OCCURRENCE AND REMEDIATION OF PIPE CLOGGING IN LANDFILL LEACHATE RECIRCULATION SYSTEMS

by

Stanislaw Lozecznik

A Thesis submitted to the Faculty of Graduate Studies of

The University of Manitoba

in partial fulfilment of the requirements of the degree of

DOCTOR OF PHILOSOPHY

Department of Civil Engineering
University of Manitoba
Winnipeg, Manitoba R3T 5V6
Canada

August, 2012

Jan Lozecznik Szyszeja
“Never say hop before jumping”

ABSTRACT

This study investigated the changes in leachate composition and clogging evolution in leachate transmission pipes and the use of methanogenesis as a leachate treatment alternative for Bioreactor landfills, by using pilot-scale and laboratory studies.

The pilot-scale study consisted of a research station built at Brady Road Landfill, housing sixteen HDPE pipes of three different diameters, conveying leachate intermittently at eight different Reynolds numbers, under reasonably controlled conditions. The pipes were tested for leachate degradation, clogging evolution and hydraulic impairment over time. The laboratory studies carried out tested (1) the effect of turbulence intensity and temperature on leachate degradation and clogging effects and (2) biological pretreatment of leachate prior to injection into a bioreactor cell.

The pilot study results showed that under the conditions tested, pipes developed a significant amount of organic and inorganic clog material in less than a year of operation. Since limited quantities of fresh leachate (approx. 3 m^3) were used during each leachate degradation analyses, the anticipated effects of clogging in a full scale injection system are expected to be more pronounced, which can negatively impact the long-term hydraulic performance, operation, and service life of a Bioreactor Landfill.

The first laboratory study showed that increasing the turbulent energy dissipation rate caused greater amounts of CO_2 evolution from the leachate, and temperature increase had an impact on dissolved Ca^{2+} under atmospheric conditions, affecting clog development.

The second and third laboratory studies showed that performing leachate methanogenesis reduces organic (COD, VFA) and inorganic (Ca^{2+}, ISS) clog constituents within the leachate However, the rate of methanogenesis was influenced by the ratio of acetate and propionate.

It is suggested that if leachate undergoes methanogenesis in a separate leachate digester prior to re-injection into a bioreactor waste cell, it may protect the pipes and other engineered landfill systems against clogging and its detrimental effects, while allowing for CH_4 recovery. However, blending of leachates from different wells or cells prior to the methanogenic digester may be needed to balance the variable concentrations and ratios of acetate and propionate over time from different landfill wells and cells.

ACKNOWLEDGEMENTS

I would like to thank my advisors Drs. J. Oleszkiewicz and Dr. S. Clark for the advice, support and guidance they have offered me in the past 5 years. Their help and valuable constructive criticism was much appreciated. The pilot study was a very challenging project which could not have been completed without the help provided by Dr. Oleszkiewicz and Dr. Clark and his selection of summer students. Special thanks also to Mr V. Wei from the Environmental Engineering Laboratory, Mr E. Penner from Mechanical Engineering, Mr. K. Lynch from Geotechnical Engineering, Ms. D. Armstrong from Chemistry, Mr. N. Ball and Ms. R. Sidhu from Geology, for their technical expertise. Thanks to my advisory committee: Dr. R. Sparling, for good technical conversation and observations; Dr. J. VanGulck, who left his research funding, trusting that I will complete the work; Dr. T. Townsend for being part of my committee and for his input and recommendations. I would also like to thank the following graduate students for their help through my research: Ms. D. Celmer, Ms.M. Paetkau, Mr. C. Goss, Mr. N. Wrana, Mr. U. Ramachandran, Mr. J. Ackerman, Ms. R. Islam, Mr. J. Chen and Ms. Q. Yuan. I'd also like to thank the following undergraduate students and friends for their help through my research: Mr. Z. Durand, Mr. J. Pawluk, Ms. A. Juneja, Mr. M. Lynch, Mr. A. Drivas, Mr. J. Nikkel and Mr. L. Diaz. Thanks to my family, especially my parents Stanislaw and Alexandra, my sisters Vanessa and Barbara, my nephew Benjamin and my grandfather Jan Lozecznik which are always a support in my life and put a smile on my face when I needed it. Finally I would like to thank the sun of my life, Irmy Nikkel, who has been with me in the good and bad times, and gave me the best gift that a man can have, our son Tadeo.

This research was financially supported by the Environmental Research and Education Foundation (EREF), Manitoba Hydro, Natural Sciences and Engineering Research Council of Canada (NSERC), Canadian Foundation for Innovation (CFI) and the City of Winnipeg.

TABLE OF CONTENTS

LIST OF APPENDICES

LIST OF TABLES

LIST OF FIGURES

CHAPTER 1: INTRODUCTION AND OBJECTIVES

1.1 BACKGROUND

Leachate recirculation in bioreactor landfills is a landfill management alternative that has been employed to enhance biological degradation of the refuse, biogas production, and waste settlement, while reducing off-site leachate treatment. Recirculation involves collection of leachate at the base of the landfill and injecting it back into the waste cell, increasing the refuse moisture and enhancing the biological activity of microorganisms (Reinhart and Townsend 1997).

Horizontal injection trenches (HIT) are commonly employed as leachate injection systems by landfill engineers because large volumes of leachate can be recirculated with limited interference to the landfill operation and reduced aesthetic and odor problems (Reinhart and Townsend 1997, Warzinski *et. al.* 2000). HIT's normally are comprised of perforated pipes surrounded by a drainage medium (e.g. granular or tire chips) and positioned at various depth within the refuse to uniformly wet the waste. Despite the common use of HIT's in bioreactor landfills around the world, there have been limited well-characterized, long-term field performance studies (Reinhart and Townsend 1997, Townsend and Miller 1998, Warzinski *et al.* 2000, and Yazdani 2002). Leachate pipes are required to operate as designed for extended periods of time (decades to centuries) because substantial amounts of leachate and gas emissions are generated during the landfill lifespan.

Field studies of leachate collection and injection systems have observed that pipes transmitting leachate can experience significant amounts of clogging over time (Brune *et al.* 1991, Turk *et al*. 1997, Fleming *et al*. 1999, Manning *et al*. 2000, Maliva *et al*. 2000, Yazdani 2002, and Bouchez *et al*. 2003). Clogging consists of a hard mineral incrustation (e.g. carbonate minerals), biological material from the leachate and biofilm. The biofilm can develop on the transmission pipe wall and perforations, as well as on the surface of the drainage material. The applicant's MSc investigated clogging in solid pipes conveying leachate intermittently at different flow rates. This study demonstrated that clogging in solid pipes depended on the hydraulic design and operation of the system (pipe material, length, inlet flow rate and pressure) and leachate composition. From these results, it was hypothesized that a clogged injection pipe at the landfill will experience a reduction in hydraulic performance for transmitting leachate, resulting in a non-uniform infiltration of leachate into the waste, thereby reducing the efficiency of waste degradation and methane gas production. Among other things, clogged leachate transmission systems seriously limit the long-term viability of the landfill design, operation, and maintenance.

Despite many researchers devoting considerable time studying the mechanisms of clogging, especially in porous material, many questions remain about mitigation methods prior to injecting leachate back into the waste cell. Turk *et al.* (1997) assessed the potential for different chemicals to clean clogged landfill pipes. However, they did not provide on-site mitigation strategies of clogging removal nor recommendations for pH control and retention time within pipelines. Renou *et al.* (1997) investigated the

amelioration of clogging on the surface of membranes used for the ultrafiltration of leachate. Nevertheless, hydrated lime $Ca(OH)_2$ was the only chemical used to pretreat the leachate against membrane fouling.

1.2 OBJECTIVES

The primary goal of this research was to develop improved engineering design and operation management strategies through clogging mitigation to extend the service life of engineered leachate transmission systems in landfills. The work involved completing pilot and laboratory studies that simulated leachate transmission pipes operating under pressurized conditions and the effects of leachate stagnation, and laboratory studies analyzing methanogenesis as an on-site leachate treatment alternative aiming to remove clog components prior to recirculation.

The objectives of this study are shown as follows.

- Correlate the rate of clog formation with the leachate composition changes and decrease in pipe hydraulic performance for different pipe sizes and hydraulic operations using a pilot-scale research station located at Brady Road landfill in Winnipeg, Manitoba, Canada.

- Investigate the role of temperature and turbulence intensity on leachate chemistry, especially CO_2, Ca^{2+} and pH under controlled conditions.

- Investigate the use of methanogenesis as an on-site biological treatment alternative to reduce the organic and inorganic clog components using real leachate from Brady Road Landfill.

1.3 THESIS OUTLINE

Chapter 2 reviews the changes in biogas and leachate composition for landfills over time, especially when the landfill becomes anaerobic. Anaerobic digestion and previous field and laboratory studies of clogging in porous media and its mechanisms are also reviewed. Finally, a conceptual development of clogging in leachate pipes during pumping and stagnation are presented. Chapter 3 describes the results from the pilot study that examine the hydraulic design and operation, leachate degradation and clogging composition and distribution of sixteen HDPE pipes operated at different Reynolds numbers. Chapter 4 describes the changes of leachate composition under different turbulent intensities by using sealed reactors with rotating impellers. In addition, a separate reactor without mixing was used to represent only the changes in temperature that can be observed in cold climate bioreactor landfills between the holding tank and inside of the bioreactor landfill. Chapter 5 and 6 present the results of the use of methanogenesis of real and synthetic leachate to remove the organic and inorganic clog components of leachate under mesophilic conditions. Chapter 7 presents the conclusions and recommendations for future work.

CHAPTER 2: LITERATURE REVIEW

2.1 BACKGROUND

A common method to dispose of municipal and industrial solid waste around the world is landfilling. Organic and inorganic waste materials located within waste layers in the landfill are typically degraded anaerobically. This is done through biological, chemical and physical interactions with emissions of biogas and, depending on the amount of moisture present, leachate production (Kjeldsen *et al*., 2002). Leachate is primarily formed as water percolates through the waste layers, where organic and inorganic components from the waste are solubilized and incorporated within it.

Modern landfills are constructed with extensively engineered infrastructure integrated into the design to safeguard the environment. An engineered leachate-collection system and a liner(s) below the waste are used to minimize leachate transport to the subsurface soil and groundwater (Rowe *et al*. 2004). The leachate collection system typically consists of a granular drainage material with embedded perforated collection pipes that control the leachate mound within the waste cell, transporting it outside for storage and treatment.

An emerging landfill management strategy known as leachate recirculation has received considerable attention in North America and major cities throughout the world (Hettiaratchi, P. 2007). Leachate recirculation involves collecting leachate at the base of the landfill and injecting it back into the waste. Various methods of leachate recirculation include methods such as surface spraying or irrigation, infiltration ponds, vertical

injection wells, and horizontal injection trenches. A horizontal injection trench (HIT) is comprised of a perforated pipe surrounded by granular material of high permeability and positioned at various depths within the refuse. HIT have the capability of recirculating large quantities of leachate without interfering with waste placement operation, compared to other recirculation strategies. Figure 2.1 shows a schematic of a HIT within a bioreactor cell.

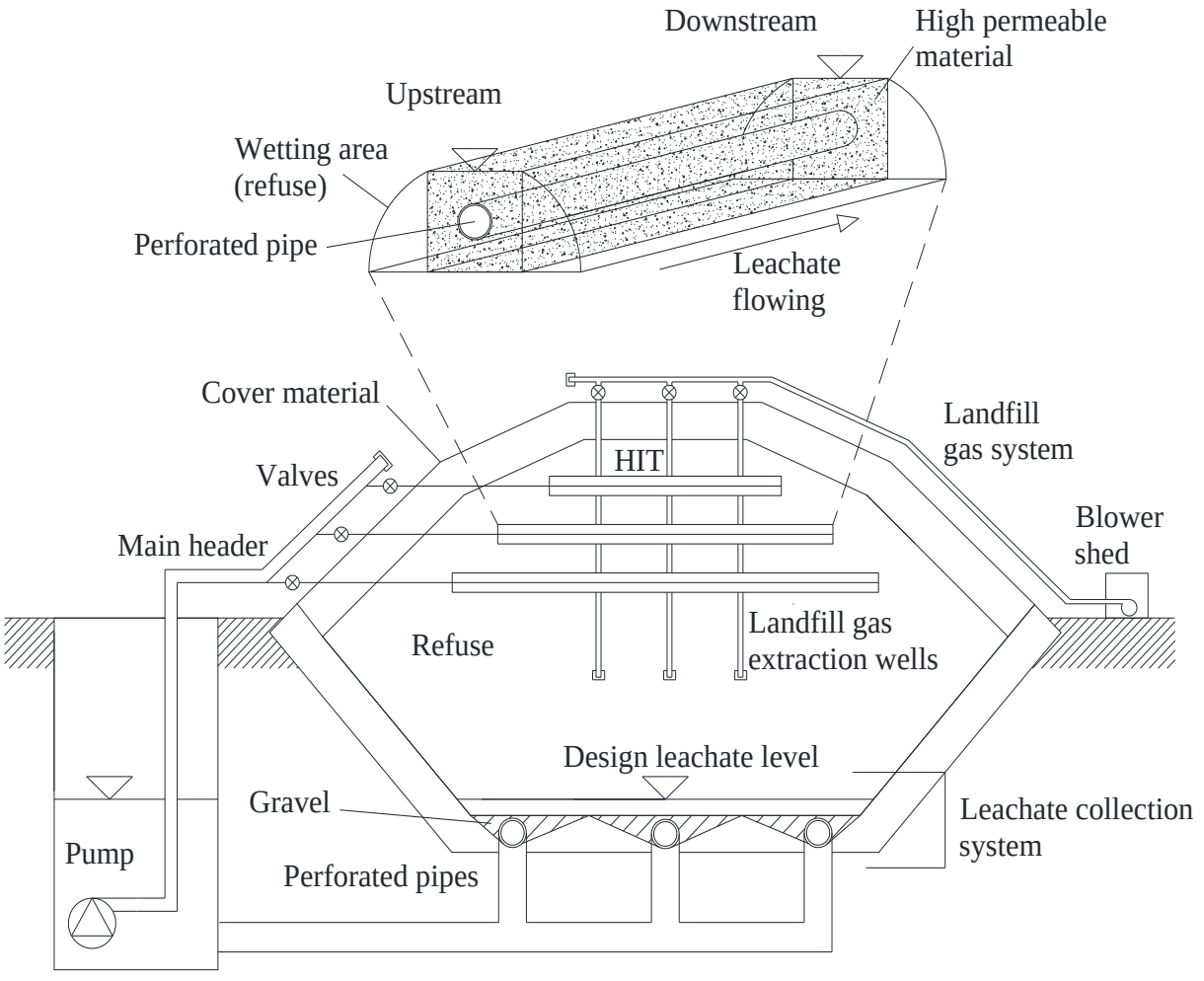

Figure 2.1. Schematic representation of a HIT in a bioreactor landfill (Not to scale). HIT are the horizontal injection trenches.

Leachate recirculation has the potential to reduce the environmental impacts of leachate and increases the volume of refuse disposed into the landfill due to increased refuse settlement (Reinhart and Townsend 1997). Furthermore, this methodology reduces the financial and environmental costs of leachate treatment by avoiding on-site chemical treatment or trucking costs. If the landfill gas (LGF) is collected it may even become an income source. Despite these advantages there has been limited long-term characterization or field performance studies of HIT used in bioreactor landfills (Townsend 1995, Reinhart and Townsend 1997, Warzinski *et al.* 2000, and Yazdani 2002, Lozecznik and VanGulck 2009).

Field and laboratory studies from around the world have reported clogging (sometimes called bio-rock) in leachate collection and injection pipes (Brune *et al.*, 1991, Turk *et al*., 1997, Fleming *et al*. 1999, Maliva *et al*., 2000, Yazdani 2002, Bouchez *et al.*, 2003). Clogging is mainly formed by the biological, physical, and chemical reactions produced by leachate and the pipe environment. Among other things, clogged leachate transmission systems seriously limit the long-term viability of the landfill design, operation, and maintenance. As leachate composition changes through time, the composition of clogging is expected to change as well. There have been, however, no reported studies regarding the effects of different leachate compositions on clog formation in leachate pipes through time.

2.2 OBJECTIVES

The first objective of this chapter is to review the changes of leachate composition over time, especially under anaerobic conditions; this review will also include the biological, physical and chemical mechanisms involved with the associated changes. The second objective is to review the hydraulic design and operation of the leachate transmission systems and the mechanisms of clogging in these systems. Investigating the capabilities and limitations of these topics will help modify existing bioreactor design and operational practices to limit clog formation, thus extending the service life of these systems. It will also aid in assessing whether anaerobic digestion can be a viable form of alternate, on-site leachate treatment prior to injection into the bioreactor landfill. If successful, anaerobic digestion of leachate may be an important secondary source of CH_4 gas.

2.3 INTRODUCTION

The composition of landfill leachate and biogas changes over time. Different theoretical landfill phases are identified as part of the aerobic and anaerobic processes that occur in the landfill. Figure 2.2 is a schematic representation of the main landfill phases, showing some general trends of biogas and VFA concentrations over time. The aerobic phase is very short as the refuse is compacted within waste layers and the oxygen trapped within the waste is rapidly depleted over a few days or weeks. During this phase, $CO_{2(g)}$ is produced by aerobic bacteria depleting $O_{2(g)}$ and leachate composition varies (Barlaz and Ham, 1993). Since the anaerobic phase is rapidly attained and can last for decades, the

biochemical processes that occur during this phase explain the changes in biogas and leachate composition measured in the landfill for decades.

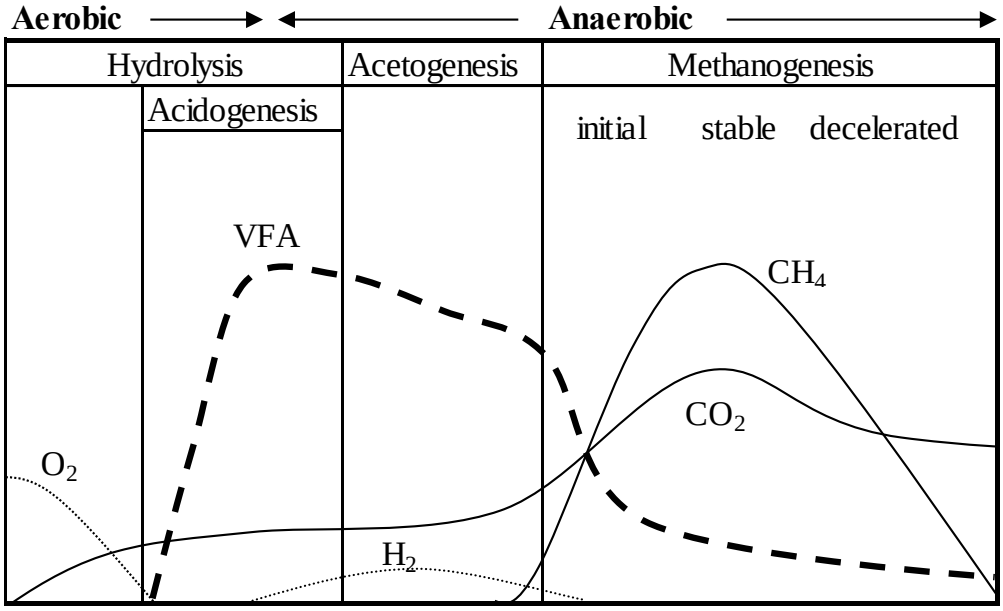

Figure 2.2. Lifetime of a landfill showing general trends in gas a leachate quality development (adapted from Kjeldsen *et al.* 2002 - Not to scale)

2.4 ANAEROBIC DIGESTION

Anaerobic digestion (AD) is generally considered a three step process: hydrolysis and acidogenesis, acetogenesis and methanogenesis, as shown in Figure 2.2. During hydrolysis, particulate material (e.g. proteins, cellulose, lignin, lipids) is converted to soluble compounds such as amino acids, glucose, fatty acids and glycerol by water and hydrolytic bacteria. These soluble compounds are transported into the cells of microorganisms to be further degraded. During acidogenesis simple carbohydrates and acids obtained from hydrolysis (amino acids, sugars and fatty acids) are used by acidogenic bacteria as an energy source, producing organic acids (e.g. acetic, propionic, formic, lactic, butyric or succinic acids), alcohols, CO_2 and H_2 as intermediate products

(Rittmann and McCarty 2001). In the following acetogenic step, acetogenic bacteria convert these organic acids and alcohols to acetate, H_2 and carbon dioxide (CO_2). There is another possible acetate formation step from H_2 and CO_2 named homoacetogenesis. The increase in organic acid concentration during acidogenesis and acetogenesis lowers the pH. Combined with the low growth rates of methanogens, this affects the start-up time of the methanogenesis (Henze *et al*. 2008).

The methanogenic steps (initial, stable and decelerated) are carried out by a group of microorganisms known collectively as methanogens. They are mainly subdivided into the hydrogenotrophic methanogenesis that convert H_2 and CO_2 into CH_4 (Equation 2.1) and the aceticlastic methanogenesis that convert acetate into CO_2 into CH_4 (Equation 2.2).

$$CO_2 + 4H_2 \rightarrow CH_4 + 2H_2O \quad (2.1)$$

$$CH_3COOH \rightarrow CH_4 + CO_2 \quad (2.2)$$

Acetate can be metabolized in anaerobic digestion to methane plus CO_2 by either methanogenic archae or some anaerobic acetate-oxidizing bacteria (Bitton *et al.* 1999, Metcalf & Eddy 2003 and Ito *et al.* 2011)**.** During the initial methanogenic phase, H_2 and CO_2, as well as organic acids accumulated during the anaerobic acid phase, are converted to CH_4 and CO_2 by methanogenic archaea reaching a steady state. As long as the organic acids concentration is constant, methane production is relatively constant. During the decelerated methanogenic phase organic acids accumulation decreases, causing an

increase in pH values. A summary of the general stages and main components of AD described before are identified in Figure 2.3.

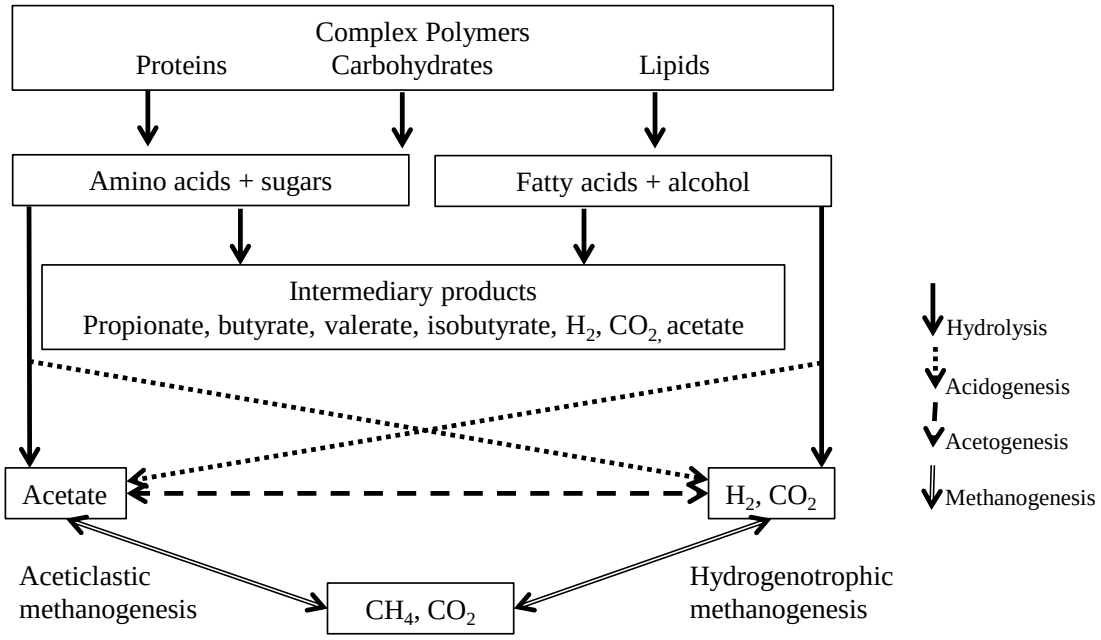

Figure 2.3. General stages of anaerobic digestion - (based on Henze *et al.* 2008 and Batstone *et al.* 2002).

2.4.1 Theoretical amount of CH_4 produced during AD

2.4.1.1 COD removal versus CH_4 production

Assuming there are no other electron acceptors available (e.g. sulphate), the theoretical amount of CH_4 produced in AD can be calculated by assuming that the removal of COD is the amount of oxygen needed to oxidize CH_4 to H_2O and CO_2 (Metcalf & Eddy 2003), as shown below

$$CH_4 + 2O_2 \rightarrow CO_2 + 2H_2O \qquad (2.3)$$

From Equation 2.3 the required oxygen needed, per mole of CH_4 produced, is 2 times (32 g O_2/mole CH_4) = 64 g O_2/mole CH_4. At standard conditions (0˚C and 1 atm) the volume of CH_4 is 22.414 L, so the CH_4 equivalent of COD converted under anaerobic conditions is 22.414/64 = 0.35 L CH_4/g COD $_{removed}$. At 35 ˚C and 1 atm, the volume of 1 mole of methane is 25.29 L; the production of CH_4 is 25.29/64 = 0.4 L CH_4/g COD $_{removed}$. These values can be used to compare CH_4 production from AD laboratory studies under the standard conditions mentioned.

2.4.1.2 Organic acids versus CH_4 production

An alternative way of estimating the theoretical amount of CH_4 produced in AD is by measuring the removal of organic acids, assuming methanogenesis is the only reaction and biomass synthesis is negligible. Speece (2008) reported the theoretical CH_4 percentage of some organic non-salt substrates containing only carbon, hydrogen and oxygen, using Equation 2.4.

$$\%CH_4 = (-12.5(n) + 50) \qquad (2.4)$$

The variable *n* is the average carbon oxidation state. For example acetic (CH_3COOH) , propionic (CH_3CH_2COOH) and butyric (CH_3CH_2 CH_2COOH) have carbon oxidation states respectively 0, -0.67 and -1,. The calculated CH_4 biogas composition from Equation 2.4 is 50%, 58.3% and 62.5%, respectively. At 35˚C and 1 atm, for example, the volume of 1 mole of methane is 25.29 L; assuming the removal of 100 mg/L of acetic, propionic and butyric acids, the production is 0.04, 0.06 and 0.07 L of CH_4. From these

stoichiometric results, it can be deduced that butyrate, followed by propionate and acetate produce the highest amount of methane. However, microbial communities and the thermodynamics of the reactions play an important role favoring the different organic acid consumption.

2.4.2 Leachate quality

Leachate is associated with the state of refuse decomposition; it contains dissolved, suspended and microbial components (Andreottola and Cannas, 1992; Kjeldsen *et al.* 2002). Changes in leachate composition are dependent on several factors. These include the nature of the waste, the sequence of landfill construction and waste layer degradation. Some authors have identified a range of values for the acidogenic and methanogenic phases explained previously and are shown in Table 2.1. Table 2.1 also includes the leachate composition from combined Winnipeg landfills, as reported by Dillon (2004); these values show a significant range that indicate different landfill phases from existing waste facilities. Leachate produced during the earlier landfill phase (acidogenic) is called "young leachate" and contains a high organic load represented by a ratio of BOD_5/COD greater than 0.4 (Ehrig 1983, Barlaz and Ham 1993, Reinhart and Grosh, 1998).

Table 2.1**.** Reported leachate composition values from landfills during acidogenic and methanogenic phases (summarized in Kjeldsen *et al.* 2002, Stegmann *et al.* 2005).

	Landfill phase***		Winnipeg Landfills
	Acidogenic	**Methanogenic**	**Combined***
pH	4.5 - 7.5	7.5-9	6.7-7.7
BOD_5	4,000-40,000	20-550	12-9,350
COD	6,000-60,000	500-4,500	NA
BOD_5/COD	> 0.4	< 0.4	NA
Calcium	10-2,500	20-600	255-880
Magnesium	50-1,150	40-350	290-720**
Iron	20-2,100	3-280	0-570
Sulfate	70-1,750	10-420	NA
Phosphorous	0.1-30	0.1-30	0.8-3.6
Ammonia	30-3,000	30-3,000	14.5-578
Zinc	0.1-120	0.03-4	0.04-6.9

NA: Not available

*Range of values obtained from Dillon (2004);

** Values obtained from the City of Winnipeg Leachate Sampling Report 2000

***Range of values taken from Kjledsen et al (2002) and Stegman et al. (2005)

During the last stages of methanogenesis, the organic load of the leachate decreases and becomes more inorganic, represented by a ratio of BOD_5/COD less than 0.4, as shown in Table 2.1. This ratio represents the biodegradability of the leachate with higher values (greater than 0.4) indicating a more biodegradable leachate than can be treated by biological means. A leachate with a BOD_5/COD ratio greater than 0.4 is therefore needed if anaerobic digestion is to be used as a treatment strategy.

The concentration of organic acids can also affect pH values and, as a consequence, the mobility of metals within the leachate. For example, Table 2.1 shows that the values of dissolved Ca^{2+} and Mg^{2+} are much higher during acidogenesis than methanogenesis. This

indicates that some metal removal may occur during the transition to methanogenesis since the pH in the acidogenic phase is typically lower than it is during the methanogenic phase.

2.4.3 Thermodynamics of AD

The Gibbs free energy value (ΔG) is commonly used to define how spontaneous (negative values), non-spontaneous (positive values), or at equilibrium ($\Delta G = 0$) a reaction proceeds. The Gibbs free energy value at its standard state ($\Delta G^{\circ'}$) is used to define whether the reaction proceeds towards the reactants or products at a specified temperature (usually 298 K) and 1 atm. In different conditions (temperature or pressure), the in-situ ΔG of the reaction is calculated by using $\Delta G^{\circ'}$ and the concentration of the products and reactants. The previously mentioned reactions occur spontaneously under the in-situ conditions. For certain intermediate reactions however, especially those requiring interspecies H_2 transfer, the in-situ ΔG must be kept away from $\Delta G^{\circ'}$ for the reactions to occur. This is shown in Figure 2.4 where some of the $\Delta G^{\circ'}$ reactions are emphasized. As can be observed from Figure 2.4, pyruvic to acetic acid ($\Delta G^{\circ'} = -47.3$), lactic to propionic acid ($\Delta G^{\circ'} = -79.9$) and acetic acid to CH_4 and CO_2 ($\Delta G^{\circ'} = -31$) are thermodynamically favorable. The reactions will proceed to the products without an external source of energy. Propionic and butyric acid degradation is, however, unfavorable. Propionic, for example, needs almost twice the energy to be degraded to acetic acid, H_2 and CO_2, compared to butyric. In addition, propionate and butyrate producing organisms need a rapid consumer of products in order to continue to synthetize

their own end-products in a thermodynamically favorable environment, if acetic acid is to be formed.

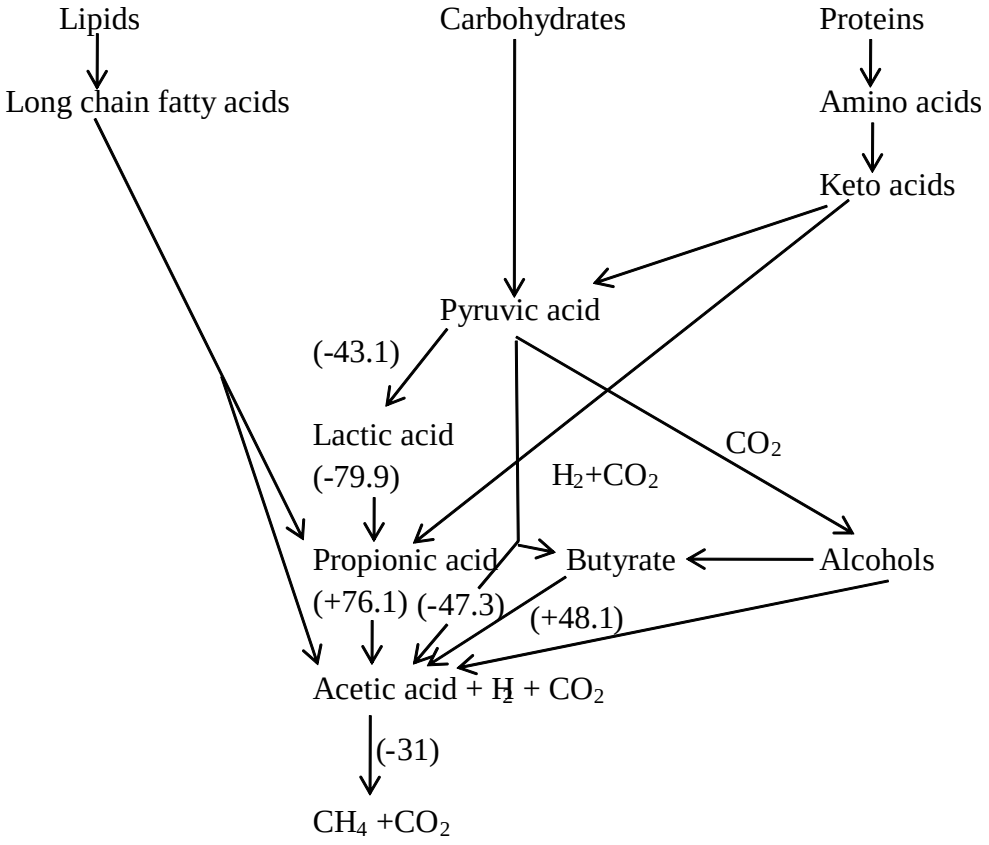

Figure 2.4. Biochemical sequences for the formation of methane and carbon dioxide by the breakdown of individual compounds under anaerobic conditions (adapted from Stafford *et al.* 1980) with their ΔG values of reactions within brackets (from Thauer *et al.* 1977).

2.4.4 Syntrophy in AD

Thauer *et al*. (1977) and Rittmann and McCarty (2001) explained that the late steps of fermentation have positive $\Delta G^{\circ'}$. They are thermodynamically possible only when consumers maintain these products at very low concentration (especially H_2). The authors described anaerobic ecosystems as a synergistic interaction in which microorganisms

benefit from the actions of their peers (syntrophy). MacInerney *et al.* (2007) reviewed several studies on syntrophic metabolisms in anaerobic digestion. Propionate and longer chains of fatty acid, alcohols, some amino acids, and aromatic compounds were reported to be degraded syntrophically to methanogenic substrates, H_2, formate and acetate. The authors suggested that the syntrophic degradation of fatty acids is often the rate limiting step of methanogenesis and biological reactors performing anaerobic digestion. James *et al.* (1998) suggested that the concentration of acetate (more than 100 mmol l^{-1}) and propionate (100 mmol l^{-1}) have an inhibitory effect on the onset of methanogenesis and butyrate oxidation, instead of the low pH. On the other hand, methanogenesis has also been reported to be a pH dependent process; pH values between 6.6 and 7.6 have been recommended (Rittmann and McCarty 2001) to avoid adverse effects. Some authors recommend a pH of 6.8 as a safe level (Metcalf & Eddy 2003; Speece 2008). The studies described above imply that syntrophic metabolism, propionate and acetate concentrations, and leachate pH may control methanogenesis in landfills.

2.4.5 Factors affecting AD

There are several factors that affect anaerobic digestion. These include temperature, alkalinity, pH, organic acids accumulation, hydraulic retention time (HRT), competition of methanogens with sulfate-reducing bacteria, and toxicants (Bitton *et al.* 1999, Speece, R.E. 1996). Thus, an understanding of the principal factors controlling and affecting the different steps of AD is necessary to maximize the stabilization of organic matter and production of biogas during AD. Based on the different biological, chemical, and physical processes involved in the anaerobic digestion phases of solid waste in sanitary

landfills, organic and inorganic components are incorporated within the leachate over time (Table 2.1). The current practice is to incorporate well designed landfill infrastructure that protects the groundwater and soil from leachate contamination. This minimizes the environmental impacts and increases the public health of sanitary landfills. Part of the engineered infrastructure, the leachate collection system, is used to control the leachate accumulation inside of the waste cell and to convey it outside for treatment purposes.

2.5 LEACHATE COLLECTION SYSTEM

Landfills have been evolving globally from simple dumps with no or little engineering design, to a new generation of modern landfills with a high level of engineering design that provides a better control of waste containments and gas emissions. A key component in landfill design is the barrier system that limits leachate release into the surrounding subsurface soils and groundwater (Rowe *et al.* 2004). The barrier system may include a leachate collection and various removal components. The system consists of a network of pipelines buried within granular material under the waste pile; a medium-size landfill has around 10 km of pipelines. The leachate collection system typically consists of a granular drainage material with embedded perforated HDPE collection pipes. These pipes control the leachate mound within the waste cell to below the design value (typically 0.3 m). This minimizes any possible advective flux of leachate and transports it outside for storage and treatment purposes (Rowe *et al.* 2004). When functioning properly leachate will enter into the drainage blanket, drain towards the collection pipe via gravity and eventually be removed from the landfill. The primary goal of the collection system is to maintain the

leachate mound on the liner within design levels, thus reducing the advective flux of contaminants through the liner. The second objective of the collection system is to collect leachate for treatment. This removes contaminant mass that would otherwise pass through the liner, therefore reducing the contaminating lifespan of the landfill. Figure 2.5 shows a typical leachate collection system representing the generic design option for primary leachate as indicated in the Ontario Regulation 232/98 for 100 years of service life (Ontario 1998).

In practice the collected leachate can be treated by disposal into the atmosphere, using some form of evaporation and/or thermal oxidation to CO_2. It can also be treated by disposal to surface water using a dedicated, separate, stand-alone treatment process or by co-treating it with other wastes such as sewage or sludge (Oleszkiewicz *et al.* 2009). A newer leachate treatment alternative is the recirculation of the leachate into the waste cell. This method has gained popularity in North America because it reduces the financial and environmental costs of leachate treatment commonly sent to the closer waste water treatment plant. This treatment method has additional benefits in that it removes the objectionable organics and BOD/COD from the leachate and produces a significant amount of biogas, which can be used as an income source.

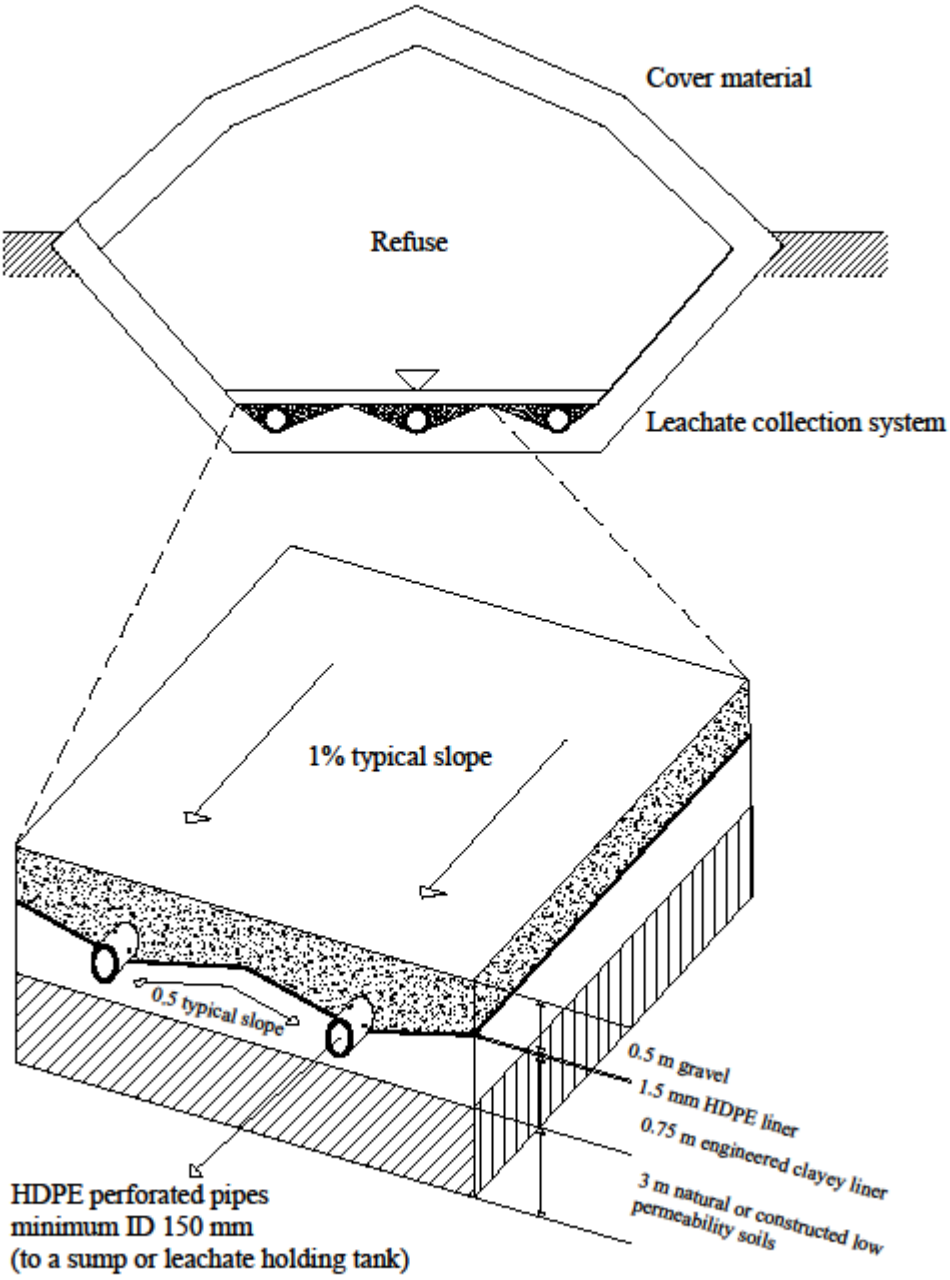

Figure 2.5. Schematic configuration of a generic design option for a primary leachate collection systems (Ontario Regulation 232/98, 1998) for 100 years of service life.

2.6 LEACHATE RECIRCULATION SYSTEM

Leachate recirculation systems are used to increase refuse moisture content in attempts to promote waste degradation, enhance waste settlement, and increase gas production (Pohland 1975, Reinhart and Townsend 1997). Generally, the benefits of leachate recirculation are maximized when the refuse moisture content is uniformly increased. The various methods used to inject leachate into the refuse include: surface spraying or irrigation, infiltration ponds, vertical injection wells, and horizontal injection trenches. Generally, leachate is collected from a leachate collection system located at the base of the landfill and transmitted through a pipe network to the injection location within or at the surface of the landfill. Compared to other methods of liquid injection, horizontal injection trenches (HIT) have the advantage of recirculating large quantities of leachate with limited interference to landfill operations (Reinhart and Townsend 1997). Horizontal injection systems commonly involve placing a highly permeable drainage material in the trench that contains a perforated pipe. Trenches are positioned at various horizontal and vertical spacing's within the waste cell.

VanGulck *et al.* (2009) described the pipe hydraulic design equations and application of design tables for the hydraulic design of perforated injection pipes in Bioreactor Landfills. A sensitivity analysis was completed for various pipe design and operational characteristics from literature reported values, showing that pipe diameter and length, perforation diameter and spacing, and inlet head and flow rate influence the perforation discharge along the length of the pipe. The design tables suggested that long perforated pipes require high inlet flow rate and hydraulic head, resulting in a non-uniform

infiltration of leachate from the perforations. In addition, the sensitivity analyses showed that literature-reported design and operational values of Bioreactor Landfills do not achieve a uniform leachate discharge along the length of the lines. This study highlighted the importance of perforated pipe hydraulics and its inclusion in the overall design and operation of leachate recirculation systems.

The hydraulic design of HIT must take into consideration capital and operating costs, liquid availability, pump operation, pipe hydraulics, and movement of fluid inside of the trench and into the surrounding refuse. During liquid injection, liquid enters the backfill material and drains into the surrounding refuse. If the liquid injection rate is higher than the drainage rate into the refuse, the fluid within the granular backfill will pressurize. The rate of liquid drainage into the refuse and pressure development within the trench is controlled by the hydraulic properties of the refuse and physical dimensions of the trench (McCreanor and Reinhart 2000, Novy *et al.*, 2005).

The development of pore water pressure within the granular material during injection induces a back-pressure on the perforation, which causes a reduction in the rate of infiltration as pore-water pressure increases (Novy *et al.*, 2005). Therefore, hydraulic interactions between the movement of liquid within the HIT and the refuse can influence the HIT placement within the landfill cell, perforation discharge (as well as back pressure), and injection time for one injection cycle. Figure 2.6 shows a schematic of a bioreactor landfill cell (Yolo County Bioreactor Landfill, California, US).

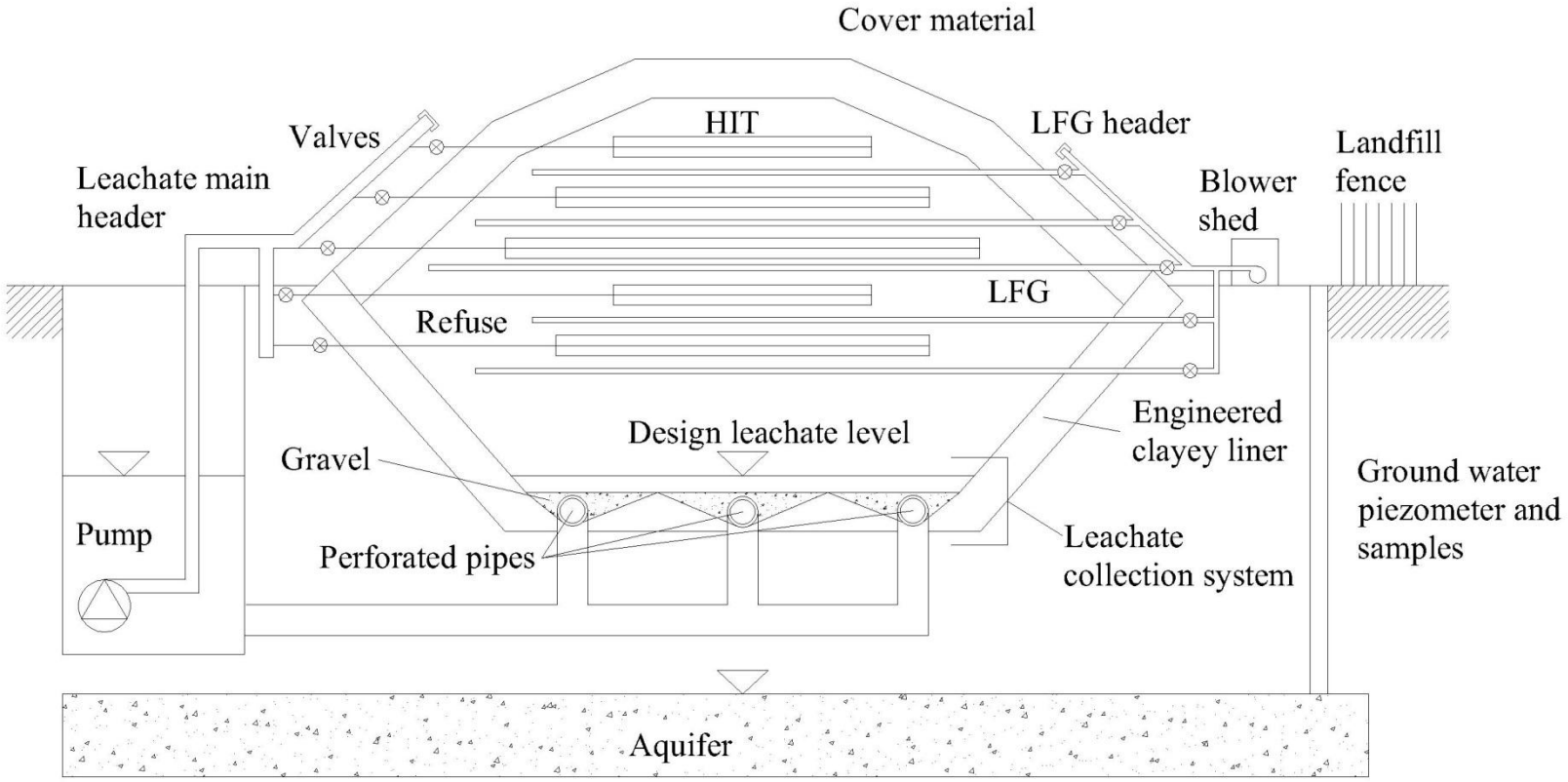

Figure 2.6. Leachate injection system configuration in Yolo County Bioreactor landfill, California, US (Not to scale). Horizontal Injection trenches (HIT) and Landfill Gas (LFG)

Different pump cycle times (pump ON/OFF) for horizontal injection trenches have been used in practice and in numerical modeling studies. This is done to assess its effect on operation and hydraulic interactions, leachate treatment, and landfill gas production. Maier and Vasuki (1996) selected pumps of variable speed for one of the landfill cells in the Southern Solid Waste Management Center (SSWMC) in Delaware; these pumps were capable of injecting up to 8 hours a day. Townsend and Miller (1998) reported different injection times based on leachate volume, starting with longer periods of injection, and then testing the systems performance for two to three days each.

A summary of HIT design and operation characteristics were consolidated from literature (summarized in Lozecznik 2006) and personal communications and shown in Table 2.2. From Table 2.2, it can be deduced that the common physical and hydraulic properties adopted for perforated pipe design in leachate injection systems from bioreactor landfill are as follows:

- High Density Polyethylene (HDPE) as the most common pipe material
- HIT lengths range between 30 to 300 m.
- Pipe external diameter ranges between 0.032 and 0.15 m.
- Inlet pipe flow rate ranges from 0.0002 to 0.0083 m^3/s.
- Inlet hydraulic head ranges from 3.6 to 60 m.
- Pipe perforations are typically circular shape with diameters ranging between 0.0024 to 0.015 m and spaced from 0.5 to 6 m.

The high range of design values raises the issue of what is an appropriate design for perforated pipes to ensure uniform waste wetting in a HIT if clog formation was considered.

Table 2.2**.** Summary of literature reported injection systems parameters (summarized from Lozecznik 2006)

Landfill	Recirculation method	Pipe Material	Pipe Diameter [m]	Pipe Length [m]	Perforation Diameter [m]	Perforation Spacing [m]	Pressure in Pipe [m]	Pipe Flow Rate [m^3/s]	Reference
Yolo County, CA, US (N-E Anaerobic Cell)	Injection pipe	HDPE	0.0318	90	0.0024	6	NA	NA	Yazdani *et al* (2000)*
Yolo County, CA, US (West Cell)	Injection line	HDPE	0.0318	100	0.0024-0.003175	6	NA	NA	Yazdani *et al* (2000)*
Lemons, MO, US	Vertical injection well	Pre cast perforated pipe	1.2	24 Max	NA	NA	NA	0.0058	Reinhart and Townsend (1997)
Central Facility, MD, US.	Vertical injection well	Pre cast perforated pipe	1.2	24 Max	NA	NA	NA	NA	Reinhart and Townsend (1997)
Coastal Regional Solid Waste Management Authority, NC, US	Iron Probe	Steel and flexible hose	0.0019-0.0032	1.5	0.0032-0.0064	NA	30.36	0.0033-0.005	Reinhart and Townsend (1997)
Pecan Row, GA, US	Horizontal trench	Corrugated	0.15	30	NA	NA	NA	0.0083	Reinhart and Townsend (1997)
Mill Seat, NY, US	Pressurized pipe loop	HDPE	0.1	NA	NA	NA	NA	0.0002-0.0012	Reinhart and Townsend (1997)
DSWA Southern SWM Center, DE, US	Injection line	HDPE	0.15	120-240	0.0127	0.1524	12-36	NA	Christopher Gabel, personal communication 2005
Onyx Orchard Hills, IL, US	Injection line	PVC/HDPE	0.15	100-300	0.0127-0.015	0.0762	NA	0.0019-0.0032	Randy Frank, personal communication 2005
Pilot project	Horizontal trench	PVC	0.08	159	0.0095	0.6	7.2	0.0054	Townsend and Miller (1998)
Buncombe County, NC, US	Injection line	HDPE	0.15	60-90	0.0127	3.048	12-60	NA	Christopher Gabel, personal communication 2005
Sainte-Sophie, Quebec, Canada	Horizontal trench	HDPE	0.15	300	NA	NA	NA	NA	Simard *et al*.(2003)

NA: Not available
Note:*Unpublished internal report

2.6.1 HIT design methodologies

Townsend (1995) and Al Yousfi and Pohland (1998) provide conceptual and mathematical design methodologies to define the HIT horizontal spacing within the bioreactor cell. The Townsend (1995) method assumes that the HIT are horizontal injection wells and act on the shape of the saturation area around it. The extension of this saturated area is a function of the pressure of fluid discharged at the pipe perforation, and a function of the hydraulic conductivity of the refuse. Some assumptions are made, such as constant fluid pressure leaving the pipe, constant refuse hydraulic conductivity, and steady state flow conditions.

The equations developed with this method estimate the vertical and horizontal dimensions of the saturated area around the HIT. The Al Yousfi and Pohland (1998) method estimates the maximum horizontal distance between two contiguous perforated pipes based on the waste properties, head mound by leachate release through pipe perforations on the waste, and overlapping of saturated refuse area. This method is based on an equal flow discharge through perforations along the pipe, and assumes that the high mound on the waste between two pipes has a parabolic shape along the perforated pipe. Other assumptions include complete waste saturation and Darcy's law applied for flow along the transversal and horizontal axis. This implies that hydraulic head along the pipe is constant.

Even though both methods have made an attempt to assess the hydraulic performance of HIT they do not consider the hydraulic changes in perforation discharge, the hydraulic head at the pipe-waste, or the pipe-trench interface along the length of the pipe. Consequently, the hydraulics of fluid flow within the perforated pipe and the influence of pipe design and operation on injection system performance are not considered. VanGulck *et al*. (2009) analyzed the design of perforated pipes under pressurized conditions, not including the hydraulic interactions between the pipe, trench, and refuse. The aim of the proposed methodology was to obtain uniform wetting of the refuse by delivering a uniform discharge of liquid along the entire length of a clean perforated pipe. Although Townsend (1995), Al Yousfi and Pohland (1998) and VanGulck *et al*. (2009) provided conceptual and mathematical approaches to assess the hydraulic performance of HITs, none of these studies considered clogging and its detrimental effects on HIT operations.

For example, VanGulck *et al* (2009) discussed the appropriate reduction in perforation discharge between the first and last perforation, assuming that 20% of difference was acceptable. Some of the general trends observed with the pipe perforations (for all other conditions being equal) in the sensitivity studies were that (1) smaller perforation diameter discharged lower flow rate and (2) the shorter the space between perforations or the higher number of perforations per spacing, the larger the volume of leachate discharge and (3) the higher the inlet head, the higher the perforation discharge. Clogging build-up within the perforations will reduce the perforation diameter, decreasing the perforation discharge and thereby reducing the difference in discharge between the first and last perforation (e.g. 20%) initially designed for a clean perforated pipe. Therefore,

clogging within the perforations will produce a non-uniform discharge along the length of the line, limiting the benefits of leachate recirculation.

If clog material is not removed it can impair the performance of these systems to the point that they can no longer perform their design functions. An understanding of the clogging processes and their control will provide a better understanding of the lifespan operation of these landfill components.

2.7 CLOGGING EVOLUTION AND MECHANISMS

There is an extensive array of studies into clogging of leachate collection systems (LCS) (e.g. Armstrong 1998, Fleming *et al*. 1999, Fleming and Rowe 2004, Rittman *et al.* 2003, Cooke *et al*. 1999, 2001, 2005, McIsaac *et al*. 2000, 2005, VanGulck *et al*. 2003, 2004a,b, Rowe *et al.* 2000a,b, 2004, 1998a,b, McIsaac and Rowe 2006). Based on the field and laboratory studies performed, clogging is a biologically mediated process initiated by the formation of biofilm within the drainage material of LCS. The growth and activity of biofilms and suspended microorganisms induces the precipitation of carbonate minerals (e.g. $CaCO_3$) and entrainment of suspended particles.

2.7.1 Biofilms

In general terms a biofilm is a community of microorganisms and their extracellular polymers (EPS) attached to a solid surface. Different microorganisms produce different EPS (i.e proteins, lipopolysaccharides or capsular polysaccharides), which further affects adhesion processes and changes of the biofilm thickness and density (Vu *et al*. 2009).

Biofilms are mainly composed of water (often > 90%), EPS (up to 90% of organic matter), cells, entrapped particles and precipitates, sorbed ions, and polar and apolar organic molecules (Flemming *et al.* 2000). Biofilms are porous; nutrients penetrate the pores and reach different layers of the biofilm and microbial colonies, thus affecting the growth of the film via mass-transport mechanisms. The compositions of biofilms vary significantly for each case depending on growth conditions (Stoodley *et al.* 1999); these conditions include nutrient availability and hydrodynamic conditions (e.g. laminar or turbulent flow). The hydrodynamic conditions have a dual effect on mass transfer in biofilms with high turbulence facilitating substrate diffusion and shear stress increasing biofilm density. This reduces the diffusivity of substrates into the biofilm (Liu and Tay 2001).

The biofilm density is a very important property as it affects how the biofilm operates. Density depends on several factors, which include bacterial species, thickness, bulk composition, hydrodynamics of the environment and biofilm age (Vu *et al.* 2009). Because the adhesive properties of EPS help retain the suspended particles at the biofilm surface, these particles can contribute significantly to the overall mass of the biofilm (Flemming *et al.* 2000). They may also hinder the transport of nutrients inside of the biofilm that are required for the microorganism's survival.

Bacterial cells are typically anionic due to the presence of carboxylate or phosphate moieties. The biofilm may acquire an anionic character, binding with metals ions (Ca^{2+}, Mg^{2+} and Fe^{3+}) and precipitating on the surface of the film (McClean *et al.* 1999).

Biofilm accumulation and growth also increases the frictional resistance in water distribution systems (Bryers and Characklis 1981), increasing the pressure drop within the systems.

Biofilm formation and growth are complex processes still being studied and analyzed. Contrary to the current interest of biofilms in wastewater engineering and its purported advantages (e.g. membrane bioreactor processes) uncontrolled biofilm growth in LCS is undesirable. Given that the design and operation of current landfills and bioreactor landfills around the world have no control over leachate composition and biofilm formation in LCS, uncontrolled biofilm growth is expected to occur.

2.7.2 Conceptual development of biofilm growth and clogging in LCS

Past research of clogging in leachate collection systems has suggested (summarized in Rowe *et al.* 2004) that biofilm growth in LCS results largely from the growth of microorganisms conducting acetogenesis of propionate and butyrate, and by the methanogenesis of acetate. The consumption of these VFA's by suspended microorganisms and the biofilm generates carbonic acid (H_2CO_3), as shown in Equations 2.5, 2.6 and 2.7.

Fermentation of propionate to acetate, carbonic acid and methane gas

$$CH_3CH_2COOH + \frac{3}{4}H_2O \rightarrow CH_3COOH + \frac{3}{4}CH_4 + \frac{1}{4}H_2CO_3 \qquad (2.5)$$

Fermentation of butyrate to acetate, carbonic acid and methane gas.

$$CH_3CH_2CH_2COOH + \frac{1}{2}H_2O + \frac{1}{2}H_2CO_3 \rightarrow 2CH_3COOH + \frac{1}{2}CH_4 \qquad (2.6)$$

Fermentation of acetate to methane and carbonic acid.

$$CH_3COOH + H_2O \rightarrow CH_4 + H_2CO_3 \qquad (2.7)$$

The accumulation of H_2CO_3 increases the carbonate (CO_3^{2-}) concentration; when combined with metals such as Ca^{2+}, which is abundant in leachate, it precipitates as $CaCO_3$. The destruction of VFA's into H_2CO_3 increases the leachate pH, potentially inducing the precipitation of carbonate based minerals formed in the leachate. Particles such as silicon (sand), which is commonly used as daily cover, travel with the leachate. They are transported and deposited in the drainage stone, thus contributing to the inorganic layer of clogging. The porosity of the medium decreases as clogging occurs, increasing the leachate velocity through the drainage material. This may control the rate of VFA consumption and the attachment/detachment of suspended or attached microorganisms; net growth in this layer occurs as a result. As clogging occurs the change in fluid flow through the porous media may affect the attachment/detachment of inorganic particles.

Although the characterization of clogging mechanisms in LCS can be estimated by conceptual and mathematical methods, the following aspects of biofilm and clogging have not been considered:

- Microbial identification (e.g. 165rDNA sequencing for identification without need for isolation, resin embedding) or sampling has been reported for biofilms clogging LCS.
- Characterization of the biofilms in LCS or its physical properties such as EPS analysis, proteins, stratification, etc.
- No studies have demonstrated where in the biofilm layers VFA consumption occurs. It may be that suspended microorganisms within the leachate or attached to the surface of the biofilm remove the majority of VFA's.
- Analyses or studies regarding the interaction between synthrophs (propionate and butyrate) and acetoclastic methanogens (acetate) with respect to clogging. As a matter of fact, some problems regarding propionate removal have been found in literature (e.g. VanGulck *et al* 2003, VanGulck and Rowe 2004a).
- The studies have not considered the impact of leachate CO_2 on Ca^{2+} precipitation or pHand the kinetics of gas transfer in the laboratory.

Although the focus of this section is to summarize the mechanisms of clogging in LCS at Municipal Solid Waste (MSW) landfills, there is evidence from literature and field reporting that clogging is also an operational problem in ash monofill landfills and ash present in co-disposal landfills (Buchholz and Landsberger 1995, Rhea, S. 2004, S., Mulla *et al.* 2005). These studies show that leachate in contact with ash contained high Ca^{2+} and metals concentrations. For example, differences up to 43 times of Ca^{2+} (5,384 against 125 mg/L) and 2.5 times of Total Dissolved Solids (24,983 against 9,777 mg/L) were found from leachate collected from West Central Florida Ash Monofill and

Southeast Florida Class I Landfill (Mulla, A *et al.* 2005). This study also shows that alkalinity was 50 time higher in the MSW leachate (7,033 against 140 mg $CaCO_3$/L) than the Ash Monofill Landfill. Rhea, S. (2004) stated that ash introduces an important source of calcium ions, while the MSW and its biological activity add the source of carbonate, which in turn can potentially form clogging, forming $CaCO_3$ minerals such as calcite. From above, it is believed that ash in co-disposal landfills will increase the metals concentrations in the leachate, especially Ca^{2+}, which, combined with the carbonate generated in the MSW fraction, will increase the potential of clogging within the LCS. However, more research is needed to further investigate this statement.

2.7.2.1 CO_2 outgassing effects on clogging in LCS

Many microorganisms in the landfill produce CO_2, part of which is dissolved within the leachate. This adds carbonate to the leachate and can lower the pH if the solution does not have enough buffering capacity. This is shown in Equations 2.8, 2.9, 2.10 and 2.11.

- Total carbonate

$$C_{TOTAL} = H_2CO_3 + HCO_3^- + CO_3^{2-} + CO_{2(aq)} \quad (2.8)$$

- Carbon dioxide to carbonic acid

$$CO_{2(g)} \rightarrow CO_{2(aq)} + H_2O \rightarrow H_2CO_{3(aq)} \quad (2.9)$$

- Carbonic acid to bicarbonate

$$H_2CO_{3(aq)} + OH^- \rightarrow H_2O + HCO_{3(aq)}^- \quad (2.10)$$

- Bicarbonate to carbonate

$$HCO_{3(aq)}^- + OH^- \rightarrow H_2O + CO_{3(aq)}^{2-} \quad (2.11)$$

Equations 2.9, 2.10, and 2.11 are pH dependent; for different leachate pH values, Equation 2.8 exhibits a different main carbonate contributor. For acidogenic (pH<6.5) and methanogenic (pH>6.5) leachate for example, carbonic acid or bicarbonate could have a higher concentration than the rest of the species in Equation 9. This is important because any increase of carbonate may bind with highly abundant Ca^{2+} within the leachate to produce calcium carbonate, as show in Equation 2.12.

- Carbonate and calcium to calcium carbonate

$$CO_{3(aq)}^{2-} + Ca^{2+} \rightarrow CaCO_{3(S)} \qquad (2.12)$$

Equation 2.12 shows the widely reported $CaCO_{3(S)}$ formation which is also commonly reported as inorganic clogging in LCS. As previously mentioned, any changes in dissolved CO_2 within the leachate affects the carbonate equilibrium, impacting inorganic clogging processes. Rittmannn *et al.* (2003) suggested that in addition to microorganism's growth and activity, and the removal of VFA, CO_2 out-gassing also affects pH values and thus clogging. This study assessed the effects of CO_2 outgassing on the changes in leachate pH and the solubility of $CaCO_3$ using a biogeochemical model (CCBATCH) with data from another leachate column study (Cooke *et al.* (2001)). Fleming and Rowe (2004) investigated the effect of different synthetic landfill gas at different headspace pressures, using 200 mL plastic flasks with real leachate. However, the synthetic landfill gas compositions was not provided nor $CO_{2(g)}$ concentration values over time. Therefore, no dissolved CO_2 values for leachate have been sampled nor assessed in laboratory or field studies with respect to clogging in leachate collection systems.

Variation in dissolved CO_2 is affected by the solubility of the CO_2 (Henry`s law constant), the partial pressure of the gas in the atmosphere, temperature, the concentration of impurities in the solution (e.g. salinity, suspended solids, etc.) and turbulence intensity (Metcalf& Eddy 2003, Malusa *et al.* 2003). Any of these variables can influence the concentration of dissolved CO_2 within the leachate, thus impacting the pH and carbonate content, forming clogging. Carbonate in solution increases the microbial conversion of VFA to H_2CO_3. At the same time, carbonate can evolve from solution as a precipitant with Ca^{2+} (as $CaCO_3$) or CO_2 outgassing. Both mechanisms increase the leachate pH, but the conversion of acetic acid to carbonic acid only produces a small increase in pH. When a gas phase exists ($CO_{2(g)}$), a portion of the carbonic acid is removed from solution, and since the lost carbonic acid cannot release H+, the net effect of this conversion is a significant increase in pH (Rittman *et al.* 2003).

2.7.3 Conceptual development of clogging in leachate injection systems

First laboratory study into clogging of pipes permeated with landfill leachate

Lozecznik and VanGulck (2009) characterized the mechanisms and rates of clogging in leachate transmission pipes for two sets of HDPE pipes of varying physical characteristics and flow rates. The pipes operated continuously during 5 months, and leachate was replaced every 2 to 3 weeks for fresh leachate. The internal diameters (ID) tested were 0.04 and 0.09 m; three different average flow rates of 0.25, 0.55 and 1.2 L/s were tested using leachate from Brady Road Landfill. Organic and inorganic material (clog) deposited within all the pipes after 5 months of operation (Figure 2.6) was

collected and sampled. Even though this study does not represent the operational conditions of bioreactor landfills as leachate was recirculated intermittently through the pipes, it provided some measurable changes of leachate degradation (e.g. COD, Ca^{2+}, TSS, etc.) as it was transmitted through testing pipes under controlled laboratory conditions. These changes were compared with the flow rates and pipe internal diameter selected from literature.

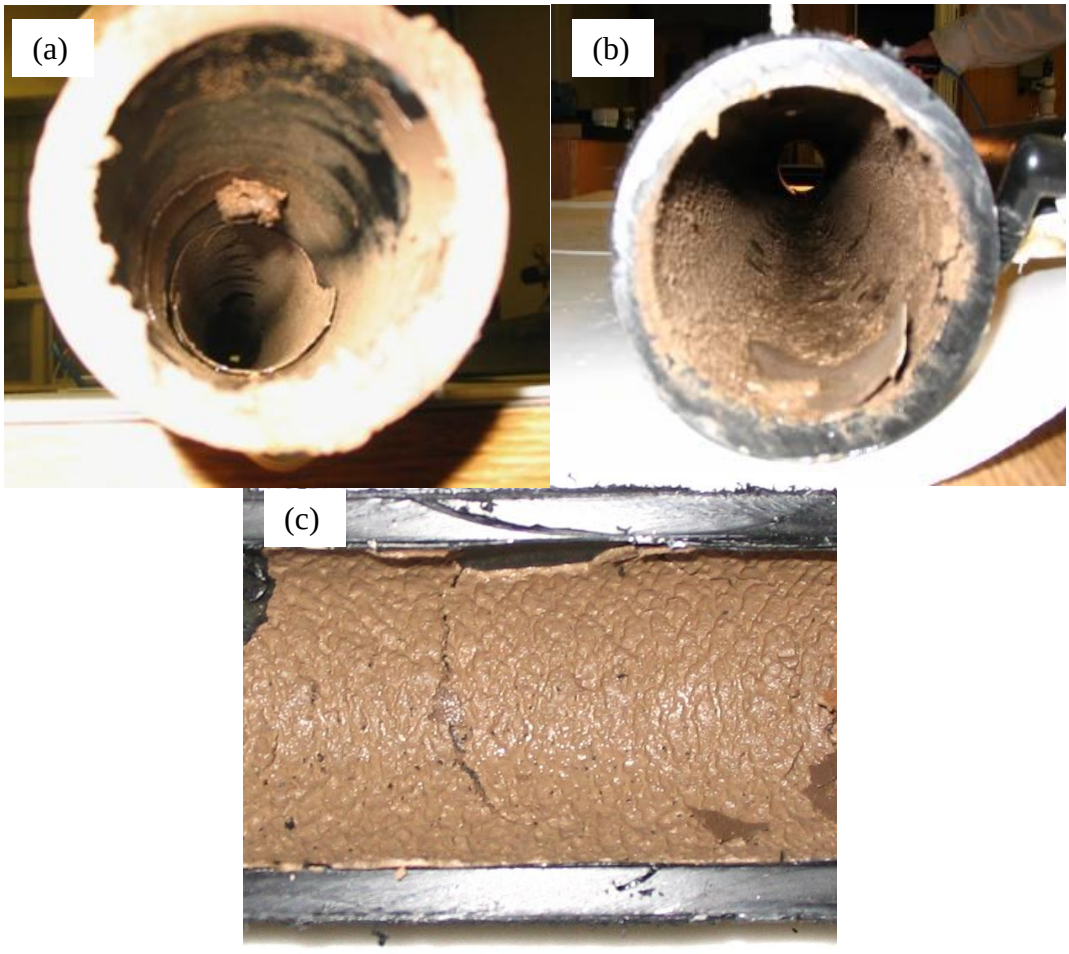

Figure 2.7. Photographs of clog within pipe series 1 for (a) top section and (b) bottom section and (c) along the length of the pipe after 5 months of operation (from Lozecznik 2006).

The most important outcomes from this research were:

- Removal of COD within the pipes varied from 10 to 25%; the greatest removal occurred during the lowest flow rate tested.
- The pH of the leachate was highest during the highest average flow rate tested; from 7.09 to 9.8 respectively.
- High leachate temperatures attained after intermittent pumping, ranged from 43 to 55°C.
- Calcium removal ranged from 25 to 50% for the different flow rates tested.
- The material that accumulated on the inner surface of the pipes contained organic and inorganic materials; this accumulation was comprised of biofilm, mineral precipitate, and retained suspended solids.
- Approximately 40% of the clog material was organic matter; it was present throughout the material.
- Magnesium, calcium and carbonate were the main inorganic clog constituents.
- Hydromagnesite ($Mg_5(CO_3)_4(OH)_2\ 4H_2O$) was the main mineral phase of the clog material that had accumulated within the four pipes.
- Small diameter pipes (0.05 m) experienced a greater reduction in cross sectional area than large diameter pipes (0.1 m).
- During the highest flow rates tested, significant CO_2 outgassing was observed.

This study showed that leachate conveyed through leachate transmission pipes can reach pH values of 7 to 9.5. Since no significant removal of COD was obtained within the testing pipes (maximum between 10 to 25%), and high amounts of gas were observed

escaping from the gas lines connected to the pipes, sump and influent tank, it was assumed that CO_2 outgassing was mainly responsible, as opposed to biological activity, for the increase in pH under turbulent flow conditions. Nevertheless, no measurements of dissolved CO2 or CO_2 outgassingat different flow rates were made. These leachate pH values will impact the methanogenesis (CH_4) at the bioreactor landfill and precipitation of carbonate type of minerals (e.g. aragonite, calcite, hydromagnesite) within the transmission pipes. The minerals type and structure can also determine the efficiency of the cleaning strategy adopted to remove the clog from the pipes. Clog material accumulated inside of the pipes may change the original pipe friction factor, thereby reducing the hydraulic efficiency of the injection system. It should be noted that the inlet pressure and head losses within the testing pipes were not measured, thus the pipe hydraulic characteristics such as friction factor or rugosity and its changes over time were not calculated.

2.7.4 Effects of leachate temperature in the degradation of VFA

As mentioned in section 2.4.5, temperature affects the performance of anaerobic processes. The laboratory study described in the previous section (2.7.3) attained high leachate temperatures within the testing pipes (43 to 55˚C), and no discussions were made on the potential effect produced on the insignificant COD removal values obtained while leachate was intermittently flowing within the pipes. In addition, it is expected that leachate stored in a sump or tank prior to recirculation will experience significant changes in temperature (e.g. 4 to 25˚C), specifically in colder winter weather locations such as Winnipeg.

Since acetate, propionate and butyrate degradation impact the rate of clogging (see Section 2.7.2), understanding the temperature effects on the thermodynamics of acetate, propionate and butyrate degradation will help to predict clogging formation within leachate injection pipes and to design a treatment system that maximizes the removal of these VFA prior to reinjection. Arrhenius equations predicts that a decrease in temperature results in a decrease in the reaction rate, for example, a temperature drop of 15˚C will decrease the biological activity by a factor of about 3 (Langenhoff and Stuckey 2000). Rebac *et al* (1995) studied the activities of methanogenic and synthrophic microorganisms under psychrophilic conditions in an expanded granular sludge bed (EGSB) reactor, using mesophilic methanogenic granular sludge and low COD synthetic wastewater. This study showed that the degradation of propionate resulted to be the most problematic, compared to the degradation of butyrate and acetate. Langenhoff and Stuckey (2000) studied the treatment effect of low temperature dilute wastewater using an anaerobic baffled reactor. This study showed that synthrophs (propionate degraders) were more affected by a decrease in temperature than acetate degrading bacteria. This study also operated a reactor at mesophilic conditions, showing higher propionate removal rates. The degradation of butyrate was stable. Speece (2008) reported several studies about the sensitivity of VFA removal at different temperatures, stating that more studies have reported elevated VFA under thermophilic conditions than mesophilic conditions. It is also reported that propionate tends to accumulate within reactors operating above 49.5˚C. These studies showed that the activity of propionate degraders is the most affected by high (thermophilic) and low (physchrophilic) temperatures, followed by acetate and then butyrate.

2.8 SUMMARY

Bioreactor landfills offer several advantages compared to traditional methods of treatment; these advantages include higher biogas production, waste settlement, and leachate reuse on-site. Horizontal injection trenches (HIT) are a common method used to recirculate leachate in bioreactor landfills to increase refuse moisture and biological activity. As described within the literature presented before, there is paucity in the design and operational values of HIT used in full-scale studies, where no design considerations of clog formation have been reported and the detrimental effects on short and long term operation have not been taken into design and operational considerations.

Although clogging has also been recognized as a nuisance for the operation and potential failure of leachate recirculation systems and the performance of bioreactor landfills, there are no laboratory or field studies of the mechanisms that contribute to its formation in these systems. So far, the mechanisms of clogging in LCS are hypothesized to occur in leachate transmission pipes, which are related to the biological, chemical, and physical processes affecting leachate degradation. Clogging in LCS is mainly produced by (1) biofilm and suspended microorganisms growth and activity, which impact the leachate VFA content and entrainment of leachate particles and (2) leachate CO_2 concentration. No field or laboratory studies of clogging in LCS have assessed the impact of leachate CO_2.

The applicant's MSc. examined leachate degradation and clog formation using laboratory pipes conveying leachate continuously (Pump On at all times) for 5 months under

controlled conditions. Nevertheless, the results of this study were very limited to scale-up as the operation adopted was very different from the bioreactor landfills (Pump On and Off). This study showed that CO_2 outgassing produced during turbulent conditions was the main clogging mechanism, but no analyses were made with regards to leachate stagnation and the effects on leachate suspended particles as occur in the field after the pump is turned off. Since leachate changes in composition depending on the landfill phase, clog composition may change over time. No studies on the rate of change or the evolution of clog composition within leachate injection systems have yet been reported.

Different individual VFA such as acetate, propionate and butyrate concentrations within the leachate are expected to change through the time as leachate changes in composition. These changes in total and individual VFA values will have a different impact in the selection, growth and activity of microorganisms responsible for clogging in LCS and leachate transmission pipes. For example, acetate, propionate and butyrate degradation was reported to drive the bioprecipitation of $CaCO_3$ in LCS. Because propionate and butyrate are degraded syntrophically to methanogenic substrates and acetate is degraded by acetoclastic methanogens, these VFA yield different carbonate concentrations or amounts causing $CaCO_3$ formation or precipitation. The predominance of acetate, with a rapid conversion step to the products (negative $\Delta G^{\circ'}$), accelerates the rate of clogging. On the other hand, the predominance of propionate or butyrate (positive $\Delta G^{\circ'}$) would have a different impact in the clogging rate.

These studies suggested that a balance between acetate and propionate concentrations is required to maximize the VFA removal and clogging rate. No studies of clogging in LCS have shown the veracity of this statement.

Leachate is commonly collected to a sump or tank prior to recirculation. Reducing the VFA content before re-injection, especially acetate and propionate, will limit the clog formation in the bioreactor landfill. To the author's knowledge, there are no studies of leachate treatment prior to recirculation to minimize clogging in the bioreactor landfill. In addition, data for the changes in concentration of the individual VFA over time for landfill leachates is scarce in the literature and most of the anaerobic degradation studies of leachate have focused on total COD and VFA values to measure the performance of the treatment. Finally, from the solid waste, leachate and clogging literature reported, there is a limited knowledge of the interactions between the different microbial communities responsible for the degradation of acetate and propionate and the possible inhibitory effects for different concentrations.

As summarized before, more field and laboratory studies are needed to understand the mechanisms behind the removal of organic and inorganic material from the leachate inside of the pipelines for different pipe sizes and hydraulic operations. Also, if the rate of clog formation and changes in composition at different time were known, this could potentially aid in the selection of cost-efficient pipe cleaning methods for type of clog material present, identify cost-effective frequency of pipe cleaning, aid in modifying existing designs to limit clog formation and to provide a comparison of clogging potential

in conventional and bioreactor landfills. As newer acidogenic leachate usually presents higher concentration of organic and inorganic materials than older leachate (decelerated methanogenic phase), a leachate treatment alternative to remove clog constituents prior injection would help to limit clog accumulation within the HIT and waste cell, especially at the earlier stages of the bioreactor landfill operation. If anaerobic digestion is used, it also has the advantage of producing another source of CH_4 inside of the landfill facility. However, the effects of different acetate and propionate concentrations on methanogenesis are needed to be evaluated as leachate changes in composition, even from well to well at the same landfill.

CHAPTER 3: PILOT STUDY OF LEACHATE TRANSMISSION PIPES

3.1 INTRODUCTION

The design and operation of Horizontal Injection Trenches (HIT) is important because leachate transmission systems (collection and injection) are required to operate as designed for extended periods of time (decades to centuries), and because substantial amounts of leachate and gas emissions are generated during the landfill lifespan. In case of failure, any attempt of trench or perforated pipe replacement from the collection or injection systems will produce odors and serious public environmental concern particularly in adjacent communities, as well as significant costs and public pressure.

Biological, physical and chemical clogging within the leachate transmission pipes (collection and injection) can occur, negatively impacting the long-term hydraulic performance, operation, and service life of the system (Yazdani *et al.* 2002, Bouchez *et al.* 2003, O'Brien, J.K. 2010). The range and paucity of data on the HIT parameters (see Table 2.2) shows that no design considerations including clog development have been reported. More laboratory and pilot studies are needed to understand the mechanisms behind the removal of organic and inorganic material from the leachate inside of the pipelines for different pipe sizes and flow conditions. Also, knowing the rate of clog formation and changes in composition with time can potentially aid in the selection of cost-efficient pipe cleaning methods for the type of clog material present. It can also help to identify cost-effective frequency of pipe cleaning, modify existing designs to limit clog

formation and provide a comparison of clogging potential in conventional and bioreactor landfills.

3.2 OBJECTIVES

The overall goal of the research is to correlate the rate of clog formation with the changes in leachate composition and the decrease in pipe hydraulic performance for different pipe sizes along with hydraulic operations using field conditions. The specific goals of this research are

- Identify the main variables impacting leachate degradation and clog formation in the pilot-scale study pipes during pumping and stagnant leachate conditions.
- Investigate the effect of CO_2 degasification versus biological activity on leachate quality and clog formation during pumping and stagnant conditions.
- Evaluate the configuration, composition and physical properties of clog formation within the pipe series over elapsed time.
- Quantify the rate of clog formation within the pipes for the different pipe diameter and hydraulic operation adopted.
- Evaluate the distribution of the final clog accumulation along the length of the pilot-scale study pipes.
- Measure pressure at the pipe inlets and head losses within the full-scale pipes at different times and calculate the changes to the pipe hydraulic characteristics (decrease in inlet pressure and friction factor) due to clog formation and accumulation, for the different pipe diameter and hydraulic operation adopted.
- Using the pilot-scale results, identify potential methods to prevent or minimize

pipe clogging with consideration given to design and operation of leachate injection systems.

3.3 METHODOLOGY

The pilot study set-up involved conveying leachate at a constant flow rate (see Table 3.1) through high-density-polyethylene (HDPE) pipes. The changes in key leachate chemical composition (discussed below) within the pipes over time were correlated with the rate of clog formation. Furthermore, the rate of clogging was correlated to the physical (i.e. diameter) and operating characteristics such as Reynolds number (i.e. turbulence) of the flow. The pipes were housed in a chamber adjacent to a manhole at the Brady Road Landfill in Winnipeg, Manitoba. The internal diameters of the pipes that were being used for this study were approximately 0.04, 0.09 and 0.13 m. These pipe sizes were selected based on existing bioreactor landfill injection systems designs (Table 2.2). The flow rates utilized in this study were selected based on reported field studies of injection rates used in HIT of 370 to 620 L/d/m of trench (Miller *et al.*, 1993). Typical trench lengths have been reported to range between 30 to 200 m (Miller *et al.* (1997), Reinhart and Townsend (1997), Townsend *et al.* (1998), GeoSyntec Consultants (2000), Yazdani *et al.* (2002). Thus, for a 30 m long trench the range of flow rate is 0.13 to 0.21 L/s, and for a 200 m long trench the range of flow rate rate is 0.86 to 1.44 L/s. Design low and high flow rates of 0.16 and 1.53 L/s, as well as other intermediate flow rates were selected for this study to compare different hydraulic operations. A testing matrix is provided in Table 3.1, showing the pipe diameter and flow rates selected for each of the testing pipes. In order to calculate the Reynolds numbers conveyed through the pipe series using real leachate

characteristics, a sample of leachate from Brady Road Landfill (from a manhole) and Summit Road Landfills (leachate impounded) both from Winnipeg, were collected on November 27 of 2009. A viscometer Cannon-Manning Semi-Micro Viscometer CMSMC (9721-Y50) Series, a stirring hot plate FISHER 11-600-49SH and a Orion 5 Star Multi WPHH equipped with a temperature probe were used in the Environmental Engineering laboratory at the University of Manitoba to calculate the viscosity of the leachate. The viscosity values were compared with water at different temperatures, as shown in Figure 3.1.

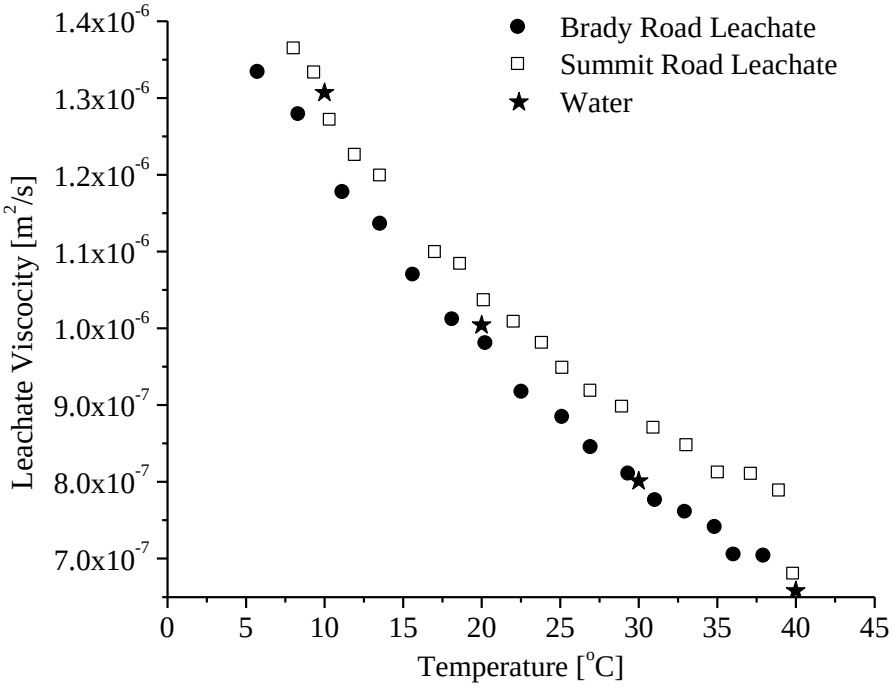

Figure 3.1. Viscosity of leachate from Brady Road Landfill, Summit Road landfill and water at different temperatures.

From Figure 3.1, it can be observed that leachate collected from Brady Road Landfill is very similar in viscosity to water at temperatures over 20˚C. On the other hand, leachate collected from Summit Road Landfill had generally higher viscosity than water and Brady Road leachate at temperatures over 20˚C and was similar to water at temperatures

below 20˚C. An estimated increase in leachate temperature during bioreactor landfill operation is expected, especially during winter months, due to the heat provided by the pump and the high temperatures reported from bioreactor landfills around the world (30 to 60˚C by Yazdani 2002, Reinhart *et al*. 2002 and Hudgins and Harper 1999). If the leachate used (impounded) in the recirculation system is similar to that from Summit Road landfill, the Reynolds number will be smaller than values calculated assuming the viscosity is equal to that of water at the same temperature. This pilot study used leachate collected from leachate wells at Brady Road Landfill, thus viscosity values are assumed to be similar to water.

As the pipe cases selected (Table 3.1) were run in duplicate, a total of sixteen HDPE pipes (SDR 11) of approximately 2 m length were analyzed with the conditions mentioned in Table 3.1. Pipe diameters, length and weight are shown in Appendix A.

Table 3.1**.** Full-scale pipe testing matrix

Pipe Test #	**Internal Diameter [cm]**	**Flow rate [L/s]**	**Reynolds Number [-]**	**Shear Stress [N/m^2]**
1	4.8	1.72	56,966	1.1
2	4.8	1.53	50,674	0.87
3	4.8	0.96	31,795	0.34
4	9.2	1.62	27,994	0.07
5	9.2	1.4	24,192	0.05
6	9.2	0.84	14,515	0.02
7	13.4	0.31	3,678	0.0006
8	13.4	0.16	1,898	0.0002

Note: For Reynolds number and shear stress calculation purposes it was assumed the kinematic viscosity of the leachate at 30˚C of 8.01×10^{-7} m^2/s and the initial friction factor of 0.02 (see Appendix J)

The research station is 2.4 m x 4.8 m with three shelves holding sixteen laboratory pipes of 4.8, 9.2 and 13.4 cm internal diameter, each 2 m long, as well as three tanks to (a) feed the pipes with leachate, (b) discharge the leachate from the pipes (both inside) and (c) an outside leachate holding tank (see Figure 3.2). The outside buried tank had a capacity of 3.5 m^3 and it was located approximately 2 m from the station to hold fresh leachate from the landfill well, and it was replenished biweekly. Inside the buried tank was two submersible pumps which were placed to supply leachate to the inside laboratory pipes and a leachate heater was installed to maintain a constant leachate temperature during the winter. A leachate discharge pipe of 15 cm external diameter was connected from the research station to the tank, allowing leachate to be collected after passing through the research station. Two 5 cm external diameter leachate feeding pipes were connected from the outside tank to the station to feed the eight submersible and eight non-submersible pumps feeding the (16 in total) laboratory pipes within the shelves (see Appendix C for pictures).

Within each of the sixteen inside laboratory pipes, five pipes rings or coupons of 2.5 cm width were placed at the end of each of the pipes to account for clog material development over time. Each of the eighty pipe rings was weighted and its diameter was measured to quantify the rate of clog formation at different periods of time throughout this research (see Appendix A). The leachate research station was well insulated and contained 2 heaters to maintain a minimum temperature inside of the shed of 20˚C all year. The temperature inside of the leachate research station averaged 26.4°C (± 4.7°C) during this study. Temperature inside of the research station was measured using a 76

MM IMM Fisher© thermometer. Pipe flow rates were measured using a hand held Doppler DYNASONICS™ ultrasonic flow meter at the 2.5 cm diameter return pipes. Leachate sample ports were placed to sample leachate concentration between upstream and downstream of the laboratory testing pipes. From the same leachate sample ports, pressure losses were measured with a calibrated pressure transducer.

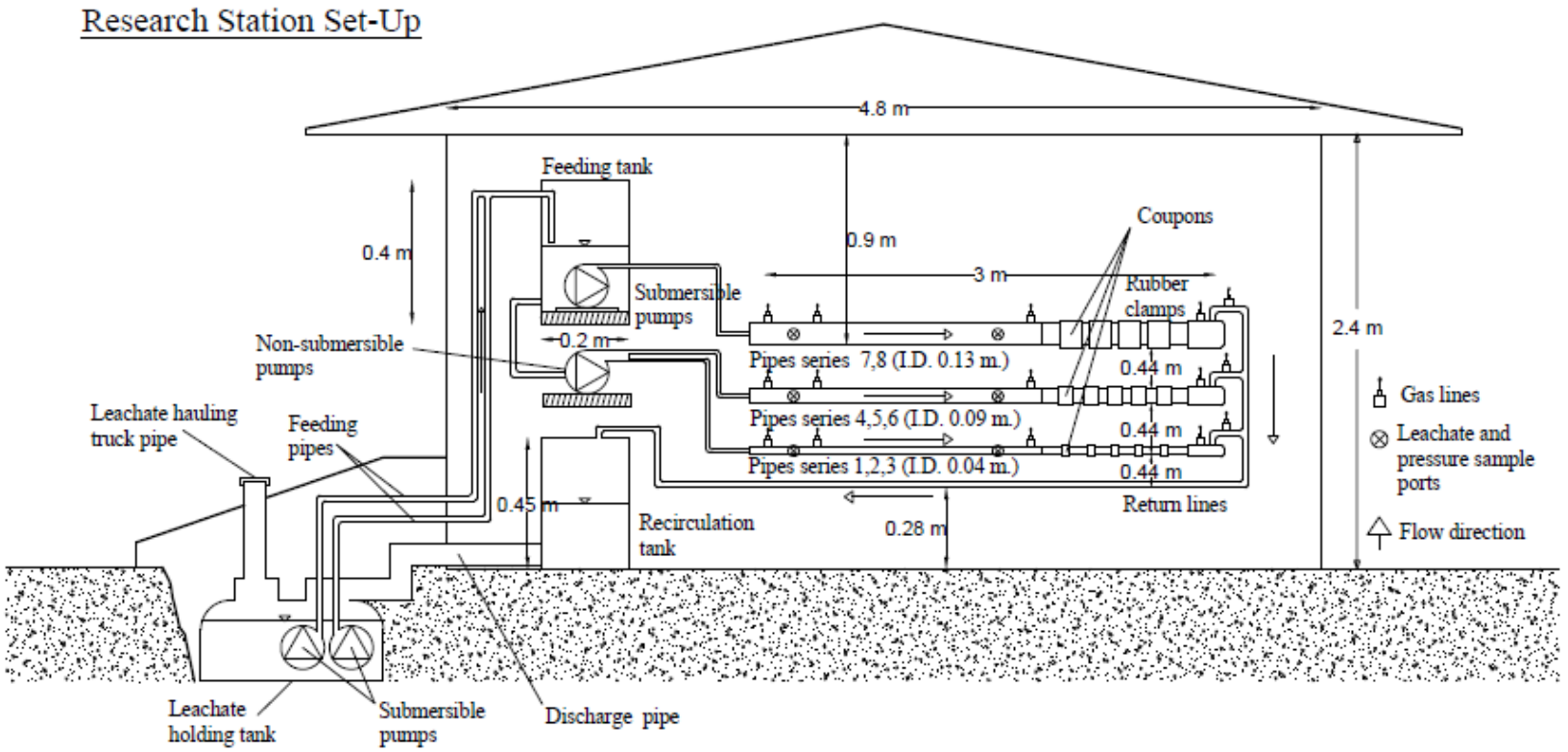

Figure 3.2. Schematic representation of the leachate research station housed at Brady Road Municipal Landfill, Winnipeg, Canada (profile view - not to scale).

3.3.1 Pilot study operation

The initial pump injection schedule selected for all the pipe series shown in Table 3.1 was 6 hrs ON and 66 hrs OFF (running twice a week – on Sunday all the pumps were OFF). Due to the electrical capacity of the research station and volume of leachate available, the appropriate pumps for the pipe series shown in Table 3.1 were operated as follows

- For pipe series 1 and 4 (cycle 1), the appropriate pumps were operated on Monday and Thursday
- For pipe series 2 and 6 (cycle 2), the appropriate pumps were operated on Tuesday and Friday
- For pipe series 3, 5, 7 and 8 (cycle 3), the appropriate pumps were operated Wednesday and Saturday

The outside submersible pumps were turned ON every time the pipe series were tested. Some changes in the pump schedules mentioned above occurred during the study due to the malfunction and excessive clogging accumulated within some pumps (not delivering the selected flow rate), so the pump schedule was re-arranged, while the pumps were fixed, to accommodate the selected time of stagnancy. In addition, due to the availability of the leachate hauling truck transporting fresh leachate to the field study and the landfill operation hours in winter and summer, the pump injection schedule was variable (Appendix B). However, the adopted leachate stagnancy time within the pipe series (66 hrs) was maintained constant during this study, as shown in Appendix B.

At the start of the testing cycle, leachate was drained from the system and then leachate from the landfill well was placed in the 3.5 m^3 exterior leachate holding tank. This new

fresh leachate was analyzed each time it was drained to the external holding tank. This sample was identified as "**fresh leachate**" and the leachate collected from the pipes after being pumped was denominated t = 0, as explained later. The main submersible pumps in the exterior tank were turned on, which pumped leachate into the interior feeding tank. The leachate overflowed into the interior recirculation tank, and then proceeded back to the exterior tank, establishing a recirculating loop. The appropriate interior pumps (submersible or non-submersible) were started (See Figure 3.1), which pumped leachate from the interior feeding tank through the appropriate testing pipes, and also through the test coupons, then through the return lines to the recirculation tank, thus establishing a second loop.

After leachate was pumped through the appropriate testing pipes (e.g. first cycle), all the pumps were turned off and leachate was maintained stagnant within these testing pipes. A sample of leachate was collected from each testing pipe at the end of Day 1 (afternoon), defined as leachate sample at t = 0 hr, and brought to the Environmental Engineering laboratory for analysis. On the morning of day 2, after 18 hours of stagnancy, leachate was collected from each pipe of cycle one (t = 18 hr) and brought to the Environmental Engineering laboratory for analysis. Cycle 2 was then started with the appropriate pumps. At the end of day 2, all pumps were tuned off. On the morning of day 3 of the testing cycle (42 hours of stagnancy for cycle 1), leachate was collected from each pipe of cycle one and brought to the Environmental Engineering laboratory for analysis. At the same time, cycle 3 was started. At the end of day 3, all pumps were turned off. On day 4, the

pipes of cycle one with the appropriate pumps were started again without testing. The testing cycle described above was followed for the pipes of cycle two and three.

Each testing cycle lasted 42 hours. The goal was to replace the pumped leachate with fresh leachate three times a month having each pipe cycle being tested at least once a month. While leachate was not being tested, the pipe cycle conveyed leachate twice a week to maintain the 6 hour on and 66 hour off operation.

3.3.2 Leachate analysis

With consideration given to the findings of biological, chemical, and physical processes that contribute to clog development from previous studies (see Rowe *et al.* 2004), leachate was collected from the sample ports once a month along the length of the pipes and tested for the following characteristics: chemical oxygen demand (COD), dissolved calcium concentration (Ca^{+2}), pH, alkalinity, total suspended solids (TSS), volatile suspended solids (VSS), inert suspended solids (ISS), volatile fatty acids (VFA) and temperature. These concentrations were measured for each batch of leachate and set of pipes. To obtain a representative sample of leachate from the pipes for the tests mentioned above, about 100 to 150 mL (2.8 to 4.1%, 0.6 to 1% and 0.3 to 0.4% of total pipe volume from pipes series 1 to 3, 4 to 6 and 7 to 8, respectively) of leachate was removed from each sample port.

COD was measured using a HACH™ COD reactor with HACH™ COD reagents. The reagents were added to the leachate and heated at 150°C for 2 hours in the reactor. The

sample was then analyzed with a HACH™ DR/2500 Spectrophotometer. Ca^{2+} concentration was obtained using a Universal Digital Titrator HACH™ Model 16900 with the proper reagents. Alkalinity was obtained using the Titration method (2320 B, Standard Methods 1992). The pH was measured using an ORION® portable pH/ORP/Temperature meter WP HH (Thermo Scientific) that is equipped with the appropriate electrical probe for each parameter. Total suspended solids (TSS) and inert suspended solids (ISS) were tested using a gravimetric measurement of the residue retained on a 0.45 μm glass fiber filter dried at 105°C and 550°C, respectively (2540 Solids D and E, Standard Methods 1992). Volatile suspended solids (VSS) concentrations were calculated as the difference between TSS and ISS concentrations.

In order to verify the consumption of VFA under stagnant conditions from each pipe series, three leachate samples were collected and analyzed for VFA at times 0, 24 and 48 hours of stagnancy. VFA concentrations in the samples were analyzed by a Varian CP 3800 gas chromatography system (GC) equipped with a flame ionization detector, CP-8400 autosampler and WCOT fused silica 25 m x 0.32 mm I.D. coating FFAP-CB capillary column. The optimized GC operating conditions were: 270°C in the injector and 300°C in the detector. Temperature in the oven was initially set at 70°C and then ramped up to 140°C at the rate of 10°C/min., from 140°C to 200°C at the rate of 25°C/min, and then from 200°C to 240°C at the rate of 30°C/min. The column was maintained at 240°C for 3.97 minutes to let the residual contaminates flush out. The total running time was 15 minutes. The gas flow rates were: helium in the column at 6.5 mL/min, hydrogen at 30 mL/min, and air at 300 mL/min. Crotonic acid was added as internal standard to improve

the analytical reproducibility and accuracy. Under the above conditions, excellent resolution and quantitative accuracy were obtained for all VFA's. Following "Standard Methods for the Examination of Water & Wastewater" (APHA, 21st Edition, 2005), samples were acidified to pH 2 using 85% O-phosphoric acid and then filtered by a 0.22 µm syringe filter prior to injection. During the last 5 months of this study, dissolved CO_2 values were sampled from the leachate collected from the landfill well and pipes. Serum bottles with a working volume of 165 mL were used, with 100 mL of sampled leachate poured into them and then sealed with butyl-rubber stoppers. After 10 seconds of gentle hand-agitation, the sample was rested for approximately one hour at room temperature to achieve equilibrium between the CO_2 dissolved-gas phases. Afterwards, CO_2 gas concentration was measured using GC, as well as leachate pH and temperature. Dissolved CO_2 concentrations were calculated using Henry's Law.

3.3.3 Clogging analysis

Pipe rings were removed at different time intervals to characterize the water and total solids content of the clog material. For the total solids content, biological and inorganic content was also sampled to characterize potential changes within leachate transmission pipes over time. From the pipe ring clog material, bulk density, non-volatile solids density and volatile density were obtained. Bulk density was obtained by measuring the weight and volume displacement of the clog material in deaerated water at constant laboratory temperature. Non-volatile and volatile clog densities were measured using a modified version of ASTM (D854) to calculate the specific gravity of soil solids. Total solids (TS) and fixed solids (FS) were tested using a gravimetric measurement of the

residue retained on a crucible dried at 105°C and 550°C, respectively (2540 Solids B and E, Standard Methods 1992). Volatile Solids (VS) were calculated as the difference between TS and FS concentrations. Water Content (WC) and Total Solids Content (TS) were calculated as the weight difference between the sample of clogging before and after drying at 105°C. Calcium (Ca^{2+}), Sodium (Na^{+}), Magnesium (Mg^{2+}) and Iron (Fe^{2+}) content within the clogging were analyzed using a Varian ICP, Model VISTA- MPX, CCD with simultaneous ICP-OES.

Mineralogy was determined by collecting an X-Ray Diffraction dataset (XRD) using Cu radiation collected from 4 to 60 degrees 2-theta, using a step width of 0.05 degrees and a dwell time of 1 sec/step, on a Philips PW1710 automated powder diffractometer. The diffractometer was configured with 1-degree divergence and anti-scatter slits and a 0.2 mm receiving slit and a curved graphite crystal monochromator. The observed data was checked against the Powder Diffraction File (PDF) database from the International Centre for Diffraction Data (ICDD) for any matching phases using the search-match capabilities of Material Data Inc.'s Jade 7+ XRD-pattern processing software.

Clog material was also analyzed with CAMBRIDGE Stereoscan 120 Scanning Electron Microscope (SEM), equipped with scanning control with EDAX Genesis 4000 software to obtain the X-ray Energy Dispersive Spectrum (EDS). The SEM and EDS analysis provided a qualitative elemental composition of the clog material. For the SEM and EDS analysis, clog samples were covered with a gold-palladium thin film deposited by an Edwards sputtering system Model S150B. The SEM was operated at 30 kV accelerating

voltage and the secondary emission detector was used for imaging the samples. The EDS spectrums were captured using a Kevex detector and an electron beam of less than 2 microns in size.

3.3.4 Pressure readings

The development of clog material on the pipe walls caused an increase in energy loss within the pipes, which was measured using pressure transducers. Pressure was measured using a Validyne DP45 Low Range Transducer and a Validyne CD280 Multi-Channel Carrier Demodulator. The voltage signal from the carrier demodulator was acquired using a National Instruments data acquisition system and Labview software. The transducer contains an internal diaphragm which deflects when a pressure difference is applied. This deflection results in an output voltage which can be converted to pressure difference after calibration. Thinner, more sensitive diaphragms can be used to measure low pressures, while more robust diaphragms are used for higher pressures. A total of two transducers with different diaphragms were selected for measuring pressure drop in the pipes. For the larger diameter and lower flow rate pipes, a number 16 diaphragm was used which accepts pressure differences of up to 3.5 cm H_2O. For the smaller diameter and higher flow rate pipes, a number 22 diaphragm was used which accepts pressure differences of up to 14 cm H_2O.

In addition to measuring pressure drop within the pipes, the pressure at the upstream sample port of each pipe was measured using a number 34 diaphragm which accepts pressure differences of up to 225 cm H_2O. This transducer had one side open to atmospheric pressure, and the other connected to the inlet pressure valve. Since the

pressure transducer was placed at a different elevation than the pipes, the resulting reading was the sum of the elevation head as well as the pressure head at this point in the pipe. The elevation of each inlet sample port was measured and subtracted from the appropriate pressure reading. All reported inlet pressures were therefore pressure head with respect to the leachate sample port elevation. While measuring pressure within the pipes, the transducers were connected to the leachate pipes at the sample ports using flexible tubing. A shut-off valve was installed on both hoses going to the sample ports from the transducers and a bypass valve going from one side of the transducer to the other to equalize the pressure on both sides of the transducer, as shown in Figure 3.3 (See Appendix C for pictures).

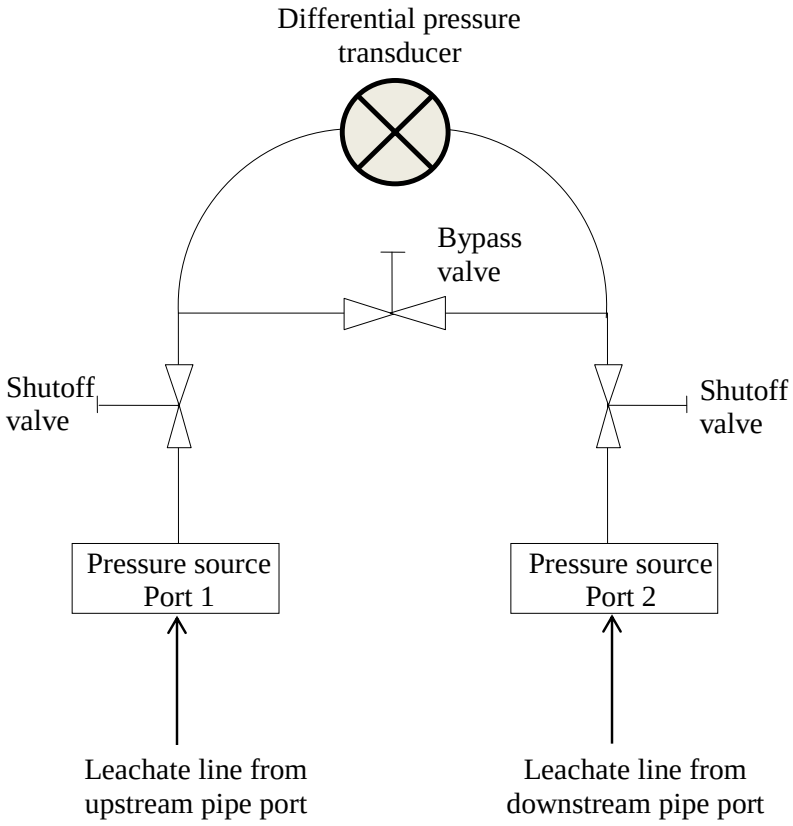

Figure 3.3. Typical valve arrangement for the Validyne transducers used (adapted from http://www.validyne.com (See picture in Appendix C).

This pressure equalization was important to minimize the risk of over pressurizing the diaphragm when applying and removing the flexible hoses from the sample ports. Over pressurizing the diaphragm can cause a zero shift and a need to recalibrate the transducer. Before taking any readings from the pipes it was necessary to follow a calibration procedure to relate the voltage output from each transducer to the measured pressure difference. To do this, each side of the pressure transducer was connected to different acrylic cylinders where the water level was known and adjustable. Starting with the same water level, and a pressure difference of zero, a reading was taken. Water was then added to the cylinder connected to the inlet side of the transducer and the water level and voltage reading were recorded. This was continued until the maximum pressure difference of the diaphragm was reached. With this, a straight line relation was obtained between pressure difference on the diaphragm and the voltage output from the transducer. These steps were repeated for the three transducers as they all had a different pressure-voltage relationship.

3.4 RESULTS AND DISCUSSION

3.4.1 Leachate composition variation within the pipes

3.4.1.1 Leachate collected from the Brady Road landfill wells

Leachate from Brady Road Municipal Landfill was collected 33 times during this study. COD and Ca^{2+} concentrations changed dramatically during the summer months (end of June to September), showing a stronger leachate (higher COD and Ca^{2+}) than the rest of the year (See Figure 3.4). The average concentrations of COD and Ca^{2+} found in the leachate collected from October 8 of 2009 to June 9, 2010 were 1,527 mg/L (standard deviation of 479 mg/L) and 212 mg/L (standard deviation of 50 mg/L). The COD and Ca^{2+} average values of leachate collected from June 16 to September 21 of 2010 were 9,463 (standard deviation of 3,720 mg/L) and 509.64 (standard deviation of 146 mg/L). These higher variations in leachate concentrations (see Figure 3.4) during the summer months could be the result of higher temperatures and the upper and fresher layers of waste being degraded more quickly in summer than winter. Based on the COD and Ca^{2+} values obtained from leachate sampled from the landfill wells during this study, the accuracy of using average values over the entire year was quite low. The following leachate analyses from the pipe series tested were divided into two main scenarios: Fall-Winter-Spring 2009-2010 and Summer 2010, as shown in Figure 3.4.

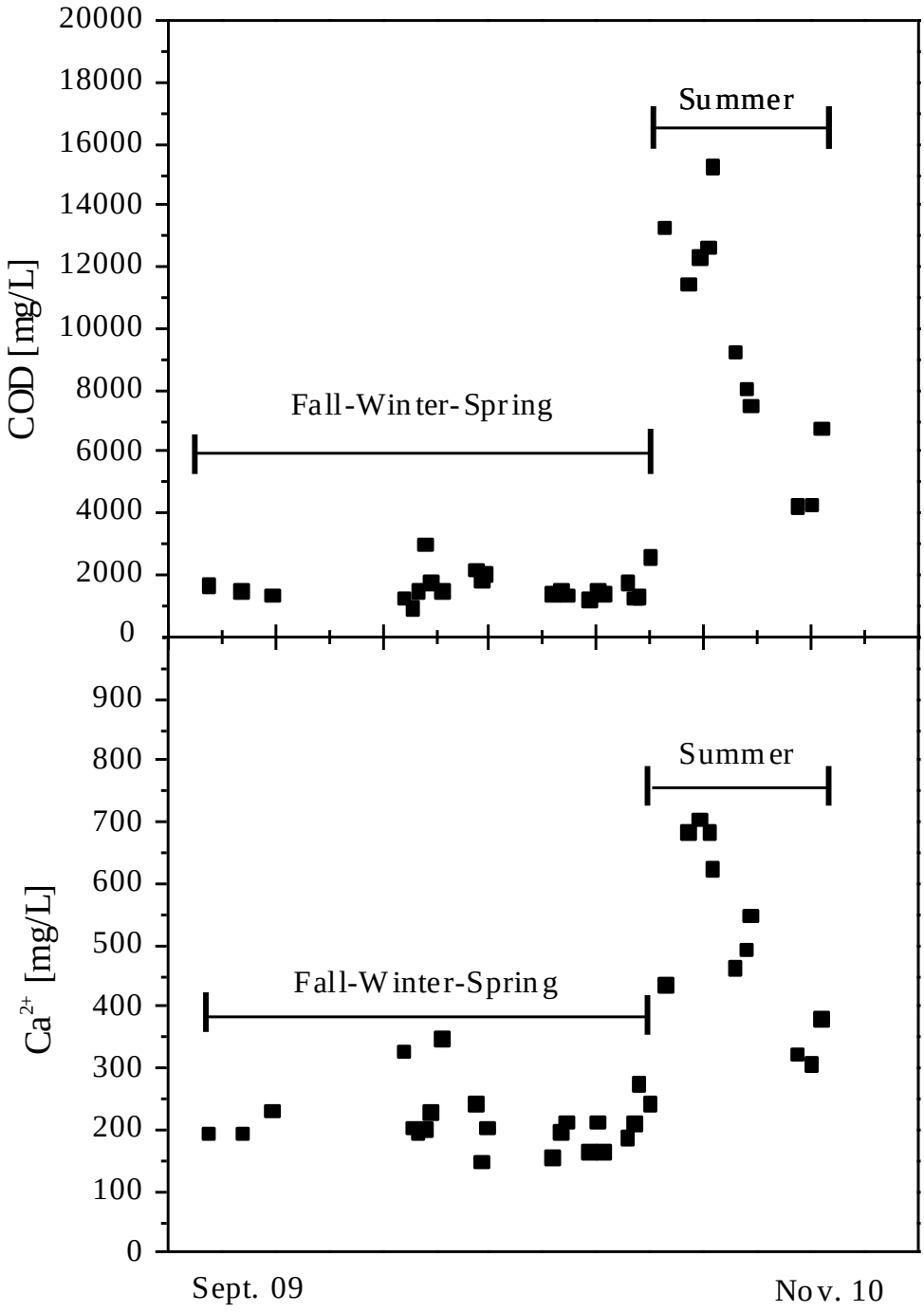

Figure 3.4. COD [mg/L] and Ca^{2+} [mg/L] variation of leachate collected during this pilot study from September 2009 to September 2010.

For the following graphs, fresh leachate represents the composition of leachate before pumping (from landfill well), t = 0 represents the composition of leachate right after pumping or when the pumps were turned off, and t = 18 and 42 hours represent the composition of leachate stagnant at that time. So, the differences between fresh leachate and t = 0 are produced during pumping and t = 0, 18 and 42 represented the changes during stagnation.

3.4.1.2 Leachate pH values during pumping and stagnation

Leachate collected from the Brady Road landfill varied in pH throughout the year, ranging from 6.97 to 7.96 during the summer of 2010 and 6.88 to 7.57 for fall, winter and spring of 2009-2010 (see data in Appendix D). Figure 3.5 (a) and (b) shows the average pH values, for both seasons, obtained during this study.

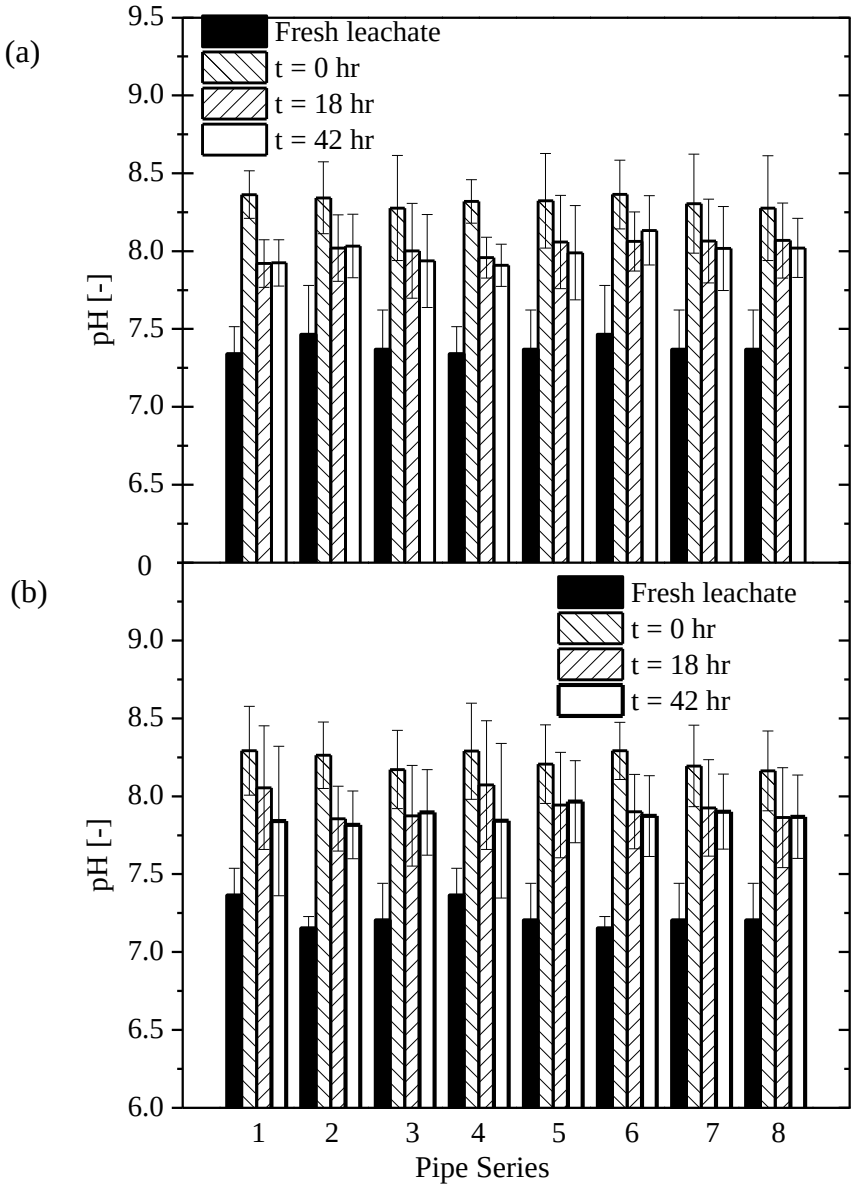

Figure 3.5. Average pH values for all testing cycles for the pipe series during (a) Sept. 2009 – June 2010 and (b) June – Sept. 2010.

The pH values increased approximately one pH unit after the leachate was pumped through the pipes for both seasons, as shown in Figure 3.5 (a) and (b). During stagnation, especially the first 18 hours, average pH values decreased for all the pipe series by an average of 0.3 pH units with a standard deviation of 0.07. The fact that average pH values

increase and decrease during pumping and stagnancy for all the pipe series raised the question whether (1) microbiological activity from suspended microorganisms and biofilm produced and consumed COD or organic acids and/or (2) physically-driven processes where CO_2 evolved from the leachate during pumping re-equilibrated with the stagnant leachate in the pipe. Since pH increased during pumping, Ca^{2+} removed as $CaCO_3$ also impacted the leachate pH by decreasing the carbonate buffering capacity of the leachate.

In order to determine whether microbiological (COD and VFA) or physical processes (CO_2 outgassing and re-equilibration) affected the pH values while leachate was pumped and stagnant within the pipes, the following results were analyzed further.

3.4.1.3 Leachate COD and VFA values during pumping and stagnation

Figure 3.6 (a) and (b) show average COD values for all pipe testing cycles performed during Sept. 2009 – June 2010 and June - September of 2010, including average values of fresh leachate drained into the outside tank and during stagnation at t = 0 hour, t = 18 hours and t = 42 hours. Figure 3.6 (a) and (b) show that different average influent COD values (June 2010 – September 2010) did affect the removal of COD within the pipe series during pumping and stagnancy. Significant COD removal values occurred during the first 18 hours of stagnancy for the pipes series tested during June – September of 2010, attaining maximum COD removal values of 5.3, 4.6 and 4.9 g/L for pipe series 1 to 3, pipe series 4 to 6 and pipe series 7 and 8, respectively (see Appendix E).

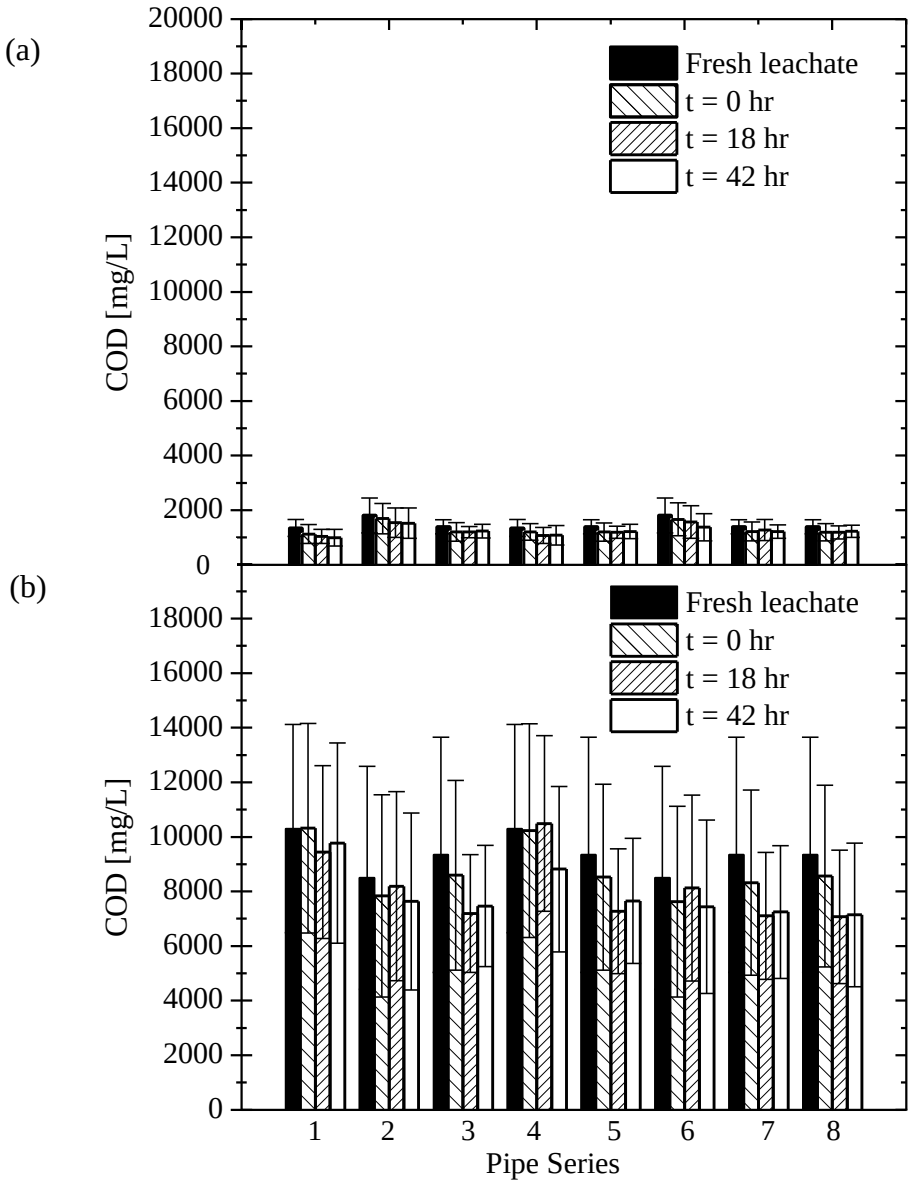

Figure 3.6. Average COD values (mg/L) for all testing cycles during (a) October 2009-June 2010 and (b) June – September of 2010.

These results show that stagnation may have impacted the leachate COD removal within the pipes by settling particles and promoting the growth and activity of suspended and attached microorganisms, thus affecting clog development. From the average COD results obtained (Figure 3.6 (a) and (b)) it can be observed that less than 14% of the

average influent COD was removed during pumping and less than 19% of the average COD was removed during stagnation for both seasons and all the pipe series. This indicates that COD removal was not the main mechanism affecting clogging within the pipes tested during pumping and stagnation. Since stagnant leachate within a pipe can promote clogging, draining the leachate after pumping may help to minimize clog formation within the pipelines. This could be incorporated into the initial leachate recirculation design by sloping the injection pipes towards the sump or tank.

In order to verify the importance of biological fermentation within the tested pipes, VFA leachate concentrations were measured during one testing cycle after a significant amount of biofilm (approx. 1 year of operation) had accumulated within the pipe series 1, 2, 4 and 6 (pipes a and b are duplicated pipes). It should be stated clearly that the disadvantage of using real leachate is the natural variability of its characteristics, so this short study represented the VFA removal ability of the testing pipes for that specific VFA concentration. These measurements were performed on September 7 and 11, 2010 and the results are shown in Figure 3.7 (a), (b) and (c). It can be observed that the leachate was higher in acetate than propionate and butyrate. For all the pipes and conditions tested, negligible amounts of VFA were removed during pumping, with maximum removal values of acetate, propionate and butyrate of 4%, 11% and 15% respectively (see Appendix E).

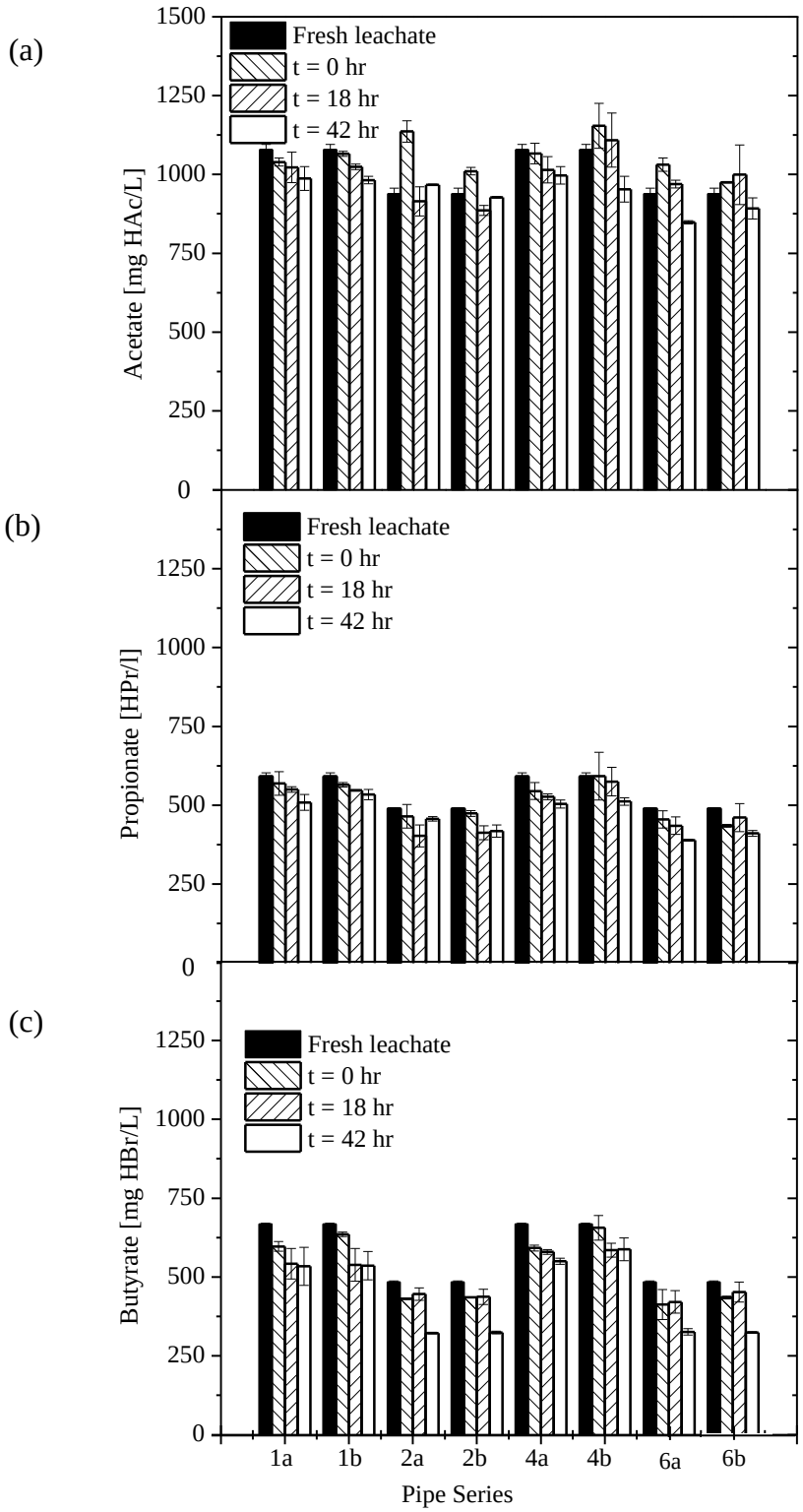

Figure 3.7. Variation in (a) acetate, (b) propionate and (c) butyrate concentrations within the pipe series 1, 2, 4 and 6 during one testing cycle.

During the 42 hours of stagnation, higher acetate removal values (52 to 201 mg HAc/L), followed by butyrate (42 to 112 mg HBu/L) and lastly propionate (32 to 61 mg HPr/L) were attained within the pipes. These removal values represented 5 to 18%, 7 to 26% and 1 to 15% of the influent acetate, butyrate and propionate leachate values left after pumping (see Appendix E). More laboratory studies under controlled conditions are needed to understand the impact of the VFA variability within the leachate and its consumption within leachate injection pipes. The relatively small amount of VFA removed can be explained by the high leachate pH values achieved after pumping (almost 1 pH unit) and the inability of the biofilm within the pipe series and the suspended bacteria within the leachate to remove VFA's at that pH. Finally, COD and VFA removal values (Figures 3.6 and 3.7) versus pH values obtained (Figure 3.5) provided a strong indication that clogging was mainly not a microbial driven process within the testing pipes.

3.4.1.4 Leachate CO_2 values during pumping and stagnation

As stated in section 2.7.2.1, dissolved CO_2 is affected by the turbulence intensity in the medium. Since CO_2 was dissolved to saturation in leachate collected from the wells, it was expected to be outgassed while the pumps were operated in the research station. To verify the changes in dissolved CO_2 (if any) while leachate was pumped and stagnant, leachate from the landfill wells and pipes was sampled for dissolved CO_2, from May – Sept 2010. Because this CO_2 sampling was mostly done during summer of 2010, no significant changes in the dissolved CO_2 concentrations (184 ±25 mg/L) of the fresh leachate collected from the landfill wells were observed, as shown in Figure 3.8.

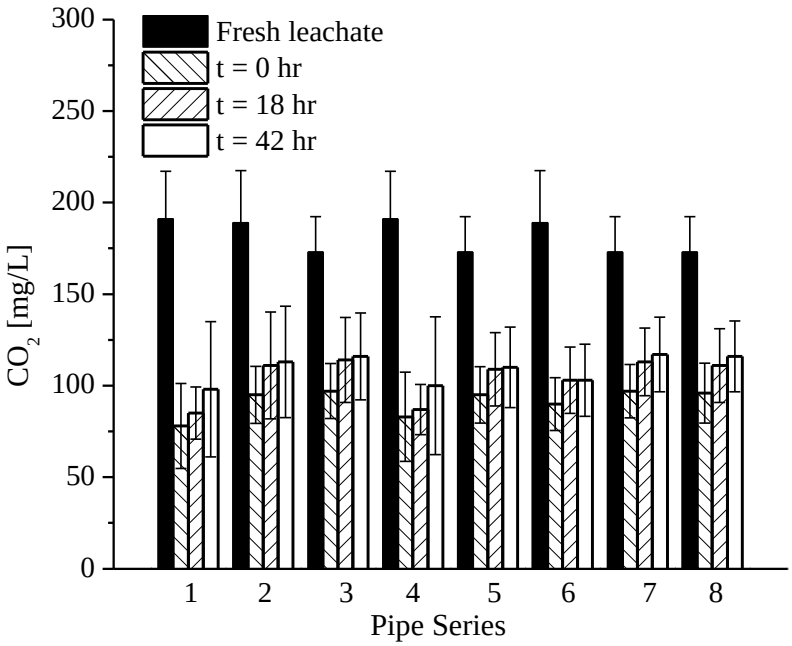

Figure 3.8. Dissolved CO_2 average concentrations (mg/L) for all testing cycles during this study.

Figure 3.8 shows that the removal of dissolved CO_2 was between 43 to 60% after pumping, with an average removal of approximately 50%. This suggests that CO_2 degasification was the main mechanism of pH increase (see Figure 3.4a and b) during pumping, which is in agreement with the observations of Lozecznik and VanGulck (2009). In contrast, after the first 18 hours of stagnation, higher average dissolved CO_2 values (between 4 to 18%) were sampled for all the pipe series. The dissolved CO_2 may have increased due to the re-equilibration of $CO_{2(gas)}$ higher in concentration within the pipe, impacting the leachate chemistry and lowering the pH, as shown in Figure 3.5a and b.

Since pH and $CO_{2(aq)}$ are known, bicarbonate (HCO_3^-) and carbonate (CO_3^{2-}) concentrations can be calculated using the Henderson-Hasselbach equation. For example

leachate collected from the landfill well averaged approximately 200 mg/L of $CO_{2(aq)}$ and pH 7.25 (see Figures 3.4.1 and 3.4.8) and assuming standard conditions, most of the carbonate will be in the form of bicarbonate (approximately 1,235 mg HCO_3^-/L) rather than carbonate (approximately 0.6 mg CO_3^{2-}/L). Because pumping increases the leachate pH (at approximately 8.2), and then $CO_{2(aq)}$ increases after 42 hours of stagnation (100 mg/L) and pH stays high at about 8, see Figures 3.4.1 and 3.4.8, CO_3^{2-} concentration will increase to approximately 30 mg/L. This increase in carbonate will be available for the removal of metals such as Ca^{2+} or Mg^{2+} as carbonate mineral precipitants.

In addition of the turbulence effects, changes in temperature also affect the solubility of CO_2 within the leachate. Temperature measurements were performed during pumping and stagnation for this study, and the average results are shown in Figure 3.9. From Figure 3.9, it can be observed that there was an average temperature increase of approximately 5˚C degrees during pumping and 9 ˚C after 18 hours of stagnation for all the pipe series. This shift in temperature was mainly produced by the pumping activity and the temperature at which the research station was set to simulate the bioreactor landfill internal temperature conditions (averaged 26.4°C with a standard deviation of 4.7°C during the entire study). This may indicate that temperature increase could have a significant effect on the CO_2 outgassing measured during this study, and potentially have a larger impact during the winter.

The relationship between turbulence, temperature and CO_2 outgassing could not be isolated as the pipes were all discharging leachate to the outside holding tank and then

pumped back to the research station by the outside submersible pumps (Figure 3.1). These submersible pumps conveyed substantially higher flow rates (approximately 5 L/s each pump) than the pumps inside of the station, producing higher turbulence than any of the inside pumps during each recirculating loop. Thus, controlled laboratory conditions are needed to isolate temperature and turbulence impact on the CO_2 kinetics within the pipes.

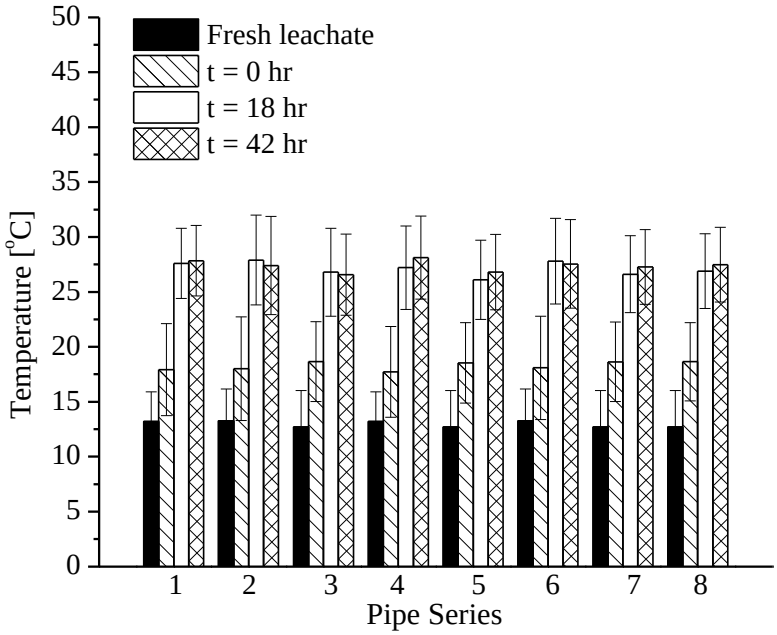

Figure 3.9. Average temperature values (˚C) for all testing cycles during this study.

During the coldest months of winter (January, February and part of March) an approximated 10 cm ice layer developed within the landfill wells. This was removed in order to gain access to the leachate by force using an industrial hose with a metal connector at the end. Even though the leachate never froze within the landfill wells, lower temperatures were measured close to the well surface (< 7˚C). For this reason, bioreactor

landfills in northern climates may face a significant challenge due to clog formation inside of the injection pipe or trench enhanced by the difference of leachate temperature between outside (< 7˚C) and inside of the landfill (> 25˚C) and the expected increase in CO_2 outgassing inside of the pipes regardless of turbulence intensity.

Temperature has an important effect on the biological activity of suspended microorganisms and the solubility of calcite ($CaCO_3$). Fleming and Rowe (2004) conducted several batch tests investigating real and synthetic leachate degradation at different temperatures. The findings from this study suggested that the precipitation of $CaCO_3$ was mainly related to the increase in pH produced by the removal of COD (organic acids) over time. When using real leachate, however, no explanations were provided about Ca^{2+} being removed during the first days while no removal of COD was detected until after 30 days. In addition, both leachate studies showed that batch tests at lower temperature (10˚C) showed higher dissolved Ca^{2+} than higher temperature leachate over time (22 and 28˚C). Abthahi *et al*. (1996) conducted a comparison between experimental data and model calculations about calcium carbonate ($CaCO_3$) precipitation and pH variations in oil field waters, using a synthetic solution saturated with CO_3^{2-}, Ca^{2+} and $CO_{2(g)}$ at different temperatures and CO_2 partial pressures. The results showed that at the same Ca^{2+} concentrations, higher CO_2 partial pressure and increase in temperature decreased the pH of the solution. This was explained as the lower solubility of the $CaCO_3$ at higher temperature and its precipitation. Domenico and Shwartz (1990) explained that one possible mechanism to enhanced calcite dissolution is the inverse relationship between calcite solubility and temperature. From above, it can be deduced that an

increase in leachate temperature will have a dual effect on the physical/chemical mechanisms of clogging within leachate injection pipes. It will enhance the rate of CO_2 outgassing and reduce the solubility of $CaCO_3$ saturated within the leachate, increasing clogging. Past research of clogging in leachate collection and injection systems has linked the increase of leachate pH with the removal of dissolved Ca^{2+} (Brune et al. 1991, Fleming et al. 1999, Maliva et al. 2000, Manning 2000, Lozecznik and VanGulck 2009).

3.4.1.5 Leachate Ca^{2+} values during pumping and stagnation

As previously mentioned, field studies that examined clog material from leachate transmission pipes have reported calcium and carbonate as the main inorganic clog constituents. As high leachate pH values were measured in this study after each pumping operation (Figures 3.5), removal of dissolved Ca^{2+} was expected to occur. Figure 3.10 (a) and (b) show the average Ca^{2+} values for all tests performed during Sept. 2009 – June 2010 and June – September 2010. Average Ca^{2+} removal values of approximately 77 mg/L (± 24 mg/L) and 319 mg/L (±11 mg/L) were obtained while pumping during Sept. 2009 – June 2010 and June – September 2010. These results show that high differences in average initial Ca^{2+} values between both seasons affected the removal of Ca^{2+}within the pipe series during pumping. Maximum Ca^{2+} removal values of approximately 68% and 77% were attained while pumping, during Sept. 2009 – June 2010 and June – September 2010. The highest removal values were achieved during longer pumping periods (3 to 6 hours) than shorter periods of pumping (see Appendix E), indicating that pump operation time influences leachate CO_2 degasification, thus leachate pH values. Ca^{2+} removed during pumping precipitated out within the tanks and pipes as calcium carbonate minerals

(see Section 3.3.2.9). These results are consistent with the observations made by Lozecznik and VanGulck (2009), showing a relationship between CO_2 degasification, pH increment and dissolved Ca^{2+} removal values and their impact on inorganic clogging deposition within the testing pipes.

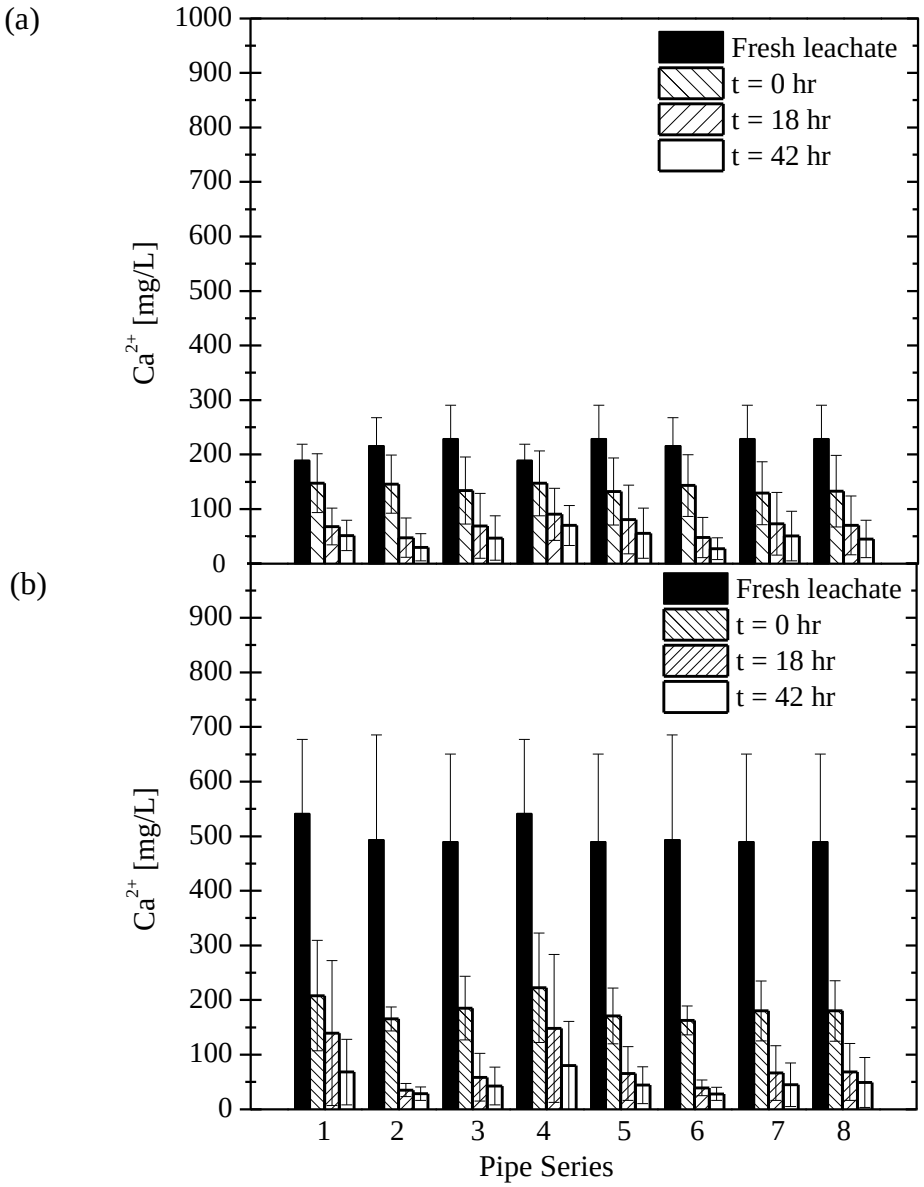

Figure 3.10. Average dissolved Ca^{2+} values (mg/L) for all testing cycles for the pipe series during (a) Fall-Winter 2009-2010 and (b) Summer 2010.

During the 42 hours of stagnation, average Ca^{2+} removal values of approximately 92 mg/L (±16 mg/L) and 136 mg/L (± 6 mg/L) were obtained within the pipe series for Fall-Winter of 2009-2010 and Summer of 2010 scenarios, respectively. This shows that while leachate pH was raised during pumping, Ca^{2+} removal occurred during both pumping and stagnation. These results show that stagnation also promotes the removal of Ca^{2+}, so

minimizing the pumping time and stagnation will minimize the inorganic clogging potential. It also showed that the rate of Ca^{2+} removal was not dependent on the Re assessed with the testing pipes. This is explained as the main turbulent effect produced by the outside feeding pipes (approximately Re = 165,000) outcompeting the highest Re adopted within the testing pipes (Re_{max} = 57,000), decreasing the overall rate of Ca^{2+} removal within the leachate. Further studies are needed to isolate the effect of Re on Ca^{2+} removal within leachate injection pipes. Finally, it also showed that as the dissolved Ca^{2+} concentrations were similarly reduced between the pipe series 1 to 8 (pipe diameters of 0.04 m, 0.09m and 0.13m) after 42 hours of stagnation, the mass load of Ca^{2+} deposited within the pipes was much larger for the largest pipe diameter (0.13 m).

As dissolved Ca^{2+} was being removed as $CaCO_3$ (see Section 3.3.2.9), a decrease in total alkalinity was expected as well. Average alkalinity values from the pipe series show an average removal rate of 9% after pumping and an average removal of 4.9% during 48 hours of stagnancy for the entire study (Appendix E).

3.4.1.6 Leachate suspend solids values (TSS, VSS and ISS) during pumping and stagnation

Changes in influent and effluent TSS, ISS and VSS within the pipes may provide an indication of the retention or production of suspended solids within the pipe. Retention of suspended particles in the pipe may result in accumulation of clog material within the testing pipe. Suspended particles may be introduced by the detachment of clog material and generated as organic (biofilm or suspended microbial activity) or inorganic ($CaCO_3$

formation) particles from the tanks, hoses and pipes into the leachate. VSS are the volatile fraction (partially comprised of microorganism and organic matter) and ISS are the inorganic fraction (partially comprised of mineral precipitate and soil particles) of TSS. Under turbulent flow conditions, suspended particles entering the pipe can settle out and accumulate on the inner pipe wall due to the following main mechanisms: gravitational, diffusional, electrostatic, and inertial forces (Friedlander and Johnstone, 1957). Shear stress acting onto the inner pipe walls can detach clogged material already formed into the passing leachate, increasing the concentration of suspended particles traveling within the leachate. Biofilm detachment may be shear stress related (Van Loosdrecht *et al.* 1995b, Rittmannn and McCarty 2001, Liu and Tay 2002, Choi and Morgenroth 2003 and Saravanan and Sreekirhnan 2006) or dependent on the biofilm growth kinetics (Characklis and Marshall 1990, Van Loosdrecht *et al.* 2002 and Hunt *et al.* 2004). The net effect of mechanisms that may decrease or increase suspended particle concentration within the pipe is captured by deducing the removed TSS concentration. The average influent TSS, VSS and ISS concentrations for Sept. 2009- June 2010 were 657 (±622), 177(±103) and 480(±544) mg/L respectively, each with a high average standard deviation. The average influent TSS, VSS and ISS concentrations for June – September 2010 were 1001(±382), 393(±182) and 608(±212) mg/L respectively, each with a relatively high average standard deviation. High standard deviations observed (especially ISS) may have been produced by the natural variability of leachate and the possibility of sampling external inert particles accumulated at the bottom of the leachate hauling truck at the time of replacing the leachate to the outside tank (approx. 3 times a month). Figure 3.11 (a) and (b) show the TSS results of this study, where two different

trends were observed after leachate was pumped through the testing pipes, for both scenarios.

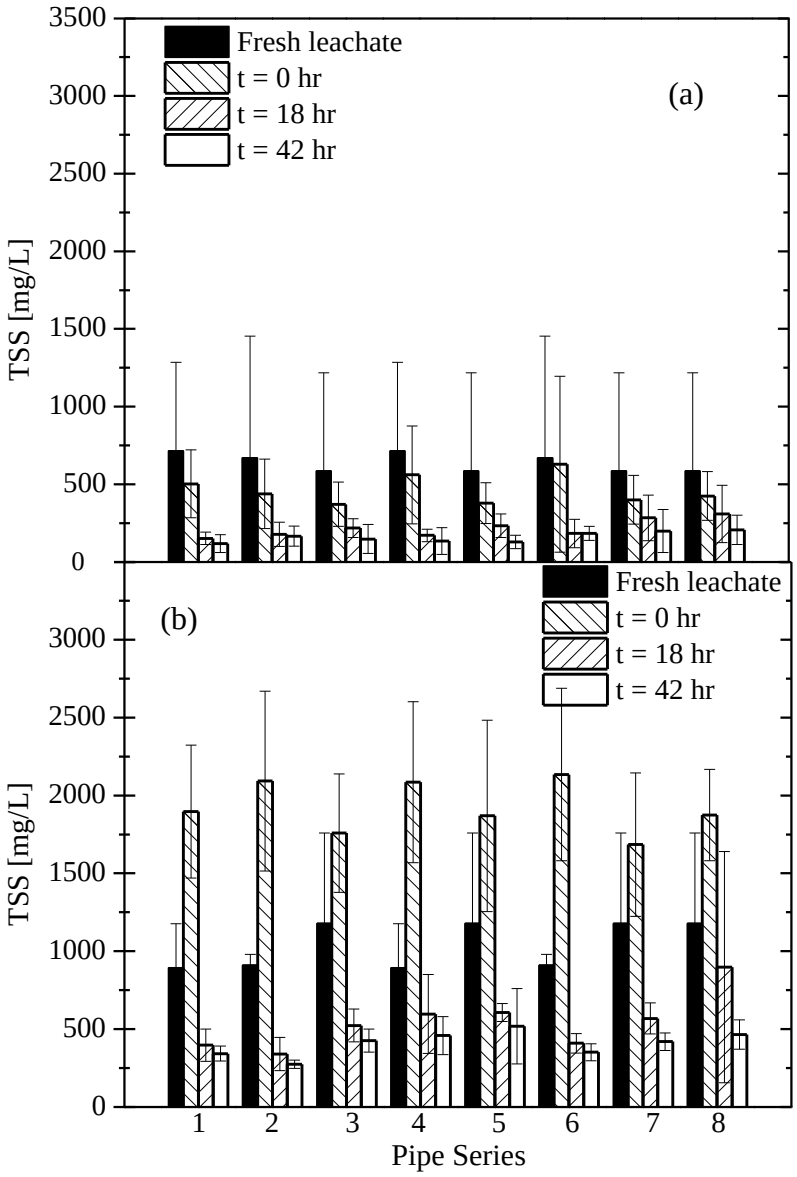

Figure 3.11. Average TSS values (mg/L) for all testing cycles for the pipe series during (a) Sept. 2009- June2010 and (b) June - September 2010.

Figure 3.11a shows that, during the period Sept. 2009-June 2010, TSS removal occurred within all the pipe series (clog formation) after pumping and stagnation. An average

removal value of 177 mg/L (standard deviation of 61 mg/L) during pumping and 303 mg/L (standard deviation of 100 mg/L) during 42 hours of stagnation was recorded.

The second trend observed during the June 2010-Sept. 2010 season (Figure 3.11b) shows an average TSS increase of 885 mg/L (±299 mg/L) immediately after pumping, and an average TSS decrease of 1518 mg/L (±211 mg/L) during the 42 hours of stagnation. Since the pilot study had already being recirculating leachate from September of 2009, it is believed that organic and inorganic clogging formed within the tanks, pumps, hoses and pipes was carried into the flow towards the testing pipes.

The importance of this trend extrapolated to full scale bioreactor landfills is that if there is a breakpoint during the operation of these systems where significant solids are attached and/or deposited within the injection system components (pumps, hoses, pipes, etc.) they will be carried over to the injection pipes, which are the end of the injection system. This will increase the rate of clogging, impairing the hydraulic performance of the pipes sooner than with clogging only formed within the pipe environment.

Based on this observation it is hypothesized that clogging formed outside and inside of the recirculation pipes may move along the perforated pipes, accumulating non-uniformly within the pipes. The pipe may eventually clog from the pipe end to the inlet.

The same trend was observed for the average ISS values (see Figure 3.12 (a) and (b)), with an average removal value of 172 mg/L (±58 mg/L) during pumping and 212 mg/L (±110 mg/L) during 42 hours of stagnation, for the first scenario. For the second scenario, an average ISS increase value of 640 mg/L (±199 mg/L) was measured immediately after

pumping, and an average ISS decrease of 1068 mg/L (±181 mg/L) , during 42 hours of stagnation.

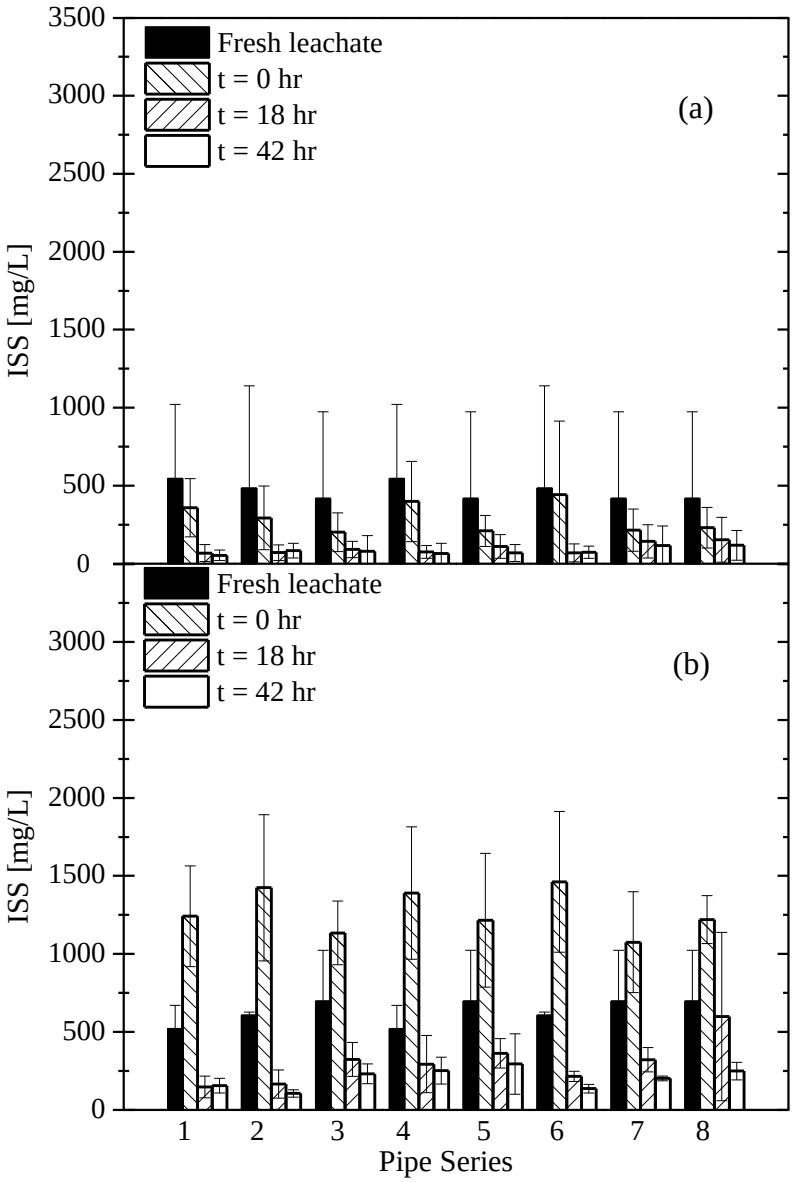

Figure 3.12. Average ISS values (mg/L) for all testing cycles for the pipe series during (a) Sept. 2009- June 2010 and (b) June - September 2010.

The ISS represented between 58 and 71% of the TSS for the leachate freshly collected from the landfill wells and between 53% and 64% of the TSS values immediately after

pumping, during Sept. 2009-June 2010 and June 2010-Sept. 2010 seasons (see Figure 3.11 (a) and (b)). After 42 hours of stagnation, the average ISS values represented over 40% and 38% of the average TSS values for each season. This may indicate that most of the ISS settled during stagnation, showing that sedimentation was the main mechanism of TSS removal during stagnation.

From the different Reynolds numbers adopted within the pipe series tested, no significant differences in TSS and ISS concentrations were observed during pumping and 42 hours of stagnation for both scenarios (Figures 3.11 and 3.12). However, the effect of mass loading and settling was significantly higher for the pipe series 7 and 8 (largest pipe diameter) than smaller pipe diameters (pipe diameter of 0.04m) for both scenarios. This results in a larger accumulation of solids during stagnation for larger diameter pipes.

Even though VSS accumulation was measured after pumping for the first scenario, the average VSS values did not clearly indicate a trend as shown with TSS and ISS. However, an average VSS removal of 91 mg/L (standard deviation of 16 mg/L) was measured within all the pipe series after 42 hours of stagnation. During the second season, an average VSS increase of 245 mg/L (standard deviation of 101 mg/L) was measured immediately after pumping, and an average VSS decrease of 450 mg/L (standard deviation of 35 mg/L) was measured during the 42 hours of stagnation.

3.4.2 Clogging accumulation and composition within the pipes

3.4.2.1 Clogging characterization

After 477 days of operation, the pilot study was completed and the pumps were turned off. A total of five coupons were collected from each pipe series during the duration of this study where the first set of coupons were collected from the pipe series 1 and 4 on December 11, 2009 and the last set of coupons were collected on November 23, 2010 from the pipe series 3, 5, 7 and 8. After the first sets of coupons were removed, clogging was found to have accumulated within all the pipe series. Figure 3.13 (a) and (b) show clogging developed inside of the 4.8 and 9.2 cm internal diameter pipes after approximately 5 months of operation. Figure 3.13 (a) shows clogging inside of the 4.8 cm pipes accumulated around the diameter of the coupon. It was mainly formed as a hard and uniform layer around the wetted perimeter of the pipes.

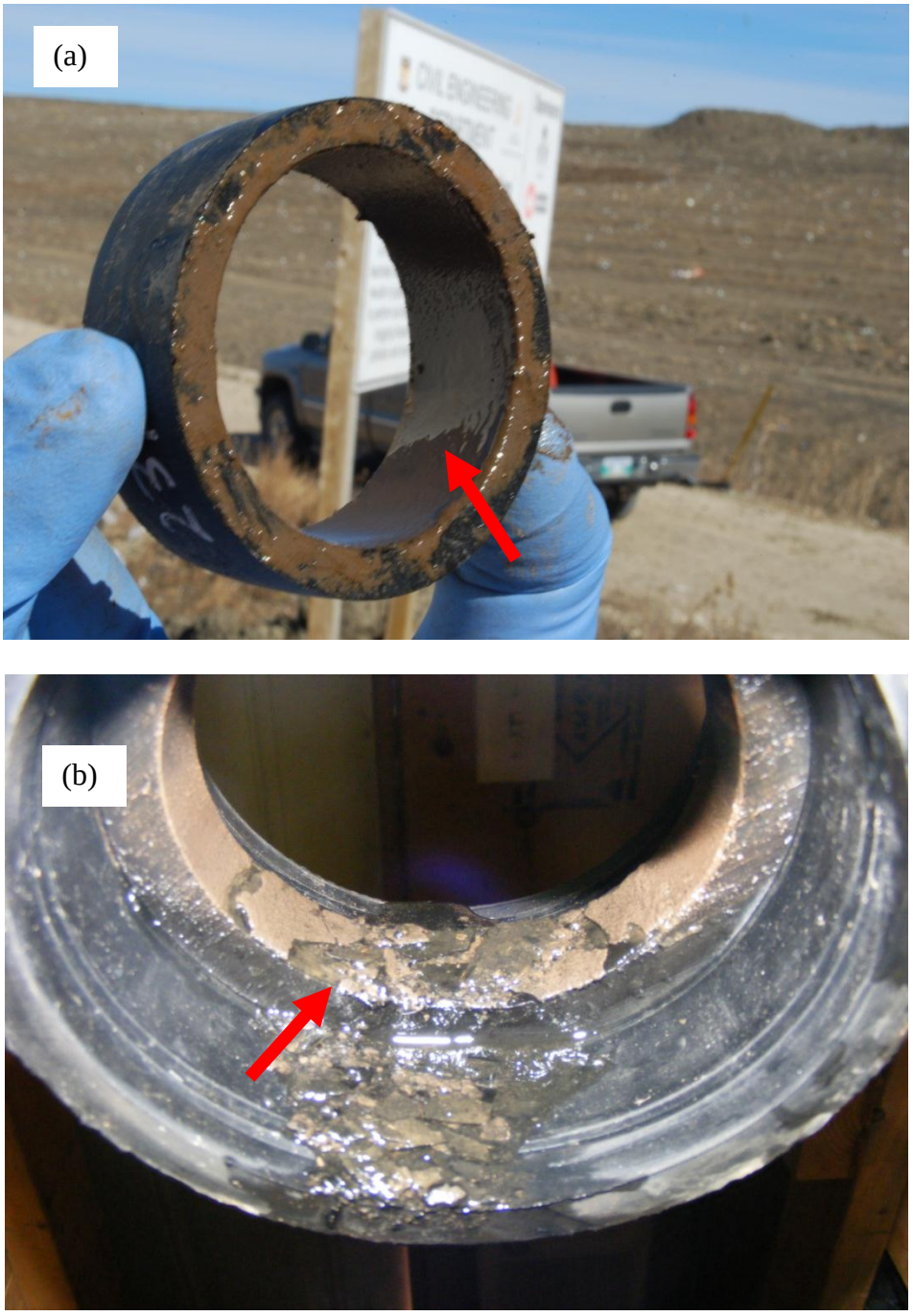

Figure 3.13. Clog development within the (a) 0.048 m and (b) 0.092 m pipes (solid arrows indicate the clog material accumulated within the pipe rings)

Figure 3.13 (b) shows clogging developed inside of the 9.2 cm diameter pipes. It was mainly formed at the bottom of the coupon and was comprised of two visible layers of

clogging: (1) a slime layer underneath of a (2) harder and more mineralized layer. The same configuration was observed within the 13.4 cm pipes. After 5 months of operation and until the end of this study, clog configuration remained similar for the 4.8 cm diameter pipes, but changed for the larger diameter pipes, accumulating as several layers of slime and harder and thin pieces of clogged material, as show in Figure 3.14.

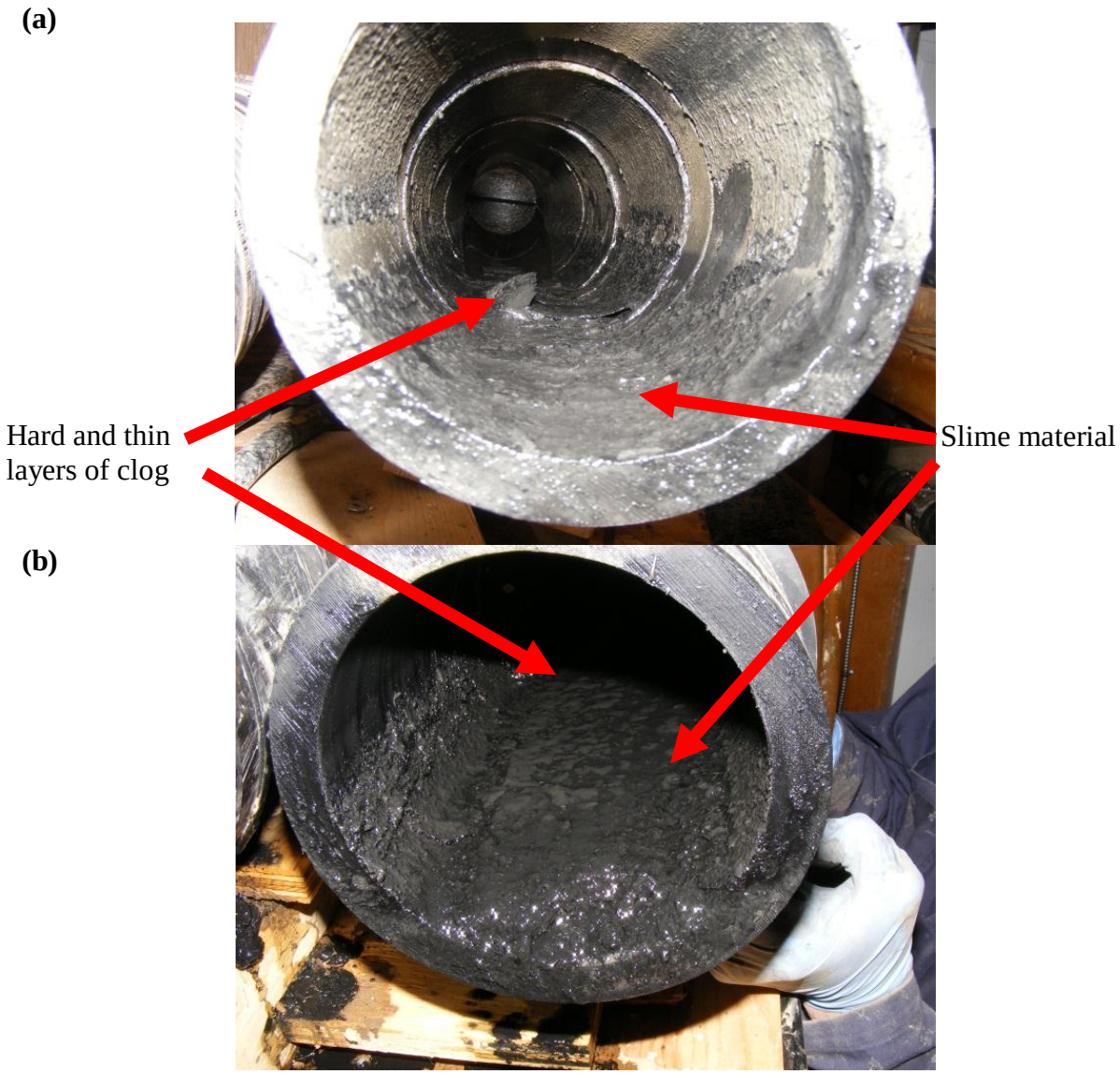

Figure 3.14. (a) and (b) show the clog development within the 9.2 and 13.4 cm internal diameter pipes (solid arrows indicate the clog material developed) after 14 months of operation

Figures 3.14 shows that most of the slimy and soft clog material was accumulated at the bottom of the pipes, where several dry clog material slices were detached from the pipe walls. The fact that pumping and stagnation were intermittent during this study may explain why clog formed within the pipe walls after the 42 hours of stagnation was then detached by the shear force exerted within the pipe walls at the beginning of each pump startup. This explains the occurrence of most of the slimy and hard material accumulated at the bottom of the pipes. In addition, it is hypothesized that clogging formed within the feeding pipes and tank may have dried and been conveyed towards the pipes.

The clog formation within the pipe series also indicate the importance of a sedimentation effect within the 9.2 and 13.4 cm pipes conveying lower flow rates than the 4.8 cm pipes, where clogging was found to be uniform around the wetted perimeter. Figure 3.15 shows the average Total Solids (TS) values per surface area [kg/m^2 of pipe surface] accumulated for the different pipes versus the Reynolds number of the pipe. Pipes with lower Reynolds numbers tended to accumulate a greater amount of clog material, and experienced greater seasonal differences (between 3 to 5 times difference).

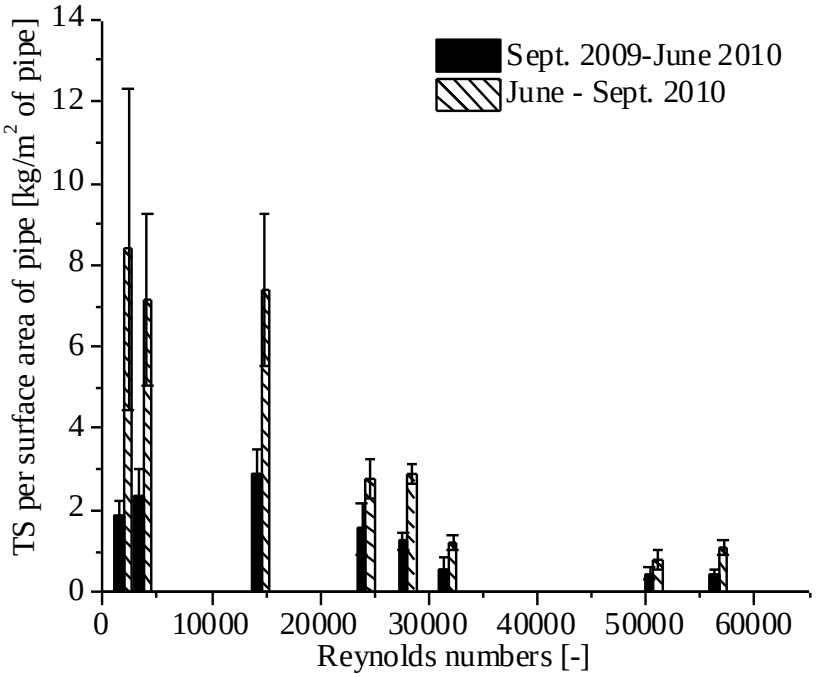

Figure 3.15. Average TS accumulated per surface area of the pipe series [kg/m^2 of pipe] for each season during the entire study

Based on these results, turbulence intensity (Reynolds number) plays a major role in the formation of clogging within the inner walls of injection pipes. Figure 3.16 shows the average mass collected from each of the five pipe rings for the different Reynolds numbers adopted within the pipe series. Since the pipe rings were collected while the pipe series were not being operated (see Section 3.3.1), the analyses of the clogging composition was performed at different times (Appendix F). Nevertheless, this "lag time" never exceeded a month between collections and analyses (Appendix F), so the average days at which pipe rings 1 to 5 were collected from all the testing pipes is shown in the following figures. This was intended to represent the evolvement of clogging within all testing pipes over time.

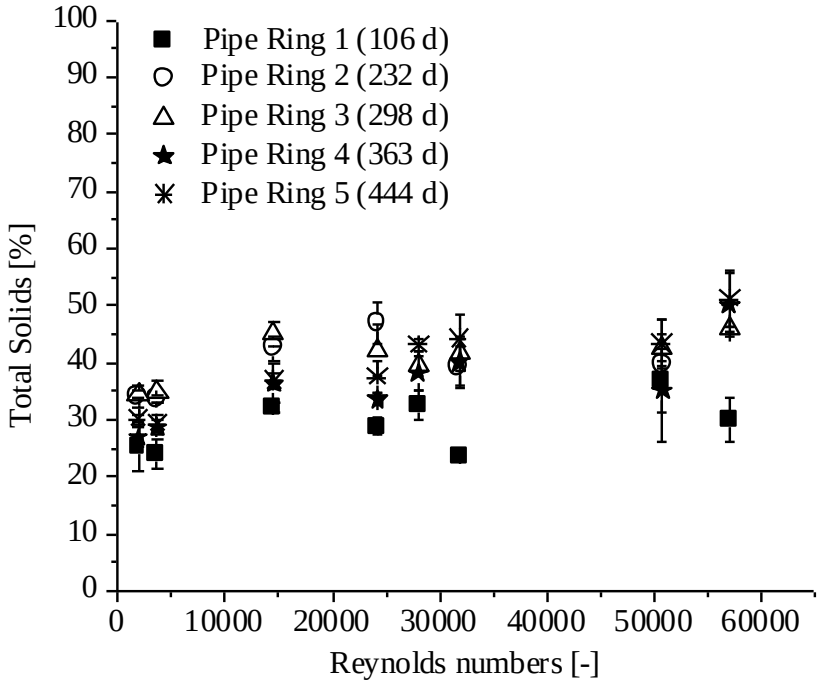

Figure 3.16. Average mass accumulated [g] collected from the pipe rings versus the different Reynolds numbers adopted for each testing pipe.

Figure 3.16 shows that for Reynolds numbers < 20,000, the mass accumulated within the pipe rings 1 and 5 increased between 4 to 5 times, where for higher Reynolds number (>20,000), the mass accumulated increased between 2 to 3 times. These results show that lower Reynolds numbers have a significant effect on the mass accumulated within the pipe rings. In addition, Reynolds number had an impact on the configuration of clog accumulated within the pipe series. For example, this study shows that at Re < 30,000, two different layers of clogging were mainly found at the bottom of the pipes, where sedimentation may have been favored over attachment/detachment of biofilm and inorganic material around the diameter of the coupons, especially at the top (Figure Figure 3.13b and Figures 3.14). At Re > 30,000, attachment/detachment may have been

favored over sedimentation, as clogging was found to have uniformly developed around the diameter of the coupons (Figure 3.13a).

From above, the hydraulic operation and design of the injection pipes may influence the cleaning methodology adopted by the landfill manager and its efficiency. For example for the pipes in this study, mechanical cleaning (e.g. pressurized water) would have been easier within the pipes conveying leachate at low Reynolds numbers.

3.4.2.2 Water and total solids content

The water and total solids content in the clog material changed with time, showing significant differences between the pipe series (see data in Appendix F). As demonstrated in Figure 3.17a and b, the pipes with the highest Reynolds numbers (31,795 to 56,696) showed the highest decrease in water content (increase in total solids), with differences from 6.5 to 22% between the first and last pipe ring collected. The Reynolds numbers between 14,515 and 27,994 showed the second largest difference from 4 to 11% between the first and last pipe ring collected. Finally, the lowest Reynolds numbers (1,898 and 3,678) showed the smallest variation, decreasing by 4 to 6% between the first and last pipe ring collected. These results show that "harder" clogging was obtained in the short term with the pipe series operated at high Reynolds numbers. These changes in composition (water versus total solids content) impact the effectiveness of the cleaning strategy (e.g. mechanical versus chemical cleaning) adopted by the landfill manager if clogging is not removed from the pipes at the earlier stages of formation.

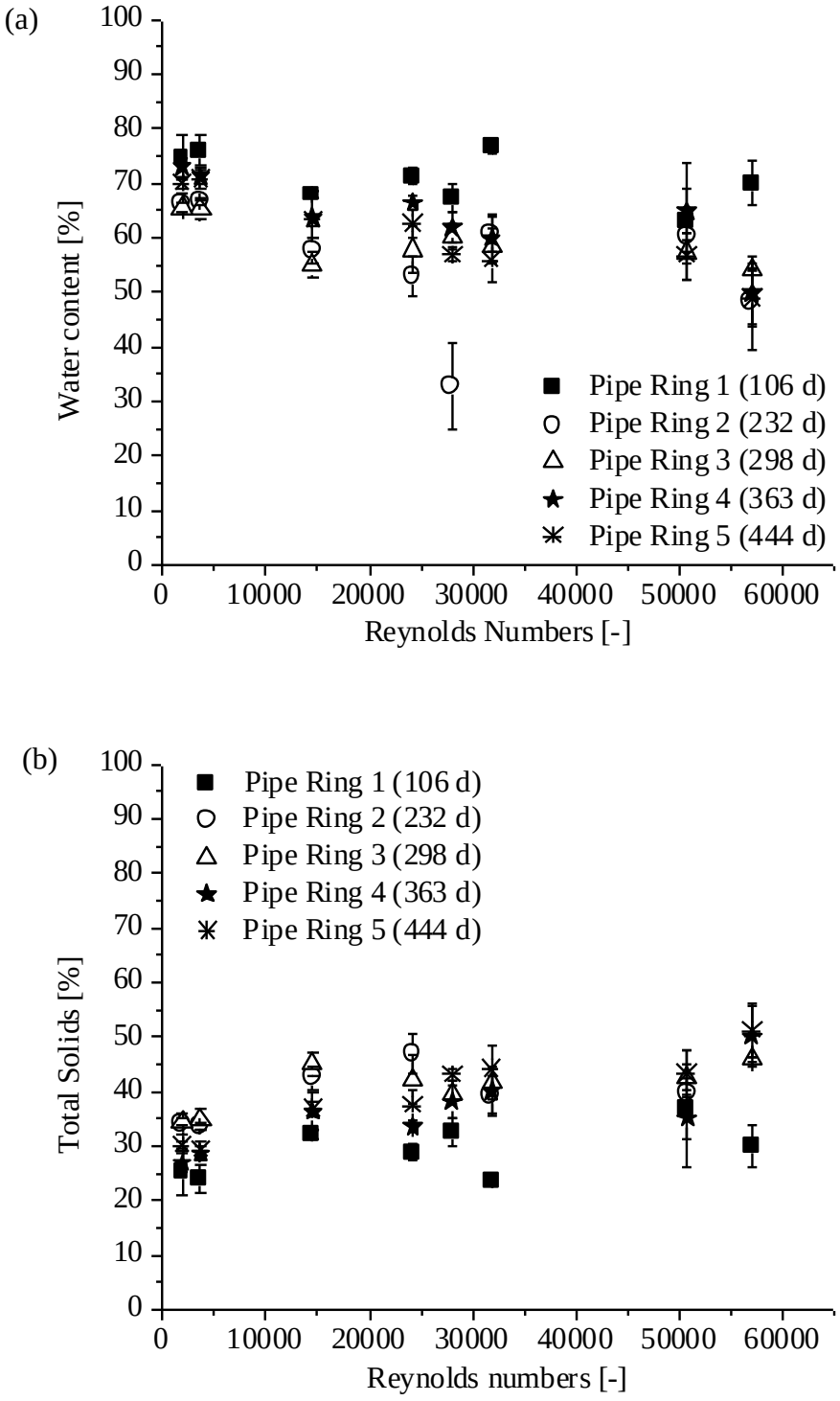

Figure 3.17. (1) Water content percentage of the total amount of clog mass accumulated inside of the pipe rings collected at different Reynolds numbers and (2) Total solid

3.4.2.3 Total mass, organic and inorganic content

The candidate's MSc thesis study showed that more clogging accumulated within pipes with larger diameters while the pipes were operated at the same flow rates over time. The effect of mass loadings (in terms of flow rate and leachate concentration) was not sufficient to explain the differences in the amount of material collected, resulting in 2 to 4.5 times greater for larger diameter pipes. Since the internal surface area of the large diameter pipes was approximately twice the small diameter pipes, higher clogging accumulation within the larger diameter pipes was explained as a combination of mass loading and pipe internal surface.

Figure 3.18a shows that more clogging accumulated within the larger pipe diameter series per length of pipe (lowest Reynolds numbers) agreeing with the applicant's M.Sc. thesis study results (see data in Appendix F). Nevertheless, the average influent mass loading during this study was substantially higher (5 fold) for the small pipe diameter series (1,103 kg of Ca^{2+}, COD, and TSS concentration) than the large pipe diameter series (246 kg of Ca^{2+}, COD, and TSS concentration). Therefore, leachate components removed during stagnation contributed significantly to the total mass of clogging material deposited within the pipes (see Figures 3.6, 3.7, 3.10 and 3.11). This has not been assessed in past injection pipe studies

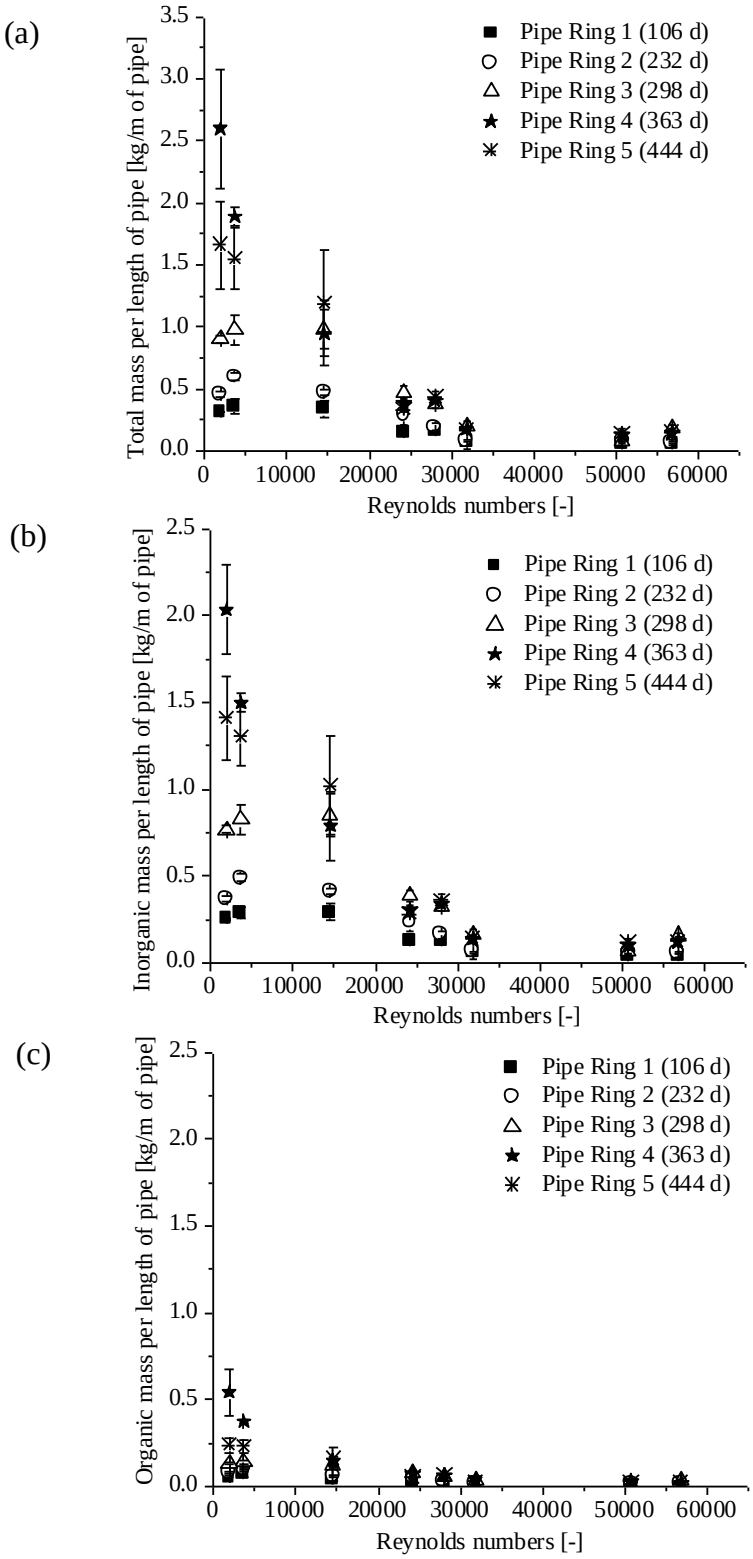

Figure 3.18. Total (a) clog mass, (b) inorganic mass and (c) organic mass per length of pipe collected inside of the coupons or pipe rings over time.

VanGulck and Rowe (2004a,b) investigated the change of clogging composition over time within columns packed with 6 mm diameter glass beads and permeated with synthetic and real leachate. Clogging evolved from containing inorganic and a soft and slime type of organic material to largely inorganic with time and the slime turned into a "biorock structure. Lozecznik and VanGulck (2009) found that for the laboratory testing pipes conveying leachates constantly (no stagnation) at different flow rates, clog material accumulated after 5 months contained higher inorganic (>43%) than organic content. Since none of the studies of clogging in leachate transmission pipes have measured clogging and its changes through time, this is the first study to do so. However, this study only shows clogging from leachate being pumped and stagnant within solid pipes by replacing the leachate source only 2-3 times a month. Bioreactor landfills recirculate leachate depending on the waste moisture target selected by the landfill engineer, which can vary from daily to once a week, depending of several factors such as rainfall events, waste compaction, permeability of the cover, etc. Therefore, this study only shows a less frequent recirculation scenario compared with full scale bioreactor landfills and further research is needed to investigate the changes produced by recirculating fresh leachate more often.

With the pipe design, hydraulic operation and leachate conditions tested, clog changed from having an average inorganic concentration of 76% (±1.7%), 84% (±3.2%) and 81% (±0.8%) for the first pipe ring collected to 83% (±1.9%), 85% (±1.4%) and 85% (±0.5%) for the last pipe ring collected, with 11 months between coupon collection (Data in Appendix F). These results indicate a slightly higher initial organic clog composition

within pipe series 1, 2 and 3 and the highest increase in inorganic clog composition through this study (average 10%) (Data in Appendix F).

Figures 3.18a, b and c show the total clog mass and organic and inorganic content of clog material per length of pipe at different Reynolds numbers. From these figures, it can be deduced that the pipe series operated at higher Reynolds numbers (>20,000) did not have significant variations of total mass, organic and inorganic content (between 0.01 to 0.15 kg/m of pipe length) over time. This shows that the higher Reynolds number flow and the higher shear stresses applied to the pipe walls maintained a fairly constant amount of mass within the pipe rings during this entire study. For the lowest Reynolds numbers adopted (< 20,000) it can be observed that high differences between total clog, inorganic and organic masses per length of pipe were observed, ranging from 0.3 to 2.6 kg/m of pipe length over time. This indicates that the lower wall shear stress were not high enough to prevent clogging from depositing at the bottom of the pipes over time.

3.4.2.4 Clogging rate

Based on the total mass of clogging collected from each coupon (Figure 3.16) over time a rate of clog accumulation was calculated for the pipe series and are plotted as a function of Reynolds number in Figure 3.19.

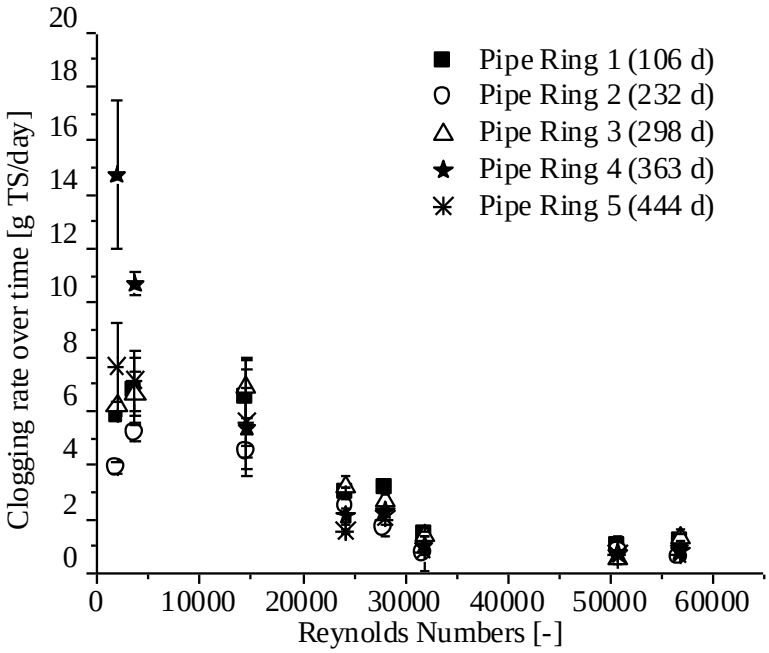

Figure 3.19. Clogging rate over time (g/day) for the different Reynolds numbers adopted over time.

From Figure 3.19, it can be observed that for the lowest Reynolds numbers (< 3,700), the highest clogging rate was found after 12 months of operation (pipe rings 4) ranging between 10.7 and 14.7 g TS/day approximately. For 3,678 < Re < 24,192 the highest increase in clogging rate was found after 10 months of operation (pipe rings 3) ranging between 3 and 7 g TS/day approximately. Finally, for higher Reynolds numbers (Re > 24,192) the maximum clogging rate was measured in the first 4 months of operation (pipe rings 1) ranging between 1 and 3.2 g TS/day approximately. These results have demonstrated that with the conditions tested, pipes operated at the lowest Reynolds numbers (Re = 1,898) presented the highest rates of clogging (10.7 and 14.7 g TS/day approximately). For Re > 30,000, the clogging rate appears to be Reynolds number independent.

3.4.2.5 COD and VFA removal rates inside of the pipe series

The measured COD and VFA removal (Figures 3.6 and 3.7) and pH increase (Figure 3.5) demonstrated that biological activity was not the primary mechanism responsible for clogging within the testing pipes. Because no other studies have assessed nor characterized clogging over time, there have not been reported rates of COD and VFA removal values performed by the biofilm developed in-situ over time, for leachate injection pipes. These rates could aid in providing a step towards understanding and predicting the capacity of the pipe biofilm to produce significant changes on the leachate chemistry and promoting clogging within injection pipes. For example, these rates indicate the effects of the biofilm developed within the pipes at different Reynolds numbers on the potential changes of clogging precursors from the leachate in the pipe environment over time. This data can be used to calibrate a biogeochemical modeling (e.g. CCBATCH (Rittman *et al.* 2003)) to predict clogging development in the pipe using the pipe design and hydraulic operation (Reynolds numbers) and leachate chemistry. Predicting clogging can be useful to determine the cleaning intervals required to limit clogging or estimating the service life of the injection pipes.

In order to calculate the maximum COD removal rate by the biofilm developed within the pipe series, the maximum COD removal was divided by the VS concentration of the biofilm and elapsed time, and the results are shown in Table 3.2.

Table 3.2**.** Maximum average COD removal rates for the pipe series

Pipe	Date Max. COD removal	COD Rem mg/L	VS mass pipe [g]	Max. COD removal rate mg COD/g VS·d
Series 1	21-Sep-10	1553	40	83
Series 2	03-Aug-10	993	56	38
Series 3	19-Jul-10	3585	76	100
Series 4	07-Jul-10	3720	131	221
Series 5	19-Jul-10	3608	155	181
Series 6	03-Aug-10	2108	306	54
Series 7	19-Jul-10	3433	775	74
Series 8	19-Jul-10	4438	1122	66

From Table 3.2, it can be observed that higher COD removal rates (221 and 181 mg COD/g VS day) were attained for the pipe series 4 and 5, representing between 23% to 34% removal of the influent COD. This may indicate that the biofilm that developed within these pipes was capable of utilizing higher amounts of COD with the conditions tested. Although these COD removal rates do not separate the biological activities of suspended biomass and biofilm kinetics, the results do indicate the overall COD removal within the pipes tested. Since COD removal values were obtained within the pipe series during stagnation, VFA concentrations were tested for pipe series 1, 2, 4 and 6 to verify if the biofilm developed within the pipe series carried out acetogenesis of propionate and butyrate and methanogenesis of acetate during stagnation. Table 3.3 shows the average VFA removal rates of acetate, propionate and butyrate for the pipe series 1, 2, 4 and 6.

From Table 3.3, higher acetate (7.89 mg HAc/g VS·d) and propionate (3.56 mg HPr/g VS·m^2·d) removal rates were attained for pipe series 4, indicating that the biofilm developed within these pipes had higher concentration of methanogens and synthrophs than the rest of the pipe series tested.

Table 3.3**.** VFA average removal rates for the pipe series

Pipe	HAc removal rate [mg HAc/g VS·d]	HPr removal rate [mg HPr/g VS·d]	HBu removal rate [mg HBu/g VS·d]
Series 1	3.55	2.51	4.26
Series 2	4.81	1.22	4.22
Series 4	7.89	3.56	3.25
Series 6	3.53	1.21	2.51

Although the COD and VFA removal rates presented in Tables 3.2 and 3.3 were calculated in an attempt to quantify the activity of the biofilm within the pipe series tested, the variability of leachate VFA's and inhibitory components of methanogens and synthrophs make this interpretation difficult and therefore further testing is required.

3.4.2.6 Clogging deposition and its movement inside of the pipe series

At the completion of this experiment, the pipes were disassembled and weighted at the pilot study location. As the pumps were operated in ON/OFF cycles, it was expected to find more clogging at the downstream end of the pipes due to the fluid force exerted on the pipe walls at the beginning of each pump startup. In order to find out the differences in clog deposition, a special tool was develop to collect clog material for each of the pipe series (3 in total for each diameter) as shown in Figure D of Appendix L. Each tool was long enough to collect material up to 13 cm down the pipes and block any excess of material from upstream or downstream. For this reason, a half diameter metal pipe piece was built at one end and at the other end a plastic "handle" piece bigger than the pipe diameter was attached to fix the maximum reach (13 cm) and to allow it to rotate as to reach the clogging developed at the top of the pipe as well as the bottom. Table 3.4 shows the total amount of clog material collected from the pipes, the theoretical amount

(uniform clog) of material developed per centimeter of pipe and the amount of clog material per centimeter of pipe weighted at the pipe inlet and outlet. Because some of the calculated clogging values were larger than the upstream and downstream values measured on-site (e.g. pipe series 2, 3 and 5), it is believed that clogging accumulated non-uniformly, creating zones of higher accumulation in the middle of the pipes.

Table 3.4**.** Summary of diameter, Reynolds Numbers, total mass accumulated, calculated average mass per centimeter of pipe, upstream and downstream mass measured per length of pipe and standard deviations respectively, for the pipe series of this study.

Pipe Series	Pipe diameter	Reynolds number	Total Mass accumulated		Mass per centimeter of pipe					
					Calculated		Measured			
					Uniform		Upstream		Downstream	
	[m]	[-]	[g]		[g/cm]		[g/cm]		[g/cm]	
#			μ	σ	μ	σ	μ	σ	μ	σ
1	0.04	56,966	67	0.01	0.33	0.04	0.07	0.06	0.32	0.15
2	0.04	50,674	83	0.03	0.62	0.15	0.07	0.01	0.45	0.09
3	0.04	31,795	148	0.01	0.72	0.07	0.42	0.09	0.65	0.11
4	0.09	27,944	155	0.003	0.76	0.01	0.19	0.02	0.95	0.22
5	0.09	24,192	181	0.01	0.88	0.05	0.30	0.13	0.86	0.13
6	0.09	14,515	1,102	0.15	5.38	0.72	0.34	0.11	8.96	1.23
7	0.13	3,678	3,280	0.31	16.01	1.52	1.38	0.81	21.96	4.54
8	0.13	1,898	4,051	0.50	19.79	2.46	1.85	1.00	25.12	0.11

Table 3.4 shows that a larger pipe diameter at lower flow rates (a) accumulated the highest amount of clogging and (b) experienced the highest differences of clogging between inlet and outlet. This may be explained as a combined effect of a larger surface area for clog formation and accumulation, and low shear stress operation, forming a more slimy and mobile clogging each time the pump was operated.

These results demonstrate that clogging is not uniform along the length of pipelines, and may indicate that the majority of the pipe clogging accumulated through time within leachate recirculation lines in bioreactor landfills could be accumulated at the end of the pipelines. This may indicate the presence of "dead injection zones" at the end of leachate recirculation systems within the bioreactor cell, affecting the zone of wetting and the benefits of leachate recirculation systems.

3.4.2.7 Clogging densities

As the amount and composition of the clogging collected from the pipe rings changed within the pipe series over time (Figures 3.15, 3.16, 3.17 and 3.18), different clog densities were also expected. Figure 3.20 summarizes the bulk density values sampled from the pipe rings collected from the pipe series through time (see data in Appendix G). The five pipe rings represent clogging accumulated within the pipe series after 4, 8, 10, 12 and 14 months of operation, respectively.

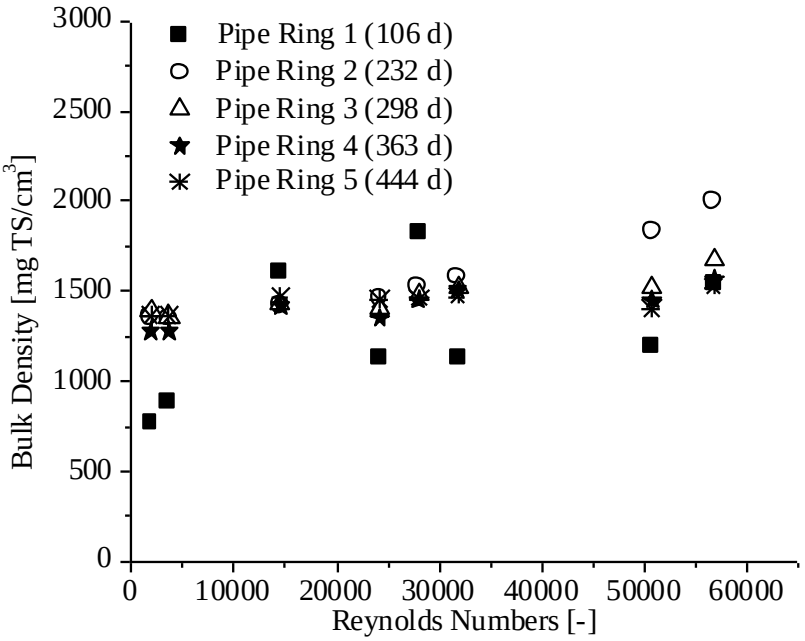

Figure 3.20. Average bulk density values [mg TS/m^3] from the clogging samples collected from pipe rings 1 to 5.

From Figure 3.20, it can be observed that the bulk density of the clog collected from the pipes with the lower Reynolds numbers adopted (< 5,000) exhibited the most significant increase from the first to the last pipe ring collected during this study (from approximately 800 to 1,360 mg TS/cm^3). After approximately a year (pipe ring 5), the bulk densities within the pipe series were similar, ranging between 1,360 to 1,520 mg TS/cm^3, due to the increase in mineral content, as it is observed in the higher inorganic content versus organic accumulated within these pipe series over time (Figure 3.17b and c). Since it was found that larger pipe diameters promote clog material with low densities, especially early-on, this might facilitate cleaning by mechanical means.

For the pipes with the higher Reynolds number adopted (>30,000), the trend was not clear. The highest bulk density was sampled after the second pipe ring was collected, and

it is hypothesized to be caused by a combined effect of mass accumulated within the pipes and shear stress effect. This suggests that for the clog mass collected from the third pipe ring, the shear stress did not prevent the excess of mass accumulating, thus lower bulk density values were obtained.

Since the larger pipes diameters also exhibited the highest increase in density values during this study, cleaning strategies must be implemented frequently, especially if low Reynolds numbers are adopted in the leachate injection pipe design for bioreactor landfills, or clogging density changes will impact its effectiveness if mechanical cleaning methods are adopted.

The density values obtained during this study were very similar to the density values reported by Lozecznik and VanGulck (2009) in their laboratory leachate pipes study, ranging from 1,300 to 1,780 (mg TS/cm^3). Even though this study recirculated leachate through pipes at a much higher flow rate than the past studies permeating leachate through a porous media, the measured clog bulk density values were within the range reported by Rowe *et al.* (2002) and VanGulck and Rowe (2004a,b) for a mature clog of about 1,320 to 2,210 (mg TS/cm^3).

None of the density values compared from the past studies mentioned above have investigated clogging and its changes in composition through time; they only assessed it once at the end of the study. Therefore, from the bulk density values and organic and inorganic mass values sampled over time, this study confirmed VanGulck and Rowe

(2004a, b) speculation, mainly for low Reynolds pipes, that clog material accumulated within the pipes changed from a mixed biological and inorganic composition to a largely inorganic composition with time.

The non-volatile density values (mg NVS/m^3) of clog collected from the pipe rings (pipe ring 1 was not sampled) are shown in Figure 3.21 (see data in Appendix G).

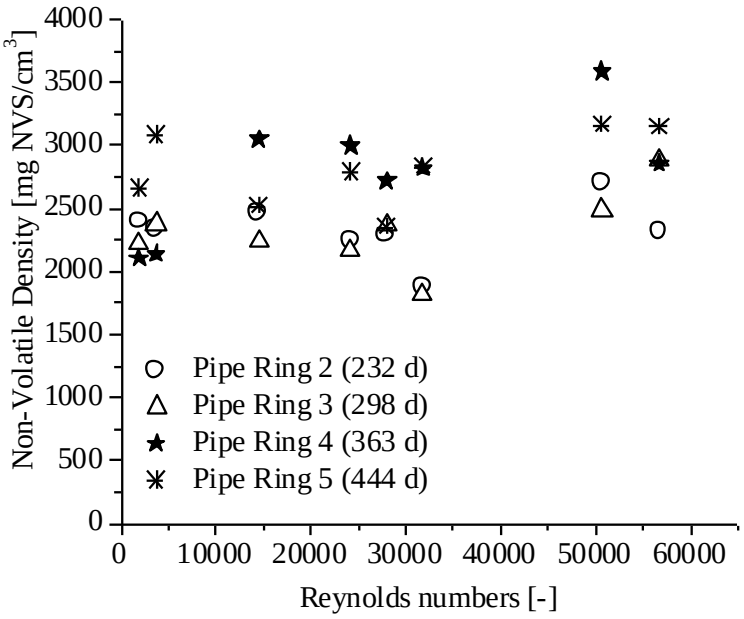

Figure 3.21. Average non-volatile density values [mg NVS/m^3] from the clogging samples collected from pipe rings 2 to 5.

From Figure 3.21, it can be observed that different non-volatile density values at different times may represent different minerals forming clogging over time. For example, calcite ($CaCO_3$), aragonite ($CaCO_3$) and monohydrocalcite ($CaCO_3 \cdot H_2O$) density values are 2,710, 2,930 and 2,380 mg NVS/cm^3 (Mineralogy Database), so Figure 3.21 may indicate the presence of some of these minerals , which were analyzed and are presented later in this section. The non-volatile density values from clog material collected from the

laboratory pipes of Lozecznik and VanGulck (2009) ranged from 2,290 to 2,870 mg NVS/cm^3, which are similar to some of the densities of this study. The fact that non-volatile densities increase through time may indicate the accumulation of carbonate minerals and solid inert particles with high densities.

The volatile density values (mg VS/m^3) were also calculated from the pipe rings collected from the pipe series as shown in Figure 3.22. The average volatile density was calculated based on the method described in Rittmann and Brunner (1984), calculating first the thickness ($L_{f,a}$) (equation 3.1) of the active film in the pipe using

$$L_{f,a} = \frac{W_e}{\rho_w A_{so}(0.99)} \qquad (3.1)$$

Where $W_e$is the mass of evaporated water in the clog sampled from the pipe ring, ρ_w is the density of the water at 21˚C, A_{so} is the internal surface area of the pipe and 99% of the water by weight is biofilm. The volatile density $\rho_v$was calculated using equation 3.2

$$\rho_v = \frac{B_v}{A_{so} L_{f,a}} \qquad (3.2)$$

Where B_v is the mass of volatile solid in the clog sampled from the pipe ring. An error in the calculated volatile density was expected, since it was assumed that half of the internal surface area of the pipe series 4 to 8 contained clog material, where in fact, most of the clogging deposited within these pipe series was accumulated at the bottom of the pipe (e.g. Figure 3.13). Despite this overestimation in volatile density due to this assumption (clogging distribution) and the differences in flow rates between this study (with approximately 4 to 6 order of magnitude higher) and clogging in porous media studies, the calculated values are within the range of the volatile density values calculated by

Rowe *et al.* (2002) and VanGulck and Rowe (2004a,b), ranging from 37 to 193 (mg VS/cm^3), as shown in Figure 3.22. On the other hand, these densities are lower than the applicant's M.Sc. thesis study. The difference may be attributed the fact that the leachate was often kept stagnant in the current study. The volatile density values showed a similar trend observed with the bulk density values for the higher Reynolds number pipes, and it is believed that the combined effect of more inorganic material accumulating and organic material leaving the pipes (lower density) and the shear stress were the responsible for the lower density values sampled after the second pipe ring was collected.

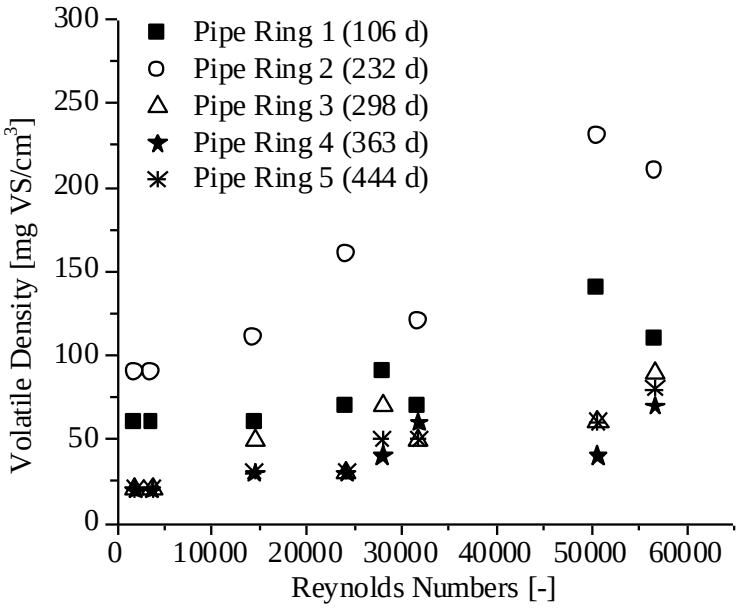

Figure 3.22. Average (μ) values of volatile density values [mg VS/m^3] from the clogging samples collected from pipe rings 1 to 5.

Garny *et al.* (2009) investigated the interaction between a heterotrophic biofilm structure and sloughing in a flow-through tube reactor, exposed to constant, limiting and non-limiting substrate conditions. In all four biofilms assessed under laminar (Re = 1,500) and turbulent conditions (Re = 3,000), the reduction in biofilm density was associated with an

increase in biofilm thickness and biofilm roughness prior to the first sloughing. These conditions were promoted by the development of small filamentous bacteria or increase in colony surface irregularity. Figure 3.22 shows a trend of smaller biofilm density values for lower Reynolds numbers adopted, perhaps indicating the existence and growth of filamentous microorganisms within clogging through time. Previous study has shown filamentous microorganisms to be responsible for clogging in pipes from activated sludge treatment (Dondero 1975). Characklis (1980) reported that under higher fluid shear stress, more rigid biofilm tends to grow. From Figure 3.22, it can be observed that higher volatile density is found within higher Reynolds numbers adopted, agreeing with the above statement.

3.4.2.8 Clogging metals analysis

Clog composition analysis for Ca^{2+}, Mg^{2+} and Fe^{2+} was performed on clog samples taken from pipe rings 2-5 from the pipe series at different times, as shown in Figures 3.23, 3.24 and 3.25. Analysis of Na^{+} was also performed, and the results are shown in Appendix H.

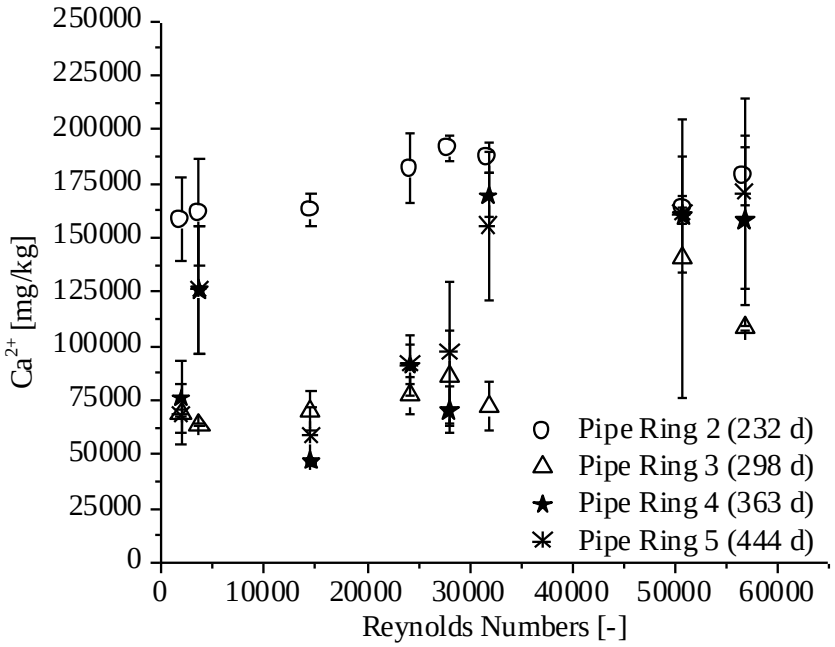

Figure 3.23. Average Ca^{2+} values ($mg \cdot kg^{-1}$) sampled from clogging collected from pipes rings 2 to 5.

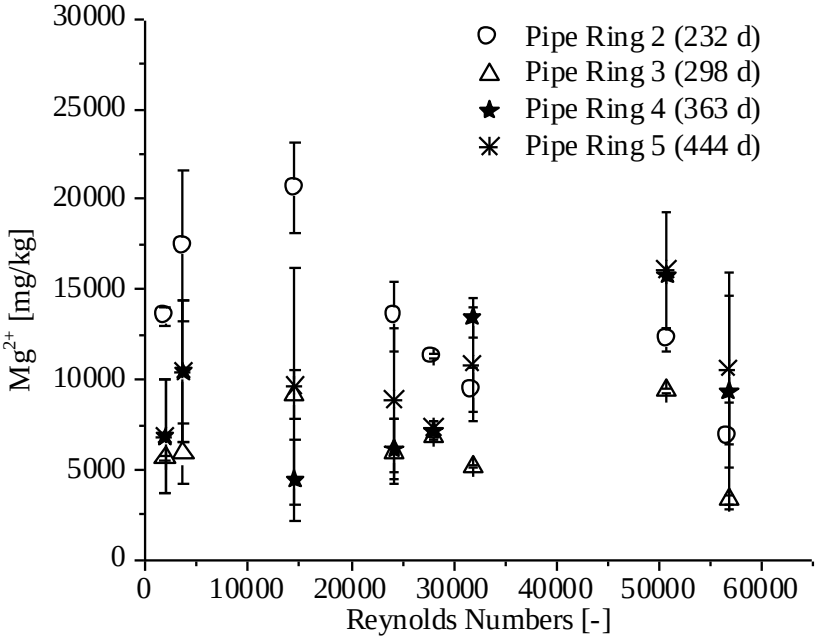

Figure 3.24. Average Mg^{2+} values ($mg \cdot kg^{-1}$) sampled from clogging collected from pipes rings 2 to 5.

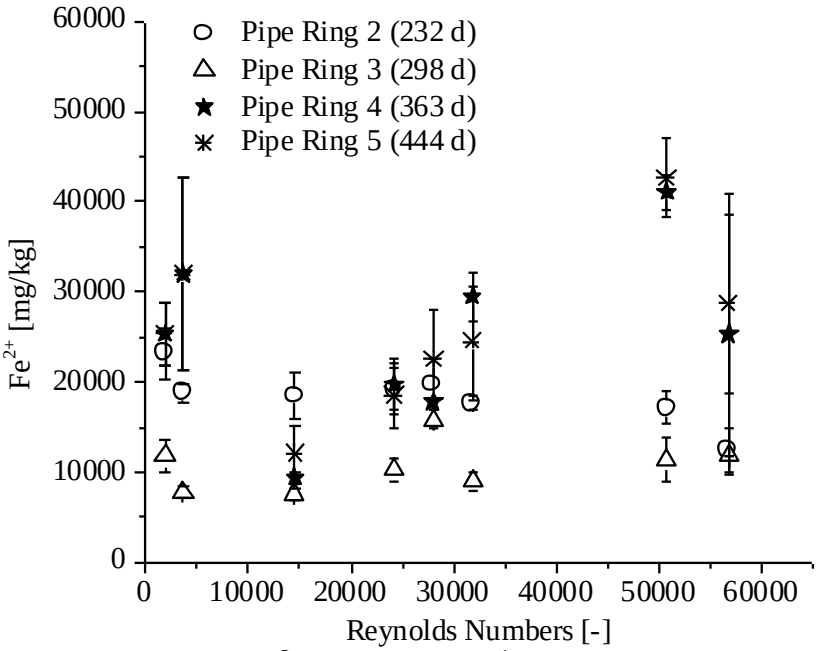

Figure 3.25. Average Fe^{2+} values ($mg \cdot kg^{-1}$) sampled from clogging collected from the pipes rings 2 to 5.

From Figures 3.23, 3.24 and 3.25, it can be observed that Ca^{2+} is the largest cation component of the clogging elements sampled from all of the pipe rings collected during this study (4.7 to 19% of the total dry mass sampled), followed by lower amounts of Fe^{2+} and Mg^{2+} concentrations, ranging between 0.4 to 4.5% of the total dry mass sampled. In addition, Figure 3.4.2 shows the lowest decrease in Ca^{2+} composition over time within the clogging collected from the pipes operated at Reynolds numbers above 30,000. This is explained as the average influent mass loading for the pipes operated at higher Reynolds numbers (1,103 kg of Ca^{2+}) was approximately 5 fold higher than the pipes operated at the lowest Reynolds numbers (246 kg of Ca^{2+}) during this study. Table 3.5 shows published compositions of clog analysis (Ca^{2+}, Mg^{2+} and Fe^{2+}) accumulated within the pore space of granular material permeated with landfill leachate and the applicant's

M.Sc. thesis study. The results of this study show a similar trend (higher Ca^{2+} than Mg^{2+} and Fe^{2+}) as the studies of clogging in porous media.

Table 3.5**.** Summary of clog composition that accumulated within porous media and pipes permeated with landfill leachate (values reported are in percentage of the total dry mass sampled).

	Ca^{2+}	Mg^{2+}	Fe^{2+}
German Landfill Brune *et al* (1991)	21	1	8
KVL-Temperature*			
21 °C	30	<1	2
27 °C Armstrong (1998)	25	1	4
Toronto Landfill Fleming *et al.* (1999)	20	2	8
KVL-Mass loading series*			
0.51 $m^3/m^2/d$	24	1	4
1.02 $m^3/m^2/d$	27	1	4
2.04 $m^3/m^2/d$ Rowe *et al.* (2000a)	27	<1	4
KVL-Particle size series*			
4 mm	24	1	4
6 mm	27	1	4
15 mm Rowe *et al.* (2000b)	27	<1	4
Synthetic Leachate*			
21 °C, 6 mm beads Rowe *et al.* (2001)	36	<1	<1
Synthetic Leachate*			
21 °C, 6 mm beads VanGulck and Rowe (2004a)	37	<1	<1
KVL-Leachate*			
21 °C, 6 mm beads VanGulck and Rowe (2004b)	29	1	3
Lozecznik (2006)			
0.05 m external diameter pipes	7	19.4	0.5
0.1 m external diameter pipes	8.1	17	1.1
Pilot Study (this study)			
0.05 m external diameter pipes	7.2-18.7	0.5-1.6	0.8-4.4
0.1 m external diameter pipes	4.7-19.1	0.4-2.1	0.8-2.7
0.16 m external pipe diameter	5.7-16.1	0.6-1.7	0.8-3.3

* Laboratory study

3.4.2.9 X-ray diffraction (XRD) and scanning electron microscope (SEM) analysis

Owen and Manning (1997) showed that landfill leachates have a strong potential to precipitate carbonate minerals as a consequence of the process of methanogenesis. Maliva *et al.* (2000) analyzed clog material flushed from leachate collection pipes at a Florida landfill (receiving incinerator ash and municipal solid waste) finding mainly calcite with low magnesium concentration. Manning *et al.* (2000) reported that leachate suspended solids and their sediment load from leachate obtained from Lancashire and West Midlands Landfills (UK) were mainly composed of calcite together with quartz and clay minerals. In the current study, X-ray diffraction analysis was completed on the clog material accumulated within the pipe rings at different times. The main type of minerals detected were calcium types such as aragonite ($CaCO_3$), monohydrocalcite ($CaCO_3H_2O$), calcite ($CaCO_3$), dolomite $CaMg(CO_3)_2$ and gypsum ($CaSO_4 \cdot 2H2O$). In addition, there were small amounts of moganite (SiO_2) and quartz (SiO_2) detected, but principally calcium containing minerals (See Appendix I). From these results, it can be deduced that as clogging changes its mineral composition over time, it will affect the landfill manager's selection of chemicals for cleaning the pipes.

According to Lozecznik (2006), laboratory pipes pumping leachate from Brady Road Landfill developed an inorganic clog layer coating the wetted perimeter of the pipes with hydromagnesite ($Mg_5(CO_3)_4(OH)_24H_2O$) as the sole phase mineral. As mentioned above, this study has shown different types of minerals sampled from the clog material collected through time. This difference can be partially attributed to the use of leachate from different wells for the current study, whereas the past study mainly collected leachate

from a single well. In addition, it was previously suggested by Lozecznik (2006) that higher Mg^{2+} than Ca^{2+} content had an impact on the mineralogy of the clogging sampled from the laboratory pipes. However, Lozecznik (2006) did not measure Mg^{2+} in the leachate.

Reddy and Wang (1980) analyzed the crystal growth inhibition of calcium carbonate ($CaCO_3$) minerals by different concentrations of Mg^{2+} in stable supersaturated solutions and concluded that Mg^{2+} concentrations close to 10^{-3} M at pH values over 8.8 inhibited calcium carbonate mineral formation. Lozecznik (2006) attained higher leachate pH values during pumping ($8.3 < pH < 9.4$) than this study ($pH < 8.8$;), and higher Mg^{2+} concentration than 10^{-3} M (approximately 24 mg/L) were historically sampled from the landfill well (City of Winnipeg Leachate Data – personal communication) used in this past study (the study did not measure Mg^{2+}), thus the main Mg^{2+} mineral type developed within the pipes ($Mg_5(CO_3)_4(OH)_24H_2O$) agrees with Reddy and Wang (1980) analysis. This is important because the inorganic minerals forming clogging impact the selection of a chemical cleaning method.

SEM photography of clog material attached within pipe series 3, 5 and 8 was performed on the second and third pipe rings collected, as shown in Figure 3.26 (all using a magnification of 2500X). Pipe series 3 (Figure 3.26a) shows a combined presence of small rod clusters with larger euhedral crystals embedded, forming a matrix of minerals and organic materials. Pipe series 5 (Figure 3.26b) shows a combined presence of small amounts of euhedral crystals with sharp spread crystals forming a matrix of minerals.

Pipe series 8 (3.26c) shows mainly rod clusters forming a matrix of minerals. Pipe series 3 operated at a higher Reynolds number (31,795) than pipe series 5 and 8 (24,192 and 1,898 respectively). Clogging in Pipe series 3 was therefore more compacted and thinner than the rest of the pipe series because of the higher wall shear stress

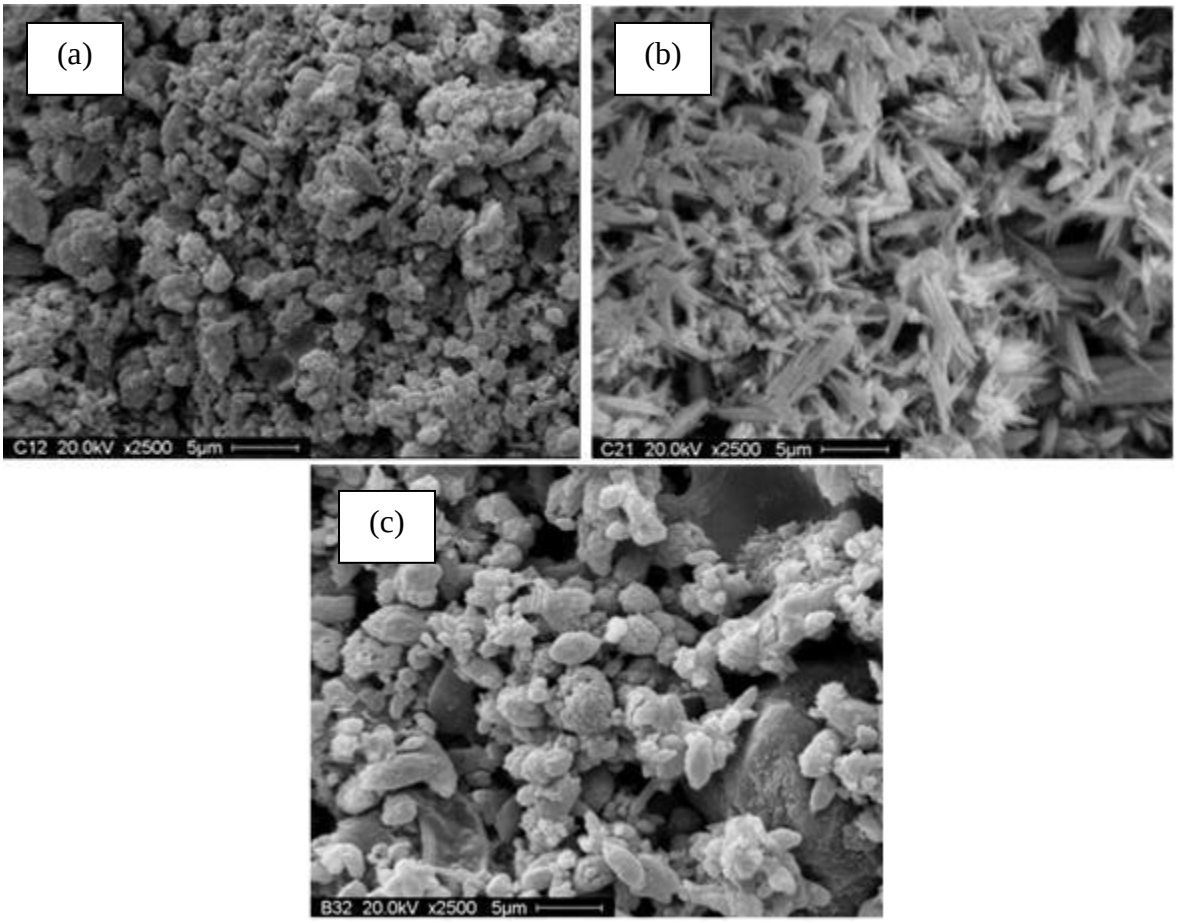

Figure 3.26. SEM photographs showing a magnification of 2500X from the mass accumulated inside of the second pipe rings for (a) pipe series 3 and the third pipe rings for (b) pipe series 5 and (c) pipe series 8.

XRD performed on pipe series 3 and 5 show monohydrocalcite as a single mineral phase; pipe series 8 was a combination of monohydrocalcite, aragonite and quartz. From above and Figure 3.4.2 it can be observed that for similar clogging mineralogy, denser clog material was developed within the highest Reynolds numbers pipes. This is explained as

higher shear forces were exerted within the pipe walls over time. This could affect the cleaning efficiency of the pipes, for example, if mechanical cleaning is adopted by the landfill manager.

From the observations of the clog material (Figures 3.13 and 3.14) and SEM (Figure 3.26), it can be deduced that the accumulation of clog material on the pipe wall will change the wall roughness, or rugosity of the pipe. A rougher pipe wall may give rise to larger head losses which may also impair the uniform discharge of leachate along the length of the pipelines, by not wetting the waste homogenously. Head losses within the pipes were measured between October, 2009 and November, 2010 (see Appendix J).

3.4.2.10 Friction factor analyses

In order to estimate the initial friction factor for the all the pipe series, clean water was ran through the testing pipes before leachate was tested for the current study. Only the 0.04 internal diameter pipes with the flow rates selected produced measurable frictional losses (ie. > 3 mm). The initial friction factors ranged from 0.018 to 0.03 for pipe series 1, 2 and 3.

As clogging accumulated within the pipes, variations in pressure readings were measured (see Appendix J). Although more clogging was collected from the pipe series with large diameters (series 7 and 8), only the smaller pipe diameters (pipe series 1, 2 and 3) showed significant head losses, hence friction factor changes at different times, as shown in

Figure 3.27. Since the pressure transducer used had a maximum accuracy of 3 mm, the larger pipe diameter (pipe series 4 to 6 and pipe series 7 and 8) had to exhibit a large amount of clog deposition (20% and 60% of blockage for pipe series 4 to 6 and 7 to 8) in order to attain a head loss value of 3 mm. Figure 3.27(a), (b) and (c) show the friction factor calculated from pipe series 1, 2 and 3 over time.

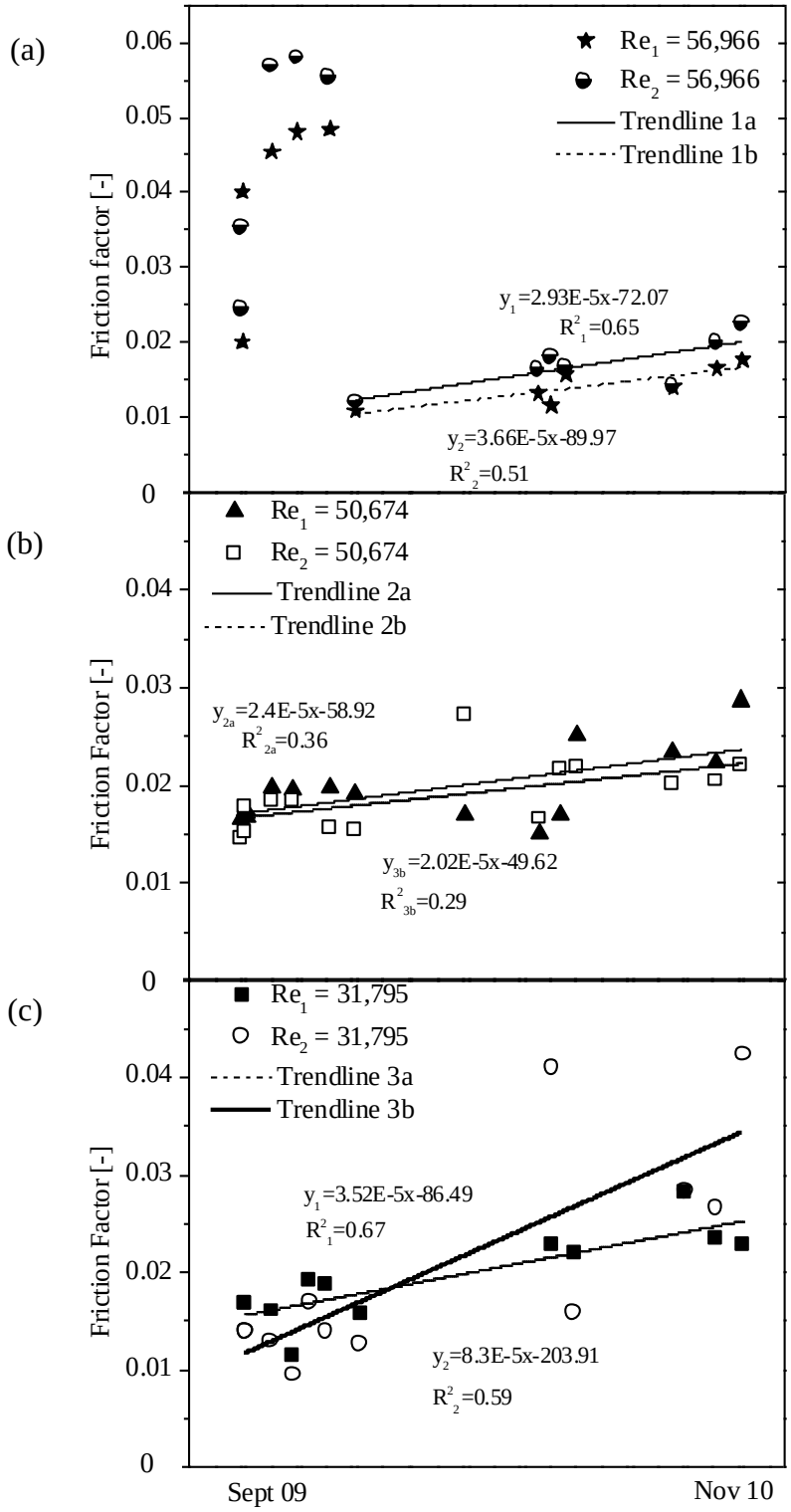

Figure 3.27. Friction factor values calculated for pipe series (a) 1, (b) 2 and (c) 3 over time (all pipes ID 0.04m).

Figures 3.27 (b) and (c) show an initial friction factor (relatively clean pipes) ranging from 0.014 to 0.017, and after a year of operation and clog accumulation, it increased between approximately 47 to 63% for pipe series 2 and 20% to 59% for pipe series 3. The relationship for an increasing friction factor was approximated with a linear trend line for pipe series 2 and 3 with HDPE pipes of 0.048 m internal diameter operating at Reynolds numbers between 30,000 and 50,000.

Figure 3.27a shows two different trends over time, where for the first two months there was a significant increase in friction factor values (ranging from 0.02 to 0.055), and for the remainder of the time there was a small increase of friction factor values over time (ranging from 0.013 to 0.018). This second trend was demonstrated by using a linear fit, as shown in Figure 3.27a. This inconsistency could be explained by the required changes made in the flow rates adopted within these pipe series after three months of operation, explained as follows.

Originally, the pipes and flow rates selected for this study were sized to achieve Reynolds numbers between 1,500 and 100,000. After over two months of operation, the pumps connected to the pipe series 1 developed a significant amount of clogging, affecting the maximum flow rates originally selected (2.3 L/s). Based on this situation, the pumps were cleaned and switched with the pumps connected to the pipe series 2, where the maximum new flow rate attained for the pumps feeding the pipe series 1 was 1.72 L/s. This new flow rate was selected after several trials were made to reach the maximum pump capacity (assuming clogging in the next year or so) and attaining a Reynolds number of

approximately 60,000. Therefore, clogging accumulated and attached at earlier stages of operation with the initial maximum flow rate selected (2.3 L/s) produced high friction factor values (0.02 to 0.06) in the short term. The new maximum flow rate selected (1.72 L/s) gave rise to a lower increase in friction factor values over time, as shown in Figure 3.27a. High friction factor values will affect the overall pump operation and result in increased cost to the landfill manager in order to homogenously wet the waste after a year of operation. From these results, it can be concluded that selecting a small pipe diameter and not cleaning frequently against clog development will decrease the benefits of leachate recirculation.

Inlet head was also measured at different times, but as clogging developed within the pumps, some of the flow rates selected for different pipe series could not be attained. Thus, pumps with clog material were removed and cleaned to continue their operation. The cleaning of the pumps resulted in a change to the inlet head delivered in some cases. Some of the submersible pumps stopped their operation and had to be replaced due to the amount of clogging accumulated outside/inside of the pump (See appendix K). This may suggest that submersible pumps may not be the most suitable pumps to convey leachate under pressurized conditions. Figures 3.28 show the inlet head required for pipes series (a) 1, 2 and 3, (b) 4, 5 and 6 and (c) 7 and 8 to deliver the flow rate selected at different elapsed times. For the first three months (September to November of 2009) there was a period of adjustment where some of the pumps did not deliver the flow rates selected (Appendix J) so changes were made. From Figure 3.28, it can be observed that after November 14 of 2009, higher inlet head values were required until the end of the study to

maintain the flow rates selected for the pipe series 1 to 6 (internal diameter 0.04m and 0.09m). Pipe series 7 and 8 (internal diameter of 13.4 cm) did not show significant changes as the inlet head values were less than 12 cm at all times. The most dramatic increase was observed within the smaller pipe diameter operated at the highest Reynolds numbers and inlet heads (pipe series 1), increasing to a maximum of approximately 1 m (72%) of head (due to clogging) until the end of the study. A dropped in inlet head for the pipe series 4, 5 and 6 was observed for the last data points (Figure 3.21b) which was as a result of the regular cleaning that was ongoing at that time for the excess of clogging collected within these pumps (Appendix K).

From these results, it can be deduced that significant increases to the required inlet head of the injection pipe systems, using small pipe diameter and high head pumps, are expected to occur after clogging develops.

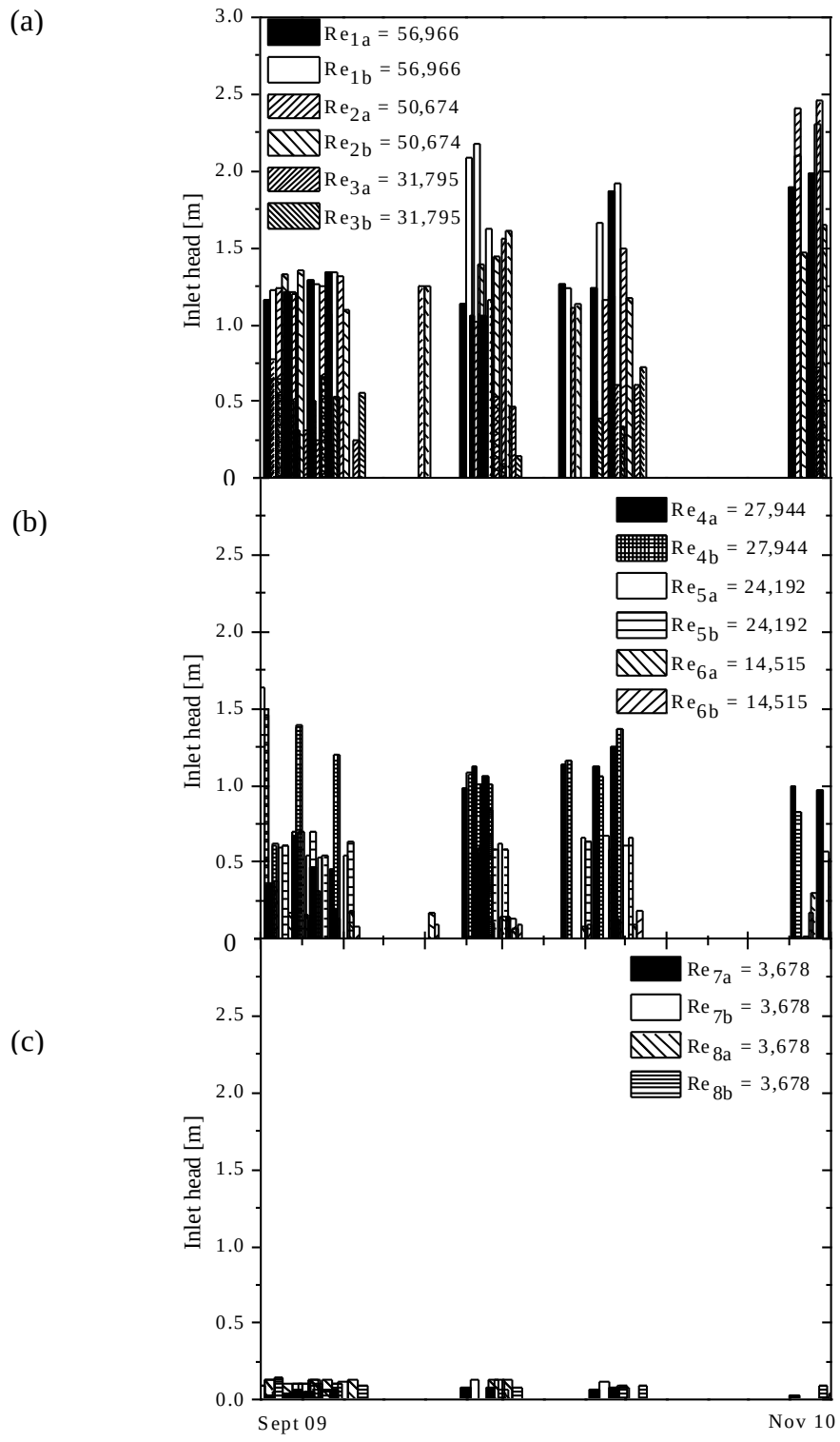

Figure 3.28. Inlet head required for pipes series (a) 1, 2 and 3 (ID 0.04m), (b) 4, 5 and 6 (ID 0.09m) and (c) 7 and 8 (ID 0.13m) to deliver the flow rate selected through time.

3.4.3 Proposed conceptual model of clogging in leachate injection systems

Based on (a) the extensive body of research of clogging in LCS explained in Section 1.6.2, (b) the applicant's M.Sc. laboratory study and (c) the results from this pilot study, the following two pipe clogging conceptual models are proposed. The proposed models are for when the leachate is flowing and for when it is stagnant.

In general terms the development of clog material in leachate transmission pipes occurs as a multilayer of inorganic and volatile material attached and deposited within the pipe walls (see Figure 3.4.28 and 3.4.29).

The conceptual models include the following mechanisms: VFA utilization in biofilm, VFA utilization in suspended microorganisms, biofilm growth and decay, CO_2 outgassing and dissolution, biogenically produced CO_2, biofilm attachment and detachment, mineral precipitation, suspended inorganic particles attachment, and detachment. The mechanisms of clogging for each case are represented by arrows in the figures below; the size of the arrows highlights the relative importance of the individual clogging mechanisms during each pump operation schedule and the direction represents the inside perimeter of the pipe where the dynamics of the mechanisms are identified.

a) Leachate flowing (Flow rate (Q) > 0 L/s)

When leachate is flowing (Q > 0 L/s), clogging is primarily controlled by the hydraulic operation of the pipe and the impact that this operation has on the dissolved CO_2 concentration within the leachate. Shear stress exerted on the organic and inorganic material accumulated within the pipe walls can also affect clogging. No significant

biofilm activity or suspended microorganisms are expected due to the short retention time that is maintained within the pipe and the shear stress magnitude (hydrodynamics) applied onto the biofilm surface. High turbulence may reduce the diffusivity of substrates in the biofilm (Liu and Tay 2002) affecting the mass-transport of VFA within the biofilm, limiting its growth. Figure 3.29 a and b represent the conceptual mechanisms of clogging inside the leachate transmission pipes when leachate is flowing and stagnant. Higher CO_2 degasification is expected due to turbulence. This increases the pH value, unbalancing the chemical equilibrium in the leachate. It may also increase leachate temperature due to (1) pump operation, (2) friction of the leachate on the pipe walls due to the growth of biofilm during stagnancy and (3) landfill temperature versus leachate temperature. The increase in temperature affects the amount of CO_2 outgassing that occurs.

This conceptual model represents an ideal section of the middle of the pipe. Clogging moves along the length of the pipe due to the shear forces acting on the pipe walls each time the pump is turned on, as shown in Section 3.4.2.6. This occurs when the pump starts operating but also during regular operation. A difference in clog accumulation within the first and the last section of the pipe can occur as a result. Greater clog accumulation at the end of the pipe may facilitate the creation of dead zones, which can lead to decreased recirculation in the landfill; this can impair bioreactor operations and limit the advantages of bioreactor treatment. No field studies have reported this observation.

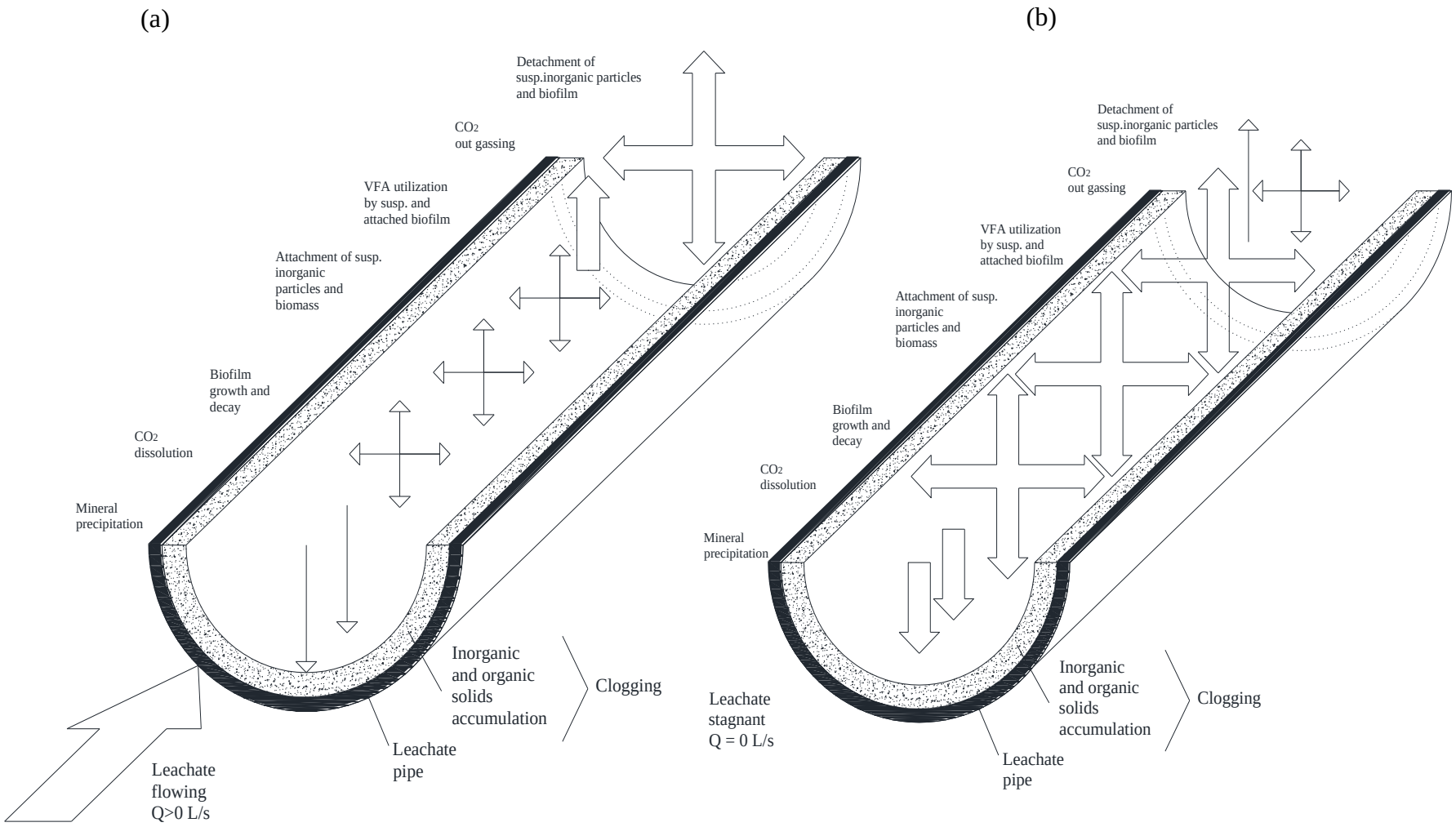

Figure 3.29. Conceptual model of clogging along the length of a leachate pipe when (a) leachate is flowing and (b) stagnant (Not to scale)

a) Leachate stagnant (Flow rate (Q) = 0 L/s)

When leachate is stagnant (Q = 0 L/s) clogging is primarily controlled by the sedimentation of suspended solids from the leachate, as leachate exits the pipe though the perforations, which are commonly located at the bottom of the pipe. In addition, the biological activities of suspended and attached biomass are expected to play an important role if the conditions in the pipe are favorable for their growth (e.g. leachate pH, etc). Leachate exits the pipe through perforations during stagnancy creating a headspace where biofilm growth and suspended microorganisms produce CO_2. Prior turbulent conditions (pipe flowing) also increases the CO_2 in leachate. Due to steeper CO_2 concentration gradients and the increase in partial pressure (PCO_2) in the headspace, CO_2 dissolution can be expected. If there is insufficient buffering capacity in the leachate CO_2 dissolution will lower the pH and increase the carbonate content of the leachate in the pipe. Carbonate (CO_3^{2-}) can then bind with Ca^{2+} from the leachate, precipitating as $CaCO_3$ minerals. Biofilm and suspended particles attach to the pipe and the deposits of minerals formed during flow and stagnant conditions.

3.5 CONCLUSIONS

This pilot study was conducted to assess leachate degradation and rate of clog formation within several HDPE pipes (internal diameter of 0.048, 0.092 and 0.134 m) operated at different flow rates and injection schedules under controlled conditions. This study was conducted inside of a specially built research facility on the site of the Brady Road Municipal Landfill in Winnipeg, Manitoba. The parallel laboratory samplings were conducted at the University of Manitoba's Environmental Engineering, Geotechnical Engineering and Geology laboratories. During this study, the leachate chemistry was significantly different for the summer months (more concentrated), so the analyses of the leachate degradation were mainly divided into two scenarios or seasons, which were Sept. 2009- June 2010 and June-Sept.2010.

The main mechanism impacting leachate degradation and clog formation during this study was the kinetics of CO_2 gas transfer, mainly controlled by the increase in leachate temperature and turbulent conditions within the pipe series. On average, 50% of the dissolved CO_2 in the leachate evolved during pumping and 4 to 18% re-equilibrated back during stagnation. This impacted the pH, hence the leachate chemistry. The average COD removal values remained small over time during pumping (<14%) and stagnation (<19%). VFA were sampled from the pipe series 1, 2, 4 and 6 during one testing cycle for 42 hours of stagnation, showing only a maximum removal of acetate, propionate and butyrate of 18%, 15% and 26%, respectively. These results indicate that the overall effect of CO_2 gas transfer was more important than biological activity within the tested pipes. These results provide significant new evidence that leachate has an important

amount of CO_2 gas and handling methods in solid waste facilities around the world (e.g. pumping) must be reviewed in order to minimize clogging. Finally, turbulence intensity, temperature increase and CO_2 outgassing could not be isolated as the testing pipes were all discharging to a common external tank, so further laboratory testing is needed.

Because significant CO_2 outgassing was measured during pumping, leachate pH values increased approximately one unit after pumping (above 8), and during stagnation decreased an average of 0.3 units, due mainly to the CO_2 equilibration and $CaCO_3$ precipitation. Since the pH increased significantly, Ca^{2+} was removed during pumping (averaged 77 mg/L during fall-winter 2009-2010 and 319 mg/L during summer of 2010 seasons) and 42 hours of stagnation (averaged 92 mg/L during fall-winter 2009-2010 and 136 mg/L summer of 2010 seasons) during the entire study, inside of the testing pipes. The removal of Ca^{2+} suggested that inorganic dissolved solids were precipitating within the testing pipes.

TSS results revealed two different trends in removal or production during fall-winter 2009-2010 and summer of 2010. For the first season, average TSS was removed in an amount of about 28% during pumping and 65% during the 42 hours of stagnation. For the second season, average TSS increased to 85% immediately after pumping, and an average TSS of 79% was removed during the 42 hours of stagnation. These results show that after significant amount of clogging formed within the tanks, hoses, and pipes, some of this material was transported with the flow to the testing pipes, enhancing the clogging rate of the pipes. A similar trend was observed with ISS and VSS, where most of the ISS

settled during stagnation, showing that sedimentation was the main mechanism of TSS removal during stagnation. These changes in concentration of Ca^{2+}, COD, alkalinity, TSS, VSS and ISS during pumping and stagnation, indicated that organic and inorganic clogging accumulated within the pipe series over time.

The configuration of the clog material accumulated within the pipe series was different within the tested pipes. For the smaller pipe diameter (0.048 m internal pipe diameter) clogging was mainly formed as a single layer around the wetted perimeter. For the larger pipe diameters (0.092 m and 0.134 m internal pipe diameter) clogging was mainly formed by multilayers of slime and harder thin layers of clogging accumulated at the bottom half of the pipe series. These different configurations may have been the result of (a) sedimentation effect during stagnation and (b) shear stress effect within the pipe walls during pumping, which was higher within the small pipes. In addition, sedimentation will impair the hydraulic performance of any perforation located at the bottom of the pipe over time.

The clog analyses of this study are unique, as to the applicant`s knowledge there has not been any other study of clogging in injection pipes that has assessed the biological, chemical and physical changes of clogging through time.

After approximately a year of operation, the accumulation of clogging was larger within the larger pipe diameter (7 to 8 kg/m^2 of pipe) than small pipe diameter (0.5 to 1.5 kg/m^2 of pipe). Clog composition changed over times within all the pipe series. There was an

important variation in water versus solids content (6.5 to 22%) within the pipes of small diameter (pipe series 1, 2 and 3) where the clog became "harder" after a year of operation. This change in composition will impact the effectiveness of the mechanical cleaning strategy (e.g. water pressure) adopted by the landfill manager if clogging is not removed at the earlier stages of formation. The bulk density results show that larger pipe diameters promote clog material with low densities (0.8 to 0.9 mg TS/m^3 for first coupon), which facilitate cleaning by mechanical means.

The organic and inorganic composition of the clogging also changed within all the pipe series through time. The inorganic content of clogging collected from the pipe series increased from approximately 65% for the first coupon to approximately 88% for the last coupon collected. These results confirm that clog material turned inorganic over time within all the pipe series. Calcium, Iron and Magnesium were the main inorganic clog constituents with aragonite ($CaCO_3$), monohydrocalcite ($CaCO_3H_2O$), calcite ($CaCO_3$), dolomite $CaMg(CO_3)_2$ and gypsum ($CaSO_4 \cdot 2H2O$) as the mainly secondary mineral sampled from the pipe series.

The maximum COD and VFA removal rates were measured within the pipe series operated at Reynolds number of 30,000, indicating that the biofilm developed within these pipes had higher concentration of methanogens and synthrophs than the rest of the pipe series.

Clog rates were substantially higher for the pipes operated at Reynolds numbers lower than 15,000 (pipe series 6, 7 and 8), increasing 3.5 to 5.5 times from the first to the last coupon sampled. This indicated that sedimentation of TSS and clog material travelling within the pipes had a significant effect on the overall clog material accumulated within the pipe series during this study.

For the distribution of final clog accumulation within the pipe series, the greatest mass differences were found within the pipes operated under the lowest Reynolds numbers (between 1,500 to 4,000 respectively), ranging between 13 to 16 times the total clog mass collected between outlet and inlet. This difference is mainly attributed to the larger and softer clogging mass developed within these pipe series and its capability of moving along the length of the pipes over time.

Pipe series operated at high Reynolds numbers (Re > 30,000) showed significant head losses, hence friction factor changes over time, increasing from 20 to 63% of the initial friction factor assessed at the beginning of the study. This increase affects the pump operation time employed to achieve the flow rate previously selected (longer pumping time), impacting the energy required and associated costs.

Higher inlet head values over time were measured for the smaller pipe diameter operated at the highest Reynolds numbers and inlet heads (pipe series 1), increasing by a maximum of approximately 1 m, 72% of the initial head due to clogging. Based on the results, small pipes and high head (and flow rate) pumps used in leachate injection

systems may be hydraulically impaired in less than one year of operation. In addition, some of the submersible pumps have had problems attaining the specified flow rates values, creating clogging issues that required stopping the operation of the system to clean or replace the pumps. Therefore, submersible pumps may not be the optimal choice for leachate injection systems.

3.6 RECOMMENDATIONS

This study has shown that pipe design and its hydraulic operation have a direct impact on leachate degradation and clogging composition within injection pipes used in bioreactor landfills. Based on the results presented above, some recommendations to minimize pipe clogging are

(a) For engineers

- By evacuating leachate standing within the pipes during the first 24 hours after each recirculation, clogging produced by TSS, VSS and FSS removal can be minimized.
- Filters can be installed within the pipes, where the injection lines are entering into the waste cell, minimizing solids carried over with the flow and accumulating along the perforated pipes. However, regular cleaning of these filters must be performed to maintain the hydraulic performance of the system.
- Since operating the injection pipes at high turbulence increases the CO_2 outgassing and low turbulence increases the solids accumulating within the pipes, it is recommended to operate the systems at low turbulence and regularly clean the lines. Adding a filter to the pipe inlet will decrease the required cleaning

intervals of the pipes. As clogging moved along the length of the pipe series over time, where potential dead recirculation zones can be formed, considerations should be given to design shorter perforated pipes that can be cleaned often or designing the pipes with an end cap that can be open and clogging can be flushed outside of the waste pile.

- The current design of perforated injection pipes with dead ends (embedded or not in trenches) has a negative effect over time, since without periodic cleaning solids accumulated within the leachate recirculation components (tanks, pumps and pipes) will be carried over to the end of the system (perforated pipes), increasing the rate of clogging. Designing perforated pipe loops inside of the Bioreactor Landfill will have the benefit of flushing the lines, limiting clogging accumulation.
- In general, larger pipe diameter and perforations are desired to minimize the hydraulic impairment of the injection pipes (for all other conditions being equal) produced by clogging in the short term. Designing the pipe perforations on the sides rather than the bottom will limit the effects of clogging formation during leachate stagnation, extending the hydraulic performance and service life of the pipe and perforations. However, pipe hydraulic design (uniform discharge between first and last perforation), leachate availability and targeted waste moisture must be taken into consideration.
- As clogging changes in quantity and quality through time, a monthly pipe cleaning strategy would help to reduce the detrimental effect of clogging within

the injection pipes and minimize the use of chemicals before substantial clogging is formed and becomes more dense.

- A chemical solution that can break the calcium carbonate ($CaCO_3$) bond may help to dissolve clogging within leachate transmission pipes.
- If leachate is treated by removing Ca^{2+}, CO_2, COD and TSS prior to recirculation, the clogging potential within the pipelines would be minimized.

(b) For operators

- After the leachate is pumped through the appropriate injection lines, the pipes must be drained.
- Regularly opening and closing valves is required to minimize the clogging effects and maintain their operation.
- The leachate tank needs to be cleaned periodically to minimize solids accumulating inside of it. If not, solids will be carried to the end of the line, increasing the clogging rate in the injection pipes.
- Constant monitoring of flow rates and pressure losses within the main header pipe and injection lines (outside of the waste cell) are required to track potential "early" clogging development within the pipes and pumps.
- If clogging is detected, immediate attention is required and the cleaning methodology adopted by the landfill engineer must be followed.
- If filters are installed within pipes to minimize clogging, these must be collected and cleaned regularly. If mechanical cleaning cannot be performed any longer

(hard encrustation), chemical cleaning is recommended (engineer recommendations).

CHAPTER 4: EFFECTS OF TURBULENCE AND TEMPERATURE ON LEACHATE CHEMISTRY

4.1 INTRODUCTION

The kinetics of CO_2 gas transfer during pumping and stagnation were the main mechanisms impacting leachate degradation and clog formation, as shown in the pilot study described in Chapter 3. These results provided new evidence that leachate contains a significant amount of dissolved CO_2 .Handling methods in solid waste facilities around the world should be reviewed to minimize CO_2 outgassing and clogging problems. Nevertheless, this study did not isolate the effects of turbulence intensity and temperature increase, so conclusions of which one of these two variables had a higher relative importance were not drawn.

Turbulence within the leachate pipes is directly affected by the hydraulic design and operation of the leachate injection systems (flow rate, pipe material, length and diameter, perforation shape and spacing) adopted by the landfill engineer. The leachate temperature outside or inside of the waste varies, depending on the weather conditions where the landfill is located and the temperature of the waste. Municipal Solid Waste (MSW) landfills around the world have reported temperatures ranging from approximately 30 to 65°C (Rowe *et al.* 2004; Southen and Rowe 2005, Hanson, J.L. *et al.* 2010). Bioreactor landfills have reported temperatures ranging from approximately 30 to 60°C (Yolo County Landfill, Yazdani 2002), 32 to 54°C (New River Regional Landfill, Reinhart *et*

Material presented in this chapter has been reported in: Lozecznik, S, Oleszkiewicz, J.A., Sparling, R., Clark, S. and VanGulck, J. (2011). Effects of turbulence and temperature on leachate chemistry. *Journal of Environmental Engineering* 138(5), 562-569.

al. (2002), and 40 to 60°C (Columbia Country Baker Place Road Landfill and Atlanta Landfill, Hudgins and Harper 1999).

While Canadian landfills may reach similar temperatures, the temperature in external holding tanks may vary seasonally between 0 and 30˚C. For example, the temperature of leachate collected from the wells during the pilot study varied between 7.5 to 18.7˚C. After pumping, leachate reached temperatures over 20˚C at all times. This suggests that bioreactor landfills in cold climates may experience a significant increase in leachate temperature after leachate is recirculated back to the waste cell. It is hypothesized that an increase in leachate temperature and turbulence will increase the CO_2 outgassing from the leachate, thus affecting the pH values. Higher leachate pH values have been linked with the removal of dissolved Ca^{2+} as calcium carbonate (CaCO3) precipitants, forming clogging.

4.2 OBJECTIVES

The overall goal of the research described here aimed to investigate the role of temperature and turbulence intensity on leachate chemistry, especially CO_2, Ca^{2+} and pH. The specific goals of this research were to

- Investigate the relationship between turbulence and CO_2 evolution under sealed (pressurized pipe) and open conditions using synthetic and real leachate.
- Evaluate the impact of temperature on leachate degradation and clogging evolvement under sealed and open conditions.

- Compare some of the results obtained in the laboratory study with the geochemical modeling software MINEQL+.
- Using the results, identify potential solutions to minimize clogging within leachate injection systems

Developing a relationship between turbulence, pH increment and CO_2 evolution can be used to provide guidance for bioreactor landfill operations to minimize clogging within the pipelines and maximize methane production within the bioreactor cell.

4.3 METHODOLOGY

Sealed reactors with rotating impellers were used to represent some of the turbulent flow conditions operated in the testing pipes of the pilot study. A control reactor with stationary leachate (no mixing) was used to help isolate the effect of leachate temperature change, as the leachate was warmed from approximately 4ºC to 22ºC (cold chamber to room temperature). This change in temperature is characteristic of what can occur during leachate reinjection in cold temperatures. After mixing, some of the leachate was kept in the sealed reactor, while some was extracted and left open to the atmosphere. The leachate samples exposed to the atmosphere represent leachate at the pipe discharge point or at perforations and any CO_2 leak along the length of the pipe.

The range of Reynolds numbers used in the pilot study (Chapter 3) were selected to be representative of design values used in Bioreactor Landfills in the US and Canada (Table 2.2). In order to mimic the turbulent flow conditions of the testing pipes in the pilot

study (and therefore the literature values) using air-tight sealed reactors, the energy dissipation rate of the chosen turbulent flow pipes were matched with the energy dissipation rate of the mixers using the formula presented by Bouyer *et al*. (2005).The energy dissipation rate per unit of mass within the pipe (ε_{pipe}) is given by:

$$\varepsilon_{pipe} = \frac{f^{3/2} U^3}{2D} \tag{4.1}$$

where f is the friction factor [-], U is the average velocity [m/s] and D is the internal pipe diameter [m].

The energy dissipation rate in the reactors ($\varepsilon_{reactor}$) can be estimated using

$$\varepsilon_{reactor} = \frac{P}{\rho V} \tag{4.2}$$

where P is the power dissipated in the mixer [$kg \cdot m^2 \cdot s^{-3}$], ρ is the density of the fluid [$kg \cdot m^3$] and V is the volume of liquid in the reactor [m^3].

In order to calculate $\varepsilon_{reactor}$, the global power dissipated in the mixer is calculated from the power number associated with the impeller as follows

$$N_p = \frac{P}{\rho N^3 d^5} \tag{4.3}$$

where N is the impeller velocity [rpm] and d is the impeller diameter [m].

There is a relationship between Reynolds number and N which is expressed as follows

$$R_e = \frac{Nd^2}{\nu} \tag{4.4}$$

where ν is the kinematic viscosity (L^2T^{-1}).

The same reactor configuration and design values were adopted from Nagata (1975) from which different N_p values were calculated.

An iterative process was required to match the energy dissipation rate of the pipe and reactor, where equations (4.1) and (4.2) must be identical. Assuming *N*, the Reynolds number in the reactor is calculated using equation (4.4). Using the graphs of N_p versus Reynolds number developed by Nagata (1975), N_p is obtained and used in equation (4.3) to calculate the energy dissipation value of the reactor ($\varepsilon_{reactor}$). This process is repeated with different values of *N* until $\varepsilon_{reactor} = \varepsilon_{pipe}$. The $\varepsilon_{reactor}$, ε_{pipe}, *N* and the Reynolds number of different flow rates evaluated for a pipe of 0.048 m internal diameter and reactors calculated using the above procedure are shown in Table 4.1.

Table 4.1**.** Pipe and mixer energy dissipation values

Flow rate [L/s]	**Reynolds number [-]**	$\boldsymbol{\varepsilon_{pipe}}$ **[m^2/s^3]**	***N*** **rpm**	$\boldsymbol{\varepsilon_{reactor}}$ **[m^2/s^3]**
0.27	8777	1.8×10^{-4}	32	1.8×10^{-4}
0.76	25171	2.9×10^{-3}	83	2.9×10^{-3}
1.75	57960	2.7×10^{-2}	180	2.7×10^{-2}

It is hypothesized that there will be a direct correlation between increasing energy dissipation values and the amount of CO_2 evolved from the leachate solution. In turn, higher volumes of evolved CO_2 are expected to be associated with higher pH values and dissolved Ca^{2+} removal.

4.3.1 Sealed reactors set-up

The reactor and impeller blade dimensions were adopted from Nagata (1975), with the reactor diameter, D_r = 0.0889 m, leachate height H = 0.137 m and blade position from the bottom of the reactor at h = 0.0475 m. The blade dimensions were 0.071 m in diameter (d) and a height of 0.019 m. Two Cole-Parmer ServoDyne® mixer heads (50008-10) and mixer controllers (50008-00) were used to rotate the impellers for the 32, 83 and 180 rpm tests. The reactor was designed to include sample ports for $CO_{2(gas)}$ and leachate composition analysis, as well a port for measurement of gas evolution as shown in Figure 4.1 (see pictures Appendix M). Influent and effluent leachate samples were taken at times 0hr, 6hr, and 24hr and tested for soluble Ca^{2+} concentration, pH, and temperature. At time 0hr and 6hr the concentration of CO_2 within the headspace of the reactor was measured.

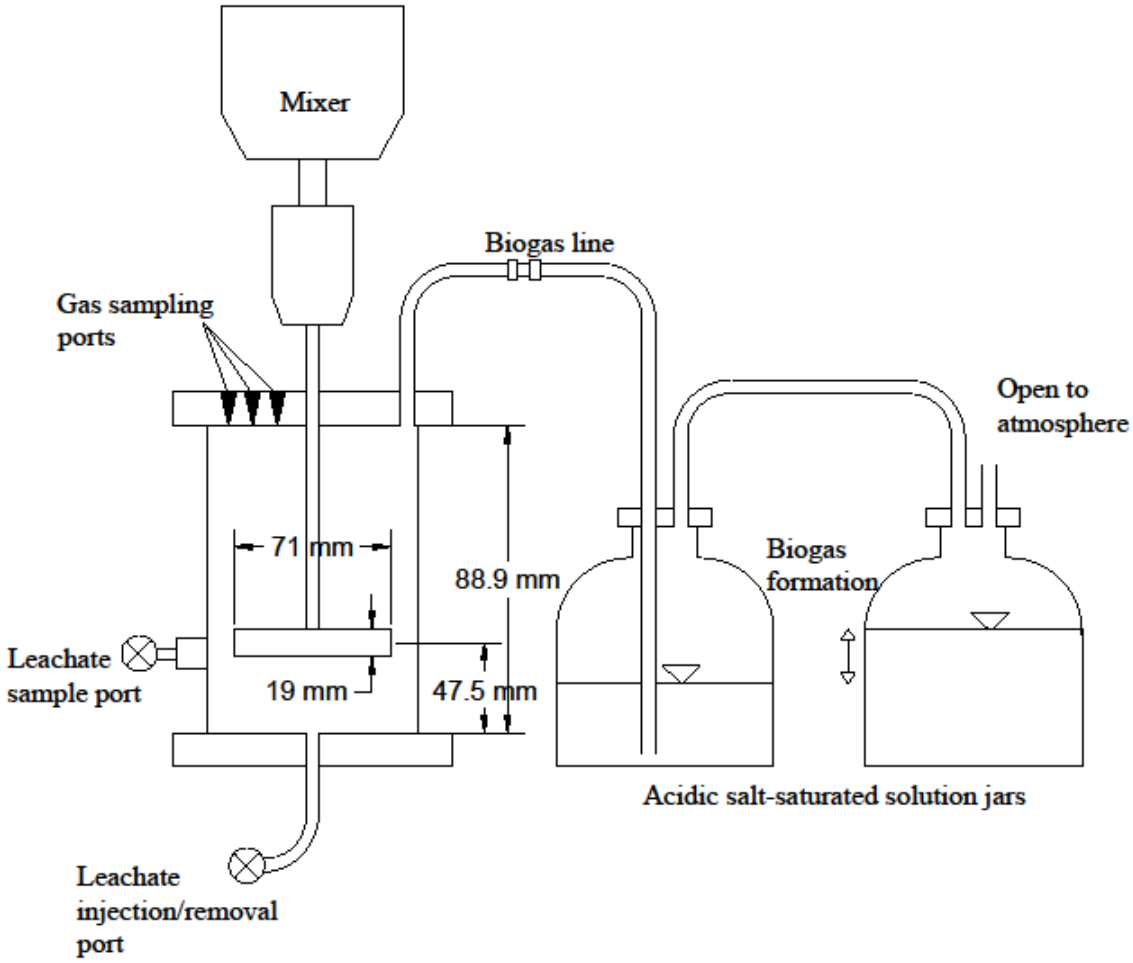

Figure 4.1. Schematic of mixer, reactors and liquid displacement set-up (not to scale)

4.3.2 Leachate preparation and analysis

Duplicate samples were taken for Ca^{2+} and CO_2 concentration. The pH, temperature and dissolved Ca^{2+} values were measured using the same laboratory equipment and methodology used in the laboratory experiments discussed in Chapter 3. The evolved CO_2 was collected and the volume was measured using a liquid displacement method in a 500 mL air-tight calibrated cylinder. The liquid inside of each vessel contained a solution of de-ionized water saturated with 350 g of NaCl, 50 mL of H_2SO_4 and 0.03 g of methyl

orange per liter of solution to prevent gas from dissolving (Puchajda 2006, Wohlgemut 2008). The synthetic leachate was prepared following the formula used by VanGulck and Rowe (2004a) that emulated the leachate characteristics of the Keele Valley Landfill in Ontario, Canada, collected between June and August 1993. This solution mainly consisted of three volatile fatty acids (acetate, propionate and butyrate) with various salts and a trace metal solution, as shown in Table 4.2.

Table 4.2**.** Composition of synthetic leachate

Component	Per litre
Acetate	0.12 M
Propionate	0.067 M
Butyrate	0.01 M
K_2HPO_4	30 mg
$KHCO_3$	312 mg
K_2CO_3	324 mg
NaCl	1440 mg
$NaNO_3$	50 mg
$NaHCO_3$	3012 mg
$CaCl_2$	2882 mg
$MgCl_2•6H_20$	3114 mg
$MgSO_4$	156 mg
NH_4HCO_3	2439 mg
$CO(NH_2)_2$	695 mg
$Na_2S•9H_2O$	Titrate to an Eh 120-180 mV
NaOH	Titrate to a pH 7.0
Trace metal solutions (TMS)	1 ml
Distilled Water	To make 1 l
<u>Composition of trace metal solution (TMS)</u>	
$FeSO_4$	2000 mg
H_3BO_4	50 mg
$ZnSO_4•7H_2O$	50 mg
$CuSO_4•5H_2O$	40 mg
$MnSO_4•7H_2O$	500 mg
$(NH_4)6Mo_7O_{24}•4H_2O$	50 mg
$Al_2(SO)_3•16H_2O$	30 mg
$CoSO_4•7H_2O$	150 mg
$NiSO_4•6H_2O$	500 mg
96% concentration H_2SO_4 (AnalR)	1 mL
Distilled water	To make 1 L

Commonly reported landfill biogas ratios are 50%-50% CH_4-CO_2, but during gas collection, landfill gas collected has higher concentration of CH_4 than CO_2 because some of the CO_2 is dissolved into the leachate forming part of the carbonate system (EPA, 2010). On the other hand, laboratory studies of leachate treatment under anaerobic conditions have shown that biogas produced contained between 60 to 80% of CH_4 (Henry *et al*. 1987, Kennedy *et al*. 1988, Chang 1989), hence CO_2 values lower than 40% were observed. Finally, leachate is commonly collected to a common sump or tank prior to recirculation. It is believed that during this time, the re-equilibration of leachate with the atmosphere (open system) will lower the amount of dissolved CO_2 within the leachate. However, no dissolved CO_2 values in leachate have been reported from laboratory or field studies of clogging in leachate collection systems.

In order to simulate CO_2 saturation conditions expected in real leachate with the synthetic leachate, the solution was saturated with gas by sparging with 20% CO_2 in N_2, and pH titration was performed simultaneously using 2.5N sodium hydroxide (NaOH). This saturation/titration was performed inside of the cold chamber (4°C) for approximately 3 hours in order to maximize the amount of CO_2 within the solution and to represent seasonal cold temperatures.

An initial leachate pH of 7 was chosen to ensure that no precipitation of calcium occurred before turbulence was induced and to represent real leachate values observed at landfills. Before injecting the synthetic leachate into the reactors, the reactors were flushed with 20% CO_2/N_2 gas to ensure the headspace within the reactors had the same conditions and

to ensure the 20% CO_2 initially within the solution. The initial average values of pH, dissolved Ca^{2+} and temperature were approximately 7, 1.0 g/L and 14ºC, respectively.

A second set of studies was performed with real leachate from Brady Road Landfill, collected from the same landfill well where leachate was used in the pilot study. This leachate is representative of waste that has been landfilled between 5 to 15 years. Leachate was drawn from this leachate well by hand (to minimize the loss of dissolved CO_2) and transported to the laboratory in 16 L jars, which were then stored at 4^{o}C to limit biological processes from occurring. Different initial pH values were selected by adding sodium hydroxide (NaOH) to represent the inherent variability of leachate. The initial average values of pH, dissolved Ca^{2+} and temperature for the real leachate were approximately 7,580 mg/L and 10ºC, respectively.

Dilution of dissolved CO_2 and Ca^{2+} by the addition of NaOH was not corrected and it was small compared with the sample of leachate titrated. At the time of transferring the leachate to the sealed reactors, for synthetic leachate, the reactors were flushed with 20% CO_2 in N_2 to ensure saturated conditions. For real leachate conditions, the reactors were flushed with N_2 to represent anaerobic conditions experienced within the pipelines. The mixers were sealed using a high grade silicone sealant as they required being air tight for a period of 24 hrs for each batch test. To test the air tight seal, the reactors were filled with distilled water to the operating leachate height and air was injected to displace the maximum amount of liquid in the volumetric measuring cylinder. The displaced volume was tested for a period of 24 hrs to ensure no loss of gas from the sealed system.

Each batch test was conducted using the following procedure. At time T = 0, the experiment was initiated, which involved running the mixer at the predetermined speed [rpm] for a period of 6 hrs, until time T = 6. At this point, the leachate was divided into two samples and was left static for 18 hrs to simulate the operation of a leachate injection line. During the static period (6 < T < 24), one of the samples was left in the sealed, air-tight reactor, while the second sample was left open to the atmosphere. At time T = 0 the leachate in the reactor was tested for initial pH, soluble Ca^{2+}, and temperature, and the height, h, was set precisely to 0.137 m. The headspace was also sampled for the initial CO_2 concentration. After 6 hrs of mixing at T = 6, the volume of gas that had evolved from the leachate was recorded and the CO_2 concentration in the headspace was measured before the mixer was turned off. A sample of leachate was removed and tested for pH, soluble Ca^{2+} and temperature at the same time. After remaining stationary for 18 hrs, at T = 24, the leachate was tested for pH, soluble Ca^{2+} and temperature.

The geochemical modeling package MINEQL+ was used to simulate the results obtained with real leachate for pH > 7.4 to understand the decrease in pH values experienced under sealed conditions. In addition, the same real leachate conditions were simulated considering 50% of CO_2 in the headspace, to represent the biogas composition observed in real scale landfills (50%-50% CH_4- CO_2).

The following assumptions were made in order to provide the program with the necessary initial data (at time T = 6) and to perform the calculations

- The total carbonate available within the reactor was calculated with the leachate alkalinity as bicarbonate (HCO^{3-}) and the CO_2 evolved and its dissolved counterpart in equilibrium contributing to HCO^{3-} using the Henderson-Hasselbalch equations

- The Ionic Strength (IS) values were taken from Gibs *et al.* (1981) where they calculated the IS values of landfill leachate from Bucks County landfill (PA) for summer (IS = 0.28) and winter (IS =0.4).

  The calculated ionic strength of the synthetic leachate (Table 4.2) was approximately 0.3, so the range of values taken form literature (0.28 and 0.4) represent the conditions tested in this study.

4.4 RESULTS AND DISCUSSIONS

4.4.1 Leachate recirculation under laboratory controlled conditions using synthetic leachate

This set of studies was performed with synthetic leachate to simulate real leachate under controlled laboratory conditions. Under sealed conditions and at mixing rates of 32, 83 and 180 rpm, no significant changes in leachate pH and dissolved Ca^{2+} were observed after the 6 hrs of mixing. Temperature increased for all the reactors from 4˚C when the sample was taken from the cold chamber, to approximately 12 to 15ºC at T = 0 hours (study start-up) and then to 20 – 23ºC at T = 6 and 24 hours. The temperature difference between the mixers and the control reactor was relatively insignificant, ranging from 1-2ºC. Table 4.3 shows the pH, quantity of evolved CO_2 and leachate temperature for the different rpm's tested after 6 hours of operation. The temperature change within the control reactor (from approx. 13 to 22˚C) caused CO_2 degasification (2.4 mL), but it was approximately 3.5 to 4.5 times lower than the measured CO_2 from the mixers. Higher turbulent energy dissipation rates were found to cause a higher amount of evolved CO_2 from solution. It is hypothesized that turbulence removes CO_2 micro bubbles within the leachate that would take much longer than 6 hrs to evolve and equilibrate under stationary conditions.

Table 4.3**.** Average (μ) and standard deviation (σ) of evolved CO_2 (mL), pH and temperature (˚C) from the mixers after 6 hrs of operation at different rpm's.

Parameter	Unit	0 rpm		32 rpm		83 rpm		180 rpm	
		μ	σ	μ	σ	μ	σ	μ	σ
$CO_{2\ (gas)}$	mL	2.43	0.63	8.45	0.51	8.65	0.26	10.73	0.74
pH	-	7.03	0.03	7.07	0.01	7.02	0.01	7.02	0.01
Temperature	˚C	21.8	0.15	21.7	0.14	21.95	0.07	22.35	0.07

These results show that CO_2 outgassing is mainly affected by the turbulence level within the mixers. No significant changes in pH were observed. The mixed reactors and the control reactor were then allowed to remain stagnant for 18 hours. A portion of the liquid was kept in the air-tight reactor, while a portion was left open to the atmosphere. At time T = 24 hours, the pH values of the synthetic leachate under sealed conditions remained around 7 and no important changes in dissolved Ca^{2+} (average 1 g/L) were measured.

For the portion of the leachate that was left open to the atmosphere in open glass beakers in the laboratory, soluble Ca^{+2}, pH and temperature were tested at time T = 24 hours. The dissolved Ca^{2+} and pH results are shown in Figure 4.2. The temperature ranged from 20 to 23 ˚C for all the mixers at 6 and 24 hours, including the control reactor (see data in Appendix N). From Figure 4.2, it can be observed that pH increased by approximately one unit after exposing the samples to atmospheric conditions (from T = 6 to 24 hrs). This increase was found to be independent of the turbulence level, as the control reactor (0 rpm) showed the same trend (Figure 4.2a). The increase in temperature and pH was found to reduce the dissolved Ca^{2+} concentration in the synthetic leachate by over 80%, (Figure 4.2b). In addition to this removal caused by the temperature increase, there is a slight increase in Ca^{2+} removal with increasing turbulence level.

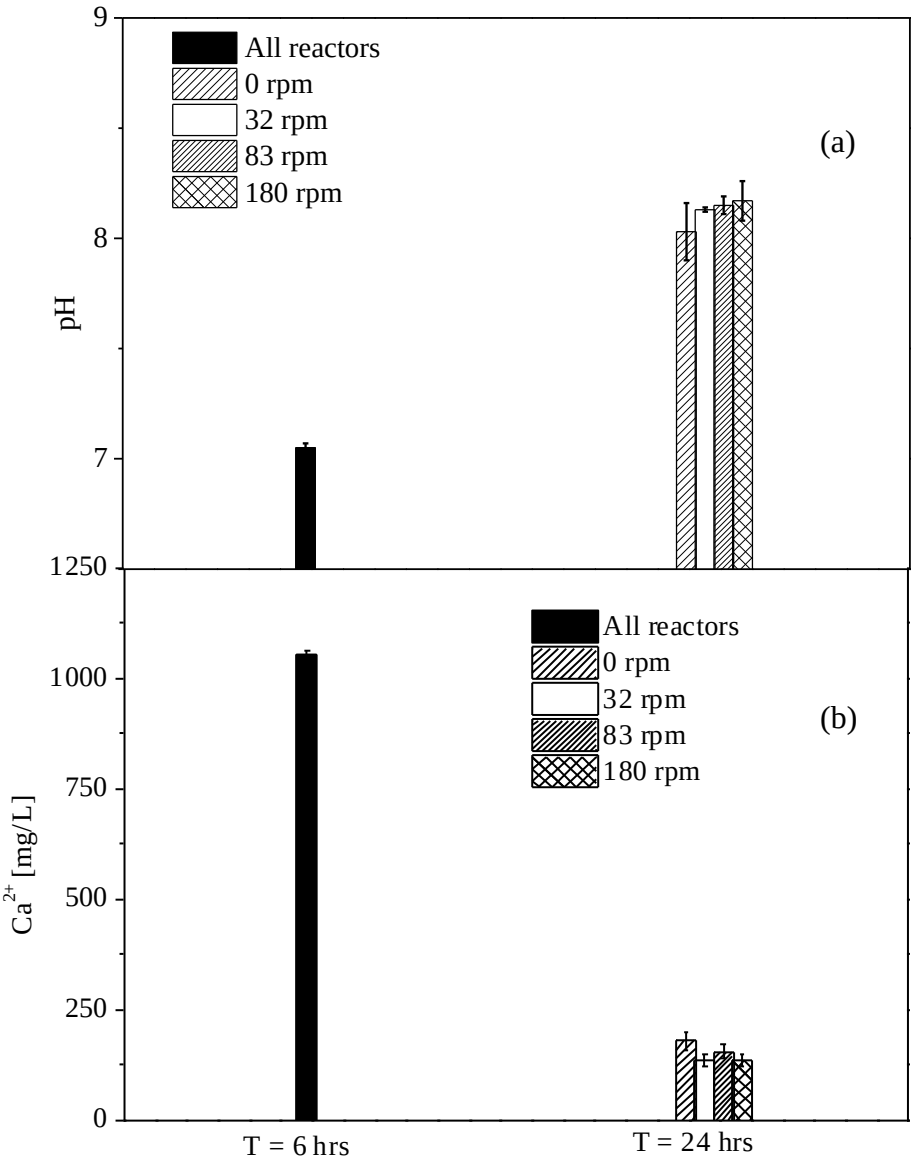

Figure 4.2. (a) Average pH values at T = 6 hrs and T = 24 hrs or after 18 hrs of exposure to atmospheric conditions. (b) Average dissolved Ca^{2+} values at T = 6 hrs and T = 24 hrs or after 18 hrs of exposure to atmospheric conditions. The black line represents the average pH and dissolved Ca^{2+} values for all the mixers and control reactors at T = 6 hours.

These results have mainly shown that as leachate temperature increased and sealed conditions were maintained, no significant changes in the leachate chemistry were measured. However, after leachate was exposed to atmospheric conditions at constant

temperature (between T = 6 and 24 hours), a significant increase in leachate pH and removal of dissolved Ca^{2+} was measured. A higher amount of CO_2 was sampled from the headspace of all reactors at T = 6 hours (sealed conditions), and between T = 6 and 24 hours (open conditions) dissolved CO_2 within the leachate re-equilibrated with the atmosphere, increasing the pH. As pH increased, Ca^{2+} was removed from solution.

4.4.2 Leachate recirculation under laboratory controlled conditions using real leachate from Brady Road Landfill, Winnipeg, Manitoba.

A second set of studies was performed using real leachate from Brady Road Landfill in Winnipeg, Manitoba. Only one control reactor and one reactor mixed at 180 rpm were used. The initial purpose of these studies was to confirm the results obtained with synthetic leachate at the highest rpm tested to demonstrate the relationship between turbulence and closed/open atmospheric conditions. The first sets of studies were performed at an initial pH close to 7. At T = 6 hours, it was found that the reactor operating under turbulent conditions had caused a significant amount of CO_2 evolution when compared to the control reactor. At time T = 24, there were no significant changes to the leachate pH and dissolved Ca^{2+} values under sealed conditions. This was similar to the results obtained from the synthetic leachate tests under sealed conditions. The portion of the leachate exposed to atmospheric conditions experienced a moderate increase in pH to an average value of 7.39, which was less than the average pH value of 8.15 reached with synthetic leachate. This can be explained by noting that the real leachate had a higher buffer capacity (7,350 as $mgCaCO_3/L$) compared with the synthetic leachate (5,900 as $mgCaCO_3/L$), hence a higher resistance to pH changes due to the kinetics of

CO_2 transfer. Since pH increased due to CO_2 evolvement during mixing and atmospheric exposure, approximately 20% of initial dissolved Ca^{2+} was removed out from solution.

Since there is significant variation in leachate composition between landfills around the world (Kjeldsen *et al.* 2002) and even within the same landfill facility (Chapter 3), the same study was repeated with real leachate, but this time with an initial pH value of approximately 7.2 (natural). Since there were no significant changes of Ca^{2+} and pH observed, it was decided to further increase the initial pH values to simulate the injection conditions of a higher leachate pH. Tables 4.4 and 4.5 shows the pH, Ca^{2+}, evolved CO_2 (mL) and temperature (˚C) values obtained by running the mixers and control reactors under the same conditions and by changing the initial pH approximately to 7.5 (study a) and 7.6 (study b) under sealed and open atmospheric conditions (see data in Appendix M). In Table 4.4 it can be observed that no significant changes were obtained with real leachate with regards to pH and dissolved Ca^{2+} values under sealed conditions during mixing and control conditions at T = 6 for the initial pH values tested. There was however, a moderate drop in pH and a moderate increase in the amount of removed Ca^{2+} during the sealed stagnant stage (6 hours < T < 24 hours) for both the mixed and control reactor. There is also a similar trend of pH change and Ca^{2+} removal assessed with synthetic and real leachate during exposure to atmospheric conditions for the mixers and control reactor, as shown in Table 4.5 (see data in Appendix M). This indicates that an increase in temperature of real leachate saturated with CO_2 at higher pH may enhance Ca^{2+} removal under open atmospheric conditions due to CO_2 re-equilibration. Nevertheless, pH dropped after 24 hrs within the control reactors for both studies under

sealed conditions, showing a trend similar to what was observed by the author within the testing pipes of the pilot study (Chapter 3).

Table 4.4**.** Average of pH, dissolved Ca^{2+}, CO_2 evolved and temperature values of real leachate from the mixers and control reactor under sealed conditions

Parameter	Elapsed Time [hr]	Study a		Study b	
		Mixers	Control	Mixers	Control
pH [-]	T = 0	7.48	7.48	7.57	7.57
	T = 6	7.4	7.33	7.57	7.55
	T = 24	7.08	7.17	7.26	7.26
Ca^{2+} [mg/L]	T = 0	385	380	370	370
	T = 6	385	360	355	320
	T = 24	280	340	224	224
CO_2 [mL]	T = 6	8.18	0.87	4.29	0.42
Temperature [˚C]	T = 0	13.7	14.6	15.65	18.1
	T = 6	23.15	22.6	22.9	22.2
	T = 24	22.85	23	21.95	21.8

Table 4.5**.** Average of pH, dissolved Ca^{2+} and temperature values of real leachate from the mixers and control reactor after being exposed to atmospheric conditions for 18 hrs after being mixed for 6 hrs at 180 rpm.

Parameter	Elapsed Time [hr]	Study a		Study b	
		Mixers	Control	Mixers	Control
pH [-]	T = 24	7.83	7.78	7.83	7.78
Ca^{2+} [mg/L]	T = 24	138	152	196	200
Temperature [˚C]	T = 24	22.5	22.2	21.4	21.4

The decrease in pH values after mixing and during stationary conditions can be explained as the decrease of the leachate buffer capacity by the removal of Ca^{2+} as $CaCO_3$, outcompeting the effect on the leachate pH with the removal of dissolved CO_2

(outgassing). In order to verify the accuracy of the results obtained with real leachate and the interpretation of the principles behind a CO_2-pH-$CaCO_3$ system under sealed conditions for a higher initial pH, geochemical modeling using MINEQL+ software was performed.

4.4.3 MINEQL+ SIMULATION

Eight different case scenarios (from Table 4.4) were analyzed, as shown in Tables 4.6 and 4.7:

Table 4.6. Dissolved Ca^{2+}, initial pH, CO_2 (%) in the headspace, total carbonate (CO^{3-}), temperature at T= 6 hours and Ca^{2+} and pH measurements after 24 hours under sealed conditions. Final pH and Ca^{2+} were obtained using MINEQL+ for IS (Ionic strength) of 0.28 and 0.4.

	Units	Case 1	Case 2	Case 3	Case 4
Reactors (T = 6 hours)					
Ca^{2+} [mg/L]	mg/L	360	385	320	355
Initial pH	-	7.33	7.4	7.55	7.57
CO_2	%	17.8	8.7	14.3	4.3
Total CO_3^{-2}	$mmol^{-1}$	0.11	0.14	0.12	0.15
Temperature	˚C	22.6	23.15	22.2	22.9
Ca^{2+} measured (T = 24 hrs)	mg/L	340	280	224	224
pH measured (T = 24 hrs)	-	7.17	7.08	7.26	7.26
MINEQL+					
Final pH (IS=0.28)	-	7.19	7.26	7.41	7.43
Final pH (IS=0.4)	-	7.18	7.25	7.4	7.42
Final Ca^{2+} (IS = 0.28)	mg/L	241	242	204	208
Final Ca^{2+} (IS = 0.4)	mg/L	246	248	208	213

From Table 4.6, a decrease of pH values can be observed for all the cases simulated with MINEQL+, agreeing with the trend obtained in the laboratory as shown in Table 4.4.

Case 1 shows the closer pH values between the geochemical modeling and this study. This may indicate that at these initial pH values, mainly dissolved Ca^{2+} outcompeted the CO_2 equilibration within the reactors. For the rest of the cases and the differences in pH, variations in IS values and important chemical elements from the leachate not incorporated within the modeling (e.g. Fe^{2+} and Mg^{2+} concentrations) could have affected the precipitation of carbonate minerals and the buffer capacity of the leachate, influencing the final pH obtained using MINEQL+.

From Table 4.7, it can be observed that increasing the CO_2 content within the headspace (50% CO_2), the total carbonate increased, but the pH values decreased to similar values as the simulations performed at 20% of CO_2.

Table 4.7. Dissolved Ca^{2+}, initial pH, CO_2 (%) assumed in the headspace, total carbonate (CO^{3-}) and temperature. Final pH and Ca^{2+} were obtained using MINEQL+ for IS (Ionic strength) of 0.28 and 0.4.

	Units	Case 1	Case 2	Case 3	Case 4
Reactors (T = 6 hours)					
Initial Ca^{2+} [mg/L]	mg/L	360	385	320	355
Initial pH	-	7.33	7.4	7.55	7.57
CO_2	%	50	50	50	50
Total CO_3^{-2}	$mmol^{-1}$	0.26	0.23	0.32	0.33
Temperature	˚C	22.6	23.15	22.2	22.9
MINEQL+					
Final pH (IS=0.28)	-	7.19	7.26	7.41	7.43
Final pH (IS=0.4)	$mmol^{-1}$	7.18	7.25	7.4	7.42
Final Ca^{2+} (IS = 0.28)	mg/L	165	193	126	137
Final Ca^{2+} (IS = 0.4)	mg/L	170	199	131	142

However, Ca^{2+} removal increased from 33% to 41% (at 20% CO_2), to 50% to 61% (50% CO_2), indicating that higher CO_2 content influences the total amount of Ca^{2+} removed from the leachate, for the rest of the conditions maintained equal. This also shows that using 20% of CO_2 in the laboratory study was representative of the calcium removal that can be observed in leachate injection pipes in a landfill with 50% of CO_2 within the biogas.

4.5 CONCLUSIONS

This study has shown that increasing the turbulent energy dissipation rate causes greater amounts of CO_2 evolution from solution. Under sealed conditions, the re-equilibration of CO_2 did not affect the dissolved Ca^{2+} removal at initial pH lower than 7.2. At initial pH higher than 7.2, dissolved Ca^{2+} was removed and pH decreased after 24 hrs. When the system was open to the atmosphere, temperature increase had an important effect on dissolved Ca^{2+} from leachate saturated with CO_2, promoting CO_2 outgassing and pH increased.

Increase in temperature had a greater impact on dissolved Ca^{2+} removal only when leachate had a higher initial pH. No significant changes were observed in dissolved Ca^{2+} concentrations at different turbulence levels under sealed conditions. This can be explained as the CO_2 evolved during mixing did not greatly affect the leachate pH due to the buffer capacity of the synthetic and real leachate. MINEQL+ simulations also showed that higher CO_2 content within the headspace (50% CO_2) affected the removal of Ca^{2+} under sealed conditions. It also showed that 20% of CO_2 used in the laboratory study represented closely the observed 50% CO_2 reported from field conditions (13 to 24% less Ca^{2+} removed).

This study has provided a better understanding of the CO_2-pH-$CaCO_3$ system for open and closed conditions. If the initial leachate pH < 7.2, no important pH changes were observed after mixing and during stagnancy under sealed conditions. However, for initial pH > 7.4, an increase of CO_2 within the headspace and its potential effect on the leachate

pH was outcompeted by the removal of Ca^{2+} as $CaCO_3$ and its impact on the buffer capacity of the leachate, decreasing the pH.

Leachate injections systems are commonly a network of solid pipes outside of the waste cell (closed system) and perforated inside of the waste cell (open system), which would have a different impact on the leachate chemistry at different sections of the pipes during operation. Leachate collected from bioreactor landfills is commonly stored in leachate tanks, sumps or wells. An increase in outside air temperature will influence CO_2 solubility and evolution, thus calcium carbonate precipitability. Leachate pH within the storage facility may affect the precipitability of Ca^{2+} within the perforated pipe. Thus, it will be important to sample leachate prior to recirculation to avoid inorganic accumulation of calcium carbonate within the pipelines caused by Ca^{2+} precipitation started within the storage facility.

Finally, this indicate that leachate may have to be pretreated prior to injection (removing dissolved Ca^{2+}) during colder seasons when the temperature gradient between the holding tank temperature and that of the pipes buried within the landfill is steepest, in order to avoid clogging within leachate injection pipelines.

CHAPTER 5: LEACHATE TREATMENT BEFORE INJECTION INTO A BIOREACTOR LANDFILL: CLOGGING POTENTIAL REDUCTION AND BENEFITS OF USING METHANOGENESIS

5.1 INTRODUCTION

Chapter 4 studied the effects of turbulence intensity and temperature increase on leachate degradation and inorganic clog formation. In this study, temperature increase was reported to impact CO_2 outgassing from the leachate, increasing the pH and affecting the stability of dissolved Ca^{2+}. It was explained that an increase in leachate temperature is expected in bioreactor landfills in cold climate countries (e.g. Canada, Northern US, Northern Europe, etc.) where leachate stored in an outdoor holding tank or sump is recirculated back into a warm waste cell (until 40 to 50˚C of differences can be expected (Krishna *et al.* 2009)). The pilot study described in Chapter 3 showed that the temperature of leachate collected from the landfill wells varied between 7.5 to 18.7˚C, and bioreactor landfills have reported temperatures ranging from 30 to 60°C. This shows that recirculating leachate during cold weather events will increase the temperature and evolved CO_2 from the leachate, promoting clog formation within the landfill engineered components.

The laboratory study described in Chapter 4 showed that turbulence intensity significantly impacted the amount of evolved CO_2 from the leachate. When leachate exposed to open atmospheric conditions were tested after having experienced turbulence

Material presented in this chapter has been reported in: Lozecznik, S., Sparling, R., Oleszkiewicz, J., Clark, S. and VanGulck, J. (2010). Leachate treatment before injection into a bioreactor landfill: Clogging potential reduction and benefits of using methanogenesis. *Waste Management* 30, 2030-2036.

(CO_2 re-equilibration), leachate pH increased by approximately one unit and dissolved Ca^{2+} was removed from solution. In turn, increased leachate pH and removal of dissolvedCa^{2+} are expected to occur within the injection pipelines in bioreactor landfills, depending on the CO_2 gradient between the perforated pipe, trench and waste cell. This is explained as the pipe design (pipe diameter and material, pipe perforations size and spacing) and the hydraulic operation (inlet flow rate and head) influence the distribution of leachate entering the refuse or trench, along the length of the line. In addition, it will also influence the amount of CO_2 in the leachate (dissolved) and pipe environment (gas phase) as presented in Chapter 4. It is expected that inside of the pipe or under sealed conditions, leachate composition will remain unchanged (as shown in Chapter 4). Since the trench and waste will have different CO_2 concentrations over time depending on the landfill phase (Figure 2.4.12), it will impact the carbonate content of leachate leaving the pipe perforations at the perforation boundary level or within the trench. In addition, due to the applied loads and waste settlement over time, injection pipes are unlikely to remain sealed for decades, and may present air leaks in the short or long term operation. During or after the turbulent operation of the leachate injection pipe, evolved CO_2 may escape through leaks present at pipe joints. The leachate that remains within the pipes may undergo a change in pH, and the associated removal of dissolved Ca^{2+} will occur within the pipe. Since CO_2 gradient between the HIT and waste and CO_2 leaks along the length of the pipeline affects leachate degradation and clog formation, clogging seems unavoidable in bioreactor landfills over time.

5.2 OBJECTIVES

The objective of this laboratory study was to assess the use of leachate methanogenesis to reduce leachate components that are known to contribute to clogging in leachate transmission pipes. In addition, the removal of dissolved Ca^{2+} under the reactor pH conditions was examined using synthetic leachate under controlled laboratory conditions.

The reduction of organic and inorganic leachate constituents may reduce the operational challenges resulting from leachate injection pipe clogging, and extend the service life of the engineered components of the bioreactor landfill, thereby maximizing its benefits over a longer period of time. In addition, treating leachate under anaerobic conditions may generate an important source of methane gas outside of the waste cell, which can provide an additional revenue source to the landfill owner.

5.3 METHODOLOGY

Brady Road Landfill in Winnipeg, Manitoba, Canada is an active landfill and the source of the leachate used in this study. Leachate was collected from the same cell and leachate well on day 1 and 70 of this 186 days of study. Select leachate characteristics from these two days are shown in Table 1. Leachate was transported to the laboratory in 25 and 45 L carboys, which were then stored at $4^{o}C$ to limit biological processes from occurring.

Table 5.1**.** Composition of leachate collected from Brady Road Landfill at day 1 and 70 of the laboratory study (Sampling was completed on July 10 and September 24 of 2009 - from the same landfill well)

Parameter	**Units**	**Brady Leachate**	
		day 1	**day 70**
COD	[mg/L]	2518	7695
Alkalinity	[mg$CaCO_3$/L]	4325	6225
pH	-	7.2	6.7
TSS	[mg/L]	240	720
VSS	[mg/L]	140	350
ISS	[mg/L]	100	370
Acetate [mg/L]	[mgHAc/L]	510	2137
Propionate [mg/L]	[mgHPr/L]	178	171
Butyrate [mg/L]	[mgHBu/L]	154	622

The leachate composition of Brady Road Landfill was representative of leachate generated from waste that is between about 5 to 15 years in age. The differences in leachate composition are inherent to the variability of the conditions within the landfill waste cell. An anaerobic sequencing batch reactor (ASBR) with a working volume of 3.4 L was operated under anaerobic conditions with leachate. The reactor was set-up to have a constant 1.4 L of biomass and 2 L of leachate (called feed). The reactor was designed to include a sample port for biogas analysis (CO_2 and CH_4) and analysis of leachate composition, as well as a port for feeding and measurement of gas production, as shown in Fig 5.1.

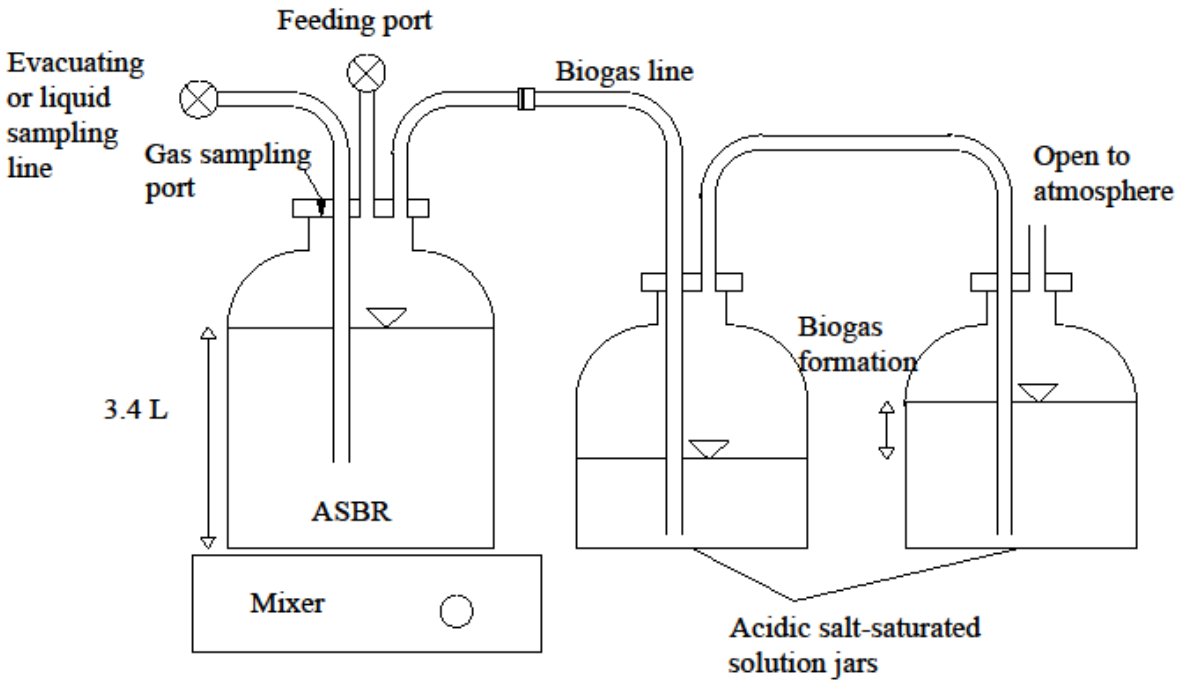

Figure 5.1. Schematic of ASBR and liquid displacement set-up (not to scale)

The ASBR was seeded at the start-up with biosolids from the anaerobic digester from the North End Water Pollution Control Center (NEWPCC) in Winnipeg, Canada. The ASBR was operated inside of a temperature controlled chamber at mesophilic temperature (35˚C). Timur and Özturk (1999) operated an ASBR for 2 years to treat leachate from 3.5 year old waste with COD ranging from 16,200 to 20,000 mg/L. This leachate was used to feed the ASBR at variable loading rates, increasing the influent COD concentrations from 3,800 to 15,940 mg/L. The highest volumetric methane production rates (1.59 to 1.85 L CH_4 $L^{-1}d^{-1}$ (STP)) were measured at the highest volumetric COD tested (14,500-15,940 mg/L), where the reactors were operated at a hydraulic retention time (HRT) ranging between 1.5 to 2 days and solids retention time (SRT) of 9 to 20 days. The highest CH_4 production rate for the COD removed measured within the

reactors was 0.29 L CH_4 (STP)/g COD removed, which is 83% of the theoretical value at STP conditions (0.35 L CH_4 (STP)/g COD removed). This work guided the selection of one HRT (48 h) and one SRT (20 days). The other HRT was selected to assess the daily treatment (24 h) and the other SRT selected (40 days) was the highest SRT evaluated by Timur and Özturk (1999), as shown in Table 5.2.

Table 5.2**.** Batch reactor SRT and HRT operation

Days	**SRT [days]**	**HRT [hours]**
0-16	20	24
16-24	40	24
24-120	40	48
120-184	40	24

After the first two weeks of operation, the sampling and feeding protocol was performed with industrial N_2(g) flushed into the reactor during each procedure to ensure anaerobic conditions. Waste activated sludge or digester samples were collected from the reactor before and after each anaerobic digestion cycle and tested on a daily basis for the following characteristics: total chemical oxygen demand (tCOD), soluble chemical oxygen demand (sCOD), oxidation reduction potential (ORP), pH, total alkalinity, total suspend solids (TSS), volatile suspend solids (VSS), inert suspend solids (ISS), volatile fatty acids (VFA) such as acetate (AA), propionate (PA) and butyrate (BA). Biogas volume and content (CO_2 and CH_4) were measured weekly. The leachate solids and supernatant extracted from the reactor were controlled daily. $Ca^{2+}$and Mg^{2+} concentrations were analyzed during one digestion cycle, on day 140. sCOD and tCOD

samples were measured using the HATCH method except that the sCOD samples were filtered through a 0.45 µm filter prior to analysis.

The TSS, ISS, VSS, pH, temperature, VFA's and CO_2 were measured using the same laboratory equipment and methodology used in the laboratory experiments discussed in Chapters 3 and 4. The ORP was measured using an Orion 5star multi WPHH equipped with the appropriate electrical probes. Prior to each pH and ORP sampling activity, a small volume from the reactor was collected (< 5 mL) and sampled for pH and ORP to calibrate the probes closer to the values existent within the reactor, before the final sampling. This was intended to have faster results with the probes at open conditions, minimizing the loss of CO_2.

CH_4 in the reactor headspace samples was analyzed by a Varian CP 3800 gas chromatographer (GC) equipped with a thermal conductivity detector. The optimized GC operating conditions were 250˚C in the injector and 180˚C in the detector. Temperature in the oven was initially set at 40˚C for 1 minute and then ramped up to 100°C at the rate of 20˚C/min for a total running time of 15 minutes. The flow rate of carrier gas helium in the column was constant at 3 mL/min. Samples were taken directly from the reactor headspace and injected into the GC. The sample volume loop was 250 µL.

The biogas was collected and the volume was measured using the same liquid displacement method used in Chapter 4, but in air-tight calibrated vessels of 10 L (see Figure 5.1). The liquid inside of each vessel contained 6 L of deionized water saturated

with 2.1 kg of NaCl, 300 mL of H_2SO_4 and 0.18 g of methyl orange to prevent gas from dissolving (Puchajda 2006, Wohlgemut 2008). Finally, Ca^{2+}, Mg^{2+} and Na^{+} were measured using a Varian ICP, Model VISTA- MPX, CCD with simultaneous ICP-OES. The CH_4 and CO_2 percentage within the biogas were monitored from day 17, while the CH_4 produced and COD removed were monitored from day 70.

A separate study was performed with synthetic leachate saturated with 20% of CO_2 (in N_2) at different pH values to illustrate the precipitability of dissolved Ca^{2+} (accumulation of ISS) observed in the ASBR. This study intended to identify the pH values for the use of an ASBR to treat leachate on-site, at which methanogenesis and removing dissolved Ca^{2+} are expected to be performed at the same time.

A volume of 500 mL of this synthetic leachate was poured into a 1 L Pyrex bottle together with a magnetic stirrer, pH meter ORION Model 420 A using an ORION 911600 THERMO semi-micro pH probe, and a gas diffuser attached to a 20% CO_2 and N_2 gas cylinder. Ca^{2+} was measured using the same laboratory equipment and methodology used in the laboratory experiments discussed in Chapter 4. Initially, the gas was bubbled via the gas diffuser for 30 min without taking any other measurement to achieve $CO_{2(aq)}$ saturation level at ambient temperature. After this 20% $CO_{2\ (aq)}$ saturation was achieved, sodium hydroxide (NaOH) of 1 N was dosed into the Pyrex bottle to increase the pH at the values chosen while bubbling. As the chosen pH values were achieved (6.5, 7, 7.21, 7.35, 7.4, 7.46 and 8.04), total calcium concentrations were sampled from the Pyrex bottle. The sampling involved taking 2 supernatant samples of 20

mL from the Pyrex bottle after settling any precipitate for 20 min. Each sample was acidified with hydrochloric acid (HCl) between pH 4 to 5 to ensure that most of the CO_2 dissolved was gasified prior to titration with the HACH method.

Since a volume of 40 mL was sampled from the Pyrex bottle at different pH values and NaOH was added to achieve the higher pH values, the Pyrex bottle volume ranged between 450 to 560 mL during this study. Thus, dilution of the total calcium sampled was small compared with the effects observed at different pH's, therefore the original measurements were not corrected for dilution effects.

5.4 RESULTS AND DISCUSSION

5.4.1 ASBR results

The performance of the digester using leachate from Brady Road Landfill changed over time as measured using tCOD and sCOD, as shown in Figure 5.2.

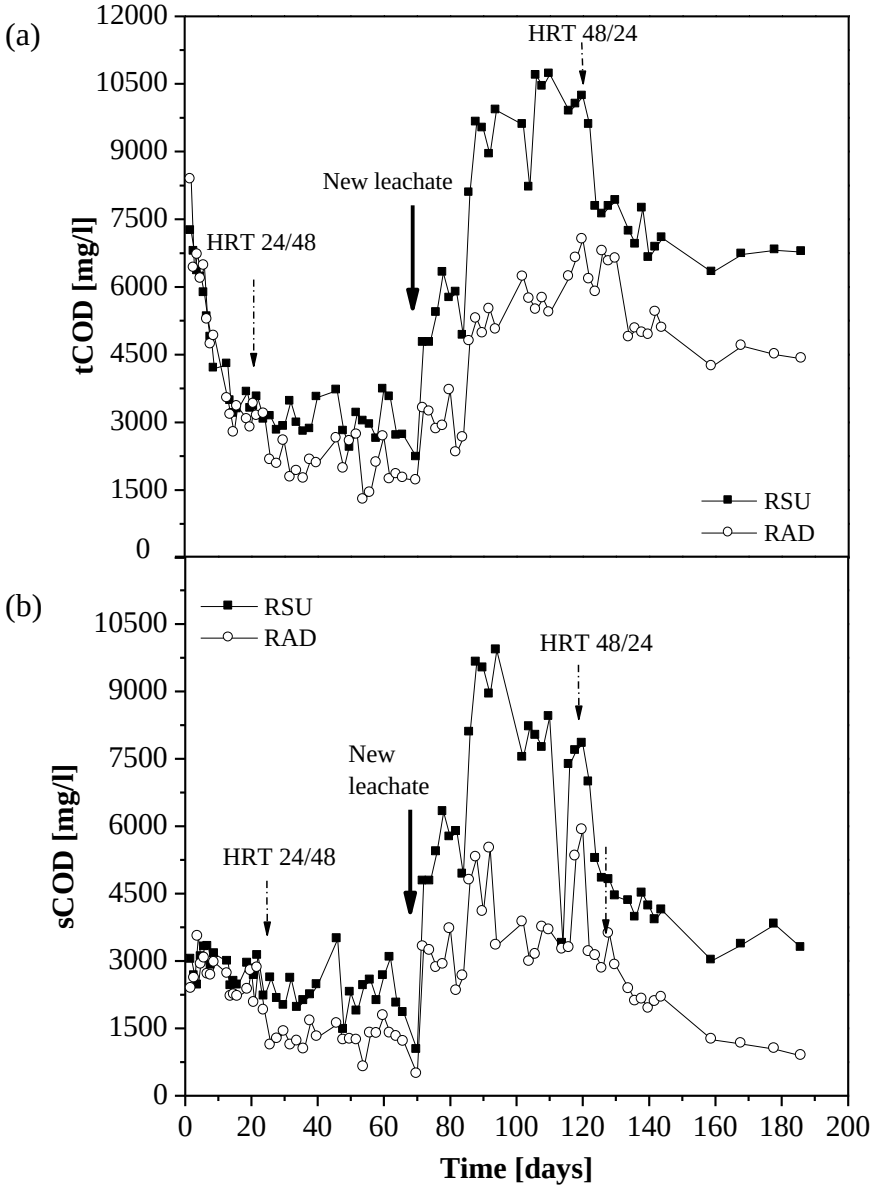

Figure 5.2. Total COD and soluble COD over time within the digester (24/48 and 48/24 correspond to the change in HRT from 24 hours to 48 hours or vice versa).

Reactor start-up (RSU) represents the composition of the reactor mixed liquor at the start-up of the digestion at each cycle (t = 0) after biomass and leachate were mixed. Reactor after digestion (RAD) represents the composition of the reactor mixed liquor at the end of the digestion cycle (t = HRT). Samples of the mix liquor from the digester were taken during each cycle to assess the performance of the digester, as well as to maintain the SRT's adopted. To assess the effects of different SRT and HRT on leachate treatability, a criterion based on a minimum percentage removal of COD (>20%) between cycles was used as a control to modify these variables at different time intervals. A settling time period of 1 hour was employed between anaerobic cycles to replace the treated leachate with fresh leachate.

For the first 16 days at SRT of 20 days, there was no substantial change in COD (<20% removal) so it was decided to increase the SRT to 40 days. A week later, little change was observed within the digester so the HRT was increased to 48 hours. After this time, the digester started COD removal over 20% and averaged 34% of tCOD removed and 43% of sCOD removed before the second batch of leachate was fed into the digester on day 72 (solid arrow shown in Figure 5.2 and b). After this second batch of leachate with higher COD concentration (Table 5.1) was fed into the reactor on day 72, the digester had higher removal rates of tCOD and sCOD that averaged approximately 42% and 48%. This higher COD removal is the result of a more degradable second batch of leachate added to the ASBR, where acetate and butyrate concentrations increased over four times for the second batch of leachate (propionate remained the same), as show in Table 5.1.

At day 120, it was decided to decrease the HRT to 24 hours to assess the performance of the reactor at shorter feeding times. After approximately 4 months, the influent tCOD and sCOD had stabilized and the average removal rates during the last 66 days of the study were around 27% and 51%, respectively. The changes of HRT at different times are indicated with the dash dot arrows in Figure 5.2.

After the 72nd day, there was an increase in pH of approximately 0.2 units during the course of each sequence batch, as shown in Figure 5.3, which is consistent with the fact that the second batch of leachate had a higher VFA content (see Table 1) and higher removal of VFA's was observed within the reactor. The pH shift was associated with the removal of tCOD and sCOD within the reactors (Figure 5.2).

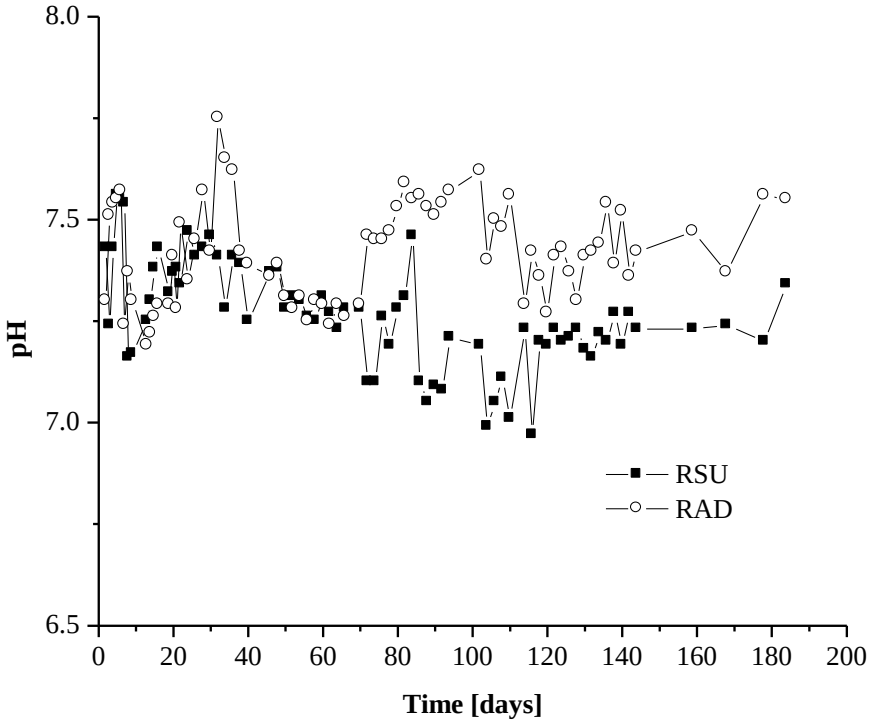

Figure 5.3. Variation in pH within the digester versus time

As shown in Figure 5.4a, b and c, the changes in tCOD and sCOD (Figure 5.2a and b) is associated with the consumption of acetate and butyrate, but not propionate. VFA removal and pH increase was measured by VanGulck *et al.* (2003), following the digestion of real leachate within columns that represented plug flow reactors. A relationship was established between the change in pH coupled with the fermentation of VFA and the biological production of carbonate and the measured removal of Ca^2 as $CaCO_3$ through the columns. The increase in VFAs measured in this study (Figures 5.4) starting from day 72 was due to the striking differences in leachate composition of the 2 batches used. The second batch of leachate had approximately 4 times higher acetate and butyrate concentrations than the first batch (Table 1). The greater amount of fermentation of these VFA after day 72 had an impact on the pH between cycles of the digester, which resulted in an increase in pH between 0.2 and 0.3 units during the course of each sequence batch (shown in Figure 5.3).

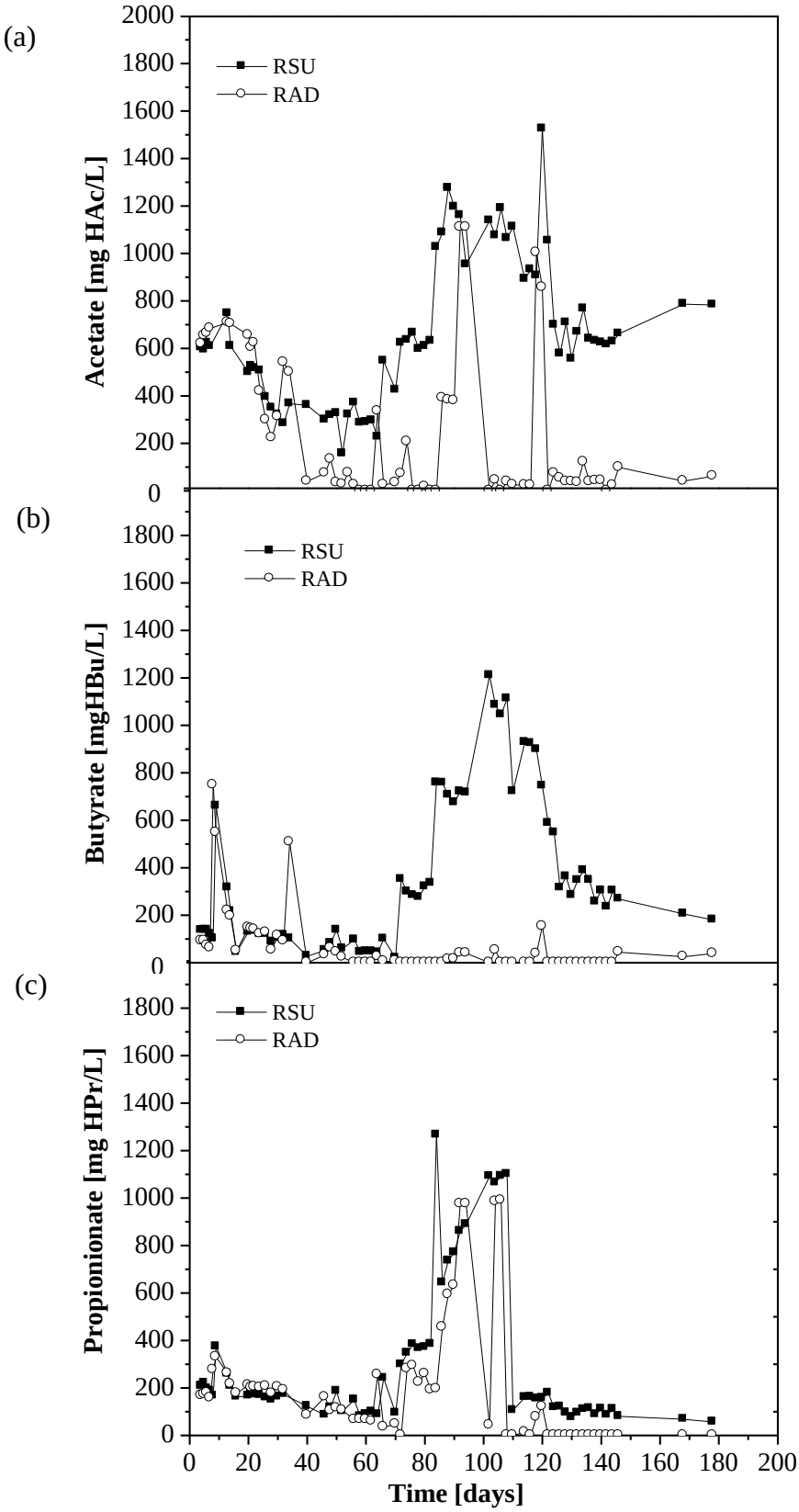

Figure 5.4. Variation in (a) acetate, (b) propionate and (c) butyrate concentrations within the digester versus time.

Rittmann *et al.* (2003) showed that the main mechanism for $CaCO_3$ precipitation from leachate was acetate fermentation producing methane (CH_4) and carbonic acid (H_2CO_3). As the pH in the digester effluent was higher than the influent and acetate was consumed within the reactor, a change in ISS was expected. Figure 5.5 shows ISS accumulation as the difference in TSS and VSS at the start of each cycle from approximately the 80th day, and increased at a nearly constant rate after the second batch of leachate was added.

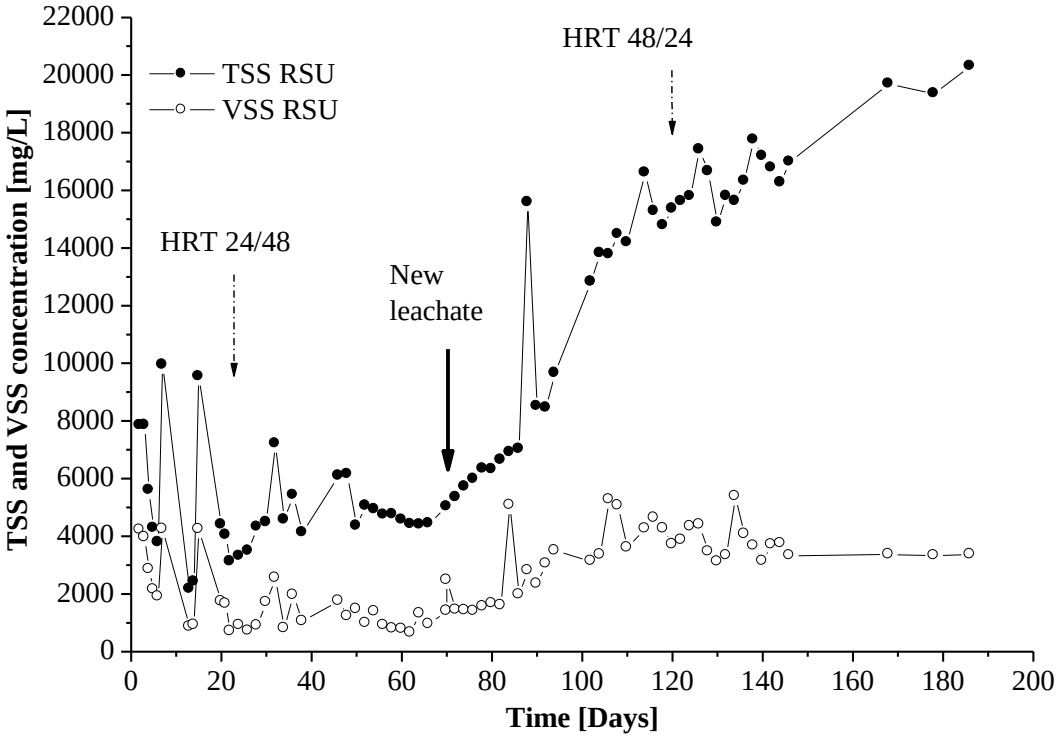

Figure 5.5. Variation in total suspend solids (TSS) and volatile suspend solids (VSS) within the digester versus time (24/48 and 48/24 correspond to the change in HRT from 24 hours to 48 hours or vice versa)

The accumulation of TSS, with a relatively constant concentration of VSS as shown in Figure 5.5, indicates a buildup of inorganic material within the digester over time. Past research on clogging in leachate columns (Rowe *et al.* 2004) have shown that changes in

pH and carbonate content combined with high concentration of metals such as Ca^{2+} or Mg^{2+}, results in carbonate mineral precipitants.

To verify whether Ca^{2+} or Mg^{2+} was lost from solution within the ASBR, a sample of leachate and supernatant was analyzed before and after the digestion cycle on day 140 for Ca^{2+} and Mg^{2+}. The results show that the leachate at the reactor start-up contained 354 and 561 mg/L of Ca^{2+} and Mg^{2+} respectively, whereas the supernatant after digestion contained 24 and 480 mg/L Ca^{2+} and Mg^{2+}, respectively. Therefore, a significant amount of Ca^{2+} was precipitated from the leachate and accumulated inside the reactor, while much less Mg^{2+} was precipitated at the operational pH of the reactor. It is believed that Ca^{2+} was mainly removed from solution as $CaCO_{3(s),}$ and Mg^{2+} removed was incorporated within the binding sites. This is explained as clogging collected from leachate collection pipes have been typically reported as an unzoned low-Mg calcite (Maliva *et al.* 2000, Manning 2000). In addition, laboratory columns studying clogging have reported magnesium-rich calcite as the main clogging component (VanGulck 2003). In order to form struvite, high dissolved ortophosphates must be presented in solution and relatively high pH values (optimum pH of 9 (Borojovich *et al*. 2010) are desired. Data provided by the City of Winnipeg from leachates sampled at Brady Road Landfill between 2006 and 2008 exhibited an average TP of 4.3 mg/L. In addition, the reactor pH increased only to an average of 7.5 between cycles, suggesting the formation of $CaCO_3$ type of minerals mainly and no struvite. However, XRD analyses were not performed within the ISS accumulated in the ASBR and further testing must be performed to verify the above assumptions.

Concurrent with VFA removal, biogas was produced during each digestion cycle. Biogas composition (CH_4 and CO_2) and production were measured weekly starting from day 17. The CH_4 and CO_2 content within the biogas and the CH_4 produced per COD removed are shown in Figure 5.6a and b. From Figure 5.6a, it can be seen that the biogas formed between digestion cycles with the first batch of leachate did not add up to 100%, which may be due to incomplete methanogenesis (with H_2 production) or an insufficient amount of biogas produced to dilute the $N_{2(gas)}$ gas used for liquid sampling and feeding the reactor. An enrichment of CH_4 and a decrease in CO_2 content was observed within the biogas starting on day 80. This CH_4 enrichment was caused by an increase in CO_2 partial pressure and mix liquor pH (organic acids consumption), increasing the rate of CO_2 transferred to the mix liquor, obtaining a higher proportion of CH_4 than CO_2 within the ASBR headspace.

From Figure 5.6b, an average of approximately 0.35 L CH_4/gCOD removed was achieved after day 80, which is smaller than the 0.4 L CH4/gCOD removed theoretically by oxidizing methane at 35˚C (calculations are shown in section 1.3.1.1). This shows that high methane (CH_4) production and COD removal can be achieved when treating leachate using well controlled anaerobic conditions.

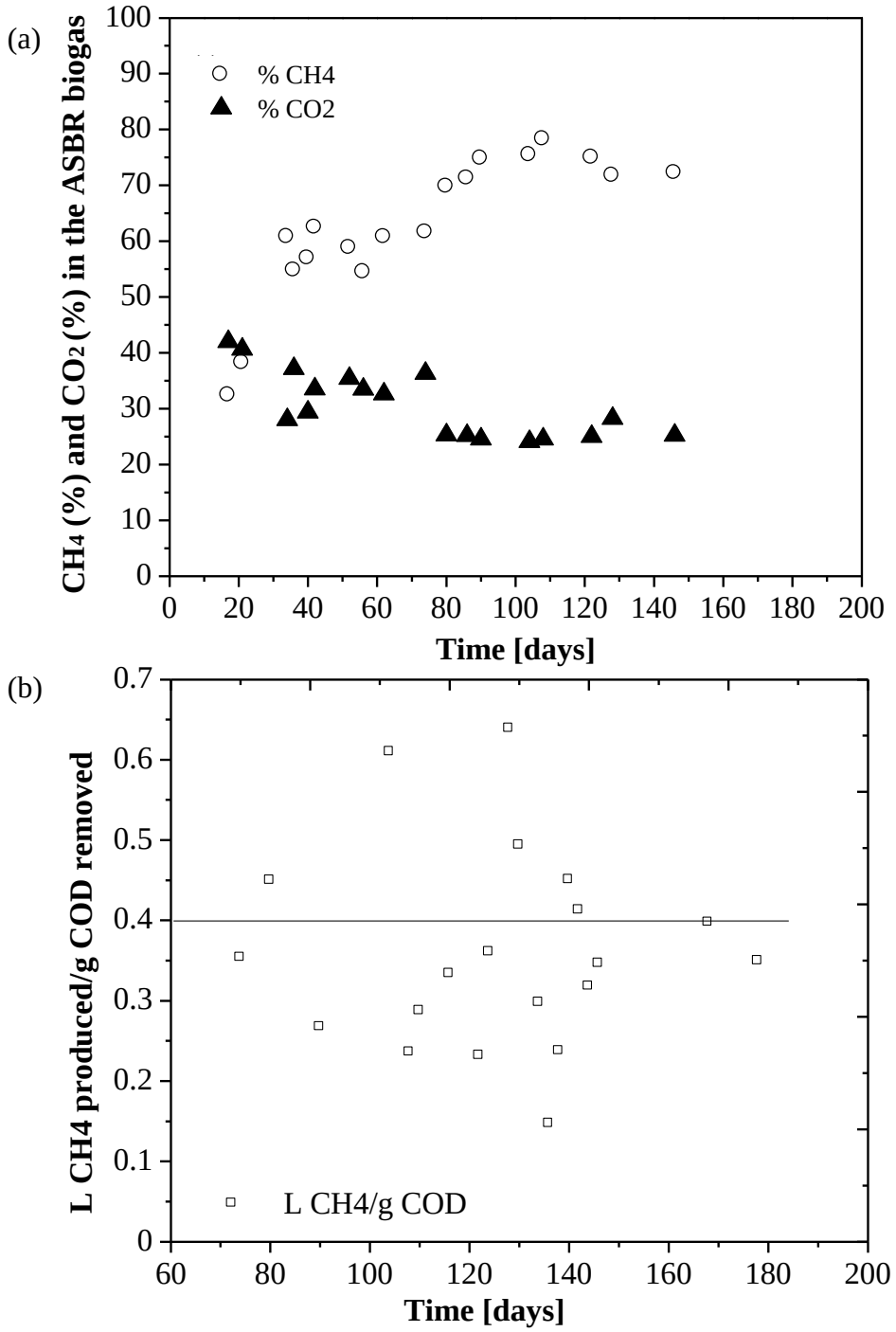

Figure 5.6. Variation of (a) percentage of CH_4 and CO_2 within the biogas produced and (b) CH_4 produced per gram of COD removed within the digester versus time

The presence of a 75% - 25% CH_4-CO_2 ratio in the digester may indicate a shifting of the carbonate equilibrium within the ASBR, where there is an increase in carbonate

availability within the ASBR as shown in Figure 5.6a. This is consistent with the observed increase in pH in the digester. The increase in carbonate content may be the cause for the increase in precipitation of carbonate minerals, as indicated by the observed ISS accumulation (Figure 5.5), within the reactor.

The results suggest that since $CO_{2(gas)}$ was produced between cycles due to biological activity and stripped out from solution depending on the mixing conditions, an increase in the partial pressure of $CO_{2(gas)}$ within the headspace of the reactor is expected. In addition, as the pH rises due to the removal of VFA's, the carbonate equilibrium between the headspace and mixed liquor is shifted towards the mixed liquor, as shown in Figure 5.6a. This increase in $CO_{2(aq)}$ at higher pH will increase the amount of carbonate available within the reactor that can be coupled with the excess metals (Ca^{2+} and Mg^{2+}) and precipitate out, as observed with the increase in ISS within the reactor.

5.4.2 Soluble Ca^{2+} removal at different pH values using synthetic leachate

In order to illustrate the effect of pH and $CO_{2\ (aq)}$ on the concentration of ISS within the digester, a parallel batch test study was carried out. Synthetic leachate was prepared and saturated with 20% of CO_2 at ambient temperature. Soluble Ca^{2+} at different pH values was measured. The results are shown in Figure 5.7 (also see Appendix N).

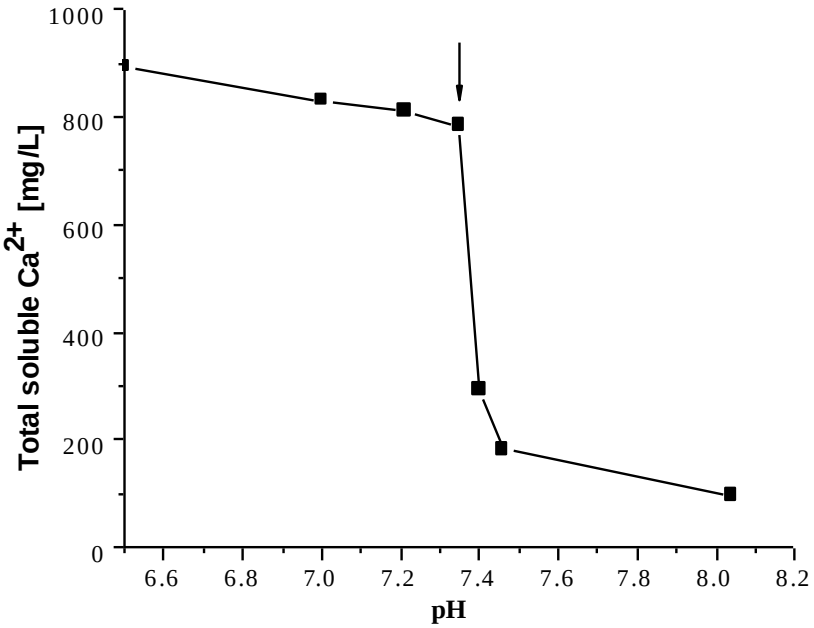

Figure 5.7. Variation of pH and total soluble calcium within the reactor (solid arrow indicate the pH at which total soluble calcium was removed from solution)

From Figure 5.7, it can be observed that between pH 7.2 and 7.46 at $CO_{2\ (aq)}$ saturation conditions (20%), the concentration of total calcium decreased between 65% to 80%, precipitating out from solution. As shown in Figure 5.3, the average pH within the ASBR before and after each digestion cycle was 7.18 and 7.46, and the CO_2 saturated conditions averaged approximately 25% (see Figure 5.6a) for the period between days 72 and 184. This explains why calcium was precipitated and accumulated within the ASBR as ISS at the pH range and CO_2 saturation conditions observed. VanGulck *et al.* (2003) permeated synthetic leachate through a leachate column, and after 300 days the leachate pH increased from the initial pH of 6 to a value of approximately 7.4. At pH 7.4, the removal of calcium from solution within the column was approximately 80%, which is similar to the result shown in Figure 5.7.

Rittmann *et al* (2003) and VanGulck *et al* (2003) concluded that the main source of the carbonate forming calcium carbonate precipitants within the column experiments was the fermentation of VFA, primarily acetate. Acetate represented approximately 44% (ranging between 5,090 and 7,990 mg HAc/L approx.) of the initial COD for the synthetic leachate used in both studies and 27% (ranging between 1,530 and 5150 mg HAc/L approx.) for the Keele Valley landfill leachate used in VanGulck *et al* (2003). For the current study, acetate represented approximately 20% (510 mg HAc/L) and 28% (2,137 mg HAc/L) of the initial COD of the first and second batch of leachate used (Table 5.1). For the second batch of leachate used, a considerable increase in ISS within the digester was measured after digestion. This is explained as the effect of the $CO_{2\ (gas)}$ produced by the removal of VFA, and its effect on the carbonate concentration of the mixed liquor during digestion. The $CO_{2\ (gas)}$ formed within the columns was degassed from the top of the columns before reacting with the leachate, increasing the carbonate content available in solution to bind with abundant Ca^{2+} from the leachate, , so its impact was not considered in the clog analysis.

5.5 CONCLUSIONS

This study showed that performing leachate fermentation reduces organic (COD, VFA) and inorganic (Ca^{2+}, ISS) clog constituents within the leachate, which otherwise may impair the operation and the service life of the recirculation pipes. CH_4 production and COD removal rates were very close to the theoretical value obtained by chemically oxidizing methane, showing that high amounts of CH_4 production and removal of COD can be performed on leachate at mesophilic temperatures under anaerobic conditions. Even higher amounts could have been achieved if propionate had been degraded in the digester during this study.

Since the variability of leachate composition (e.g. VFA) affected the ISS production rates (approximately 1.9 g ISS produced/ day, after day 70^{th}) within the ASBR, more studies are needed to investigate the effects of the changes in the organic content of leachate (e.g. acetate and propionate) with the removal of clogging components using methanogenesis. To the author's knowledge, this is the first laboratory study of leachate treatment that shows the effect of CO_2 production and dissolution under sealed and anaerobic conditions on the removal of dissolved Ca^{2+}.

A decrease in the CO_2 gas content was measured within the reactor after the second batch of leachate was added, evolving to the aqueous phase, increasing the carbonate content within the reactor and binding with the excess of dissolved Ca^{2+}, accumulating as ISS. This effect also caused an increase in CH_4 content within the headspace of the digester, thus producing a cleaner biogas with regards to CO_2. This enrichment of CH_4 was

observed within the ASBR when the digestion of organic acids increased the reactor pH from an initial average of 7.2 to a value higher than 7.4.

Solid waste engineers may be able to use fermentation of leachate prior to leachate recirculation as a way of controlling clogging in recirculation pipes. When doing so, consideration should be given to a) an equalization tank to control the influent to the ASBR to ensure consistent concentrations of leachate constituents and b) a pH control (adding NaOH or HCl depending on the leachate pH) to achieve the pH values at which methanogenesis is performed and Ca^{2+} concentration is reduced. By causing the precipitation of mineral carbonates, methanogenic treatment of leachate prior to recycling has the potential to reduce pipe clogging during leachate injection, while the methane generated can be collected for energy production

CHAPTER 6: ACETATE AND PROPIONATE IMPACT ON THE METHANOGENESIS OF LANDFILL LEACHATE AND THE REDUCTION OF CLOGGING COMPONENTS

6.1 INTRODUCTION

An extensive array of studies have been devoted to the characterization of the mechanisms controlling clogging in porous media (see Section 6.2), and to the author's knowledge, there have been few studies investigating clogging mitigation methods. Turk *et al.* (1997) provided the only reported study to assess the potential for different chemicals to clean clogged landfill pipes. Turk's study was useful for identifying chemicals appropriate for removing clog material. However, it did not provide on-site mitigation strategies of clogging removal nor recommendations for pH control and retention time within pipelines. The study described in Chapter 5 assessed the use of leachate methanogenesis prior to recirculation as a method to reduce leachate components that are known to contribute to clogging in leachate transmission pipes. This study demonstrated that performing methanogenesis of leachate prior to recirculation reduces the organic (COD and VFA) and inorganic (Ca^{2+}, FSS) material responsible for clogging and as an added benefit, produced a large amount of CH_4 gas (0.35 L CH_4 produced per g of COD removed). In practice this methane could be used as an additional source of on-site energy. However, due to the natural variability of leachate characteristics, different COD and VFA concentrations are expected to be found within the leachate from different landfill cells or from the same cell over time.

Material presented in this chapter has been submitted in: Lozecznik, S., Sparling, R., Clark, S., VanGulck, J and Oleszkiewicz, J.A. (2011). Acetate and propionate impact on the methanogenesis of landfill leachate and the reduction of clogging components. *Bioresource Technology* 104, 37-43.

These differences will cause a varying amount of COD and VFA removal and CH_4 production, as measured in Chapter 5.

The composition of landfill leachate and its changes over time has been well documented for landfills around the world (Kjeldsen et al. 2002, Rowe et al. 2004), but there is a lack of reported data with regards to the landfill age and individual VFA values such as acetate, propionate and butyrate. Table 1 shows acetate, propionate and butyrate ranges reported from landfills in Europe and North America. Table 6.1 demonstrates the large range of VFA concentrations that can be observed between landfills. Furthermore, significant differences in concentrations were also found within the same landfill well over time as observed in Owen and Manning (1997) and this thesis (Chapters 3 and 5). These wide ranges of VFA concentration and its changes over time will impact any on-site biological leachate treatment, unless an equalization tank is designed to balance the variable load and flow of leachate on a continuous steady-state basis.

An understanding of the principal factors controlling and affecting the activity of the microorganisms involved in the fermentation of acetate and propionate will provide better knowledge to maximize VFA removal and thus increase the production of biogas under anaerobic conditions. Thauer *et* al (1977) and Rittmannn and McCarty (2001) explained that the intermediate steps of fermentation have low energy yields and are thermodynamically possible only when the microorganisms acting as consumers maintain their products at very low concentration (especially H_2 formation).

Table 6.1**.** Concentrations of acetate, propionate and butyrate (mg/L) in leachate from landfills in Europe and North America.

Country	Landfill	Acetate mg HAc/L	Propionate mg HPr/L	Butyrate mg HBu/L	Author
Netherlands	NA[1]	1,230-10,800	470-4,390	1,210-9,810	Hoeks and Borst (1982)
Canada (ON) [2]	Keele Valley	3,533 -4,010	4,125 - 4,475	598-738	Cooke *et al.* (2005)
Canada (MB) [3]	Brady Road	510 -2,137	171-178	154-622	Chapter 3
Canada (MB) [3,4]	Summit Road	2,000-7,500	170-700	600-4,100	Personal sampling
England [4]	Bell House Pit	4,560-16,860	2,664-5,550	370-1,760	Nedwell and Reynolds (1995)
England [4]	Arpley	390-4580	1070-2350	0-1730	Owen and Manning (1997)
England [4]	Maw Green	0-960	0-480	0-470	Owen and Manning (1997)
US (IL)	NA[1]	1,748	509	3,075	Chian (1977)

[1]NA: not available
[2] Standard deviation values for acetate, propionate and butyrate are 1,699-1,521, 1,652-1,497 and 458-558 of leachate collected during the performance of this study.
[3]Samples collected from the same landfill well at different elapsed times during 2008
[4]Impounded leachate from a closed landfill cell during 2008
[5]Samples collected from the same landfill well at different elapsed times during 1993 and 1994

The anaerobic ecosystem was described as a synergistic interaction in which some key microorganisms benefit from the metabolic actions of their peers to maintain thermodynamically favorable conditions for growth (syntrophy). MacInerney *et al.* (2008) reviewed several studies on syntrophic metabolism in anaerobic digestion where propionate, longer chains of fatty acids, alcohols, some amino acids, and aromatic compounds were reported to be degraded syntrophically to the methanogenic substrates: H_2, formate and acetate. They suggested that the syntrophic degradation of fatty acids is often the rate limiting step of methanogenesis and biological reactors performing anaerobic digestion.

Thauer *et al*. (1977) and Rittmann and McCarty (2001) suggested that the syntrophic degradation of fatty acids (e.g. propionate degraders) is often the rate limiting step of methanogenesis in biological reactors. The study described in Chapter 5 showed that methanogenesis of leachate was greater at 2137 mg/L (35.6 mmol/L) of acetate, than at 510 mg/L (8.5 mmol/L) of acetate (both at low propionate concentration < 178 mg HPr/L (2.4 mmol/L)). However, higher VFA concentrations have been reported to hinder methanogenesis, and the most common explanation for reactor failure at lower operating pH is related to the concentration of un-dissociated fatty acids, particularly propionic acid (Taconi *et al.* 2008). VanGulck *et al*. (2003) studied the removal of leachate components (e.g. VFA such as acetate, propionate and butyrate) through column studies emulating the porous media of leachate collection systems. Problems with acetate removal at high concentrations (for example 6,000 mg/L) were not encountered, but no discussion was made on the inability of the columns to remove propionate from synthetic and real

leachate while acetate concentration in the influent was over 2,000 mg/L. James (1998) studied the effects of VFA concentration on the methanogenesis of landfill leachate, concluding that (a) 6,000 mg/L (100 mmol/L) of acetate inhibited methane production, (b) 7,400 mg/L (100 mmol/L) of propionate inhibited butyrate oxidation, and (c) elevated concentrations of butyrate did not affect methanogenesis at pH values between 7.11 and 7.57. The inhibition of methanogenesis caused by high acetate and propionate concentrations may be mitigated if such high VFA leachates are blended with leachate having lower acetate and propionate concentrations from older cells on-site.

6.2 OBJECTIVES

The objective of this laboratory study was to investigate the effects of different initial acetate to propionate concentrations on methanogenesis and the removal of Ca^{2+} from synthetic leachate under anaerobic and mesophilic conditions. Finding the optimum range of acetate and propionate concentrations will help to define the optimum influent loads for an on-site anaerobic digester that can be used to maximize methanogenesis and reduce dissolved Ca^{2+}. Removing dissolved Ca^{2+} prior to injection would help to minimize the potential precipitation of $CaCO_3$ as inorganic clogging within the injection pipes.

6.3 METHODOLOGY

The biomass used in this study was collected from the anaerobic sequencing batch reactor (ASBR) study described in Chapter 5, where the biomass was acclimated in the ASBR with landfill leachate at a hydraulic retention time (HRT) of 24 hours and solid retention time (SRT) of 40 days. The total suspended solids (TSS) concentration in the biomass was approximately 100 g/L at 24% of VSS. The synthetic leachate was prepared following the formula used by VanGulck and Rowe (2004a), and was identical to the synthetic leachate used in the laboratory study described in Chapter 4 (Table 4.2). This solution consisted mainly of acetate, propionate and butyrate (0.12 M, 0.067 M and 0.01M respectively), various salts and a trace metal solution.

Past studies of clogging in drainage material (VanGulck et al. 2003, Cooke et al. 2005) had tested synthetic and real leachate from Keele Valley Landfill at an approximate molar ratio of 1:1 for acetate and propionate. From Table 6.1, several molar ratios are reported from different landfills around the world, so testing different acetate to propionate ratios and molar proportions will cover the range of values that are typically experienced in field conditions.

This laboratory study was performed using Balch tubes (Bellco Glass Co.) with a working volume of 27 mL, containing 5 mL of media (synthetic leachate) and 5 mL of inoculum (biomass). The final VFA concentration of the medium tested (leachate and biomass) was expected to change as equal volume of synthetic leachate and biomass were digested, and are shown in Table 6.2. Butyrate was maintained constant at 25 mmol/L.

Table 6.2**.** Average (μ) and standard deviation (σ) of acetate, propionate, approximate molar ratio, butyrate and pH of synthetic leachate at hour T = 0 from tests 1 to 6.

Pipe Test #	Acetate [mg HAc/L]		Propionate [mg HPr/L]		Molar Ratio [HAc/HPr]	Butyrate [mg HBu/L]		pH [-]	
	μ	σ	μ	σ		μ	σ	μ	σ
1	2400	93	592	0	5	924	48	6.97	0.01
2	1840	49	1024	30	2	997	45	7.00	0.01
3	1530	33	1776	0	1	1071	36	6.97	0.01
4	1697	153	1735	120	1	1040	107	6.99	0.01
5	1124	32	2168	60	0.5	1108	47	6.99	0.01
6	505	40	3313	318	0.2	738	51	6.97	0.01

A total of 12 Balch tubes were prepared for each of the leachate combinations, sampling three Balch tubes (triplicate) each at times 0, 24, 48 and 72 hours after the anaerobic digestion cycle. Due to the amount of tubes assessed, this study was conducted over two consecutive weeks. During the first week, tests 1, 2 and 3 were completed (higher acetate than propionate concentration values) and during the second week tests 4, 5 and 6 were finished. Test 3 and 4 contained roughly the same acetate and propionate concentration values to compare the reproducibility of the results, as shown in Table 6.2.

Each tube was tested for pH, acetate, propionate and butyrate concentrations at 0, 24, 48 and 72 hours. Biogas content (CO_2 and CH_4) was tested at 24, 48 and 72 hrs was measured from the gas phase. An initial leachate pH of 7 was chosen to ensure that no precipitation of calcium occurred and to represent real leachate values observed at landfills. The tubes were air-sealed with butyl-rubber stoppers, crimped with aluminum seals and were gassed and degassed (1:4 minutes) four times with 100% nitrogen (N_2) to maintain anaerobic conditions (Daniels *et al.* 1986) at 1.5 atm overpressure.

The Balch tubes were placed on an orbital shaker (Scientific Co. Inc.) at a medium speed inside of a temperature controlled chamber at mesophilic temperature (35˚C). The pH, temperature, Ca^{2+} and CO_2 were measured using the same laboratory equipment and methodology used in the laboratory experiments discussed in Chapter 4. VFA concentrations and CH_4 from the Balch tubes were analyzed identically as discussed in the laboratory experiments of Chapter 5. Acetate, propionate and butyrate concentrations were measured in duplicates from each Balch tube. The pH, CO_2 and CH_4 were measured once from each Balch tube and Ca^{2+} values were measured from two of the three Balch tubes collected at different elapsed times.

6.4 RESULTS AND DISCUSSION

6.4.1 Acetate, propionate and butyrate concentrations over time

Figure 6.1 shows the different average concentrations of acetate, propionate and butyrate over time for the different digestion tests. The highest average removal values of acetate after 72 hours of digestion were attained in Tests 2, 3 and 4, averaging 1,466, 1,482 and 1,698 mg HAc/L (24 to 29 mmol/L) respectively, indicating nearly complete removal of available acetate (between 80 to 100%). These tests also had the highest removal of butyrate (44% and 55%). Since tests 3 and 4 were prepared with the same acetate and propionate molar ratios, the acetate to propionate molar ratios of 2:1 and 1:1 exhibited the highest acetate and butyrate removal rates. In the case of propionate, test 5 (acetate to propionate molar ratio of 1:2) shows the highest removal value at 565 mg HPr/L (7.6 mmol/L), and at the same time, the second highest percentage removal of acetate

(approximately 88%). Tests 2 and 5 attained similar amounts of acetate removal after 72 hours.

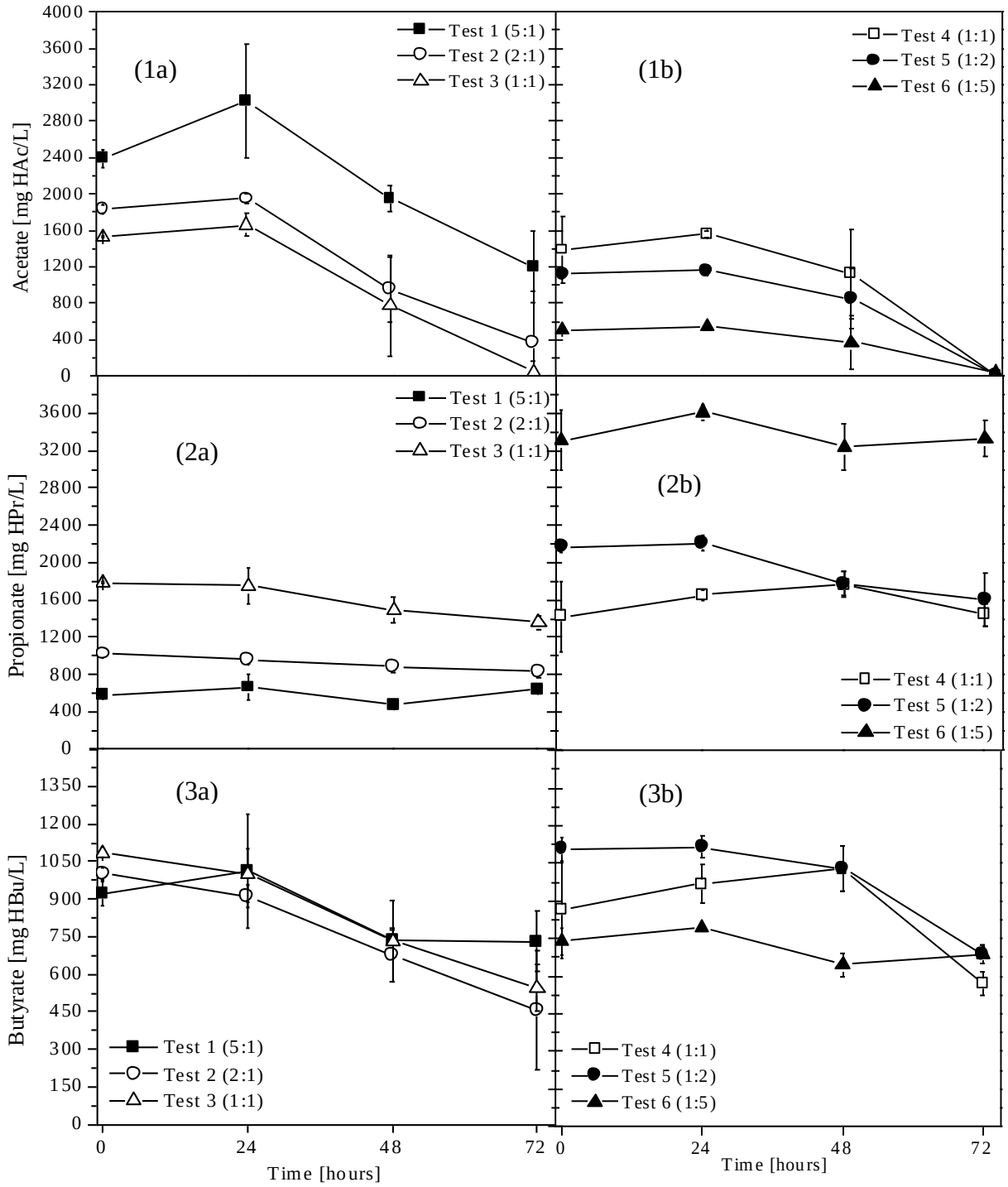

Figure 6.1. Average of (1) acetate, (2) propionate and (3) butyrate in tests (a) 1, 2 and 3 and (b) 4, 5 and 6 with time. The numbers in parenthesis represent the acetate to propionate molar ratio tested.

Test 1 with the highest concentration of acetate (2,400 mg HAc/L- see Table 6.2), showed 50% acetate removal after 72 hours of digestion (> 1000 mgL^{-1} removed), but no propionate removal was measured. Test 6 with the highest concentration of propionate (3,313 mg HPr/L), showed very little removal of butyrate and virtually no propionate removal during the 72 hours of digestion. Despite removing 30% of the acetate over the 72 hours of digestion, this only represented 10% of the acetate removal observed in Tests 2, 3 and 4. Overall, Test 6 shows the worst performance for VFA removal. For Tests 2, 3, 4 and 5, acetate and propionate removal values were observed after 72 hours of digestion. These results suggest that equalization of high initial concentrations of acetate and propionate is required in order to maximize the anaerobic treatment of leachate, favoring the activity of synthrophic bacteria. Since test 5 showed approximately 20% removal of propionate during the 72 hours of digestion, synthrophic communities were also present within the inoculum.

6.4.2 pH and dissolved Ca^{2+} concentrations

Given the removal of acetate in all tests, and butyrate and propionate removal in some of the tests, pH values were expected to increase, as shown in Figure 6.2. The largest increase in pH was attained for Tests 3 and 4, followed by Test 2. This is consistent with the acetate and butyrate removal values observed in Figure 6.1. The study described in Chapter 5 tested the removal of dissolved Ca^{2+} at different pH values in synthetic leachate saturated with CO_2 under controlled laboratory conditions. This study showed

that between pH 7.2 and 7.4, the concentration of dissolved Ca^{2+} decreased between 65% and 80%.

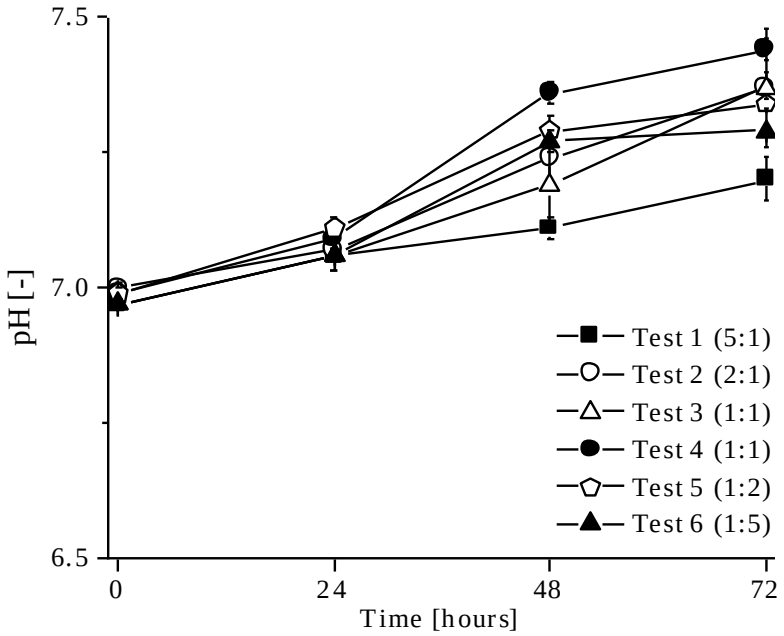

Figure 6.2. Variation of pH in tests 1 to 6 with time. The numbers in parenthesis represent the acetate to propionate molar ratio tested.

For the current tests 1 to 6, average dissolved Ca^{2+} percentage removal values of 34.8, 67.8, 55.8, 50, 43.5 and 33.3% after 72 hours of digestion were obtained, as pH values were higher than 7.2. Tests 1 and 6 show the lowest percentage removal of dissolved Ca^{2+} and the smallest increase in pH (Figure 6.2 and Appendix Q).

6.4.3 CH_4 and CO_2

As VFA's were removed, biogas was formed within the headspace of the Balch tubes. Figures 6.3 show the average CO_2 and CH_4 (mg/L) concentrations measured in the headspace of the Balch tubes after 24, 48 and 72 hours of digestion for Tests 1 to 6.

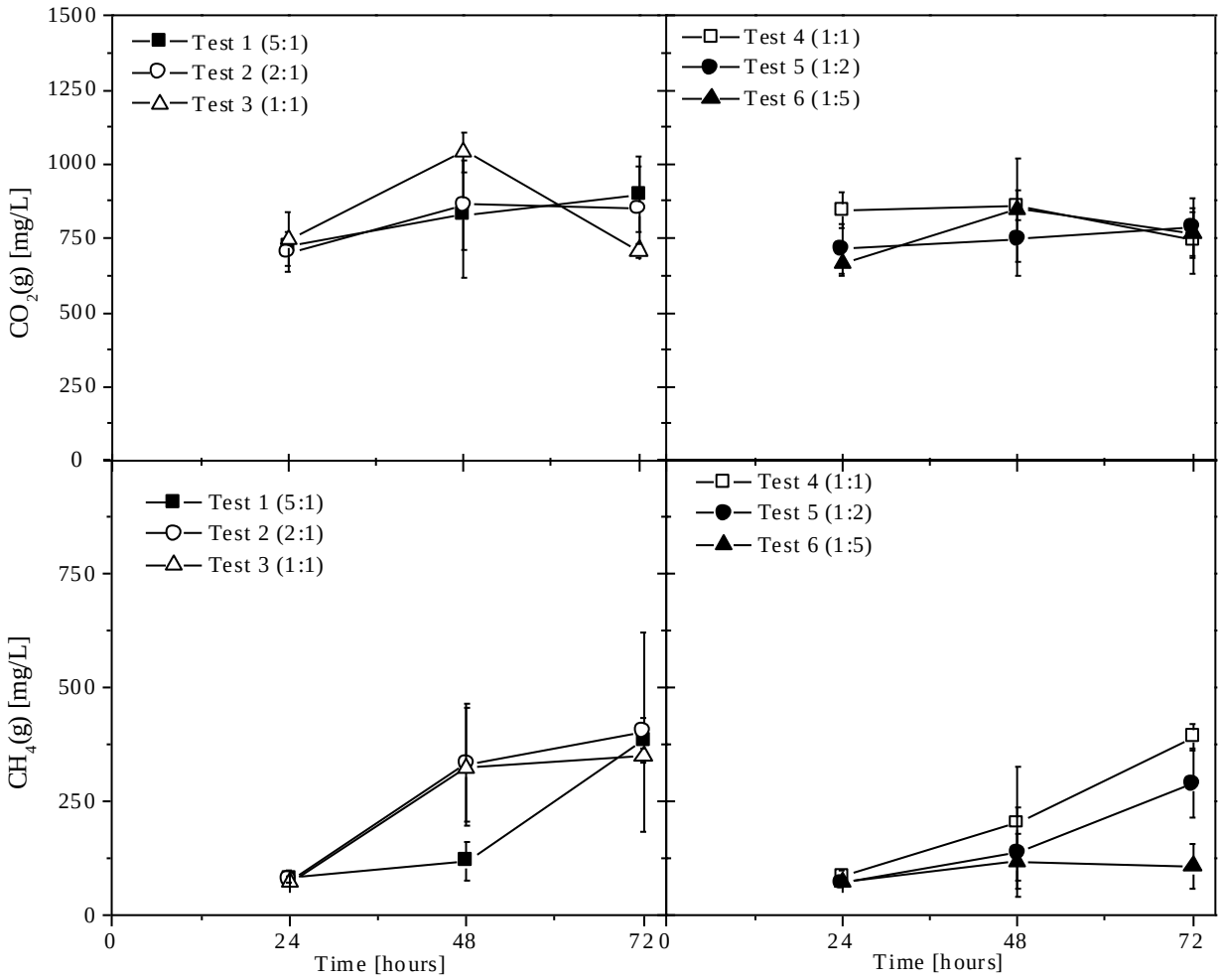

Figure 6.3. Average values of (1) CO_2 and (2) CH_4 values (mg/L) measured in the headspace of the Balch tubes after 24, 48 and 72 h of digestion for tests 1 to 6. The numbers in parenthesis represent the acetate to propionate molar ratio tested.

During tests 2, 3 and 4, a rapid increase of the CH_4/CO_2 ratio was measured in the headspace as shown in Figure 6.4. Tests 1 and 5 show a slow CH_4/CO_2 ratio increase during the first 48 hours, where Test 6 did not show a CH_4/CO_2 ratio increase during this study.

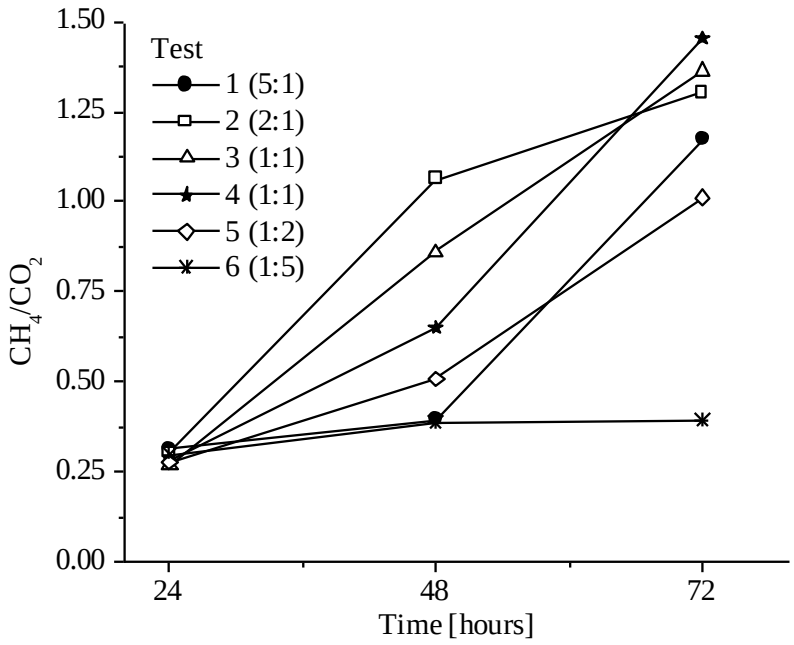

Figure 6.4. CH_4/CO_2 ratios in the headspace for tests 1 to 6 during the 24, 48 and 72 hours of digestion. The numbers in parenthesis represent the acetate to propionate molar ratio tested.

These differences of CH_4/CO_2 ratio in the headspace over time are explained as the effect of VFA removal on the pH values, and the increase of CO_2 converted into carbonate, eventually causing the removal of dissolved Ca^{2+} as $CaCO_3$. As pH in the medium and CO_2 in the headspace of the Balch tubes increased (see Figure 6.2 and 6.3), a shift in the carbonate equilibrium of the medium was expected, increasing the carbonate availability within the tubes. This was verified by calculating the average dissolved CO_2 concentrations, HCO_3^- and CO_3^{2-} in the medium using Henry's law and the Hendersen-Hasselbalch equation, and is shown in Tables 6.3 and 6.4. These calculations of CO_2 concentration in the medium used the measured pH of the medium and CO_2 concentration in the headspace at 24, 48 and 72 hours of digestion for Tests 1 to 6.

Table 6.3**.** Average dissolved CO_2 (mg/L), bicarbonate (HCO^{3-}) and carbonate (CO_3^{2-}) concentrations in the medium calculated for 24, 48 and 72 hours of digestion for Tests 1 to 3. The numbers in parenthesis represent the acetate to propionate molar ratio tested.

Parameter	Unit	TESTS								
		1 (5:1)			2 (2:1)			3 (1:1)		
		24	48	72	24	48	72	24	48	72
CO_2	mg/L	402	461	499	391	479	472	415	578	394
HCO_3-		3137	4013	5350	3136	5671	7782	3254	6129	6309
CO_3^{2-}		2	3	5	2	6	11	2	5	8

Table 6.4**.** Average dissolved CO_2 (mg/L), bicarbonate (HCO^{3-}) and carbonate (CO_3^{2-}) concentrations in the medium calculated for 24, 48 and 72 hours of digestion for Tests 4 to 6. The numbers in parenthesis represent the acetate to propionate molar ratio tested.

Parameter	Unit	TESTS								
		4 (1:1)			5 (1:2)			6 (1:5)		
		24	48	72	24	48	72	24	48	72
CO_2	mg/L	468	478	412	396	414	438	370	470	424
HCO_3-		3902	7437	7681	3475	5559	6501	2884	5887	5659
CO_3^{2-}		3	9	12	2	6	8	2	6	6

To verify the quality of our gas measurements relative to the substrate concentration, a mass balance was performed for the 72 hour digestion period. In order to account for the dissolution of gases (mostly CO_2) into the medium and the carbon loss, CO_2, HCO_3^-, and CO_3^{2-} were calculated as explained above and shown in Tables 6.3 and 6.4. Due to the pH values measured within the Balch tubes, it was expected to find most of the C converted into HCO_3^-, as shown in Tables 6.3 and 6.4. The conversion of dissolved CO_2 to HCO_3^- was calculated using a pKa of 6.3 and a pressure of 1.5 atm. In addition, the carbon loss due to dissolved Ca^{2+} removed as $CaCO_3$ was also determined. Table 6.4 shows the

CH_4/CO_2 ratio calculated from the removal of acetate, propionate and butyrate values removed after 72 hours of digestion. Column (b) of Table 4 indicates the CH_4/CO_2 ratio calculated from the values measured within the headspace and calculated from the dissolved phase. Finally, column (c) shows the ratio of carbon formed versus carbon consumed, calculated as CH_4 and CO_2 presence in the gas and dissolved phases against the carbon removed by the consumption of acetate, propionate and butyrate after 72 hours of digestion.

Table 6.5**.** (a) CH_4/CO_2 ratio calculated from the removal of acetate, propionate and butyrate values removed after 72 hours of digestion, (b) CH_4/CO_2 ratio calculated from the headspace measurements at 72 hours and (c) carbon formed as the CH_4 and CO_2 presence in the gas and dissolved phases versus carbon consumed from the VFA removed within 72 hours of digestion.

Tests	(a) CH_4/CO_2	(b) CH_4/CO_2	(c) $C_{formed}/C_{consumed}$
1	1.1	1.17	1.2
2	1.2	1.30	1.2
3	1.2	1.36	0.8
4	1.2	1.45	0.9
5	1.2	1.01	1.0
6	1.1	0.39	2.7

Note: Pressure at 1.5 atm

From Table 6.5, it can be observed that Tests 1 to 5 present similar theoretical and measured CH_4/CO_2 ratios, showing a balance of gases formed in both phases, and carbon balance from products (gases) and substrate (VFA). The inhibition of methanogenesis observed in Test 6 (high propionate) gave rise to a different CH_4/CO_2 measured than theoretical ratio value expected. The observation that more carbon was formed than consumed may be attributed to the lower amount substrate consumed and gases produced (CH_4 and CO_2) as well as possible measurement error.

From Figure 6.4 and Table 6.3, the following observations can be made.

- The average CH_4 increased (ranging from 70 to 403 mg/L) for all the tests, except test 6 (highest propionate) between 48 and 72 hrs of digestion
- The average CO_2 increased (ranging from 713 to 899 mg/L) with time for test 1 and 5. For tests 2, 3, 4 and 6 there was a decrease in the average amount of CO_2 measured in the gas phase between 48 and 72 hrs (ranging from 863 to 741 mg/L).
- The highest amount of average CH_4 (134 mg/L*day) was achieved during test 2 after 72 hours of digestion, followed by test 1, 3 and 4 (117, 128 and 131 mg/ L*day).
- Methanogenesis stopped after 48 hours for the Balch tubes with the highest concentration of propionate (average 3,313 mg HPr/L – Test 6).
- The CH_4/CO_2 ratio increased in the gas phase over time for all tests. It was highest for the Balch tubes with the acetate to propionate molar ratio of 1:1, achieving an average value of 1.45 after 72 hours of digestion.
- Total dissolved CO_2 (CO2, HCO_3^-, CO_3^{2-}) increased over time for all tests, except for the Balch tubes with the highest concentration of propionate, between 48 and 72 hours.

6.4.4 Mechanisms of $CaCO_3$ precipitation

To better represent the mechanisms observed within the digestion tests (especially tests 2, 3 and 4) performed in this study, a conceptual framework that identifies key variables

affecting the precipitation of $CaCO_3$(s) during methanogenesis of leachate under sealed conditions is presented in Fig. 6.5.

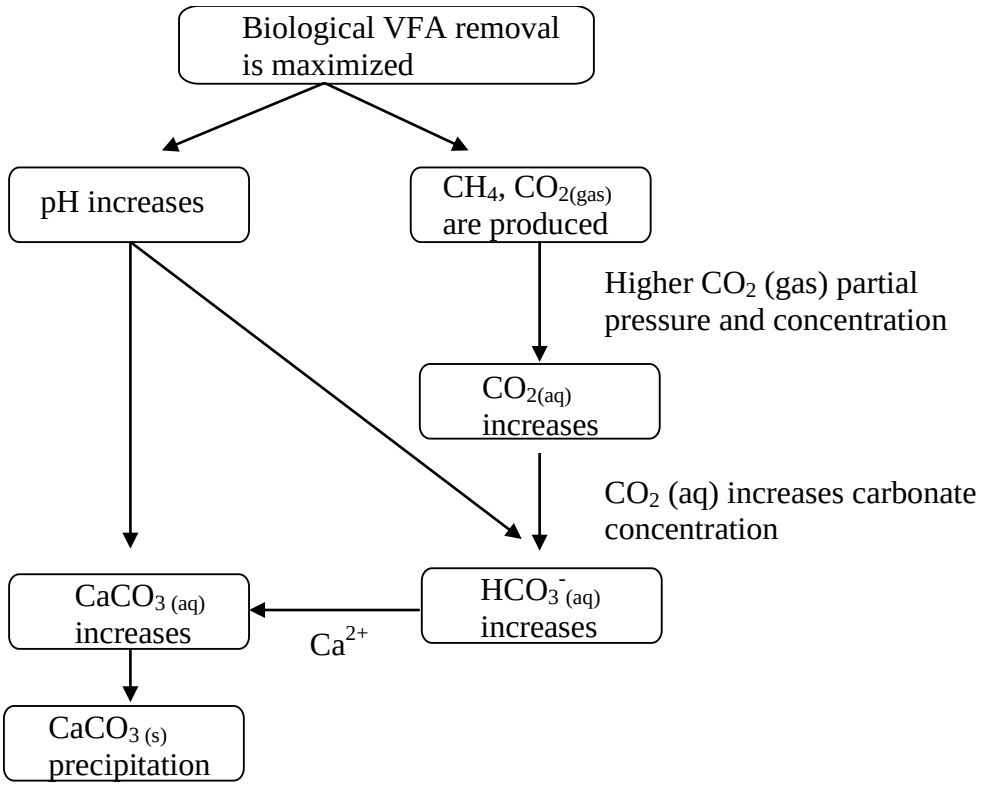

Figure 6.5. A flowchart describing the relationship between VFA methanogenesis and the mechanisms of $CaCO_3$ precipitation (inorganic clogging) in the Balch tubes as a model for inorganic clogging in landfill pipes.

Figure 6.5 depicts a flowchart describing the relationship between VFA removal and the mechanisms of $CaCO_3$ precipitation observed in tests 2, 3 and 4. When optimum influent acetate and propionate concentrations are metered into the digester, VFA removal is maximized thereby increasing the pH of the medium and producing CO_2 and CH_4 as biogas most quickly. The increase of $CO_{2(g)}$ in the headspace increases the partial pressure and concentration of the gas, increasing the concentration of $CO_{2(aq)}$. This

increase in $CO_{2(aq)}$ destabilizes the carbonate equilibrium of the medium, with more CO_2 converted to bicarbonate. This increase in carbonate is further accentuated by the pH increase, as the pH goes further away from the pK_a. This increase in bicarbonate and the availability of significant amount of Ca^{2+} within the leachate leads to $CaCO_{3\,(aq)}$ which at pH values higher than 7.2 at 20% CO_2 (Figure 5.7 of Chapter 5) precipitates as $CaCO_{3(s)}$.

6.5 CONCLUSIONS

This study has shown that methanogenesis of leachate-like media was influenced by the ratio of acetate and propionate. Methanogenesis was the highest at acetate to propionate molar ratios of 2:1 and 1:1. It was also shown that methanogenesis was inhibited at acetate to propionate molar ratio of 1:5.

Methanogenesis of VFA increased the digester pH, which increased the concentration of CO_2, as carbonate and bicarbonate in solution. This in turn can lead to the precipitation of $CaCO_3$. It is suggested that if leachate undergoes methanogenesis in a separate leachate digester prior to re-injection into a bioreactor waste cell, it may protect the pipes and other engineered landfill systems against calcium carbonate precipitation and its detrimental effects, while allowing for methane recovery from the digester gas phase.

However, blending of leachates from different wells or cells prior to the methanogenic digester may be needed to balance the variable concentrations and ratios of acetate and propionate over time from different landfill wells and cells. Metering leachate on a continuous basis will likely be required.

CHAPTER 7: CONCLUSIONS AND RECOMMENDATIONS

7.1 RESEARCH OVERVIEW

This thesis investigated the changes in leachate composition and clogging evolution in leachate injection systems and the use of methanogenesis as a leachate treatment alternative, using a pilot-scale and laboratory studies. The pilot-scale study consisted of a research station built at Brady Road Landfill in Winnipeg, housing sixteen HDPE pipes of three different diameters, conveying leachate intermittently (Pump On and Off times) at different Reynolds numbers, under reasonably controlled conditions. The pipes were tested for leachate degradation, clogging evolution and hydraulic impairment over time. The laboratory studies carried out tested (1) turbulence intensity and temperature effect on leachate degradation and clogging effects and (2) biological pretreatment of leachate prior to injection into a bioreactor cell. This chapter provides a summary and the conclusions of the work presented in this thesis with the engineering significance and recommendations for future work.

7.2 SUMMARY AND CONCLUSIONS

Chapter 2 presented a general review of leachate and biogas composition during the different landfill phases was reported through the literature review. A more specific description of the anaerobic mechanisms and the main types of bacteria involved in the different biological, physical and chemical reactions was shown. Leachate collection systems were superficially explained, and literature design and operational values of leachate injection systems were shown. Clogging mechanisms in porous media of

leachate collection systems and the conceptual processes that may contribute to clogging within leachate injection systems in bioreactor landfills were explained. Finally, the main results obtained from the applicant's MSc investigating leachate degradation and clog formation using laboratory pipes were presented. This study was designed to understand the mechanisms of clogging in leachate injection pipes, but it only analyzed leachate degradation while it passed through the laboratory pipes intermittently for 5 months. The results of this study were very difficult to scale-up as leachate injection schedule is dependent on the targeted waste moisture and the daily schedule of the landfill operator. It was suggested that leachate stagnant within the pipes, after the pumps are turned off, may play a significant role in accelerating clogging within the injection pipes.

Chapter 3 presented the results of the pilot study, showing that under the Reynolds numbers operated within the testing pipes and leachate composition values, pipes developed a significant amount of organic and inorganic clog material in less than a year of operation. Since leachate recirculation in full scale bioreactor landfills could be performed every day of the week, depending on the waste moisture targeted by the landfill engineer, this study does not represent the worst case scenario. This means that significant clogging can occur in full scale leachate transmission pipes in less than a year of operation. Finally, conceptual representations of clog development within leachate injection pipe systems while (1) leachate is pumped and (2) leachate is stagnant (pump OFF) were proposed.

Since high pH values (above 8 at all times) were measured within the pipes tested after each pumping experiment, and limited removal of COD over time was obtained (average value removed 11%), compared with the 50% average removal values of dissolved CO_2 after pumping, this indicated that CO_2 degasification was the main mechanism of pH increase during pumping, rather than biological activity. As the pH increased, Ca^{2+} was being removed while pumping, precipitating out within the tanks and pipes. During stagnation, leachate had already attained high pH values (pH > 8) from pumping, so more Ca^{2+} removal was observed. In addition, TSS mass removal (averaging approximately 65%) was observed during the first 24 hrs of stagnancy during each pumping cycle, indicating the importance of evacuating leachate during the first 24 hours of stagnancy to avoid clogging produced by TSS, VSS and FSS removal. Therefore, settlement of suspend solids was the main clogging mechanism within the pipes tested during stagnant conditions. As Ca^{2+}, COD, alkalinity, TSS, VSS and FSS masses were removed from the leachate during pumping and stagnation over time, organic and inorganic clogging accumulated within the pipes.

Clog material collected from the testing pipes changed over time. There was a significant increase in inorganic versus organic content (65% to 88%) over time and clogging became "harder" over time as water versus total solids content increase from 6.5% to 22%. Ca^{2+} was the main cation component of clogging (ranging from 4.7 to 19.1%), which was similar to studies of clog accumulated within porous media. Mg^{2+} values sampled from clogging collected in this study were significantly lower (0.8 to 4.4%) than Lozecznik and VanGulck (2009) (17 to 19.4%). Throughout this chapter, the author

denominated as biofilm the 20 to 30% of volatile solids measured from the clogging accumulated within the testing pipes over time. Even though the organic matter was not characterized (e.g. EPS, proteins, stratification, etc.) nor was microbial identification performed, the pipe testing results showed that COD and VFA were removed within the pipes over time. This was explained as the result of the suspended microorganisms and biofilm activity within the pipe environment. In addition, Lozecznik (2006) performed resin embedding and light microscopy within the volatile solids accumulated within the laboratory pipes (same material) that conveyed leachate from Brady Road Landfill under intermittent conditions. This analysis showed an important amount of organic matter accumulated around the wetted perimeter of the pipes and through the clog thickness. For the reasons presented above, based on the biofilm literature (see section 2.7.1) and on the presence and importance of biofilm in the clogging mechanisms of leachate collection systems (section 2.7.2), the author maintains the presence of biofilm within the slime material collected from the testing pipes over time. Further studies are needed to characterize the biofilm developed with the clog material accumulated in leachate injection pipes.

The reason may be the lower pH values attained during this research due to shorter periods of pumping, hence CO_2 outgassing effects. XRD analysis confirmed this larger amount of Ca^{2+} sampled from the clog material collected, showing mainly calcium carbonate type of materials such as aragonite ($CaCO_3$), monohydrocalcite ($CaCO_3H_2O$), calcite ($CaCO_3$), dolomite $CaMg(CO_3)_2$ and gypsum ($CaSO_4 \cdot 2H2O$). In addition, there were small amounts of moganite (SiO_2) and quartz (SiO_2) detected.

Head loss measurements from the pipes showed that small pipe diameters had the most significant head losses (increased from 16 to 60% of the initial values measured for the clean pipes). In addition, some of the centrifugal pumps had problems attaining the specified flow rates due to excessive clogging, requiring to stop the operation of the system to clean the pumps. This may indicate that centrifugal pumps are not the optimal choice for leachate injection systems. Finally, larger diameter pipes had the largest amounts of clogging and differences in clogging mass between pipe inlet and outlet, showing that clogging is not uniform along the length of the pipelines.

Chapters 4, 5 and 6 presented the results of the laboratory investigations. Based on the results obtained from the pilot study (Chapter 3), Chapter 4 presented the results from laboratory studies investigating the effects of turbulence level and temperature on the $CO_{2\ (gas)}$ concentration and leachate degradation (dissolved Ca^{2+} and pH) using synthetic and real leachate. Sealed reactors with rotating propellers were used to mimic leachate flow through the testing pipes and they were operated under turbulent conditions for 6 hours ON and 18 hrs OFF. A control reactor was operated parallel to the reactors at 0 Reynolds number. During the OFF phase, the reactors were either sealed or open to the atmosphere.

Under sealed conditions and pH values lower than 7.2, no significant changes in chemistry were observed for the synthetic or real leachate. However, for the mixers and control reactors containing real leachate at pH values higher than 7.4, the pH dropped approximately by 0.3 to 0.4 units. The drop in pH is explained by Ca^{2+} removal as $CaCO_3$

decreasing the carbonate buffering capacity of the leachate, out-competing the re-equilibration of CO_2 evolved to the headspace of the reactors and its pH effect. The geochemical modeling software MINEQL+ was used to verify this interpretation, and showed the same trend in pH decrease. Under open conditions, CO_2 evolution, as it equilibrated with the atmospheric concentration, was responsible for increasing the pH by one unit for the synthetic leachate and between 0.35 to 0.45 units for the real leachate. Temperature increase (from 4˚C at storage room to 22˚C at room temperature), without turbulence, had an important effect on pH increment and leachate degradation as observed within the control reactors. This temperature effect is relevant for cold climate landfills as leachate is commonly collected to a sump or tank, and seasonal temperature variation can decrease significantly the leachate temperature as it is evacuated from the bottom of landfill. For the leachate sampled from the landfill wells at Brady Road Landfill showed that temperature fluctuated between 7.5˚C to 18.7˚C. Since Bioreactor Landfills have been reported to reach internal temperatures over 30˚C, recirculation of this leachate will affect the CO_2 evolution from it, and create clogging issues during recirculation. Due to the different results obtained between the synthetic and real leachate tests at identical laboratory controlled conditions, the future use of this is discredited, especially to represent physical/chemical degradation processes.

Chapter 5 presented the results of the laboratory study that treated real leachate from Brady Road Landfill by using methanogenesis. This study investigated the use of methanogenesis as a leachate treatment strategy to reduce the organic and inorganic clogging precursors from leachate prior to injecting leachate into a bioreactor landfill. In

this study, an anaerobic sequencing batch reactor (ASBR) was operated with leachate from Brady Road Municipal Landfill in Winnipeg, Manitoba, Canada. The ASBR was seeded at the start-up with biosolids from the anaerobic digester from Winnipeg's North End Water Pollution Control Center (NEWPCC). This study has shown that high levels of methanogenesis can be achieved with leachate..

Amounts of methane averaging 0.35 L/g CODrem (removed) were produced, which are close to the 0.4 L CH_4/g CODrem theoretical value obtained by chemically oxidizing methane at 35˚C. Concurrent with the removal of COD and VFA, an increase of approximately 0.3 pH units was observed during each cycle (from pH 7.2 to 7.5). CO_2 also was produced between cycles at constant temperature where a fraction of the CO_2 became dissolved, shifting the CO_2/bicarbonate/carbonate equilibrium. In addition to the increase in pH and carbonate, an accumulation of inert suspend solids (ISS) was observed within the ASBR, indicating a build-up of inorganic material over time. From the ISS effect produced, Ca^{2+} and Mg^{2+} were measured within the reactor on day 140, indicating that most of the dissolved Ca^{2+} was removed during digestion.

A parallel study investigated this observation using synthetic leachate under controlled laboratory conditions. The results of the study indicate that leachate with high concentration of Ca^{2+} under CO_2 saturation conditions (20%) can precipitate out $CaCO_3$ at the pH values obtained between digestion cycles of the ASBR. From the studies performed, it can be concluded that methanogenesis of leachate impacts the removal of organic (COD, VFA) as well as inorganic (FSS, Ca^{2+}) clog constituents from the leachate that otherwise will accumulate inside of the recirculation pipe in bioreactor landfills.

Since the variability of leachate composition (e.g. VFA) affected the ISS removal rates within the ASBR (Chapter 5), the study described in Chapter 6 aimed to quantify the effect on leachate methanogenesis produced by the variation of acetate and propionate concentrations under controlled laboratory conditions. Batch studies of synthetic leachate with different initial concentrations of acetate (500-2,500 mg HAc/L) and propionate (500-3,500 mg HPr/L) were treated with active biomass collected from the prior study under anaerobic mesophilic conditions for 72 hours. The highest removal of acetate (80-100%) and propionate (15-35%) were achieved in tests with initial concentrations ranging from 1,500-1,900 mg HAc/L (25-30 mmol/L) and 1,000-1,800 mg HPr/L (13-24 mmol/L) or acetate to propionate molar ratios of 2:1 and 1:1. Concurrent with the removal of acids, pH increased between 0.3 to 0.45 units, removing 50 to 70% of dissolved Ca^{2+} as $CaCO_3$. This study showed that lower acetate to propionate molar ratio impacted leachate methanogenesis. By combining various sources of leachate with different ratios of propionic and acetic acids (e.g. from different cells at a landfill), aiming to achieve the concentrations shown above in an equalization tank, leachate methanogenesis prior to injection would be maximized.

The laboratory studies from Chapters 4, 5 and 6 were connected to the pilot-scale study of Chapter 3 by exploring the individual parameters that promoted clogging within the testing pipes and could not be assessed in the field. Chapter 4 showed that leachate under turbulent and sealed conditions did not change in composition for the conditions tested. However, under turbulent and open conditions it showed changes in composition for the

real and synthetic leachate. These results changed the dynamics of clogging while leachate is flowing within the pipe (Figure 3.29), for example, the buffer capacity of the leachate can outcompete the pH effects of CO_2 outgassing, leaving the leachate pH unchanged. Chapter 4 also investigated the effects of temperature and CO_2 outgassing during stagnation, demonstrating that temperature differential can be an important mechanism of clogging during stagnation (Figure 3.30), especially during winter months where higher differences in temperature can be observed between the leachate stored in the sump or tank and the inside of the Bioreactor Landfill. The results from Chapter 5 agreed with the conceptual effect of the biological activity on the dynamics of CO_2 within the pipe environment, as shown in Figure 3.30. But it also changes the VFA utilization rates predominance depending on the leachate composition. Chapter 6 showed that acetate to propionate molar ratio within the leachate influenced the VFA utilization rate, hence leachate methanogenesis. Since leachate changes in composition from well to well, even from day to day from the same well (Chapter 3 and Chapter 5), the importance of these mechanisms will vary in Figures 3.29 and 3.30.

7.3 ENGINEERING SIGNIFICANCE

The work presented addressed several issues related to the design and operation of bioreactor landfills. The pilot study has shown that pipes conveying leachate have limited service life due to a significant accumulation of organic and inorganic material known as clogging or biorock during the first year of operation. The experimental results indicated that the hydraulic operation (flow rate, inlet head pressure) of the pipes and their physical characteristics (diameter, pipe length and material) impacted clogging composition and

accumulation. Designing liquid injection systems with low flow rates and inlet head values to uniformly inject leachate into the waste is necessary in order to minimize turbulence and CO_2 evolvement, thus minimizing the increase in leachate pH values. This will minimize the removal of inorganic dissolved solids that are known to contribute to the development of clog material.

One alternative could be to design liquid injection systems with shorter pipes distributed uniformly within the waste cell to maximize the zone of wetting. It is also important during operation to limit leachate stagnation within the pipes, avoiding the settlement of suspended solids, thereby preventing the performance impairment of the pipe perforations commonly located at the bottom of the pipes. To help lessen this impairment of performance, it is recommended to change the location of the pipe perforations to the sides or top of the pipe. This will limit the effects of TSS settling within the perforations during leachate stagnation. Considering the impact of perforation locations and the hydraulic behavior must therefore be previously evaluated.

As demonstrated in the clogging results of the pilot study, the distribution and composition of clogging changed within the pipe series and over time. Clogging accumulated as a hard film material forming a uniform coat around the wetted perimeter of the pipe series operated at Reynolds numbers higher than 30,000. For the pipe series operated at Reynolds numbers lower than 30,000, clogging accumulated as several layers of organic and inorganic material, mainly at the bottom of the pipes. For all the pipe series, clog material became denser over time. These changes impact the effectiveness

and costs of the cleaning strategy adopted by the landfill manager such as the types and amounts of chemicals needed. The effectiveness of the mechanical cleaning strategy (e.g. water pressure) adopted by the landfill manager is also impacted if clogging is not removed at the earlier stages of formation. For each pipe ring removed, calcium types of minerals (e.g. aragonite, monohydrocalcite) were mainly found within the clogging collected at different times. This has a direct impact on the chemical chosen for pipe cleaning, aiming mainly to break the calcium carbonate bond. On the operational cost side, clogging also impacts the energy required at the pipe inlet to discharge leachate uniformly along the length of the pipe over time.

Head losses were greater within small diameter pipes and inlet head losses were greater within higher inlet head pumps. From these results, there is a need to select pumps with low head values and perforated pipes producing small head losses at the flow rates selected to reduce operational costs due to clogging formation.

Clogging was demonstrated to be non-uniform along the length of the pipes, accumulating more at the pipe end. This clog material formation will affect the moisture distribution of bioreactor landfills that employ leachate injection pipes with dead ends, rather than the pressurized pipe loops, generating zones of non-wetting within the refuse, especially on the waste located under the end of the pipe. This limits the benefits of leachate recirculation, impairing the hydraulic interactions between the pipe, trench and refuse. From these results, it can be concluded that selecting small pipe diameter and not

cleaning frequently against clog development will negatively impact the benefits of leachate recirculation in less than a year.

From the results obtained from the bench scale work, it can be inferred that the turbulence intensity selected by the landfill manager to operate the injection system affects the rate of clogging. If the system is not perfectly sealed (e.g. pipe CO_2 leak) pH values will increase dramatically, affecting dissolved Ca^{2+} removal and clogging accumulation within the pipelines. As temperature variation affects leachate pH values, the operation of the injection lines during winter may have a larger impact on leachate degradation than during the summer season. This temperature effect can be avoided if a temperature equalization tank or a leachate pre-treatment reactor requiring higher temperature prior to injection is operated.

From the leachate treatment results, performing methanogenesis prior to injection into the bioreactor landfill reduces the clog components of the leachate (COD, VFA, Ca^{2+}) and produces an extra source of energy (CH_4), adding revenue to the landfill management. Nevertheless, significant differences in VFA removal and CH_4 gas formation were observed with leachate collected from the same leachate well, mainly due to the differences in leachate composition (COD and VFA such as acetate and butyrate) and its inherent variability in landfills. It was also shown that establishing a constant source of carbon from different leachate sources in an equalization tank prior to methanogenesis (for example 1,500-1,900 mg HAc/L and 1,000-1,800 mg HPr/L) will help to maximize

the removal of VFA, a key clog component, and maximize CH_4 formation at the landfill facility.

7.4 FUTURE WORK

Despite the clogging studies that have indicated that dissolved CO_2 and VFA are the main parameters affecting the increase in leachate pH and removal of dissolved Ca^{2+}as $CaCO_3$, the majority of the landfill leachate reports (pages 14 and 172) mainly include organics (e.g. COD), metals (Ca^{2+} and Mg^{2+}) and alkalinity within the leachate composition analysis. As CO_2 and VFA are important for clog development, knowing the general trend over time would help to understand clogging potential in bioreactor landfills. Therefore, dissolved CO_2 and individual VFA composition values within the leachate need to be reported during the different landfill phases. In addition, analysis of TSS within leachates and its sedimentation time with respect to pipe sizes will help to minimize clogging issues during stagnation.

The pilot study in Chapter 3 did not measure the ORP and Eh leachate values during collection, pumping and stagnation within the testing pipes. Since leachate is commonly stored outside of the waste cell in a tank or sump prior to recirculation, it is anticipated that storage time will increase the ORP and Eh of the leachate. The recirculation of a more aerobic leachate will change the characteristics of any biofilm developed within the injection pipes under anaerobic conditions, for example, it is expected to find aerobic/anaerobic alternating bacteria within the biofilm and suspension. In addition, the change in Redox environment within the pipe after leachate is pumped will influence the

activity of suspended microorganisms and biofilm, such as the ability to remove VFA. Changes in Redox environment between the tank or sump (aerobic) and the injection pipes (anaerobic) can also affect the mobility and precipitation of metals within the leachate, for example, metal sulfides precipitate when the system becomes reduced (Domenico and Schwartz 1990). Verification of the above statements is recommended in future investigations to clarify the effects, if any, of the changes in leachate redox and clogging formation within the injection pipes.

The analysis of clog material collected from injection systems in bioreactor landfills is required in order to generalize the results obtained with this study. Pipe design and operation, location within the waste cell and zones of wetting to minimize the impact of clogging requires further study as a system rather than individual components of leachate injection systems.

Further research is needed to fully understand the interactions between synthrophic bacteria and acetoclastic methanogens for leachate treatment purposes. This study and past studies of clogging (VanGulck *et* al. 2003, VanGulck and Rowe 2004a) have shown poor removal values of propionate, so selecting the conditions that maximize the activity of both groups will maximize the removal of clog components and produce an important amount of CH_4 on-site.

From the results of the study of methanogenesis with different acetate and propionate ratios, it is not clear what the impact would be of the individual VFA on the methanogens

and synthrophs in the bioreactor cell. Future research determining the ideal concentration of VFA that will maximize methanogenesis in the bioreactor landfill may help to define the level of leachate treatment required prior to injection. This research could aid in the design of the equalization tank prior to methanogenesis (outside of the waste cell), defining the required VFA effluent concentration needed from the methanogenic pretreatment reactor.

Future research is needed to investigate the effects of landfill temperature on leachate changes in temperature and degradation during recirculation for colder seasons. If leachate methanogenesis under mesophilic conditions (35˚C) is performed prior to recirculation, constant leachate temperature and VFA concentrations will be achieved in the effluent, benefiting the growth and activity of methanogens and synthrophs inside the bioreactor cell.

REFERENCES

Abtahi, M., Kaasa, B., Vindstad, J. and Øtvold, T. (1996). Calcium carbonate precipitation and pH variations in oil field water. A comparision between experimental data and model calculations.

Al-Yousfi, A.B. and Pohland, F.G. (1998) Strategies for simulation, design and management of solid waste disposal sites as landfill bioreactors, *Practice Periodical of Hazardous Toxic and Radioactive Waste Management* 2(1), 13-21.

Al-Yousfi, A. B. 1992. Modeling of leachate and gas production and composition at sanitary landfills, PhD Thesis, University of Pittsburg, Pittsburg, USA.

Andreottola, G. and Cannas, P. 1992. Chemical and biological characteristics of landfill leachate, in *Landfilling of Waste: Leachate*, Christensen, T.H., Cossu, R. and Stegmann, R., Eds., Elsevier Applied Science, London, UK, 1992, pp. 65.

Armstrong, M.D. (1998). Laboratory program to study clogging in a leachate collection system. M.E.Sc. thesis, The University of Western Ontario, London, Ontario, CANADA.

ASTM D854. Standard test methods for specific gravity of soil solids by water pycnometer. The American Society for Testing and Materials, West Conshohocken, PA, U.S.A.

Batstone, D. J., Keller, J., Angelidaki, I., Kalyuzhnyi, S., Pavlostathis, S. G., Rozzi, A., Sanders, W. T. M., Siegrist, H., and Vavilin, V. A. (2002). Anaerobic digestion model no. 1 (ADM1). *Scientific and Technical Report No. 13*, IWA Task Group for Mathematical Modelling of Anaerobic Digestion Process, London, UK.

Barlaz, M.A. and Ham, R.K. (1993). Leachate and gas generation. Geotechnical practice for waste disposal, D.E. Daniel, Ed., Chapman and Hall, London, pp 113.

Bitton, G. (1999). Wastewater microbiology, second edition. Wiley Series in Ecological and Applied Microbiology, Ralph Mitchell, Series Editor. pp 578.

Borojovich, E., Münster, M., Rafailov, G. and Porat, Z. (2010). Precipitation of ammonium from concentrated industrial wastes as struvite: A search for the optimal reagents. *Water Environment Research* 82(7), 586-591.

Bouchez, T., Munoz, M-L., Vessigaud, S., Bordier, C., Aran, C. and Duquennoi, C. (2003). Clogging of MSW landfill leachate collection systems: prediction methods and in situ diagnosis. *Proceedings, 9th International Landfill Symposium*, Calgliari, Italy (CD-ROM).

Bouyer, D., Escudie, R and Line, A. (2005). Experimental analysis of hydrodynamics in a jar-test. *Process Safety and Environmental Protection* 83(1), 22-30.

Bryers, J. and Characklis, W. (1981). Early fouling biofilm formation in a turbulent flow system: overall kinetics. *Water Research* 15, 483-491.

Brune, M., Ramke, H.G., Collins, H., and Hanert, H.H. (1991). Incrustations process in drainage systems of sanitary landfills. *Proceedings Sardinia 91, Third International Landfill Symposium*, CISA publisher, Cagliari, Italy (CD-ROM).

Buchholz, B.A. and Landsbrger, S. (1995). Leachate dynamics studies of municipal solid waste incinerator ash. *Air and Waste Management Association* 45, 579-590.

Chang, J.E. (1989). Treatment of landfill leachate with an upflow anaerobic reactor combining a sludge bed and a filter. *Water Science and Technology* 21, 133-143.

Characklis, W.G. and Marshall, K.C. (1990). Biofilms: a basis for an interdisciplinary

approach. in: Characklis, W.G. and Marshall, K.C., editors. Biofilms. New York, John Wiley & Sons.

Characklis, W.G. (1980). Biofilm development and destruction. *Electrical Power Research Institute.* RP921-1, Palo Alto, CA.

Chian, E.S.K. and DeWalle, F.B. (1977). Characterization of soluble organic matter in leachate. *Environmental Science and Technology* 11(2), 158-163.

Choi, Y.C. and Morgenroth, E. (2003). Monitoring biofilm detachment under dynamic changes in shear stress using laser-based particle size analysis and mass fractionation. *Water Science and Technology* 47(5), 69-76.

Cooke, A J., Rowe, R.K., VanGulck, J.F. and Rittmannn, B.E. (2005). Application of the BioClog model for landfill leachate clogging of gravel-packed columns, *Canadian Geotechnical Journal* 42, 1600-1614.

Cooke, A.J., Rowe, R.K., Rittmannn, B.E. and Fleming, I.R. (1999). Modelling biochemically driven mineral precipitation in anaerobic biofilms. *Water Science and Technology* 39(7), 57-64.

Cooke, A.J., Rowe, R.K., Rittmannn, B.E., VanGulck, J.F. and Millward, S.C. (2001). Biofilm growth and mineral precipitation in synthetic leachate columns. *Journal of Geotechnical and Geoenvironmental Engineering, ASCE* 127(10), 949-856.

Cooke, A.J., Rowe, R.K., Rittmannn, B.E. (2005). Modeling species fate and porous media effects for landfill leachate flow. *Canadian Geotechnical Journal*, 42(9), 1116-1132.

Daniels, L., Rajagopal, B.S., and Belay, N. (1986). Assimilatory reduction of sulfate and

sulfite by methanogenic bacteria. *Applied Environmental Microbiology* 51, 703-709.

Dillon (2004). City of Winnipeg leachate management opportunities. Final Report April. Dillon Consulting Ltd, Winnipeg MB.

Domenico, P. and Schwartz, F. (1990). Physical and chemical hydrogeology. John Wiley & Sons, Inc., New York, pp. 494.

Dondero, F.C. (1975). The *Sphaerorilus-Leptuthrix* group. *Annual Review of Microbiology* 29, 407-428.

Ehrig, H.J. (1983). Quality and quantity of sanitary landfill leachate. *Waste Management. Research* 1, 53-68

EPA (2010). See. http://www.epa.gov/climatechange/wycd//waste/downloads/landfilling-chapter10-28-10.pdf

Fleming, I.R., Rowe, R.K., and Cullimore, D.R. (1999). Field observations of clogging in a landfill leachate collection system. *Canadian Geotechnical Journal* 36(4), 289-296.

Fleming, I.R. and Rowe, R.K. (2004). Laboratory studies of clogging of landfill leachate collection and drainage systems. *Canadian Geotechnical Journal* 41, 134-153.

Flemming H. C. , Szewczyk U., Griebe T., 2000, Biofilms – investigative methods & applications, Technomic Publishing Company Inc., Lancaster, Pennsylvania, USA, pp. 247

Friedlander, S.K. and Johnstone, H.F. (1957). Deposition of suspend particles from turbulent gas streams. *Industrial and Engineering Chemistry* 49(7), 1151-1156.

Garny, K., Neu, T.R. and Horn, H. (2009). Sloughing and limited substrate conditions

trigger filamentous growth in heterotrophic biofilms – measurements in flow-through tube reactor. *Chemical Engineering Science* 64(11), 2723-2732.

GeoSyntec Consultants (2000) Application for project XL: King George County Landfill and Recycling Center, and Maplewood Recycling and Waste Disposal Facility, Virginia Waste Facility, Virginia Waste Management, Inc, *Report submitted to Waste Management, Inc*, Charles City, VG,USA.

Gibs, J., Schoenberger, R.J. and Suffet, I.H. (1982). A simplified capacity model for sanitary landfill leachate. *Water Research* 16(5), 699-705.

HACH Company. See http://www.hach.com/fmmimghach?/CODE%3AL70531494|1

Hanson, J.L., Yesiller, N. and Oettle, N.K. (2010). Spatial and temporal temperature distribution in municipal solid waste landfills. *Journal of Environmental Engineering*, ASCE 136(8), 804-814.

Henry, J.G., Prasad, D. and Young, H. (1987). Removal of organics from leachates by anaerobic filter. *Water Research* 21(11), 1395-1399.

Henze, M., Van Loosdrecht, M.C.M., Ekama, G.A. and Brdjanovic, D. (2008). Biological Wastewater Treatment: Principles, Modelling and Design. IWA Publishing, London, UK. pp. 511

Hettiaratchi, J.P.A. (2007). New trends in waste management: North American Perspective. *Proceedings of the International Conference on Sustainable Solid Waste Management, 5-7 September, Chennai, India.* 9-14.

Hoeks, J. and Borst, R.J. (1982). Anaerobic digestion of free volatile fatty acids in

soils below waste tips. *Water, Air and Soil Pollution* 17, 165-173.

Hudgins, M. and Harper, S. (1999). Operational characteristics of two aerobic landfill systems. *Proceedings Sardinia 99, Seventh International landfill Symposium*, Calgliari, Italy (CD-ROM).

Hunt M.S. , 2004 , Theoretical investigation of biofilm detachment and protection from killing using the bacterium level automata model, PhD Thesis Civil Engineer Department, Montana State University, Bozeman, Montana, USA.

Ito, T., Yoshiguchi, K., Ariesyady, H.D. and Okabe, S. (2011). Identification of a novel acetate-utilizing bacterium belonging to Synergistes group 4 in anaerobic digestion sludge. *International Society of Microbial Ecology (ISME) Journal* 5, 1844-1856.

James, A.G., Watson-Craik, I..A, and Senior, E. (1998). The effects of organic acids on the methanogenic degradation of the landfill leachate molecules butyrate and valerate. *Water Research* 32(3), 792-800.

Kennedy, K.J., Hamoda, M.F. and Guiot, S.G. (1988). Anaerobic treatment of leachate of using fixed film and sludge bed systems. *Journal of the Water Pollution Control Federation* 60, 1675-1683.

Kjeldsen, P., Barlaz, M.A., Rooker, A.P., Baun, A., Ledin, A. and Christensen, T.H., (2002). Present and long term composition of MSW landfill leachate: A review. *Environmental Science and technology* 32(4), 297-336

Reddy, K., Grellier, S., Carpenter, P. and Bogner, J. (2009). Geophysical monitoring of leachate recirculation at Orchard Hills Landfill. *Final Project Report Submitted to:* Environmental Research and Education Foundation. pp. 88

Langenhoff, A. and Stuckey, D. (2000). Treatment of dilute wastewater using an anaerobic baffled reactor: Effect of low temperature. *Water Research 34(15), 3867-3875.*

Liu Y., Tay J.H., 2001, The essential role of hydrodynamic shear force in the formation of biofilm and granular sludge, *Water Research*, 36, 1653- 1665

Lozecznik, S and VanGulck, J.F. (2009). Full-Scale laboratory study into clogging of pipes permeated with landfill leachate. *Practice Periodical of Hazardous Waste, Toxic and Radioactive Waste Management* 13(4), 261-269.

Lozecznik, S. (2006). Hydraulic design, operation and clogging of leachate injection pipes in bioreactor landfills. M.Sc. Thesis Civil Engineer Department, University of Manitoba,Winnipeg, Manitoba, CANADA.

Maier, T.B. and Vasuki, N.C. (1996). Expected benefits of a full-scale bioreactor landfill. *Proceedings of the Fifth International Landfill Symposium*, Cagliari, Italy.

Maliva, R.G., Missimer, T.M., Leo, K.C., Statom, R.A., Dupraz, C., Lynn, M., and Dickson, J.A.D. (2000). Unusual calcite stromatolites and pisoids from a landfill leachate collection system. *Geology* 28(10), 931-934.

Malusa , J., Overby, S.T. and Parnell, R.A. (2003). Potential for travertine formation: Fossil Creek, AZ, *Applied Geochemistry* 18, 1081-1093.

Manning, D.A.C. (2000). Carbonates and oxalates in sediments and landfill: monitors of death and decay in natural and artificial systems. *Journal of the Geological Society of London* 157(1), 229-238.

McInerney, M.J., Struchtemeyer, C.G., Sieber, J., Mouttaki, H., Stams, A.J.M., Schink, B., Rohlin, L. and Gunsalus, RP. (2008). Physiology, ecology, phylogeny and genomics of microorganisms capable of syntrophic metabolism. *Annals of the New York Academy of Sciences* 1125, 58-72.

McLean, R.J.C., Fuqua, C., Siegele, D.A., Kirkland, B.L., Adams, J.L. and Whiteley, M. (1999). Biofilm growth and illustrations of its role in mineral formation. *Proceedings of the 8th International Symposium on Microbial Ecology*, Halifax, CANADA.

McIsaac, R., Rowe, R.K., Fleming, I.R. and Armstrong, M.D. (2000). Leachate collection system design and clog development. *Proceedings 6th Canadian Environmental Engineering Conference*, London, Ontario, 66-73.

McIsaac, R. and Rowe, R.K. (2005). Change in leachate chemistry and porosity as leachate permeates through tire shreds and gravel. *Canadian Geotechnical Journal* 42(4), 1173-1188.

Metcalf & Eddy (2003). Wastewater Engineering. Treatment, Disposal, and Reuse. McGraw-Hill, 4rd Edition.

Miller,W. Lamar, Townsend, T.G., Earle, J.F.K., Lee, H., Reinhart, D., and Paladuga, P. (1993). Leachate recycle and the argumentation of biological decomposition at municipal solid waste landfills. Presented at the FCSHWM First Annual Research Symposium, Orlando, Florida.

Miller, D.E. and Emge, S.M. (1997). Enhancing landfill leachate recirculation system

performance, *Practice Periodical of Hazardous Toxic and Radioactive Waste Management* (1),113-119.

Mullah, A., Levine, A., Harwood, V., Cardoso, A., Rhea, L., Nayak, B., Dodge, B., Decker, M., Dzama, G., Jones, L. and Haller, E. (2005). Assessment of biogeochemical deposits in landfill leachate drainage systems. Final reported submitted to the Florida Center for Solid and Hazardous Waste Management. Report #0332006-05.

Nagata, S. (1975). Mixing – principles and applications. Halsted press/John Wiley & Sons, New York. pp. 458

Nedwell, D.B. and Reynolds, P.J. (1996). Treatment of landfill leachate by methanogenic and sulphate-reducing digestion. *Water Research* 30(1), 21-28.

Novy, L., VanGulck, J., Ferguson, G. (2005). Role of refuse hydraulic properties on liquid injection system design, *Proceedings 58th Canadian Geotechnical Student Conference*, Saskatoon, SK, CANADA

O`Brien, J.K. (2010). The solid waste manager`s guide to the bioreactor landfill – a 2009 update. *Municipal Solid Waste Magazine* May: 14-23.

Oleszkiewicz, J.A., Lozecznik, S. and Hyuk Hwang, J. (2008). Management of leachate in the City of Winnipeg. Report to the Water and Waste Department, City of Winnipeg.

Ontario Landfill Standards (1998). http://www.ene.gov.on.ca/envision/gp/3651e.htm

Owen, J.A. and Manning, D.A.C. (1997). Silica in landfill leachates: Implications for clay mineral stabilities. *Applied Geochemistry* 12, 267-280.

Pohland, F.G. (1975). Accelerated solid waste stabilization and leachate treatment by leachate recycle through sanitary landfills, *Progress in Water Technology* 7,753-765.

Puchajda, B. (2006). Increased energy recovery and enhanced pathogen inactivation through anaerobic digestion of thickened wastewater sludge. PhD Thesis, University of Manitoba.

Rebac, S., Ruskova, J., Gerbens, S., Van Lier, J., Stams, A. and Lettinga, G. (1995). High-rate anaerobic treatment of wastewater under psychrophilic conditions. *Journal of Fermentation and Bioengineering* 80(5), 499-506.

Reddy, M.M. and Wang, K.K. (1980). Crystallization of calcium carbonate in the presence of metals ions: Inhibition by magnesium ions at pH 8.8 and 25˚C. *Journal of Crystal Growth* 50(2), 470-480.

Reinhart, D.R. and Townsend, T.G. (1997). Landfill bioreactor design and operation. CRC Press LLC, Florida, USA, pp 189.

Reinhart, D.R., Townsend, T.G. and McCreanor, P (2002). Florida bioreactor demonstration project instrumentation. Waste Tech 2002 – Landfill Conference.

Reinhart, D.R. and Grosh, C.J. (1998). Analysis of Florida MSW landfill leachate quality, Florida Center for Solid and Hazardous Management, Gainesville, Fl.

Renou, S., Poulain, S., Givaudan, J.G. and Moulin, P. (2009). Amelioration of ultrafiltration process by lime treatment: Case of landfill leachate. *Desalination* 249, 72-82.

Rhea, L. (2004). Mineral solubilization from municipal solid waste combustion residues: Implications for landfill leachate collection systems. MSc. Thesis , Department of Civil Engineering University of South Florida, USA.

Rittmannn, B.E., Banazak, J., Cooke, A.J., and Rowe, R.K. (2003). Biogeochemical evaluation of mechanisms controlling $CaCO_3$ precipitation in landfill leachate collection systems. *Journal of Environmental Engineering, ASCE* 129 (8), 723 – 730.

Rittmannn, B.E. and McCarty, P.L. (2001). Environmental biotechnology: principles and applications, McGraw and Hill, New York, pp 754.

Rittmannn, B.E. and Brunner, C. W. 1984. "The non-steady state biofilm process for advanced organics removal". *Journal of Water Pollution and Control Federation* **56**(7), 874-880.

Rowe, R.K. (1998a). "Geosynthetics and the minimization of contaminant migration through barrier systems beneath solid waste". *Proceedings. 6th International Conference on Geosynthetics,* Atlanta, March, Vol 1, pp. 27-103, Industrial Fabrics Association International, St. Paul, MN.

Rowe, R.K. (1998b). "From the past to the future of landfill engineering through case histories". *Keynote Lecture, Proc. Fourth International Conference on Case Histories in Geotechnical Engineering,*, St. Louis, pp. 145-166.

Rowe, R.K., Armstrong, M.D. and Cullimore, D.R. 2000a. Mass loading and the rate of clogging due to municipal solid waste leachate. *Canadian Geotechnical Journal* 37, 355-370.

Rowe, R.K., Armstrong, M.D. and Cullimore, D.R. 2000b. Particle size and clogging of granular media permeated with leachate. *Journal of Geotechnical and Geoenvironmental Engineering, ASCE* 126(9), 775-786.

Rowe, R.K. and VanGulck, J.F. 2001. Clogging of leachate collections systems: From laboratory and field study to modeling and prediction. *Keynote lecture, 2nd Australian-New Zealand Conference on Environmental Geotechnics*, Newcastle, November, pp. 1-22

Rowe, R.K., VanGulck, J. and Millward, S.C. (2002). Biologically induced clogging of a granular medium permeated with synthetic leachate. *Journal of Environmental Engineering and Science* 1(2), 135-156.

Rowe, R.K., Quigley, R.M., Brachman, R.W.I., Booker., J.R., 2004. Barrier systems for waste disposal facilities 2nd Edition. Spon Press, New York, pp 587.

Saravanan, V. and Sreekrishnan, T.R. (2009). Modelling anaerobic biofilm reactors – A review. *Journal of Environmental Management* 81(1), 1-18.

SCS Engineers 2000. Literature review and research needs for landfill bioreactors. Final report submitted to Environmental Research and Education Foundation, File # 02200028.00.

Simard, A., Norstrom, and Bourquet, H. (2003) Constructing, operating and monitoring of a bioreactor landfill in Saint-Sophie, Quebec, Canada. *Proceedings Sardinia 91, Ninth International Waste Management and Landfill Symposium*, CISA publisher, Cagliari, Italy.

Speece, R.E. (1996). Anaerobic biotechnology for industrial wastewater. Archae Press, Nashville, pp 394

Speece, R.E. (2008). Anaerobic biotechnology and odor/corrosion control for municipalities and industries. Archae Press, Nashville, pp 585.

Southen, J.M., Rowe, R.K. (2005). Modelling of thermically induced desiccation of geosynthetic clay liners, *Geotextiles and Geomembranes* 23(10), 425-442.

Standard Methods for the Examination of Water and Wastewater, 21th edition, (2005). Edited by Eaton, A. (AWWA), Clesceri, L.S. (WEF), Rice, E.W. and Greenberg A.E. (APHA). ISBN 0-87553-047-8.

Standard Methods for the Examination of Water and Wastewater, 18th edition, (1992). Edited by Greenberg A.E. (APHA), Clesceri, L.S. (WEF), Eaton, A.D. (AWWA). ISBN 0-87553-207-1.

Stafford, D.A., Hawkes, D.L and Horton, R. (1980). Methane production from waste organic matter. CRC Press, Florida, pp.285.

Stegman, R., Heyer, K.U., Cossu, R. (2005). Leachate treatment in *Proceedings Sardinia 2005,* Tenth International Landfill Symposium, Italy.

Stoodley P, Lewandowski Z, Boyle JD, Lappin-Scott HM. (1999). Structural deformation of bacterial biofilms caused by short-term fluctuations in fluid shear: An insitu investigation of biofilm rheology. *Biotechnology and Bioenergy* 65, 83–92.

Thauer, R.K, Jungermann, K and Decker, K. (1977). Energy conservation in chemotrophic anaerobic bacteria. *Bacteriological Review* 41(1), 100-180.

Timur, H. and Özturuk, I., 1999. Anaerobic sequencing batch reactor treatment of landfill leachate. *Water Research* 33(15), 3225-3230.

Townsend, T.G. (1995) Leachate recycle at solid landfills using horizontal injection, PhD

Thesis, Civil Engineer Department University of Central Florida, USA.

Townsend, T.G. and Miller, W.L. (1998) Leachate recycling using horizontal injection. *Advances in Environmental Research* 2(2), 129-138.

Turk, M., Collins, H-J., Wittmaier, M., Harborth, P. and Hanert, H-H. (1997). Advanced landfill liner systems. Edited by H. August, U. Holzlohner & T. Meggyes; London: Tehomas Telford Pub., pp 389

VanGulck, J.F., Lozecznik, S and Murdock, J.H., (2009). Hydraulic design tables for horizontal injection systems in bioreactor landfills. *Practice Periodical of Hazardous Waste, Toxic and Radioactive Waste Management* 13(3), 147-155.

VanGulck, J.F. and Rowe, R.K., (2004a). Influence of landfill leachate suspended solids on clog (biorock) formation. *Waste Management* 24(2), 723-728.

VanGulck, J.F. and Rowe, R.K., (2004b). Evolution of clog formation with time in column permeated with synthetic landfill leachate. *Journal of Contaminant Hydrology* 75, 115-135

VanGulck, J.F., Rowe, R.K., Rittmannn, B.E. and Cooke, A.J. (2003). Predicting biogeochemical calcium precipitation in landfill leachate collection systems. *Biodegradation* 14(5), 331-346.

VanGulck, J.F. (2003). Biologically induced clogging of granular media and leachate collection systems. Ph.D. thesis, Queen's University, Kingston, Ontario, CANADA.

Van Loosdrecht, M.C.M., Eikelboom D, Gjaltema A, Mulder A,Tijhuis, L. and Heijnen, J.J. (1995) Biofilm structures. *Water Science and Technology* 32(8), 35-43.

Van Loosdrecht, M.C.M., Heijnen, J.J., Eberl, H., Kreft, J. and Picioreanu, C. (2002). Mathematical modelling of biofilm structures. *Antonie van Leeuwenhoek – International Journal of General and Molecular Microbiology* 81(1), 245-256.

Vu, B., Chen, M., Crawford, R.J. and Ivanova, E.P. (2009). Bacterial extracellular polysaccharides involved in biofilm formation. *Molecules* 14, 2535-2554.

Warzinski, J., Watermolen, B. T., Torresani, M. and Genthe, D.R. (2000). A superior approach to recirculation. http://waste360.com/wag/waste superior approach recirculation

Wohlgemut, O., (2008). Co-digestion of hog manure with glycerol to boost biogas and methane production. MSc. Thesis, University of Manitoba, Winnipeg, CANADA.

Yazdani, R., Kieffer, J., and Akau, H. (2002). Full scale landfill bioreactor project at the Yolo County central landfill. Final report submitted to USEPA- Project XL, pp. 114.

APPENDIX A : PIPES AND RINGS DIMENSIONS, AND RINGS PLACEMENT WITHIN THE TESTING PIPES.

1) Pipe length, weight and diameter.

Pipe series #	Pipe ID	Length [m]	Weight [kg]	Diameter [m]
1	a	2.05	1.99	0.048
	b	2.05	1.98	0.048
2	a	2.05	1.98	0.048
	b	2.05	1.97	0.048
3	a	2.05	1.97	0.048
	b	2.05	1.98	0.048
4	a	2.04	7.01	0.092
	b	2.05	6.87	0.092
5	a	2.04	6.92	0.092
	b	2.04	6.95	0.092
6	a	2.05	6.87	0.092
	b	2.05	6.87	0.092
7	a	2.05	15.26	0.135
	b	2.05	15.25	0.134
8	a	2.05	15.23	0.134
	b	2.05	15.21	0.135

2) Pipe rings

a. Pipe rings placement within pipe series.

Pipe Series	Pipe ID	Pipe ring collected/Pipe Ring 1st	2nd	3rd	4th	5th
1	a	270	251	250	247	223
	b	237	236	234	233	212
2	a	238	228	225	224	218
	b	232	231	221	220	216
3	a	260	258	257	256	242
	b	207	206	205	203	202
4	a	437	422	419	418	403
	b	439	431	409	402	401
5	a	435	433	432	405	404
	b	413	412	411	407	406
6	a	426	421	420	416	415
	b	451	444	430	410	408
7	a	13,37	1,36,52	56,4	71	40
	b	23,24	72,73,74	14,15	77	75
8	a	54,57	8,9,10	33,34	64	65
	b	17,18	39,44,48	67,79	7	2

Note: 1st is the first pipe ring collected and the last positioned within the pipe series and 5th is the last connected and first positioned from the pipe outlet

b. Pipe rings (PR), internal diameter (ID) and weight (W) for the pipe series tested

Pipe Series 1						Pipe Series 2					
a			b			a			b		
PR #	ID [cm]	W [gr]	PR #	ID [cm]	W [gr]	PR #	ID [cm]	W [gr]	PR #	ID [cm]	W [gr]
270	48.63	24.5	237	48.65	23.6	238	48.33	23.7	232	48.41	22.8
251	48.44	23.4	236	48.39	22.5	228	48.43	22.6	231	48.1	23.6
250	48.55	25.3	234	48.49	23.3	225	48.27	24.4	221	48.44	22.4
247	48.47	24	233	48.43	23.5	224	48.39	22.3	220	48.37	23.7
223	48.4	23.1	212	48.02	23.4	218	48.43	23.1	216	48.33	23.9

Pipe Series 3						Pipe Series 4					
a			b			a			b		
PR ID	ID [cm]	W [gr]	PR ID	ID [cm]	W [gr]	PR ID	ID [cm]	W [gr]	PR ID	ID [cm]	W [gr]
260	48.45	24.6	207	48.77	22.3	437	92.29	84.3	439	92.15	84.7
258	48.41	25.1	206	48.38	22.8	422	92.37	83.3	431	92.29	81.4
257	48.37	23.6	205	48.4	23.2	419	91.96	81.7	409	92.55	84.7
256	48.27	25.6	203	48.79	23.5	418	91.91	83.8	402	92.01	82.5
242	48.47	24	202	48.58	23.4	403	91.84	77.1	401	91.97	83.6

Pipe Series 5						Pipe Series 6					
a			b			a			b		
PR ID	ID [cm]	W [gr]	PR ID	ID [cm]	W [gr]	PR ID	ID [cm]	W [gr]	PR ID	ID [cm]	W [gr]
435	91.91	78.8	413	92.33	79.5	426	91.83	84.6	451	92.31	83.5
433	92.26	81.5	412	92.31	79.4	421	92.39	78	444	92.33	82.5
432	91.99	86.2	411	91.84	78.5	420	92.11	82.6	430	92.05	82.6
405	92.37	83.7	407	91.74	81.6	416	92.14	83.3	410	92.11	83.4
404	92.09	81.6	406	91.9	78.8	415	92.07	81	408	92.02	81.7

Pipe Series 7						Pipe Series 8					
a			b			a			b		
PR ID	ID [cm]	W [gr]	PR ID	ID [cm]	W [gr]	PR ID	ID [cm]	W [gr]	PR ID	ID [cm]	W [gr]
13	135.03	178.9	23	135.22	172.2	54	134.97	184.9	17	135.17	179.3
37	135.17	174.8	24	134.92	175.2	57	134.99	183.1	18	134.77	179.6
1	135.01	179.2	72	134.89	185.3	8	134.91	180.7	39	134.99	172.7
36	135.05	182.7	73	135.48	174.8	9	135.11	184.5	44	134.99	174.7
52	135.14	174.6	74	135.4	187.9	10	134.94	184	48	135.05	174.9
56	134.89	170.5	14	134.99	175	33	135.05	172.7	67	135.12	179.9
4	135.35	173.2	15	135.15	182.3	34	134.89	179.9	79	135.08	186.2
71	135.21	203.8	77	135.32	185.5	64	135.17	187.7	7	135.11	175.5
40	134.91	184.9	75	135	194.7	65	135.13	186.1	2	135.17	180.1

APPENDIX B : PUMPS OPERATION DURING EACH TESTING CYCLE

1) Pumps operation time.

Pipe Series					
1 and 4		2 and 6		3,5,7 and 8	
Date	[hour]	Date	[hour]	Date	[hour]
27-Oct-10	2	08-Oct-10	6	13-Nov-09	0.25
01-Feb-10	1	27-Jan-10	2	04-Feb-10	5
11-Feb-10	1	08-Feb-10	2	18-Feb-10	3
12-Mar-10	0.1	09-Mar-10	4	15-Mar-10	6
21-Apr-10	2	26-Apr-10	3	29-Apr-10	3
17-May-10	5	12-May-10	6	20-May-10	6
07-Jun-10	5	03-Jun-10	4	09-Jun-10	0.25
07-Jul-10	3	16-Jun-10	0.25	24-Jun-10	5
21-Jul-10	4	14-Jul-10	5	19-Jul-10	5
09-Aug-10	4	03-Aug-10	3	12-Aug-10	7
21-Sep-10	6	07-Sep-10	2.5	15-Sep-10	4

APPENDIX C : PILOT STUDY PICTURES

2) Field study pictures.

Front of the research station

Signage with sponsors

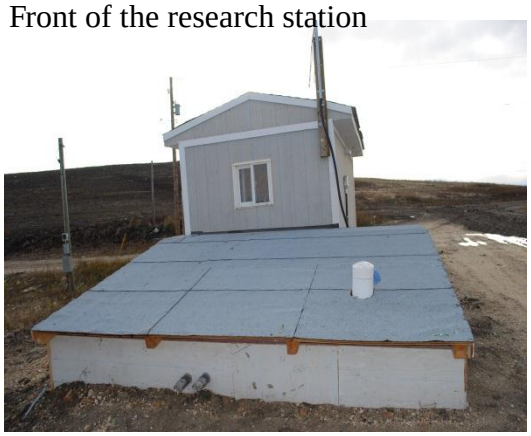

Back of the station with outside tank

Electrical pump and heater wiring connection

Leachate feeding lines and evacuating valves

Electrical panel with 3 separate circuits

Computer with pressure transducer and software

Pressure transducers

Pipes within the shelves

Air venting lines

End of pipes with pipe rings inside of the pumps rubber clamps and pipe outlet

Return lines and non-submersible

APPENDIX D : LEACHATE DATA COLLECTED FROM BRADY ROAD LANDFILL WELLS

- Pipe Series 1 and 4

Date	COD [mg/L]	CO_2 [mg/L]	pH [-]	Ca^{2+} [mg/L]	TSS [mg/L]	VSS [mg/L]	FSS [mg/L]	Alk [mg/L]	Temp. [˚C]
27-Oct-10	1368	-	7.06	190	170	140	30	6300	-
01-Feb-10	825	-	7.46	200	215	65	150	4750	7.5
11-Feb-10	1680	-	7.51	224	875	150	725	5250	9.1
12-Mar-10	1710	-	7.52	144	335	115	220	3975	9.1
21-Apr-10	1278	-	7.18	152	1565	390	1175	2350	13.9
17-May-10	1420	169	7.37	208	710	175	-	2255	15.4
07-Jun-10	1152	171	7.29	206	1135	170	965	2200	13.4
07-Jul-10	11360	197.3	7.57	680	1100	430	670	6650	13.7
21-Jul-10	15205	239	7.19	620	760	300	460	7600	15
09-Aug-10	7950	193.5	7.26	490	1155	545	610	5200	17
21-Sep-10	6695	178.2	7.44	376	555	215	340	6450	12.2

- Pipe Series 2 and 6

Date	COD [mg/L]	CO_2 [mg/L]	pH [-]	Ca^{2+} [mg/L]	TSS [mg/L]	VSS [mg/L]	FSS [mg/L]	Alkalinity [mg/L]	Temp. [˚C]
08-Oct-10	1598	-	7.1	190	210	165	45	6200	-
27-Jan-10	1155	-	7.44	325	390	95	295	3550	-
08-Feb-10	2918	-	7.96	197	2375	475	1900	7750	9.6
09-Mar-10	2090	-	7.66	240	175	95	80	4200	12.5
26-Apr-10	1388	-	7.23	192	235	140	95	2750	12.7
12-May-10	1140	169.47	7.35	160	495	170	325	2350	11
03-Jun-10	1668	192.15	7.18	184	1995	-		2000	16.8
16-Jun-10	2490	155.4	7.81	240	815	180	635	5600	17.9
14-Jul-10	12220	194.48	7.07	700	850	265	585	5700	15.9
03-Aug-10	9160	185.42	7.18	460	985	360	625	5850	11.7
07-Sep-10	4130	238.65	7.21	320	895	285	610	5400	11.3

- Pipe Series 3,5,7 and 8

Date	COD [mg/L]	CO_2 [mg/L]	pH [-]	Ca^{2+} [mg/L]	TSS [mg/L]	VSS [mg/L]	FSS [mg/L]	Alk [mg/L]	Temp. [˚C]
13-Nov-09	1270	-	6.97	228	95	75	20	6000	10
04-Feb-10	1395	-	7.52	192	1975	325	1650	4675	8.2
18-Feb-10	1394	-	7.42	344	305	110	195	5050	9.1
15-Mar-10	1940	-	7.56	200	310	145	165	3775	11
29-Apr-10	1242	-	7.38	208	505	135	370	2775	10.9
20-May-10	1294	163	7.09	160	360	165	195	2350	11.8
09-Jun-10	1184	155	7.65	272	555	230	325	3050	16.1
24-Jun-10	13215	165.8	7.2	432	1730	745	985	6650	15.9
19-Jul-10	12570	194	6.88	680	685	320	365	7750	14.3
12-Aug-10	7395	199.8	7.31	544	1630	660	970	6500	18.7
15-Sep-10	4200	158.5	7.43	304	670	200	470	5400	13.8

APPENDIX E : LEACHATE DATA COLLECTED FROM THE PIPE SERIES AT T = 0, 24 AND 48 HRS AT DIFFERENT ELAPSED TIMES.

a. Average COD values.

i. Pipe Series 1, 2, 4 and 6.

Date	Pipe ID	Pipe Series 1 COD [mg/L]			Pipe Series 4 COD [mg/L]			Date	Pipe Series 2 COD [mg/L]			Pipe Series 6 COD [mg/L]		
		t = 0	t = 24	t = 48	t = 0	t = 24	t = 48		t = 0	t = 24	t = 48	t = 0	t = 24	t = 48
27-Oct-10	a	2000	1278	1205	1628	1395	1323	08-Oct-10	2290	2160	1678	2418	2260	1818
	b	1408	1210	1353	1488	1363	1295		2315	2088	1865	2478	2363	1878
01-Feb-10	a	825	640	830	705	520	890	27-Jan-10	1430	1075	1003	1110	1095	963
	b	680	560	845	765	565	735		1110	1040	925	1170	1035	1003
11-Feb-10	a	1504	1410	1200	1554	1464	1308	08-Feb-10	2174	2130	2280	2280	2238	2178
	b	1516	1434	1148	1460	1394	1318		2332	2226	2260	2266	2232	1890
12-Mar-10	a	1403	1118	1343	1455	1123	1843	09-Mar-10	1828	1548	1573	1838	1630	1520
	b	1498	1115	1185	1418	1190	1278		1842.5	1580	1595	1720	1635	1583
21-Apr-10	a	1046	1044	826	1158	1060	870	26-Apr-10	1096	896	952	1084	934	904
	b	1132	958	836	1216	1016	830		1032	858	928	1060	798	932
17-May-10	a	1012	942	1096	1052	1100	1166	12-May-10	990	1105	1532	1086	1108	1094
	b	974	1136	1188	1164	984	1164		1280	1270	1960	996	1012	1178
07-Jun-10	a	1034	822	420	824	908	648	03-Jun-10	1258	1166	850	1116	1128	748
	b	1120	852	430	974	864	458		1296	1050	724	1278	1080	614
07-Jul-10	a	15205	12530	14440	15205	12990	11500	16-Jun-10	2372	2232	2212	2332	2194	1858
	b	15205	11465	13810	15205	12500	11470		2384	2202	2034	2382	2312	1852
21-Jul-10	a	12100	12070	11270	12575	12980	11590	14-Jul-10	10915	12065	11145	10350	11985	11165
	b	12450	11900	11580	11925	12700	11520		11290	11920	11570	10650	11795	11575
09-Aug-10	a	6955	8975	8045	6815	10980	6990	03-Aug-10	8455	8410	7575	8245	8365	6105
	b	7690	8965	9200	7210	10850	7600		8380	8255	7275	8480	7985	6405
21-Sep-10	a	6315	4370	4750	6645	5740	4960	07-Sep-10	3955	4105	4105	4015	3800	5555
	b	6630	5265	5090	6240	5195	4905		4035	4405	4145	4035	4835	3830

ii. Pipe Series 3, 5, 7 and 8.

Date	Pipe ID	Pipe Series 3 COD [mg/L]			Pipe Series 5 COD [mg/L]			Pipe Series 7 COD [mg/L]			Pipe Series 8 COD [mg/L]		
		t = 0	t = 24	t = 48	t = 0	t = 24	t = 48	t = 0	t = 24	t = 48	t = 0	t = 24	t = 48
13-Nov-09	a	1525	1460	1394	1562	1471	1342	1521	1442	1406	1532	1547	1374
	b	1529	1449.5	1416	1505	1465	1428	1492	1449	1457	1536.5	1509	1335.5
04-Feb-10	a	562.5	1003	1188	568	953	1083	583	953	1098	572.5	992.5	1070
	b	557.5	1098	1103	470	1070	1020	473	938	1078	472.5	1002.5	1122.5
18-Feb-10	a	1384	1394	1653	1400	1376	1738	1332	1528	1628	1362	1364	1565
	b	1362	1352	1653	1294	1346	1670	1296	1396	1618	1358	1460	1510
15-Mar-10	a	1800	1373	1328	1608	1460	1305	1613	2298	1223	1495	1377.5	1360
	b	1200	1478	1410	1463	1340	1353	1725	1633	1370	1260	1355	1560
29-Apr-10	a	1258	1034	1038	1088	938	900	1146	860	992	1124	1002	950
	b	1082	1002	860	1066	996	900	1208	994	1016	1226	944	1012
20-May-10	a	1106	1052	1060	1226	920	1208	1074	1122	972	1280	1038	1098
	b	1184	1076	1154	1152	1282	1138	1236	1150	1172	1232	1192	1160
09-Jun-10	a	1190	974	1038	1140	992	962	1236	984	938	1154	948	960
	b	1126	1008	960	1218	988	1010	1128	1016	942	1122	872	1060
24-Jun-10	a	10565	9725	9480	9550	9615	9710	9465	9735	8750	10110	9620	11745
	b	9780	9265	9055	10340	9955	9680	10265	9815	10225	9675	10055	8500
19-Jul-10	a	12930	8220	9500	12650	8160	8360	12390	7960	8865	12455	7815	8495
	b	12840	7565	9100	12540	7970	9615	12575	7650	9235	12810	8090	7895
12-Aug-10	a	7025	7855	6670	7860	7380	7630	6410	6960	6955	7750	7220	6325
	b	7155	6810	7400	7380	7270	7840	7350	7210	6150	7430	6620	6490
15-Sep-10	a	4095	4160	4285	3890	4385	4510	4150	4025	3825	4080	3480	3600
	b	4380	3895	4245	3980	3485	3890	3965	3500	3980	4210	3660	4070

b. Dissolved CO_2 average leachate pipes measurements.

i. Pipe Series 1, 2, 4 and 6.

Date	Pipe ID	Pipe Series 1 CO_2 [mg/L]			Pipe Series 4 CO_2 [mg/L]			Date	Pipe Series 2 CO_2 [mg/L]			Pipe Series 6 CO_2 [mg/L]		
		t = 0	t = 24	t = 48	t = 0	t = 24	t = 48		t = 0	t = 24	t = 48	t = 0	t = 24	t = 48
17-May-10	a	82	84	91	86	89	96	12-May-10	88	105	84	83	89	88
	b	82	85	89	84	87	92		83	93	83	82	89	87
07-Jun-10	a	79	87	88	84	87	91	03-Jun-10	83	88	98	78	85	82
	b	81	89	93	82	92	93		78	85	89	77	86	83
07-Jul-10	a	105	92	171	115	94	170	16-Jun-10	126	171	168	118	127	114
	b	106	103	167	108	94	170		122	162	166	118	130	125
21-Jul-10	a	32	54	49	41	64	47	14-Jul-10	86	87	88	78	85	88
	b	34	64	53	33	59	50		81	86	87	78	85	87
09-Aug-10	a	91	100	101	104	106	105	03-Aug-10	102	128	135	94	119	132
	b	89	99	100	95	101	104		96	115	123	94	123	134
21-Sep-10	a	77	82	88	84	83	91	07-Sep-10	102	108	120	90	107	114
	b	75	83	87	79	84	89		96	109	116	89	104	105

ii. Pipe Series 3, 5, 7 and 8.

Date	Pipe ID	Pipe Series 3 CO_2 [mg/L]			Pipe Series 5 CO_2 [mg/L]			Pipe Series 7 CO_2 [mg/L]			Pipe Series 8 CO_2 [mg/L]		
		t = 0	t = 24	t = 48	t = 0	t = 24	t = 48	t = 0	t = 24	t = 48	t = 0	t = 24	t = 48
20-May-10	a	94	104	101	92	100	99	96	101	99	94	99	100
	b	91	89	97	92	96	97	93	99	98	92	100	98
09-Jun-10	a	132	152	122	123	142	155	129	143	134	131	132	129
	b	123	152	153	127	138	132	124	124	117	129	144	150
24-Jun-10	a	94	103	97	87	105	99	89	114	140	92	131	126
	b	87	107	105	85	102	95	90	126	118	90	101	124
19-Jul-10	a	96	133	163	96	131	134	96	133	151	95	132	135
	b	97	134	140	96	126	131	96	133	145	95	125	134
12-Aug-10	a	96	88	114	79	84	88	85	87	101	81	85	94
	b	79	88	90	79	82	86	82	87	98	80	83	94
15-Sep-10	a	89	111	104	90	102	102	89	104	102	89	103	105
	b	91	107	107	90	101	103	90	106	100	88	103	100

c. Dissolved Ca^{2+} average leachate pipes measurements.

i. Pipe Series 1, 2, 4 and 6.

Date	Pipe ID	Pipe Series 1 Ca^{2+} [mg/L]			Pipe Series 4 Ca^{2+} [mg/L]			Date	Pipe Series 2 Ca^{2+} [mg/L]			Pipe Series 6 Ca^{2+} [mg/L]		
		t = 0	t = 24	t = 48	t = 0	t = 24	t = 48		t = 0	t = 24	t = 48	t = 0	t = 24	t = 48
27-Oct-10	a	176	56	32	192	156	66	08-Oct-10	148	14	10	158	17	10
	b	184	128	65	208	108	67		156	14	10	156	13	11
01-Feb-10	a	200	112	112	200	168	128	27-Jan-10	224	116	8	224	112	8
	b	200	112	112	200	168	128		224	116	6	224	116	8
11-Feb-10	a	172	56	56	172	112	112	08-Feb-10	108	5	4	108	5	4
	b	172	112	38	172	112	112		108	5	4	108	5	4
12-Mar-10	a	216	64	48	200	74	66	09-Mar-10	152	52	46	176	52	32
	b	208	70	52	216	80	76		160	56	52	176	48	34
21-Apr-10	a	96	48	38	108	50	48	26-Apr-10	116	46	36	128	44	32
	b	104	48	42	104	52	46		132	46	36	112	44	36
17-May-10	a	80	40	30	80	72	26	12-May-10	96	36	34	88	32	32
	b	88	32	32	64	32	32		96	34	25	64	32	28
07-Jun-10	a	80	34	34	74	42	34	03-Jun-10	80	28	26	72	28	28
	b	88	36	28	70	38	36		80	22	20	72	34	34
07-Jul-10	a	392	312	168	312	384	208	16-Jun-10	228	80	72	208	112	72
	b	312	384	152	328	344	208		224	88	88	216	72	64
21-Jul-10	a	216	108	64	248	104	64	14-Jul-10	168	38	31	152	43	26
	b	184	92	68	336	100	64		168	34	34	152	50	30
09-Aug-10	a	184	72	24	192	84	26	03-Aug-10	192	48	42	200	48	38
	b	184	80	30	184	76	30		184	48	36	192	52	44
21-Sep-10	a	104	32	22	92	48	20	07-Sep-10	144	22	14	144	20	14
	b	88	36	16	88	44	18		136	20	12	136	22	16

ii. Pipe Series 3, 5, 7 and 8.

Date	Pipe ID	Pipe Series 3 Ca^{2+} [mg/L]			Pipe Series 5 Ca^{2+} [mg/L]			Pipe Series 7 Ca^{2+} [mg/L]			Pipe Series 8 Ca^{2+} [mg/L]		
		t = 0	t = 24	t = 48	t = 0	t = 24	t = 48	t = 0	t = 24	t = 48	t = 0	t = 24	t = 48
13-Nov-09	a	268	188	130	248	204	136	248	174	104	264	196	122
	b	236	200	126	248	210	154	236	204	172	270	176	94
04-Feb-10	a	104	56	21.6	104	56	32.8	104	56	26.4	104	56	29.6
	b	104	56	20.8	104	56	31.2	104	56	34.4	104	56	26.4
18-Feb-10	a	112	18	14.4	112	30	20	112	30	13.6	112	34	12
	b	112	18	11.2	112	28	17.6	112	32	20	112	28	13.6
15-Mar-10	a	72	24	24	64	36	24	72	24	24	72	30	28
	b	68	22	18	72	38	28	60	44	32	72	26	26
29-Apr-10	a	136	56	40	128	56	44	112	48	36	112	56	40
	b	104	60	48	112	60	40	136	56	48	120	52	40
20-May-10	a	96	36	26	80	48	30	80	36	20	80	38	14
	b	88	30	16	88	40	24	88	34	22	80	42	26
09-Jun-10	a	192	98	78	188	132	96	182	94	48	176	104	76
	b	180	104	82	192	138	102	160	134	106	178	84	82
24-Jun-10	a	184	56	42	144	72	46	128	58	36	152	70	40
	b	176	60	40	128	42	36	144	68	38	168	66	46
19-Jul-10	a	264	112	100	232	136	96	272	160	108	224	152	128
	b	248	136	92	256	148	96	232	124	108	272	144	112
12-Aug-10	a	200	36	15.2	180	32	22.4	200	28	15.2	200	24	14.4
	b	200	24	20	180	32	19.2	200	36	16	200	32	15.2
15-Sep-10	a	104	20	14.4	120	30	16	144	28	20.8	120	30	16
	b	104	24	17.6	128	32	20.8	120	28	16	104	28	20.8

d. Total Suspend Solids (TSS) average leachate pipes measurements.

i. Pipe Series 1, 2, 4 and 6.

Date	Pipe ID	Pipe Series 1 TSS [mg/L]			Pipe Series 4 TSS [mg/L]			Date	Pipe Series 2 TSS [mg/L]			Pipe Series 6 TSS [mg/L]		
		t = 0	t = 24	t = 48	t = 0	t = 24	t = 48		t = 0	t = 24	t = 48	t = 0	t = 24	t = 48
27-Oct-10	a	215	205	195	330	215	115	08-Oct-10	340	95	125	365	115	145
	b	245	150	155	300	145	185		315	130	105	335	125	135
01-Feb-10	a	310	210	80	285	160	125	27-Jan-10	390	135	195	430	210	220
	b	315	225	75	315	160	85		365	205	200	330	270	185
11-Feb-10	a	655	125	60	510	195	60	08-Feb-10	645	240	265	1080	385	235
	b	655	145	50	635	185	50		594	230	295	2410	235	215
12-Mar-10	a	335	110	100	345	140	120	09-Mar-10	245	135	105	375	155	160
	b	430	110	110	330	150	120		210	160	80	365	190	130
21-Apr-10	a	585	115	80	570	130	80	26-Apr-10	255	110	125	295	110	110
	b	650	120	110	925	170	90		180	110	120	240	105	155
17-May-10	a	-	-	-	-	-	-	12-May-10	430	150	135	425	55	255
	b	-	-	-	-	-	-		450	125	145	550	95	230
07-Jun-10	a	855	145	225	1205	265	350	03-Jun-10	-	-	-	675	140	245
	b	770	160	175	980	130	240		-	-	-	570	250	250
07-Jul-10	a	1890	540	355	2095	945	640	16-Jun-10	910	315	195	805	265	185
	b	1710	535	425	1880	875	620		810	340	225	810	245	205
21-Jul-10	a	2225	355	350	2915	365	450	14-Jul-10	2405	405	320	2340	410	310
	b	2625	390	330	2520	560	420		2295	250	255	2665	470	310
09-Aug-10	a	2080	355	365	2020	815	420	03-Aug-10	2650	350	285	2415	330	455
	b	1915	375	325	2355	485	485		2485	375	280	2515	495	335
21-Sep-10	a	1350	220	250	1630	475	315	07-Sep-10	1365	180	260	1495	375	355
	b	1380	400	340	1270	250	315		1360	475	245	1375	370	340

ii. Pipe Series 3, 5, 7 and 8.

Date	Pipe ID	Pipe Series 3 TSS [mg/L]			Pipe Series 5 TSS [mg/L]			Pipe Series 7 TSS [mg/L]			Pipe Series 8 TSS [mg/L]		
		t = 0	t = 24	t = 48	t = 0	t = 24	t = 48	t = 0	t = 24	t = 48	t = 0	t = 24	t = 48
13-Nov-09	a	205	110	160	200	135	160	210	130	315	210	125	160
	b	210	155	160	190	125	160	175	140	165	195	410	165
04-Feb-10	a	465	210	95	345	240	105	230	330	90	425	180	105
	b	350	325	120	425	235	75	270	220	30	450	455	305
18-Feb-10	a	375	250	100	285	230	95	370	515	175	365	270	190
	b	255	240	120	255	335	125	295	225	180	455	460	155
15-Mar-10	a	390	250	130	450	195	95	455	490	115	345	830	120
	b	220	175	95	395	220	145	340	240	140	375	190	205
29-Apr-10	a	590	165	80	390	255	65	625	135	85	445	175	205
	b	265	265	75	365	260	90	625	140	140	605	195	215
20-May-10	a	320	175	450	395	340	120	415	460	235	360	280	330
	b	390	285	175	355	365	175	420	355	265	385	320	445
09-Jun-10	a	660	260	140	630	165	180	590	450	600	830	210	135
	b	500	180	160	625	160	200	580	140	250	495	220	150
24-Jun-10	a	1930	460	535	1715	600	430	1135	740	530	1770	815	635
	b	1720	550	445	1955	615	505	2270	525	465	2155	520	480
19-Jul-10	a	1915	315	365	2005	535	450	1695	545	410	2130	585	440
	b	2005	535	440	1775	600	480	1540	545	405	1960	590	515
12-Aug-10	a	2205	560	460	2070	520	1105	2380	455	360	2135	505	295
	b	1930	485	295	3110	695	405	1835	695	375	1945	2715	480
15-Sep-10	a	1245	660	395	1095	650	345	1445	555	435	1395	760	435
	b	1120	615	470	1230	635	425	1175	485	370	1505	685	440

e. Fixed Suspend Solids (FSS) average leachate pipes measurements.

i. Pipe Series 1, 2, 4 and 6.

Date	Pipe ID	Pipe Series 1 FSS [mg/L]			Pipe Series 4 FSS [mg/L]			Date	Pipe Series 2 FSS [mg/L]			Pipe Series 6 FSS [mg/L]		
		t = 0	t = 24	t = 48	t = 0	t = 24	t = 48		t = 0	t = 24	t = 48	t = 0	t = 24	t = 48
27-Oct-10	a	120	100	55	155	110	40	08-Oct-10	145	10	85	155	5	75
	b	120	65	65	160	50	70		115	15	60	130	5	70
01-Feb-10	a	210	165	30	205	115	50	27-Jan-10	325	65	110	365	65	125
	b	260	165	40	265	125	25		320	110	125	260	125	110
11-Feb-10	a	400	20	35	345	70	25	08-Feb-10	445	25	180	755	190	105
	b	480	65	25	475	115	15		420	50	115	1925	60	80
12-Mar-10	a	210	15	30	215	35	30	09-Mar-10	105	60	15	230	70	20
	b	315	5	15	205	45	35		100	70	5	240	90	25
21-Apr-10	a	380	60	60	395	70	40	26-Apr-10	115	50	65	155	55	65
	b	485	90	60	680	120	50		75	55	55	100	55	115
17-May-10	a	-	-	-	-	-	-	12-May-10	310	80	55	285	0	45
	b	-	-	-	-	-	-		280	45	55	360	0	0
07-Jun-10	a	705	20	140	910	35	240	03-Jun-10	-	-	-	535	0	235
	b	605	40	80	770	10	155		-	-	-	430	30	255
07-Jul-10	a	1210	240	155	1360	515	365	16-Jun-10	715	165	100	620	120	80
	b	1115	245	210	1225	465	350		635	180	135	620	125	105
21-Jul-10	a	1575	80	145	2200	90	305	14-Jul-10	1730	180	85	1655	190	105
	b	1885	135	230	1860	240	275		1590	85	85	1895	230	115
09-Aug-10	a	1145	125	145	1055	510	190	03-Aug-10	1825	145	145	1665	160	185
	b	1060	155	105	1275	285	235		1745	150	115	1775	230	145
21-Sep-10	a	955	45	90	1205	180	155	07-Sep-10	825	95	110	885	235	130
	b	985	150	155	945	60	135		830	335	90	895	245	135

ii. Pipe Series 3, 5, 7 and 8.

Date	Pipe ID	Pipe Series 3 FSS [mg/L]			Pipe Series 5 FSS [mg/L]			Pipe Series 7 FSS [mg/L]			Pipe Series 8 FSS [mg/L]		
		t = 0	t = 24	t = 48	t = 0	t = 24	t = 48	t = 0	t = 24	t = 48	t = 0	t = 24	t = 48
13-Nov-09	a	95	20	40	80	50	40	85	40	140	75	40	30
	b	80	50	45	90	55	30	65	70	50	65	235	40
04-Feb-10	a	295	95	25	215	95	25	135	140	20	290	25	55
	b	240	145	60	275	65	5	175	70	5	285	225	155
18-Feb-10	a	195	50	35	185	20	65	245	190	85	195	90	85
	b	135	60	65	165	160	90	180	70	65	280	185	85
15-Mar-10	a	195	110	60	245	90	35	235	215	60	175	575	65
	b	55	70	0	175	90	20	160	95	25	185	65	80
29-Apr-10	a	350	55	20	235	135	25	460	60	25	270	75	115
	b	150	115	20	210	175	40	380	45	50	370	120	120
20-May-10	a	140	115	405	180	255	170	75	390	215	100	195	255
	b	75	205	145	85	250	150	50	280	225	110	210	385
09-Jun-10	a	475	145	85	385	50	120	375	255	465	545	20	75
	b	340	30	105	405	35	135	375	80	190	275	70	95
24-Jun-10	a	1185	220	350	1060	295	240	575	275	230	1015	425	330
	b	1155	280	225	1130	295	315	1460	225	210	1365	230	245
19-Jul-10	a	1220	195	185	1235	370	185	1070	340	200	1375	380	245
	b	1235	370	230	1120	340	245	930	365	185	1250	405	305
12-Aug-10	a	1385	310	270	1310	235	760	1575	205	190	1370	295	170
	b	1240	255	125	2190	365	250	1105	400	210	1250	1900	290
15-Sep-10	a	880	475	230	780	500	160	1060	410	200	1010	600	200
	b	770	480	230	905	495	195	825	355	185	1120	550	205

f. Volatile Suspend Solids (VSS) average leachate pipes measurements.

i. Pipe Series 1, 2, 4 and 6.

Date	Pipe ID	Pipe Series 1 VSS [mg/L]			Pipe Series 4 VSS [mg/L]			Date	Pipe Series 2 VSS [mg/L]			Pipe Series 6 VSS [mg/L]		
		t = 0	t = 24	t = 48	t = 0	t = 24	t = 48		t = 0	t = 24	t = 48	t = 0	t = 24	t = 48
27-Oct-10	a	95	105	140	175	105	75	08-Oct-10	195	85	40	210	110	70
	b	125	85	90	140	95	115		200	115	45	205	120	65
01-Feb-10	a	100	45	50	80	45	75	27-Jan-10	65	70	85	65	145	95
	b	55	60	35	50	35	60		45	95	75	70	145	75
11-Feb-10	a	255	105	25	165	125	35	08-Feb-10	200	215	85	325	195	130
	b	175	80	25	160	70	35		174	180	180	485	175	135
12-Mar-10	a	125	95	70	130	105	90	09-Mar-10	140	75	90	145	85	140
	b	115	105	95	125	105	85		110	90	75	125	100	105
21-Apr-10	a	205	55	20	175	60	40	26-Apr-10	140	60	60	140	55	45
	b	165	30	50	245	50	40		105	55	65	140	50	40
17-May-10	a	-	-	-	-	-	-	12-May-10	120	70	80	140	85	210
	b	-	-	-	-	-	-		170	80	90	190	110	235
07-Jun-10	a	150	125	85	295	230	110	03-Jun-10	-	-	-	-	-	-
	b	165	120	95	210	120	85		-	-	-	-	-	-
07-Jul-10	a	680	300	200	735	430	275	16-Jun-10	195	150	95	185	145	105
	b	595	290	215	655	410	270		175	160	90	190	120	100
21-Jul-10	a	650	275	205	715	275	145	14-Jul-10	675	225	235	685	220	205
	b	740	255	100	660	320	145		705	165	170	770	240	195
09-Aug-10	a	935	230	220	965	305	230	03-Aug-10	825	205	140	750	170	270
	b	855	220	220	1080	200	250		740	225	165	740	265	190
21-Sep-10	a	395	175	160	425	295	160	07-Sep-10	540	85	150	610	140	225
	b	395	250	185	325	190	180		530	140	155	480	125	205

ii. Pipe Series 3, 5, 7 and 8.

Date	Pipe ID	Pipe Series 3 VSS [mg/L]			Pipe Series 5 VSS [mg/L]			Pipe Series 7 VSS [mg/L]			Pipe Series 8 VSS [mg/L]		
		t = 0	t = 24	t = 48	t = 0	t = 24	t = 48	t = 0	t = 24	t = 48	t = 0	t = 24	t = 48
13-Nov-09	a	110	90	120	120	85	120	125	90	175	135	85	130
	b	130	105	115	100	70	130	110	70	115	130	175	125
04-Feb-10	a	170	115	70	130	145	80	95	190	70	135	155	50
	b	110	180	60	150	170	70	95	150	25	165	230	150
18-Feb-10	a	180	200	65	100	210	30	125	325	90	170	180	105
	b	120	180	55	90	175	35	115	155	115	175	275	70
15-Mar-10	a	195	140	70	205	105	60	220	275	55	170	255	55
	b	165	105	95	220	130	125	180	145	115	190	125	125
29-Apr-10	a	240	110	60	155	120	40	165	75	60	175	100	90
	b	115	150	55	155	85	50	245	95	90	235	75	95
20-May-10	a	180	60	45	215	85	0	340	70	20	260	85	75
	b	315	80	30	270	115	25	370	75	40	275	110	60
09-Jun-10	a	185	115	55	245	115	60	215	195	135	285	215	60
	b	160	150	55	220	125	65	205	60	60	220	190	55
24-Jun-10	a	745	240	185	655	305	190	560	465	300	755	390	305
	b	565	270	220	825	320	190	810	300	255	790	290	235
19-Jul-10	a	695	120	180	770	165	265	625	205	210	755	205	195
	b	770	165	210	655	260	235	610	180	220	710	185	210
12-Aug-10	a	820	250	190	760	285	345	805	250	170	765	210	125
	b	690	230	170	920	330	155	730	295	165	695	815	190
15-Sep-10	a	365	185	165	315	150	185	385	145	235	385	160	235
	b	350	135	240	325	140	230	350	130	185	385	135	235

g. Alkalinity average leachate pipes measurements.

i. Pipe Series 1, 2, 4 and 6.

Date	Pipe ID	Pipe Series 1 Alkalinity [$mgCaCO_3/L$]			Pipe Series 4 Alkalinity [$mgCaCO_3/L$]			Date	Pipe Series 2 Alkalinity [$mgCaCO_3/L$]			Pipe Series 6 Alkalinity [$mgCaCO_3/L$]		
		t = 0	t = 24	t = 48	t = 0	t = 24	t = 48		t = 0	t = 24	t = 48	t = 0	t = 24	t = 48
27-Oct-10	a	5800	5225	5200	5825	5500	5300	08-Oct-10	5600	5300	5225	5475	5250	5225
	b	5800	5350	5350	5800	5425	5350		5450	5200	5150	5500	5225	5450
01-Feb-10	a	4850	4550	4500	4725	4625	4450	27-Jan-10	3950	3300	3300	4100	3500	3400
	b	4850	4550	4450	4750	4650	4500		3950	3300	3300	4050	3400	3300
11-Feb-10	a	5425	5325	4650	5600	5300	5250	08-Feb-10	6750	6675	6550	6850	6750	6600
	b	5500	5150	5200	5650	5275	5250		6875	6675	6575	6900	6750	6650
12-Mar-10	a	4575	2725	2800	4075	2825	2800	09-Mar-10	3825	3700	3625	3875	3650	3550
	b	4625	2775	2775	4255	2800	2800		3875	3750	3700	3825	3625	3550
21-Apr-10	a	2225	2050	2100	2275	2050	2050	26-Apr-10	2500	2425	2300	2550	2300	2225
	b	2225	2100	2075	2275	2050	2050		2600	2400	2350	2575	2375	2375
17-May-10	a	2500	2000	1900	2500	1900	1750	12-May-10	1950	2050	3225	2400	2000	1800
	b	2400	1950	1800	2650	1850	1850		2100	2100	3200	2350	1950	1850
07-Jun-10	a	2000	1850	1800	1850	1550	1575	03-Jun-10	1700	1500	1600	1500	1550	1550
	b	2050	1750	1750	1800	1750	1650		1600	1600	1700	1500	1700	1550
07-Jul-10	a	4900	6100	5850	5500	5700	6050	16-Jun-10	4900	4700	4300	5600	4750	4650
	b	6050	5950	5800	6650	5900	5750		5050	4850	4700	4900	4900	4650
21-Jul-10	a	5550	5950	5725	4700	5250	5800	14-Jul-10	4200	4500	4900	4350	4850	4950
	b	6050	5850	5725	5600	5650	5750		4400	4600	5000	4450	4800	4800
09-Aug-10	a	5100	5200	4600	4450	5300	4700	03-Aug-10	6050	5300	4850	6200	5400	4650
	b	4650	5500	4800	4450	5300	4800		6100	5250	4700	6150	5300	5000
21-Sep-10	a	6200	4900	5300	5850	4650	5300	07-Sep-10	4950	5100	4200	4750	4750	4250
	b	5800	5250	5450	5850	4650	5400		4800	5150	4150	4900	5100	4300

ii. Pipe Series 3, 5, 7 and 8.

Date	Pipe ID	Pipe Series 3 Alkalinity [$mgCaCO_3/L$]			Pipe Series 5 Alkalinity [$mgCaCO_3/L$]			Pipe Series 7 Alkalinity [$mgCaCO_3/L$]			Pipe Series 8 Alkalinity [$mgCaCO_3/L$]		
		t = 0	t = 24	t = 48	t = 0	t = 24	t = 48	t = 0	t = 24	t = 48	t = 0	t = 24	t = 48
13-Nov-09	a	6150	6000	5900	6100	5750	5725	6075	5750	5750	6100	5850	5700
	b	6150	6000	5800	6050	5750	5850	6100	5875	5925	6100	5900	5700
04-Feb-10	a	4400	4175	4225	4400	4325	4300	4375	4200	4200	4300	4200	4250
	b	4350	4225	4100	4400	4350	4200	4400	4350	4250	4375	4250	4100
18-Feb-10	a	5050	4950	4750	5000	4675	4750	4950	4800	4725	4900	4775	4825
	b	4850	4725	4825	4950	4775	4800	4925	4700	4900	5000	4775	4800
15-Mar-10	a	2575	2750	2800	2675	2950	2800	2725	2850	2750	2425	2950	2800
	b	2775	2825	2850	2725	2950	2850	2780	2925	2875	2475	2850	2850
29-Apr-10	a	2600	2450	2450	2600	2500	2475	2600	2450	2350	2600	2400	2400
	b	2600	2450	2425	2625	2500	2500	2600	2500	2475	2600	2400	2400
20-May-10	a	2450	2400	1950	2300	2000	2100	2300	2050	1850	2350	2350	1950
	b	2150	2000	2200	2250	1950	2100	2300	2150	2000	2250	2100	2100
09-Jun-10	a	2250	4000	4600	3050	4800	4700	3000	4575	4300	2750	4700	4650
	b	3050	4650	4700	3250	4900	4600	3100	4700	4800	2450	4550	4100
24-Jun-10	a	6050	5550	5400	6150	5500	5500	6250	6200	6050	6150	6200	5800
	b	6250	5750	5550	6200	5700	6050	6400	6150	5700	6100	6100	5600
19-Jul-10	a	5850	5200	4950	5700	5050	5250	5750	5200	5100	5550	5150	5000
	b	5700	5100	4750	5700	5150	5000	5800	5300	5500	5500	5050	5200
12-Aug-10	a	5400	4500	5400	5200	4550	4900	5600	4600	5100	5050	4600	5700
	b	5750	4250	4750	4900	4700	5000	5150	4400	5300	5700	4950	4950
15-Sep-10	a	4800	5400	4150	4900	5450	4300	5200	5600	4300	4900	5350	4250
	b	4950	5600	4750	5050	5500	4600	5150	5800	4450	5000	5750	4650

h. pH average leachate pipes measurements.

i. Pipe Series 1, 2, 4 and 6.

Date	Pipe ID	Pipe Series 1 pH [-]			Pipe Series 4 pH [-]			Date	Pipe Series 2 pH [-]			Pipe Series 6 pH [-]		
		t = 0	t = 24	t = 48	t = 0	t = 24	t = 48		t = 0	t = 24	t = 48	t = 0	t = 24	t = 48
27-Oct-10	a	-	-	-	8.22	8.11	8.16	08-Oct-10	7.97	7.83	7.92	8	7.88	7.96
	b	8.24	8.05	8.08	8.22	8.1	8.13		7.96	7.88	7.95	7.98	7.89	7.99
01-Feb-10	a	8.15	7.65	7.64	8.12	7.76	7.74	27-Jan-10	8.08	7.76	7.82	8.14	7.8	7.81
	b	8.18	7.64	7.68	8.15	7.78	7.7		8.09	7.74	7.85	8.12	7.87	7.82
11-Feb-10	a	8.28	7.9	8.13	8.25	7.94	7.92	08-Feb-10	8.51	8.35	8.34	8.55	8.36	8.4
	b	8.28	7.93	7.94	8.29	7.96	7.94		8.54	8.39	8.34	8.56	8.45	8.52
12-Mar-10	a	8.28	7.95	7.95	8.25	7.95	7.92	09-Mar-10	8.45	8.06	8.18	8.47	8.21	8.39
	b	8.31	7.98	7.96	8.28	7.93	7.87		8.47	8.07	8.18	8.47	8.2	8.39
21-Apr-10	a	8.4	7.86	7.86	8.31	7.83	7.82	26-Apr-10	8.43	7.95	7.79	8.43	8.11	8.12
	b	8.38	7.84	7.84	8.33	7.79	7.74		8.47	7.95	7.92	8.46	8	8.07
17-May-10	a	8.6	7.94	7.91	8.52	8.09	7.93	12-May-10	8.55	8.18	8.11	8.57	7.94	7.94
	b	8.62	7.95	7.91	8.56	7.97	7.87		8.62	8.15	8.18	8.59	7.95	7.93
07-Jun-10	a	8.5	8.16	8.13	8.47	8.15	8	03-Jun-10	8.52	8.22	8.18	8.56	8.21	8.34
	b	8.5	8.12	7.99	8.5	8.06	7.99		8.53	8.21	8.22	8.55	8.19	8.2
07-Jul-10	a	8.12	7.55	7.22	8.1	7.49	7.18	16-Jun-10	8.14	7.79	7.78	8.18	8.01	8.19
	b	8.12	7.54	7.21	8.12	7.5	7.17		8.15	7.79	7.76	8.19	7.93	8.06
21-Jul-10	a	8.27	7.89	7.71	8.24	8.12	7.79	14-Jul-10	8.37	7.99	7.89	8.41	8.03	7.96
	b	8.26	7.91	7.74	8.27	7.92	7.79		8.4	8.02	7.97	8.4	8.04	7.99
09-Aug-10	a	8.05	8.24	7.97	8.02	8.21	7.92	03-Aug-10	7.97	7.59	7.51	8.05	7.59	7.55
	b	8.05	8.23	7.96	8.03	8.24	7.93		8.01	7.59	7.57	8.06	7.6	7.55
21-Sep-10	a	8.71	8.55	8.46	8.76	8.56	8.51	07-Sep-10	8.4	7.95	7.98	8.41	8.1	8.17
	b	8.76	8.53	8.46	8.78	8.54	8.45		8.43	8	7.98	8.42	8.05	8.02

ii. Pipe Series 3, 5, 7 and 8.

Date	Pipe ID	Pipe Series 3 pH [-]			Pipe Series 5 pH [-]			Pipe Series 7 pH [-]			Pipe Series 8 pH [-]		
		t = 0	t = 24	t = 48	t = 0	t = 24	t = 48	t = 0	t = 24	t = 48	t = 0	t = 24	t = 48
13-Nov-09	a	7.51	7.56	7.43	7.79	7.64	7.44	7.7	7.7	7.73	7.58	7.68	7.67
	b	7.78	7.6	7.45	7.75	7.62	7.6	7.71	7.66	7.46	7.67	7.76	7.76
04-Feb-10	a	8.49	8.25	8.23	8.49	8.32	8.28	8.49	8.33	8.18	8.49	8.29	8.25
	b	8.5	8.41	8.26	8.5	8.34	8.3	8.5	8.32	8.27	8.47	8.32	8.23
18-Feb-10	a	8.3	8.03	8.09	8.44	8.1	8.08	8.42	8.17	8.21	8.41	8.13	8.13
	b	8.45	8.11	8.11	8.43	8.15	8.12	8.44	8.12	8.08	8.41	8.14	8.12
15-Mar-10	a	8.6	8.36	8.18	8.65	8.52	8.39	8.64	8.44	8.35	8.62	8.42	8.26
	b	8.66	8.55	8.43	8.66	8.57	8.46	8.64	8.53	8.43	8.65	8.46	8.25
29-Apr-10	a	8.43	7.85	7.92	8.49	8.02	7.94	8.49	8.03	8.1	8.43	7.97	7.98
	b	8.44	7.91	7.79	8.52	8.04	8	8.48	8.01	7.99	8.44	8.07	7.95
20-May-10	a	8.38	7.96	7.78	8.39	7.96	7.84	8.38	7.96	7.85	8.37	7.97	7.91
	b	8.4	7.98	7.94	8.4	7.97	7.91	8.38	7.97	7.96	8.36	7.98	7.95
09-Jun-10	a	7.94	7.71	7.79	8.01	7.78	7.71	7.98	7.91	7.91	7.96	7.79	7.89
	b	8	7.75	7.72	8	7.8	7.79	8.01	7.77	7.72	8	7.98	7.93
24-Jun-10	a	8.04	7.86	7.92	8.04	7.93	7.92	7.94	7.86	7.8	8.04	7.77	7.82
	b	8.04	7.92	7.87	8.04	7.95	7.81	8.02	7.82	7.86	7.95	7.71	7.88
19-Jul-10	a	7.83	7.36	7.43	7.93	7.4	7.61	7.93	7.47	7.54	7.88	7.43	7.44
	b	7.9	7.4	7.53	7.92	7.46	7.62	7.95	7.51	7.59	7.87	7.43	7.5
12-Aug-10	a	8.3	8.07	8.07	8.34	8.2	8.23	8.33	8.16	8.11	8.32	8.11	8.06
	b	8.34	8.13	8.15	8.34	8.23	8.24	8.35	8.17	8.09	8.32	8.14	8.06
15-Sep-10	a	8.47	8.11	8.09	8.52	8.17	8.13	8.52	8.2	8.11	8.46	8.18	8.12
	b	8.46	8.15	8.11	8.52	8.21	8.17	8.52	8.22	8.11	8.47	8.14	8.07

i. Temperature average leachate pipes measurements.

i. Pipe Series 1, 2, 4 and 6.

Date	Pipe ID	Pipe Series 1 Temperature [˚C]			Pipe Series 4 Temperature [˚C]			Date	Pipe Series 2 Temperature [˚C]			Pipe Series 6 Temperature [˚C]		
		t = 0	t = 24	t = 48	t = 0	t = 24	t = 48		t = 0	t = 24	t = 48	t = 0	t = 24	t = 48
01-Feb-10	a	11	22.3	23.2	10.8	19.7	21.4	27-Jan-10	9.8	19.8	20.3	9.8	20.3	21.4
	b	11.1	21.6	23.4	10.8	20.8	22.3		9.9	20.2	20.8	9.8	20.8	22
11-Feb-10	a	13.3	22.6	21.9	13	20.6	20.7	08-Feb-10	14.6	21.1	21	14.8	21.9	21.9
	b	13.6	22.5	21.4	13.2	21.6	21.5		14.8	21.8	21.7	14.7	21.7	21.8
12-Mar-10	a	15.7	26.6	27	15.7	25.6	27.4	09-Mar-10	16.8	27.2	21.9	16.8	26.9	22.6
	b	15.6	26	25.9	15.4	26.8	28.2		16.8	26.8	22.4	17	26.9	22.5
21-Apr-10	a	16.2	29.1	29.7	17.1	28.1	30.1	26-Apr-10	16.4	30.2	31.3	16.3	30.1	30.1
	b	16.2	28.7	29.3	16.2	29.2	30.5		16.1	29.8	29.6	16.1	29.4	29.8
17-May-10	a	18.4	29.7	29.2	18.3	28.4	29.1	12-May-10	17.4	30.2	30	18.1	29.7	30
	b	18.6	29.2	29.1	18.5	29.7	30.1		17.5	29.8	29	18.5	29.2	29.5
07-Jun-10	a	20.3	29.2	29.7	20.1	28.8	30	03-Jun-10	21.5	30.7	30.7	21.4	30.2	30.2
	b	20.5	28.8	29.6	20.2	29.3	30.6		21.3	30.1	29.9	21.4	30.4	30.2
07-Jul-10	a	18.6	30.8	30.5	18.2	30.1	30.7	16-Jun-10	16.6	31.3	30.5	16.3	30.8	30.3
	b	18.7	30.5	30.2	18.1	31	31.3		16.6	30.7	29.7	16.7	30.8	30.1
21-Jul-10	a	22.5	29.3	30.3	22.4	29.1	30.1	14-Jul-10	26.5	31	32	26.5	30.5	31.1
	b	22.7	29.1	30.1	22.3	29.4	30.7		26.5	30.2	31	26.5	30.5	31
09-Aug-10	a	24.7	30.8	30.5	24.3	30.7	30.7	03-Aug-10	22.7	30.8	31	22.5	30.4	30.6
	b	24.6	30.7	30.1	24.2	30.9	30.8		22.5	30.5	30.2	22.5	30.6	30.6
21-Sep-10	a	19.1	25.7	28.2	19.2	24.8	28.1	07-Sep-10	17.3	29.7	28.5	17.1	29	30
	b	18.9	24.9	27.8	19.2	26.2	29		17.1	29.3	29.1	17	29.1	29.6

ii. Pipe Series 3, 5, 7 and 8.

Date	Pipe ID	Pipe Series 3 Temperature [˚C]			Pipe Series 5 Temperature [˚C]			Pipe Series 7 Temperature [˚C]			Pipe Series 8 Temperature [˚C]		
		t = 0	t = 24	t = 48	t = 0	t = 24	t = 48	t = 0	t = 24	t = 48	t = 0	t = 24	t = 48
13-Nov-09	a	14.3	22.9	22.7	14.4	20.5	22.7	14.5	22.9	23.5	14.6	22.1	22.5
	b	14.6	21.1	21.2	14.5	22.1	21.4	14.6	21.4	21.9	14.6	22.8	23
04-Feb-10	a	16.3	20.9	20.3	16.4	21.2	21.7	16.3	21.2	22	16.5	21.4	21.7
	b	16.3	20.4	20.8	16.4	20.2	20.9	16.4	20.3	21.4	16.7	21.5	22
18-Feb-10	a	13.9	20.3	20.7	14.1	21.9	22.3	14.1	21.8	22.3	13.9	21.7	22.3
	b	14.1	21.1	21.4	13.8	20.8	21.4	14.2	21.1	21.8	14.2	22.1	22.3
15-Mar-10	a	21.6	27.8	27.5	21.4	25.5	27.3	21.3	26.8	27.7	21.5	26.7	27.8
	b	21.5	24.1	25.8	21.5	24.1	26.1	21.5	25.9	27.3	21.3	26.6	27.5
29-Apr-10	a	15.8	28.9	28.1	15.7	27	27.8	15.7	27.9	28.4	15.6	27.7	28.3
	b	16	26.3	26.2	15.6	25.5	27.1	16.1	26.5	27.8	15.8	27.8	28.2
20-May-10	a	19.2	29.4	29.2	18.9	28.9	29.3	18.9	29.1	29.6	19.8	29.3	29.8
	b	19	28	28.5	18.9	28	28.8	19.1	28.5	29.2	19.1	28.3	29.5
09-Jun-10	a	16	30.1	29	16	28.6	28.8	16	29.2	29.3	16.3	29.4	29.6
	b	16.8	28	28.2	16	27.1	28	16.6	27.5	28.5	16.5	29.3	29.4
24-Jun-10	a	21.8	31.7	30.6	21.7	30.5	30.5	21.7	31	31.2	21.9	31.2	31.4
	b	21.8	30	30.8	21.8	29.6	31.4	21.8	31.1	31.1	21.7	31.5	30.2
19-Jul-10	a	21.7	31.7	31	21.2	30.5	30.4	21.3	29.8	30.7	21.3	29.8	30.9
	b	21.6	30.1	29.9	21.2	29.6	30.1	21.6	29.7	30.6	21	29.4	30.9
12-Aug-10	a	25.8	30.8	30.5	26.1	30.1	29.6	26	29.8	29.8	25.8	30.7	30.1
	b	26.1	29.8	28.7	26.1	29.6	29.2	26.2	29.6	29.6	26	29.8	30.2
15-Sep-10	a	18.1	29.3	26.8	18.1	27	27.7	17.9	26.6	28.3	18.1	26.8	28.5
	b	18.1	26.2	26.6	18	25.8	26.8	18.2	26.7	28.2	18	26.6	28.5

j. VFA leachate and pipes measurements values.

i. Pipe series 1 and 4

Date	VFA	Leachate	Pipe ID	Pipe Series 1 Acetate [mg HAc/L]			Pipe Series 4 Acetate [mg HAc/L]		
				t = 0	t = 24	t = 48	t = 0	t = 24	t = 48
21-Sep-11	Acetate mgHAc/L	1090	a	1030	1056	960	1089	985	1016
				1048	988	1014	1043	1044	977
		1066	b	1070	1018	990	1103	1048	982
				1059	1030	973	1204	1169	924
	Propionate mgHPr/L	599	a	542	543	526	564	520	513
				595	556	491	526	533	495
		583	b	560	548	545	538	543	520
				570	545	522	645	607	503
	Butyrate mgHBu/L	670	a	608	576	576	598	585	543
				586	508	491	585	574	557
		666	b	632	575	567	628	601	562
				637	502	504	683	570	613

ii. Pipe series 2 and 6

Date	VFA	Leachate	Pipe ID	Pipe Series 2 Acetate [mg HAc/L]			Pipe Series 6 Acetate [mg HAc/L]		
				t = 0	t = 24	t = 48	t = 0	t = 24	t = 48
07-Sep-11	Acetate mgHAc/L	930	a	1160	882	965	1046	978	851
				1112	947	968	1016	961	844
		947	b	1018	875	925	976	1066	915
				1001	897	929	973	932	868
	Propionate mgHPr/L	487	a	471	378	452	436	454	391
				458	427	462	474	415	387
		491	b	467	428	404	455	492	417
				480	397	431	451	429	404
	Butyrate mgHBu/L	486	a	429	432	324	379	446	333
				432	460	320	446	396	319
		481	b	435	420	327	432	475	326
				436	454	321	438	430	322

APPENDIX F : CLOGGING COMPOSITION DATA FROM THE PIPE RINGS (5) ACCUMULATED WITHIN THE PIPE SERIES AT DIFFERENT ELAPSED TIMES.

a. Summary of average (μ) and standard deviation (σ) values of clog mass [gr] accumulated within the pipe series at different elapsed times

Pipe Ring 1				Pipe Ring 2			Pipe Ring 3		
Pipe Series	Date Sampled	Mass collected [gr] μ	σ	Date Sampled	Mass collected [gr] μ	σ	Date Sampled	Mass collected [gr] μ	σ
1	16-Dec-09	1.53	0.60	27-Apr-10	1.72	0.06	28-Jun-10	4.83	0.45
2	18-Dec-09	1.36	0.46	07-Apr-10	2.09	0.30	23-Jun-10	2.01	0.65
3	18-Dec-09	1.92	0.15	28-Apr-10	2.10	1.93	30-Jun-10	5.09	1.15
4	16-Dec-09	4.06	0.13	27-Apr-10	4.94	0.86	28-Jun-10	9.75	0.93
5	18-Dec-09	3.94	0.22	28-Apr-10	7.27	2.10	30-Jun-10	11.79	1.65
6	18-Dec-09	8.55	1.77	07-Apr-10	12.06	0.53	23-Jun-10	24.91	4.12
7	21-Dec-09	9.16	1.61	28-Apr-10	15.2	0.79	30-Jun-10	24.70	3.12
8	21-Dec-09	7.9	0.04	28-Apr-10	11.47	0.58	30-Jun-10	22.95	0.73

Pipe Ring 4				Pipe Ring 5		
Pipe Series	Date Sampled	Mass collected [gr] μ	σ	Date	Mass collected [gr] μ	σ
1	03-Sep-10	3.65	0.07	20-Nov-10	3.78	0.15
2	30-Aug-10	3.25	0.07	14-Nov-10	3.67	0.69
3	31-Aug-10	4.47	0.28	27-Nov-10	4.37	0.49
4	03-Sep-10	10.33	0.35	20-Nov-10	11.01	1.28
5	31-Aug-10	9.67	1.12	27-Nov-10	8.51	0.42
6	30-Aug-10	24.05	6.72	14-Nov-10	30.26	10.80
7	31-Aug-10	48.02	1.89	23-Nov-10	39.35	6.24
8	31-Aug-10	66.03	12.23	23-Nov-10	42.23	9

b. Summary of average (μ) and standard deviation (σ) values of water content values [%] in the clog mass accumulated within the pipe series at different elapsed times

Pipe Ring 1				Pipe Ring 2			Pipe Ring 3		
Pipe Series	Date Sampled	Water Content [%] μ	σ	Date Sampled	Water Content [%] μ	σ	Date Sampled	Water Content [%] μ	σ
1	16-Dec-09	70.03	4.04	27-Apr-10	48.02	8.47	28-Jun-10	54.21	0.35
2	18-Dec-09	63.14	10.69	07-Apr-10	60.24	2.70	23-Jun-10	57.34	2.24
3	18-Dec-09	76.52	0.98	28-Apr-10	60.79	3.48	30-Jun-10	58.44	3.19
4	16-Dec-09	67.33	2.66	27-Apr-10	32.81	7.87	28-Jun-10	60.28	2.07
5	18-Dec-09	71.28	1.53	28-Apr-10	53.02	3.59	30-Jun-10	57.76	4.35
6	18-Dec-09	67.89	0.65	07-Apr-10	57.55	2.26	23-Jun-10	55.05	2.32
7	21-Dec-09	76.00	2.64	28-Apr-10	66.51	0.62	30-Jun-10	65.14	1.79
8	21-Dec-09	74.74	4.21	28-Apr-10	66.02	1.91	30-Jun-10	65.48	0.77

Pipe Ring 4				Pipe Ring 5		
Pipe Series	Date Sampled	Water Content [%] μ	σ	Date Sampled	Water Content [%] μ	σ
1	03-Sep-10	49.84	5.56	20-Nov-10	48.81	5.03
2	30-Aug-10	64.87	4.07	14-Nov-10	56.68	4.35
3	31-Aug-10	59.90	4.06	27-Nov-10	55.83	4.02
4	03-Sep-10	61.83	2.88	20-Nov-10	56.82	1.08
5	31-Aug-10	66.46	1.13	27-Nov-10	62.56	2.61
6	30-Aug-10	63.68	3.56	14-Nov-10	63.22	1.27
7	31-Aug-10	71.30	1.40	23-Nov-10	70.72	1.53
8	31-Aug-10	72.98	1.67	23-Nov-10	69.96	0.79

c. Summary of average (μ) and standard deviation (σ) values of Total Solids content [%] in the clog mass accumulated within the pipe series at different elapsed times

	Pipe Ring 1			Pipe Ring 2			Pipe Ring 3		
Pipe	Date	Total Solids [%]		Date	Total Solids [%]		Date	Total Solids [%]	
Series	Sampled	μ	σ	Sampled	μ	σ	Sampled	μ	σ
1	16-Dec-09	29.97	4.04	27-Apr-10	51.98	8.47	28-Jun-10	45.79	0.35
2	18-Dec-09	36.86	10.69	07-Apr-10	39.76	2.70	23-Jun-10	42.66	2.24
3	18-Dec-09	23.48	0.98	28-Apr-10	39.21	3.48	30-Jun-10	41.56	3.19
4	16-Dec-09	32.67	2.66	27-Apr-10	67.19	7.87	28-Jun-10	39.72	2.07
5	18-Dec-09	28.72	1.53	28-Apr-10	46.98	3.59	30-Jun-10	42.24	4.35
6	18-Dec-09	32.11	0.65	07-Apr-10	42.45	2.26	23-Jun-10	44.95	2.32
7	21-Dec-09	24.00	2.64	28-Apr-10	33.49	0.62	30-Jun-10	34.86	1.79
8	21-Dec-09	25.26	4.21	28-Apr-10	33.98	1.91	30-Jun-10	34.52	0.77

	Pipe Ring 4			Pipe Ring 5		
Pipe	Date	Total Solids [%]		Date	Total Solids [%]	
Series	Sampled	μ	σ	Sampled	μ	σ
1	03-Sep-10	50.16	5.56	20-Nov-10	51.19	5.03
2	30-Aug-10	35.13	4.07	14-Nov-10	43.32	4.35
3	31-Aug-10	40.10	4.06	27-Nov-10	44.17	4.02
4	03-Sep-10	38.17	2.88	20-Nov-10	43.18	1.08
5	31-Aug-10	33.54	1.13	27-Nov-10	37.44	2.61
6	30-Aug-10	36.32	3.56	14-Nov-10	36.78	1.27
7	31-Aug-10	28.70	1.40	23-Nov-10	29.28	1.53
8	31-Aug-10	27.02	1.67	23-Nov-10	30.04	0.79

d. Summary of average (μ) and standard deviation (σ) values of Inorganic mass [gr] in the clog mass accumulated within the pipe series at different elapsed times

	Pipe Ring 1			Pipe Ring 2			Pipe Ring 3		
Pipe	Date	Inorganic mass[gr]		Date	Inorganic mass[gr]		Date	Inorganic mass[gr]	
Series	Sampled	μ	σ	Sampled	μ	σ	Sampled	μ	σ
1	16-Dec-09	1.14	0.39	27-Apr-10	1.39	0.05	28-Jun-10	4.05	0.36
2	18-Dec-09	1.02	0.23	07-Apr-10	1.60	0.19	23-Jun-10	1.59	0.39
3	18-Dec-09	1.48	0.07	28-Apr-10	1.70	1.29	30-Jun-10	4.24	0.76
4	16-Dec-09	3.30	0.09	27-Apr-10	4.12	0.56	28-Jun-10	8.28	0.61
5	18-Dec-09	3.24	0.14	28-Apr-10	5.98	1.45	30-Jun-10	9.89	0.89
6	18-Dec-09	7.45	1.25	07-Apr-10	10.49	0.40	23-Jun-10	21.69	3.14
7	21-Dec-09	7.36	0.92	28-Apr-10	12.52	0.54	30-Jun-10	21.18	2.19
8	21-Dec-09	6.46	0.15	28-Apr-10	9.48	0.31	30-Jun-10	19.63	0.56

	Pipe Ring 4			Pipe Ring 5		
Pipe	Date	Inorganic mass[gr]		Date	Inorganic mass[gr]	
Series	Sampled	μ	σ	Sampled	μ	σ
1	03-Sep-10	3.16	0.03	20-Nov-10	3.20	0.04
2	30-Aug-10	2.56	0.06	14-Nov-10	2.98	0.50
3	31-Aug-10	3.53	0.27	27-Nov-10	3.69	0.35
4	03-Sep-10	8.71	0.37	20-Nov-10	9.24	0.98
5	31-Aug-10	7.75	0.67	27-Nov-10	7.22	0.26
6	30-Aug-10	20.26	5.09	14-Nov-10	26.14	7.33
7	31-Aug-10	38.41	1.38	23-Nov-10	33.42	4.34
8	31-Aug-10	52.12	6.58	23-Nov-10	36.13	6.27

e. Summary of average (μ) and standard deviation (σ) values of Organic mass [gr] in the clog mass accumulated within the pipe series at different elapsed times

	Pipe Ring 1			Pipe Ring 2			Pipe Ring 3		
Pipe Series	Date Sampled	Organic mass[gr] μ	σ	Date Sampled	Organic mass[gr] μ	σ	Date Sampled	Organic mass[gr] μ	σ
1	16-Dec-09	0.39	0.11	27-Apr-10	0.33	0.00	28-Jun-10	0.77	0.04
2	18-Dec-09	0.34	0.14	07-Apr-10	0.49	0.06	23-Jun-10	0.42	0.15
3	18-Dec-09	0.43	0.06	28-Apr-10	0.40	0.29	30-Jun-10	0.85	0.19
4	16-Dec-09	0.76	0.04	27-Apr-10	0.81	0.15	28-Jun-10	1.47	0.15
5	18-Dec-09	0.69	0.04	28-Apr-10	1.28	0.27	30-Jun-10	1.90	0.49
6	18-Dec-09	1.10	0.22	07-Apr-10	1.56	0.07	23-Jun-10	3.21	0.23
7	21-Dec-09	1.80	0.41	28-Apr-10	2.68	0.13	30-Jun-10	3.51	0.37
8	21-Dec-09	1.44	0.14	28-Apr-10	1.99	0.17	30-Jun-10	3.31	0.16

	Pipe Ring 4			Pipe Ring 5		
Pipe Series	Date Sampled	Organic mass[gr] μ	σ	Date Sampled	Organic mass[gr] μ	σ
1	03-Sep-10	0.49	0.06	20-Nov-10	0.58	0.09
2	30-Aug-10	0.69	0.03	14-Nov-10	0.68	0.09
3	31-Aug-10	0.94	0.06	27-Nov-10	0.68	0.06
4	03-Sep-10	1.62	0.12	20-Nov-10	1.76	0.16
5	31-Aug-10	1.92	0.25	27-Nov-10	1.29	0.11
6	30-Aug-10	3.79	0.52	14-Nov-10	4.12	1.50
7	31-Aug-10	9.60	0.28	23-Nov-10	5.93	0.90
8	31-Aug-10	13.90	3.42	23-Nov-10	6.10	1.10

APPENDIX G : CLOG MATERIAL DENSITIES FOR THE PIPE SERIES

a. Pipe Series clog bulk density data

i. Pipe Ring 1

Pipe Series	Pipe ID	Date Sampled	Initial Vol. [mL]	Initial Weight [gr]	Final Vol. [mL]	Final Weight [gr]	Difference Vol. [mL]	Difference Weight [gr]	Density [gr/mL]
1	a	16-Dec-09	-	-	-	-	-	-	-
	b		13	68.05	13.25	68.434	0.25	0.384	1.54
2	a	18-Dec-09	-	-	-	-	-	-	-
	b		13	68.09	13.2	68.329	0.2	0.239	1.20
3	a	18-Dec-09	13	68.124	13.4	68.666	0.4	0.542	1.36
	b		13	68.138	13.4	68.501	0.4	0.363	0.91
4	a	16-Dec-09	13	68.052	13.4	68.781	0.4	0.729	1.82
	b		13	68.169	13.3	68.718	0.3	0.549	1.83
5	a	18-Dec-09	13	68.138	14.2	69.482	1.2	1.344	1.12
	b		13	68.14	14.2	69.505	1.2	1.365	1.14
6	a	18-Dec-09	13	68.03	13.3	68.49	0.3	0.46	1.53
			13	68.01	13.8	69.303	0.8	1.293	1.62
	b		13	68.05	13.2	68.364	0.2	0.314	1.57
			13	68.051	13.3	68.572	0.3	0.521	1.74
7	a	21-Dec-09	11	66.092	12	66.987	1	0.895	0.90
	b		10	76.029	11.1	77.016	1.1	0.987	0.90
8	a	21-Dec-09	10	43.041	11.4	44.082	1.1	1.041	0.74
	b		10	43.175	11.7	44.506	1.7	1.331	0.78

ii. Pipe Ring 2

Pipe Series	Pipe ID	Date Sampled	Initial Vol. [mL]	Initial Weight [gr]	Final Vol. [mL]	Final Weight [gr]	Difference Vol. [mL]	Difference Weight [gr]	Density [gr/mL]
1	a	27-Apr-10	13	68.09	13.2	68.488	0.2	0.398	1.99
	b		13	68.08	13.2	68.48	0.2	0.4	2.00
2	a	07-Apr-10	13	68.08	13.2	68.442	0.2	0.362	1.81
	b		-	-	-	-	-	-	-
3	a	28-Apr-10	13	68.083	13.6	69.063	0.6	0.98	1.63
	b		13	68.08	13.7	69.149	0.7	1.069	1.53
4	a	27-Apr-10	13	68.086	13.6	69.001	0.6	0.915	1.53
	b		13	68.083	14	69.593	1	1.51	1.51
5	a	28-Apr-10	13	68.08	14	69.662	1	1.582	1.58
	b		13	68.081	15.4	71.305	2.4	3.224	1.34
6	a	07-Apr-10	13	68.078	14.6	70.325	1.6	2.247	1.40
	b		13	68.072	13.7	69.074	0.7	1.002	1.43
7	a	28-Apr-10	13	68.082	15.4	71.358	2.4	3.276	1.37
	b		13	68.081	15.2	70.998	2.2	2.917	1.33
8	a	28-Apr-10	13	68.082	14.8	70.549	1.8	2.467	1.37
	b		13	68.083	15	70.76	2	2.677	1.34

iii. Pipe Ring 3

Pipe Series	Pipe ID	Date Sampled	Initial Vol. [mL]	Initial Weight [gr]	Final Vol. [mL]	Final Weight [gr]	Difference Vol. [mL]	Difference Weight [gr]	Density [gr/mL]
1	a	28-Jun-10	5	44.653	5.2	44.993	0.2	0.34	1.70
	b		5	44.655	5.4	45.32	0.4	0.665	1.66
2	a	23-Jun-10	5	44.676	5.2	44.956	0.2	0.28	1.40
	b		5	44.672	5.2	44.999	0.2	0.327	1.64
3	a	30-Jun-10	5	44.655	5.4	45.301	0.4	0.646	1.62
	b		5	44.655	5.6	45.505	0.6	0.85	1.42
4	a	28-Jun-10	5	44.654	6	46.126	1	1.472	1.47
	b		5	44.647	6	46.138	1	1.491	1.49
5	a	30-Jun-10	5	44.654	5.8	45.817	0.8	1.163	1.45
	b		5	44.66	5.8	45.759	0.8	1.099	1.37
6	a	23-Jun-10	13	68.056	15	70.935	2	2.879	1.44
	b		5	44.676	6.1	46.223	1.1	1.547	1.41
7	a	30-Jun-10	5	44.654	5.6	45.483	0.6	0.829	1.38
	b		5	44.658	5.8	45.732	0.8	1.074	1.34
8	a	30-Jun-10	5	44.646	5.8	45.749	0.8	1.103	1.38
	b		5	44.638	5.8	45.753	0.8	1.115	1.39

iv. Pipe Ring 4

Pipe Series	Pipe ID	Date Sampled	Initial		Final		Difference		Density
			Vol. [mL]	Weight [gr]	Vol. [mL]	Weight [gr]	Vol. [mL]	Weight [gr]	[gr/mL]
1	a	03-Sep-10	5	44.66	5.2	44.954	0.2	0.294	1.47
	b		5	44.66	5.2	44.993	0.2	0.333	1.67
2	a	30-Aug-10	5	44.669	5.2	44.961	0.2	0.292	1.46
	b		5	44.671	5.2	44.958	0.2	0.287	1.43
3	a	31-Aug-10	5	44.655	5.2	44.954	0.2	0.299	1.50
	b		5	44.655	5.2	44.957	0.2	0.302	1.51
4	a	03-Sep-10	5	44.653	5.6	45.512	0.6	0.859	1.43
	b		5	44.66	5.4	45.245	0.4	0.585	1.46
5	a	31-Aug-10	5	44.665	5.4	45.201	0.4	0.536	1.34
	b		5	44.66	5.4	45.204	0.4	0.544	1.36
6	a	30-Aug-10	5	44.669	5.4	45.241	0.4	0.572	1.43
	b		5	44.673	5.4	45.235	0.4	0.562	1.40
7	a	31-Aug-10	5	44.664	5.8	45.667	0.8	1.003	1.25
	b		5	44.671	5.6	45.455	0.6	0.784	1.31
8	a	31-Aug-10	5	44.663	5.6	45.42	0.6	0.757	1.26
	b		5	44.672	5.6	45.446	0.6	0.774	1.29

v. Pipe Ring 5

Pipe Series	Pipe ID	Date Sampled	Initial Vol. [mL]	Initial Weight [gr]	Final Vol. [mL]	Final Weight [gr]	Difference Vol. [mL]	Difference Weight [gr]	Density [gr/mL]
1	a	20-Nov-10	5	44.677	5.2	44.979	0.2	0.302	1.51
	b		5	44.665	5.2	44.971	0.2	0.306	1.53
2	a	14-Nov-10	5	44.659	5.4	45.223	0.4	0.564	1.41
	b		5	44.679	5.4	45.23	0.4	0.551	1.38
3	a	27-Nov-10	5	44.649	5.4	45.235	0.4	0.586	1.46
	b		5	44.647	5.4	45.233	0.4	0.586	1.46
4	a	20-Nov-10	5	44.665	5.2	44.956	0.2	0.291	1.46
	b		5	44.666	5.2	44.956	0.2	0.29	1.45
5	a	27-Nov-10	5	44.65	5.4	45.223	0.4	0.573	1.43
	b		5	44.652	5.4	45.237	0.4	0.585	1.46
6	a	14-Nov-10	5	44.653	5.4	45.254	0.4	0.601	1.50
	b		5	44.661	5.4	45.232	0.4	0.571	1.43
7	a	23-Nov-10	5	44.66	5.4	45.2	0.4	0.54	1.35
	b		5	44.659	5.4	45.201	0.4	0.542	1.36
8	a	23-Nov-10	5	44.654	5.4	45.213	0.4	0.559	1.40
	b		5	44.657	5.6	45.447	0.6	0.79	1.32

b. Dry density data.

i. Pipe Ring 2

Pipe Ring #1**Pipe Series 1a**	
Mass Tare [g]	18.633
Mass of Flask + Water + Ash [g]	72.216
Temperature of suspension (T) [˚C]	23.9
Time under vacuum [min]	Overnight
Mass of Tare + Dry Ash [g]	18.859
Specific Gravity of water at 20 ˚C	0.9982
Mass of Ash [g]	0.226
Mass of Flask + Water at T [g]	72.08
Specific Gravity of Water at T	1.00
Specific Gravity of Soil	**2.46**
Dry Ash Density [kg/m^3]	2461.15

Pipe Series 1b	
Mass Tare [g]	18.654
Mass of Flask + Water + Ash [g]	72.25
Temperature of suspension (T) [˚C]	24.4
Time under vacuum [min]	Overnight
Mass of Tare + Dry Ash [g]	18.894
Specific Gravity of water at 20 ˚C	0.9982
Mass of Ash [g]	0.24
Mass of Flask + Water at T [g]	72.08
Specific Gravity of Water at T	1.00
Specific Gravity of Soil	**3.41**
Dry Ash Density [kg/m^3]	3411.33

Pipe Series 2a	
Mass Tare [g]	18.779
Mass of Flask + Water + Ash [g]	72.167
Temperature of suspension (T) [˚C]	25.6
Time under vacuum [min]	Overnight
Mass of Tare + Dry Ash [g]	18.91
Specific Gravity of water at 20 ˚C	1.00
Mass of Ash [g]	0.13
Mass of Flask + Water at T [g]	72.08
Specific Gravity of Water at T	1.00
Specific Gravity of Soil	**3.26**
Dry Ash Density [kg/m^3]	3261.50

Pipe Series 3a	
Mass Tare [g]	18.663
Mass of Flask + Water + Ash [g]	72.349
Temperature of suspension (T) [˚C]	24.9
Time under vacuum [min]	Overnight
Mass of Tare + Dry Ash [g]	19.09
Specific Gravity of water at 20 ˚C	1.00
Mass of Ash [g]	0.43
Mass of Flask + Water at T [g]	72.08
Specific Gravity of Water at T	1.00
Specific Gravity of Soil	**2.74**
Dry Ash Density [kg/m^3]	2741.89

Pipe Series 3b	
Mass Tare [g]	18.7
Mass of Flask + Water + Ash [g]	72.415
Temperature of suspension (T) [˚C]	24.7
Time under vacuum [min]	Overnight
Mass of Tare + Dry Ash [g]	19.15
Specific Gravity of water at 20 ˚C	1.00
Mass of Ash [g]	0.45
Mass of Flask + Water at T [g]	72.08
Specific Gravity of Water at T	1.00
Specific Gravity of Soil	**4.04**
Dry Ash Density [kg/m^3]	4035.17

Pipe Series 4a	
Mass Tare [g]	18.63
Mass of Flask + Water + Ash [g]	72.341
Temperature of suspension (T) [˚C]	25.3
Time under vacuum [min]	Overnight
Mass of Tare + Dry Ash [g]	19.03
Specific Gravity of water at 20 ˚C	1.00
Mass of Ash [g]	0.40
Mass of Flask + Water at T [g]	72.08
Specific Gravity of Water at T	1.00
Specific Gravity of Soil	**2.95**
Dry Ash Density [kg/m^3]	2951.74

Pipe Series 4b	
Mass Tare [g]	18.623
Mass of Flask + Water + Ash [g]	72.492
Temperature of suspension (T) [˚C]	23.5
Time under vacuum [min]	Overnight
Mass of Tare + Dry Ash [g]	19.32
Specific Gravity of water at 20 ˚C	1.00
Mass of Ash [g]	0.70
Mass of Flask + Water at T [g]	72.08
Specific Gravity of Water at T	1.00
Specific Gravity of Soil	**2.40**
Dry Ash Density [kg/m^3]	2404.25

Pipe Series 5a	
Mass Tare [g]	18.286
Mass of Flask + Water + Ash [g]	72.854
Temperature of suspension (T) [˚C]	24.7
Time under vacuum [min]	Overnight
Mass of Tare + Dry Ash [g]	19.51
Specific Gravity of water at 20 ˚C	1.00
Mass of Ash [g]	1.22
Mass of Flask + Water at T [g]	72.08
Specific Gravity of Water at T	1.00
Specific Gravity of Soil	**2.72**
Dry Ash Density [kg/m^3]	2720.66

Pipe Series 5b	
Mass Tare [g]	18.668
Mass of Flask + Water + Ash [g]	72.577
Temperature of suspension (T) [˚C]	24.7
Time under vacuum [min]	Overnight
Mass of Tare + Dry Ash [g]	19.35
Specific Gravity of water at 20 ˚C	1.00
Mass of Ash [g]	0.68
Mass of Flask + Water at T [g]	72.08
Specific Gravity of Water at T	1.00
Specific Gravity of Soil	**3.69**
Dry Ash Density [kg/m^3]	3694.33

Pipe Series 6a	
Mass Tare [g]	18.683
Mass of Flask + Water + Ash [g]	72.596
Temperature of suspension (T) [˚C]	25.3
Time under vacuum [min]	Overnight
Mass of Tare + Dry Ash [g]	19.44
Specific Gravity of water at 20 ˚C	1.00
Mass of Ash [g]	0.75
Mass of Flask + Water at T [g]	72.08
Specific Gravity of Water at T	1.00
Specific Gravity of Soil	**3.21**
Dry Ash Density [kg/m^3]	3214.28

Pipe Series 6b	
Mass Tare [g]	18.199
Mass of Flask + Water + Ash [g]	72.302
Temperature of suspension (T) [˚C]	25.2
Time under vacuum [min]	Overnight
Mass of Tare + Dry Ash [g]	18.56
Specific Gravity of water at 20 ˚C	1.00
Mass of Ash [g]	0.36
Mass of Flask + Water at T [g]	72.08
Specific Gravity of Water at T	1.00
Specific Gravity of Soil	**2.63**
Dry Ash Density [kg/m^3]	2632.66

Pipe Series 7a	
Mass Tare [g]	18.763
Mass of Flask + Water + Ash [g]	72.718
Temperature of suspension (T) [˚C]	25.6
Time under vacuum [min]	Overnight
Mass of Tare + Dry Ash [g]	19.79
Specific Gravity of water at 20 ˚C	1.00
Mass of Ash [g]	1.03
Mass of Flask + Water at T [g]	72.08
Specific Gravity of Water at T	1.00
Specific Gravity of Soil	**2.65**
Dry Ash Density [kg/m^3]	2645.72

Pipe Series 7b	
Mass Tare [g]	18.717
Mass of Flask + Water + Ash [g]	72.92
Temperature of suspension (T) [˚C]	25.3
Time under vacuum [min]	Overnight
Mass of Tare + Dry Ash [g]	19.92
Specific Gravity of water at 20 ˚C	1.00
Mass of Ash [g]	1.20
Mass of Flask + Water at T [g]	72.08
Specific Gravity of Water at T	1.00
Specific Gravity of Soil	**3.33**
Dry Ash Density [kg/m^3]	3331.39

Pipe Series 8a	
Mass Tare [g]	18.763
Mass of Flask + Water + Ash [g]	72.718
Temperature of suspension (T) [˚C]	25.6
Time under vacuum [min]	Overnight
Mass of Tare + Dry Ash [g]	19.79
Specific Gravity of water at 20 ˚C	1.00
Mass of Ash [g]	1.03
Mass of Flask + Water at T [g]	72.08
Specific Gravity of Water at T	1.00
Specific Gravity of Soil	**2.65**
Dry Ash Density [kg/m^3]	2645.72

Pipe Series 8b	
Mass Tare [g]	18.717
Mass of Flask + Water + Ash [g]	72.92
Temperature of suspension (T) [˚C]	25.3
Time under vacuum [min]	Overnight
Mass of Tare + Dry Ash [g]	19.92
Specific Gravity of water at 20 ˚C	1.00
Mass of Ash [g]	1.20
Mass of Flask + Water at T [g]	72.08
Specific Gravity of Water at T	1.00
Specific Gravity of Soil	**3.33**
Dry Ash Density [kg/m^3]	3331.39

ii. Pipe Ring 3

Pipe Series 1a	
Mass Tare [g]	18.625
Mass of Flask + Water + Ash [g]	48.774
Temperature of suspension (T) [˚C]	22.7
Time under vacuum [min]	Overnight
Mass of Tare + Dry Ash [g]	18.801
Specific Gravity of water at 20 ˚C	0.9982
Mass of Ash [g]	0.176
Mass of Flask + Water at T [g]	48.66
Specific Gravity of Water at T	1.00
Specific Gravity of Soil	**2.89**
Dry Ash Density [kg/m^3]	2894.90

Pipe Series 1b	
Mass Tare [g]	18.713
Mass of Flask + Water + Ash [g]	48.872
Temperature of suspension (T) [˚C]	23.4
Time under vacuum [min]	Overnight
Mass of Tare + Dry Ash [g]	19.021
Specific Gravity of water at 20 ˚C	0.9982
Mass of Ash [g]	0.308
Mass of Flask + Water at T [g]	48.66
Specific Gravity of Water at T	1.00
Specific Gravity of Soil	**3.28**
Dry Ash Density [kg/m^3]	3276.45

Pipe Series 2a	
Mass Tare [g]	18.776
Mass of Flask + Water + Ash [g]	48.721
Temperature of suspension (T) [˚C]	25.8
Time under vacuum [min]	Overnight
Mass of Tare + Dry Ash [g]	18.86
Specific Gravity of water at 20 ˚C	1.00
Mass of Ash [g]	0.09
Mass of Flask + Water at T [g]	48.65
Specific Gravity of Water at T	1.00
Specific Gravity of Soil	**4.64**
Dry Ash Density [kg/m^3]	4643.24

Pipe Series 2a	
Mass Tare [g]	18.626
Mass of Flask + Water + Ash [g]	48.756
Temperature of suspension (T) [˚C]	25.1
Time under vacuum [min]	Overnight
Mass of Tare + Dry Ash [g]	18.78
Specific Gravity of water at 20 ˚C	1.00
Mass of Ash [g]	0.15
Mass of Flask + Water at T [g]	48.65
Specific Gravity of Water at T	1.00
Specific Gravity of Soil	**3.00**
Dry Ash Density [kg/m^3]	2999.52

Pipe Series 3a	
Mass Tare [g]	18.754
Mass of Flask + Water + Ash [g]	48.851
Temperature of suspension (T) [˚C]	23.1
Time under vacuum [min]	Overnight
Mass of Tare + Dry Ash [g]	19.03
Specific Gravity of water at 20 ˚C	1.00
Mass of Ash [g]	0.28
Mass of Flask + Water at T [g]	48.66
Specific Gravity of Water at T	1.00
Specific Gravity of Soil	**3.28**
Dry Ash Density [kg/m^3]	3282.61

Pipe Series 3b	
Mass Tare [g]	18.576
Mass of Flask + Water + Ash [g]	48.854
Temperature of suspension (T) [˚C]	23.6
Time under vacuum [min]	Overnight
Mass of Tare + Dry Ash [g]	18.86
Specific Gravity of water at 20 ˚C	1.00
Mass of Ash [g]	0.28
Mass of Flask + Water at T [g]	48.66
Specific Gravity of Water at T	1.00
Specific Gravity of Soil	**3.32**
Dry Ash Density [kg/m^3]	3317.32

Pipe Series 4a	
Mass Tare [g]	18.659
Mass of Flask + Water + Ash [g]	49.082
Temperature of suspension (T) [˚C]	23.4
Time under vacuum [min]	Overnight
Mass of Tare + Dry Ash [g]	19.32
Specific Gravity of water at 20 ˚C	1.00
Mass of Ash [g]	0.67
Mass of Flask + Water at T [g]	48.66
Specific Gravity of Water at T	1.00
Specific Gravity of Soil	**2.76**
Dry Ash Density [kg/m^3]	2758.01

Pipe Series 4b	
Mass Tare [g]	18.624
Mass of Flask + Water + Ash [g]	49.104
Temperature of suspension (T) [˚C]	24.5
Time under vacuum [min]	Overnight
Mass of Tare + Dry Ash [g]	19.27
Specific Gravity of water at 20 ˚C	1.00
Mass of Ash [g]	0.65
Mass of Flask + Water at T [g]	48.66
Specific Gravity of Water at T	1.00
Specific Gravity of Soil	**3.21**
Dry Ash Density [kg/m^3]	3214.58

Pipe Series 5a	
Mass Tare [g]	18.65
Mass of Flask + Water + Ash [g]	48.951
Temperature of suspension (T) [˚C]	23
Time under vacuum [min]	Overnight
Mass of Tare + Dry Ash [g]	19.11
Specific Gravity of water at 20 ˚C	1.00
Mass of Ash [g]	0.46
Mass of Flask + Water at T [g]	48.66
Specific Gravity of Water at T	1.00
Specific Gravity of Soil	**2.75**
Dry Ash Density [kg/m^3]	2745.35

Pipe Series 5b	
Mass Tare [g]	18.694
Mass of Flask + Water + Ash [g]	48.927
Temperature of suspension (T) [˚C]	23.7
Time under vacuum [min]	Overnight
Mass of Tare + Dry Ash [g]	19.10
Specific Gravity of water at 20 ˚C	1.00
Mass of Ash [g]	0.41
Mass of Flask + Water at T [g]	48.66
Specific Gravity of Water at T	1.00
Specific Gravity of Soil	**2.99**
Dry Ash Density [kg/m^3]	2986.85

Pipe Series 6a	
Mass Tare [g]	18.198
Mass of Flask + Water + Ash [g]	72.882
Temperature of suspension (T) [˚C]	24.4
Time under vacuum [min]	Overnight
Mass of Tare + Dry Ash [g]	19.34
Specific Gravity of water at 20 ˚C	1.00
Mass of Ash [g]	1.14
Mass of Flask + Water at T [g]	72.08
Specific Gravity of Water at T	1.00
Specific Gravity of Soil	**3.35**
Dry Ash Density [kg/m^3]	3352.68

Pipe Series 6b	
Mass Tare [g]	18.68
Mass of Flask + Water + Ash [g]	49.068
Temperature of suspension (T) [˚C]	26
Time under vacuum [min]	Overnight
Mass of Tare + Dry Ash [g]	19.29
Specific Gravity of water at 20 ˚C	1.00
Mass of Ash [g]	0.61
Mass of Flask + Water at T [g]	48.65
Specific Gravity of Water at T	1.00
Specific Gravity of Soil	**3.15**
Dry Ash Density [kg/m^3]	3149.27

Pipe Series 7a	
Mass Tare [g]	18.661
Mass of Flask + Water + Ash [g]	48.845
Temperature of suspension (T) [˚C]	23.5
Time under vacuum [min]	Overnight
Mass of Tare + Dry Ash [g]	18.93
Specific Gravity of water at 20 ˚C	1.00
Mass of Ash [g]	0.26
Mass of Flask + Water at T [g]	48.66
Specific Gravity of Water at T	1.00
Specific Gravity of Soil	**3.44**
Dry Ash Density [kg/m^3]	3435.31

Pipe Series 7b	
Mass Tare [g]	18.77
Mass of Flask + Water + Ash [g]	48.857
Temperature of suspension (T) [˚C]	22.8
Time under vacuum [min]	Overnight
Mass of Tare + Dry Ash [g]	1.00
Specific Gravity of water at 20 ˚C	0.34
Mass of Ash [g]	48.66
Mass of Flask + Water at T [g]	1.00
Specific Gravity of Water at T	2.40
Specific Gravity of Soil	**2398.59**
Dry Ash Density [kg/m^3]	

Pipe Series 8a	
Mass Tare [g]	18.689
Mass of Flask + Water + Ash [g]	48.903
Temperature of suspension (T) [˚C]	24.3
Time under vacuum [min]	Overnight
Mass of Tare + Dry Ash [g]	19.05
Specific Gravity of water at 20 ˚C	1.00
Mass of Ash [g]	0.36
Mass of Flask + Water at T [g]	48.66
Specific Gravity of Water at T	1.00
Specific Gravity of Soil	**3.12**
Dry Ash Density [kg/m^3]	3115.33

Pipe Series 8b	
Mass Tare [g]	18.272
Mass of Flask + Water + Ash [g]	48.91
Temperature of suspension (T) [˚C]	23.2
Time under vacuum [min]	Overnight
Mass of Tare + Dry Ash [g]	18.68
Specific Gravity of water at 20 ˚C	1.00
Mass of Ash [g]	0.41
Mass of Flask + Water at T [g]	48.66
Specific Gravity of Water at T	1.00
Specific Gravity of Soil	**2.64**
Dry Ash Density [kg/m^3]	2641.69

iii. Pipe Ring 4

Pipe Series 1a	
Mass Tare [g]	18.193
Mass of Flask + Water + Ash [g]	48.709
Temperature of suspension (T) [˚C]	26.3
Time under vacuum [min]	3 Hours
Mass of Tare + Dry Ash [g]	18.283
Specific Gravity of water at 20 ˚C	0.9982
Mass of Ash [g]	0.09
Mass of Flask + Water at T [g]	48.65
Specific Gravity of Water at T	1.00
Specific Gravity of Soil	**2.79**
Dry Ash Density [kg/m^3]	2794.44

Pipe Series 1b	
Mass Tare [g]	18.684
Mass of Flask + Water + Ash [g]	48.731
Temperature of suspension (T) [˚C]	24.1
Time under vacuum [min]	3 Hours
Mass of Tare + Dry Ash [g]	18.823
Specific Gravity of water at 20 ˚C	0.9982
Mass of Ash [g]	0.139
Mass of Flask + Water at T [g]	48.66
Specific Gravity of Water at T	1.00
Specific Gravity of Soil	**2.14**
Dry Ash Density [kg/m^3]	2143.37

Pipe Series 2a	
Mass Tare [g]	18.754
Mass of Flask + Water + Ash [g]	48.718
Temperature of suspension (T) [˚C]	24.4
Time under vacuum [min]	3 Hours
Mass of Tare + Dry Ash [g]	18.83
Specific Gravity of water at 20 ˚C	1.00
Mass of Ash [g]	0.08
Mass of Flask + Water at T [g]	48.66
Specific Gravity of Water at T	1.00
Specific Gravity of Soil	**4.39**
Dry Ash Density [kg/m^3]	4389.84

Pipe Series 2a	
Mass Tare [g]	18.635
Mass of Flask + Water + Ash [g]	48.71
Temperature of suspension (T) [˚C]	23.4
Time under vacuum [min]	3 Hours
Mass of Tare + Dry Ash [g]	18.71
Specific Gravity of water at 20 ˚C	1.00
Mass of Ash [g]	0.07
Mass of Flask + Water at T [g]	48.66
Specific Gravity of Water at T	1.00
Specific Gravity of Soil	**3.37**
Dry Ash Density [kg/m^3]	3371.43

Pipe Series 3a	
Mass Tare [g]	18.624
Mass of Flask + Water + Ash [g]	48.709
Temperature of suspension (T) [˚C]	24
Time under vacuum [min]	3 Hours
Mass of Tare + Dry Ash [g]	18.72
Specific Gravity of water at 20 ˚C	1.00
Mass of Ash [g]	0.09
Mass of Flask + Water at T [g]	48.66
Specific Gravity of Water at T	1.00
Specific Gravity of Soil	**2.24**
Dry Ash Density [kg/m^3]	2237.50

Pipe Series 3b	
Mass Tare [g]	18.658
Mass of Flask + Water + Ash [g]	48.709
Temperature of suspension (T) [˚C]	25
Time under vacuum [min]	3 Hours
Mass of Tare + Dry Ash [g]	18.74
Specific Gravity of water at 20 ˚C	1.00
Mass of Ash [g]	0.09
Mass of Flask + Water at T [g]	48.65
Specific Gravity of Water at T	1.00
Specific Gravity of Soil	**2.70**
Dry Ash Density [kg/m^3]	2696.05

Pipe Series 4a	
Mass Tare [g]	18.713
Mass of Flask + Water + Ash [g]	48.873
Temperature of suspension (T) [˚C]	25.3
Time under vacuum [min]	3 Hours
Mass of Tare + Dry Ash [g]	19.01
Specific Gravity of water at 20 ˚C	1.00
Mass of Ash [g]	0.30
Mass of Flask + Water at T [g]	48.65
Specific Gravity of Water at T	1.00
Specific Gravity of Soil	**3.69**
Dry Ash Density [kg/m^3]	3694.47

Pipe Series 4b	
Mass Tare [g]	18.619
Mass of Flask + Water + Ash [g]	48.788
Temperature of suspension (T) [˚C]	24.5
Time under vacuum [min]	3 Hours
Mass of Tare + Dry Ash [g]	18.83
Specific Gravity of water at 20 ˚C	1.00
Mass of Ash [g]	0.21
Mass of Flask + Water at T [g]	48.66
Specific Gravity of Water at T	1.00
Specific Gravity of Soil	**2.69**
Dry Ash Density [kg/m^3]	2689.64

Pipe Series 5a	
Mass Tare [g]	18.675
Mass of Flask + Water + Ash [g]	48.79
Temperature of suspension (T) [˚C]	24.7
Time under vacuum [min]	3 Hours
Mass of Tare + Dry Ash [g]	18.86
Specific Gravity of water at 20 ˚C	1.00
Mass of Ash [g]	0.18
Mass of Flask + Water at T [g]	48.66
Specific Gravity of Water at T	1.00
Specific Gravity of Soil	**3.82**
Dry Ash Density [kg/m^3]	3822.43

Pipe Series 5b	
Mass Tare [g]	23.943
Mass of Flask + Water + Ash [g]	48.71
Temperature of suspension (T) [˚C]	23.4
Time under vacuum [min]	3 Hours
Mass of Tare + Dry Ash [g]	24.08
Specific Gravity of water at 20 ˚C	1.00
Mass of Ash [g]	0.14
Mass of Flask + Water at T [g]	48.66
Specific Gravity of Water at T	1.00
Specific Gravity of Soil	**1.59**
Dry Ash Density [kg/m^3]	1590.92

Pipe Series 6a	
Mass Tare [g]	18.568
Mass of Flask + Water + Ash [g]	48.737
Temperature of suspension (T) [˚C]	24
Time under vacuum [min]	3 Hours
Mass of Tare + Dry Ash [g]	18.69
Specific Gravity of water at 20 ˚C	1.00
Mass of Ash [g]	0.12
Mass of Flask + Water at T [g]	48.66
Specific Gravity of Water at T	1.00
Specific Gravity of Soil	**3.10**
Dry Ash Density [kg/m^3]	3104.64

Pipe Series 6b	
Mass Tare [g]	24.784
Mass of Flask + Water + Ash [g]	48.778
Temperature of suspension (T) [˚C]	25
Time under vacuum [min]	3 Hours
Mass of Tare + Dry Ash [g]	24.95
Specific Gravity of water at 20 ˚C	1.00
Mass of Ash [g]	0.17
Mass of Flask + Water at T [g]	48.65
Specific Gravity of Water at T	1.00
Specific Gravity of Soil	**3.80**
Dry Ash Density [kg/m^3]	3803.04

Pipe Series 7a	
Mass Tare [g]	18.659
Mass of Flask + Water + Ash [g]	48.844
Temperature of suspension (T) [˚C]	25
Time under vacuum [min]	3 Hours
Mass of Tare + Dry Ash [g]	18.94
Specific Gravity of water at 20 ˚C	1.00
Mass of Ash [g]	0.28
Mass of Flask + Water at T [g]	48.65
Specific Gravity of Water at T	1.00
Specific Gravity of Soil	**2.99**
Dry Ash Density [kg/m^3]	2990.40

Pipe Series 7b	
Mass Tare [g]	18.706
Mass of Flask + Water + Ash [g]	48.809
Temperature of suspension (T) [˚C]	24.7
Time under vacuum [min]	3 Hours
Mass of Tare + Dry Ash [g]	18.93
Specific Gravity of water at 20 ˚C	1.00
Mass of Ash [g]	0.22
Mass of Flask + Water at T [g]	48.66
Specific Gravity of Water at T	1.00
Specific Gravity of Soil	**3.20**
Dry Ash Density [kg/m^3]	3202.31

Pipe Series 8a	
Mass Tare [g]	18.268
Mass of Flask + Water + Ash [g]	48.774
Temperature of suspension (T) [˚C]	23.9
Time under vacuum [min]	3 Hours
Mass of Tare + Dry Ash [g]	18.46
Specific Gravity of water at 20 ˚C	1.00
Mass of Ash [g]	0.19
Mass of Flask + Water at T [g]	48.66
Specific Gravity of Water at T	1.00
Specific Gravity of Soil	**2.57**
Dry Ash Density [kg/m^3]	2573.63

Pipe Series 8b	
Mass Tare [g]	18.618
Mass of Flask + Water + Ash [g]	48.81
Temperature of suspension (T) [˚C]	25
Time under vacuum [min]	3 Hours
Mass of Tare + Dry Ash [g]	18.83
Specific Gravity of water at 20 ˚C	1.00
Mass of Ash [g]	0.21
Mass of Flask + Water at T [g]	48.65
Specific Gravity of Water at T	1.00
Specific Gravity of Soil	**3.63**
Dry Ash Density [kg/m^3]	3631.47

iv. Pipe Ring 5

Pipe Series 1a	
Mass Tare [g]	18.562
Mass of Flask + Water + Ash [g]	48.722
Temperature of suspension (T) [˚C]	23.4
Time under vacuum [min]	3 Hours
Mass of Tare + Dry Ash [g]	18.676
Specific Gravity of water at 20 ˚C	0.9982
Mass of Ash [g]	0.114
Mass of Flask + Water at T [g]	48.66
Specific Gravity of Water at T	1.00
Specific Gravity of Soil	**2.28**
Dry Ash Density [kg/m^3]	2281.35

Pipe Series 1b	
Mass Tare [g]	18.765
Mass of Flask + Water + Ash [g]	48.728
Temperature of suspension (T) [˚C]	23.8
Time under vacuum [min]	3 Hours
Mass of Tare + Dry Ash [g]	18.881
Specific Gravity of water at 20 ˚C	0.9982
Mass of Ash [g]	0.116
Mass of Flask + Water at T [g]	48.66
Specific Gravity of Water at T	1.00
Specific Gravity of Soil	**2.56**
Dry Ash Density [kg/m^3]	2557.47

Pipe Series 2a	
Mass Tare [g]	18.618
Mass of Flask + Water + Ash [g]	48.797
Temperature of suspension (T) [˚C]	23.9
Time under vacuum [min]	3 Hours
Mass of Tare + Dry Ash [g]	18.87
Specific Gravity of water at 20 ˚C	1.00
Mass of Ash [g]	0.25
Mass of Flask + Water at T [g]	48.66
Specific Gravity of Water at T	1.00
Specific Gravity of Soil	**2.29**
Dry Ash Density [kg/m^3]	2291.12

Pipe Series 2a	
Mass Tare [g]	18.669
Mass of Flask + Water + Ash [g]	48.8
Temperature of suspension (T) [˚C]	24
Time under vacuum [min]	3 Hours
Mass of Tare + Dry Ash [g]	18.89
Specific Gravity of water at 20 ˚C	1.00
Mass of Ash [g]	0.22
Mass of Flask + Water at T [g]	48.66
Specific Gravity of Water at T	1.00
Specific Gravity of Soil	**2.91**
Dry Ash Density [kg/m^3]	2905.08

Pipe Series 3a	
Mass Tare [g]	18.186
Mass of Flask + Water + Ash [g]	48.795
Temperature of suspension (T) [˚C]	24.1
Time under vacuum [min]	3 Hours
Mass of Tare + Dry Ash [g]	18.40
Specific Gravity of water at 20 ˚C	1.00
Mass of Ash [g]	0.22
Mass of Flask + Water at T [g]	48.66
Specific Gravity of Water at T	1.00
Specific Gravity of Soil	**2.73**
Dry Ash Density [kg/m^3]	2729.61

Pipe Series 3b	
Mass Tare [g]	18.652
Mass of Flask + Water + Ash [g]	48.803
Temperature of suspension (T) [˚C]	24.4
Time under vacuum [min]	3 Hours
Mass of Tare + Dry Ash [g]	18.87
Specific Gravity of water at 20 ˚C	1.00
Mass of Ash [g]	0.22
Mass of Flask + Water at T [g]	48.66
Specific Gravity of Water at T	1.00
Specific Gravity of Soil	**3.12**
Dry Ash Density [kg/m^3]	3118.02

Pipe Series 4a	
Mass Tare [g]	18.621
Mass of Flask + Water + Ash [g]	48.717
Temperature of suspension (T) [˚C]	23.9
Time under vacuum [min]	3 Hours
Mass of Tare + Dry Ash [g]	18.72
Specific Gravity of water at 20 ˚C	1.00
Mass of Ash [g]	0.09
Mass of Flask + Water at T [g]	48.66
Specific Gravity of Water at T	1.00
Specific Gravity of Soil	**2.75**
Dry Ash Density [kg/m^3]	2750.21

Pipe Series 4b	
Mass Tare [g]	18.635
Mass of Flask + Water + Ash [g]	48.715
Temperature of suspension (T) [˚C]	23.8
Time under vacuum [min]	3 Hours
Mass of Tare + Dry Ash [g]	18.73
Specific Gravity of water at 20 ˚C	1.00
Mass of Ash [g]	0.09
Mass of Flask + Water at T [g]	48.66
Specific Gravity of Water at T	1.00
Specific Gravity of Soil	**2.54**
Dry Ash Density [kg/m^3]	2543.47

Pipe Series 5a	
Mass Tare [g]	18.686
Mass of Flask + Water + Ash [g]	48.803
Temperature of suspension (T) [˚C]	24.5
Time under vacuum [min]	3 Hours
Mass of Tare + Dry Ash [g]	18.90
Specific Gravity of water at 20 ˚C	1.00
Mass of Ash [g]	0.21
Mass of Flask + Water at T [g]	48.66
Specific Gravity of Water at T	1.00
Specific Gravity of Soil	**3.22**
Dry Ash Density [kg/m^3]	3224.09

Pipe Series 5b	
Mass Tare [g]	18.612
Mass of Flask + Water + Ash [g]	48.792
Temperature of suspension (T) [˚C]	24.8
Time under vacuum [min]	3 Hours
Mass of Tare + Dry Ash [g]	18.83
Specific Gravity of water at 20 ˚C	1.00
Mass of Ash [g]	0.22
Mass of Flask + Water at T [g]	48.66
Specific Gravity of Water at T	1.00
Specific Gravity of Soil	**2.70**
Dry Ash Density [kg/m^3]	2698.22

Pipe Series 6a	
Mass Tare [g]	18.268
Mass of Flask + Water + Ash [g]	48.751
Temperature of suspension (T) [˚C]	24.5
Time under vacuum [min]	3 Hours
Mass of Tare + Dry Ash [g]	18.44
Specific Gravity of water at 20 ˚C	1.00
Mass of Ash [g]	0.17
Mass of Flask + Water at T [g]	48.66
Specific Gravity of Water at T	1.00
Specific Gravity of Soil	**2.32**
Dry Ash Density [kg/m^3]	2317.15

Pipe Series 6b	
Mass Tare [g]	18.571
Mass of Flask + Water + Ash [g]	48.766
Temperature of suspension (T) [˚C]	23.1
Time under vacuum [min]	3 Hours
Mass of Tare + Dry Ash [g]	18.74
Specific Gravity of water at 20 ˚C	1.00
Mass of Ash [g]	0.17
Mass of Flask + Water at T [g]	48.66
Specific Gravity of Water at T	1.00
Specific Gravity of Soil	**2.84**
Dry Ash Density [kg/m^3]	2844.12

Pipe Series 7a	
Mass Tare [g]	24.785
Mass of Flask + Water + Ash [g]	48.775
Temperature of suspension (T) [˚C]	24.6
Time under vacuum [min]	3 Hours
Mass of Tare + Dry Ash [g]	24.95
Specific Gravity of water at 20 ˚C	1.00
Mass of Ash [g]	0.17
Mass of Flask + Water at T [g]	48.66
Specific Gravity of Water at T	1.00
Specific Gravity of Soil	**3.39**
Dry Ash Density [kg/m^3]	3391.15

Pipe Series 7b	
Mass Tare [g]	18.646
Mass of Flask + Water + Ash [g]	48.778
Temperature of suspension (T) [˚C]	24.4
Time under vacuum [min]	3 Hours
Mass of Tare + Dry Ash [g]	18.83
Specific Gravity of water at 20 ˚C	1.00
Mass of Ash [g]	0.18
Mass of Flask + Water at T [g]	48.66
Specific Gravity of Water at T	1.00
Specific Gravity of Soil	**3.05**
Dry Ash Density [kg/m^3]	3054.09

Pipe Series 8a	
Mass Tare [g]	18.631
Mass of Flask + Water + Ash [g]	48.772
Temperature of suspension (T) [˚C]	24.1
Time under vacuum [min]	3 Hours
Mass of Tare + Dry Ash [g]	18.81
Specific Gravity of water at 20 ˚C	1.00
Mass of Ash [g]	0.18
Mass of Flask + Water at T [g]	48.66
Specific Gravity of Water at T	1.00
Specific Gravity of Soil	**2.89**
Dry Ash Density [kg/m^3]	2892.49

Pipe Series 8b	
Mass Tare [g]	23.93
Mass of Flask + Water + Ash [g]	48.795
Temperature of suspension (T) [˚C]	24.7
Time under vacuum [min]	3 Hours
Mass of Tare + Dry Ash [g]	24.15
Specific Gravity of water at 20 ˚C	1.00
Mass of Ash [g]	0.22
Mass of Flask + Water at T [g]	48.66
Specific Gravity of Water at T	1.00
Specific Gravity of Soil	**2.71**
Dry Ash Density [kg/m^3]	2706.68

c. Ash density data.

i. Pipe Ring 2

Pipe Series 1a	
Mass Tare [g]	18.627
Mass of Flask + Water + Ash [g]	72.192
Temperature of suspension (T) [˚C]	25.2
Time under vacuum [min]	Overnight
Mass of Tare + Dry Ash [g]	18.823
Specific Gravity of water at 20 ˚C	0.9982
Mass of Ash [g]	0.196
Mass of Flask + Water at T [g]	72.08
Specific Gravity of Water at T	1.00
Specific Gravity of Soil	**2.39**
Dry Ash Density [kg/m^3]	2388.54

Pipe Series 1b	
Mass Tare [g]	18.647
Mass of Flask + Water + Ash [g]	72.197
Temperature of suspension (T) [˚C]	24.4
Time under vacuum [min]	Overnight
Mass of Tare + Dry Ash [g]	18.859
Specific Gravity of water at 20 ˚C	0.9982
Mass of Ash [g]	0.212
Mass of Flask + Water at T [g]	72.08
Specific Gravity of Water at T	1.00
Specific Gravity of Soil	**2.22**
Dry Ash Density [kg/m^3]	2222.72

Pipe Series 2a	
Mass Tare [g]	18.776
Mass of Flask + Water + Ash [g]	72.154
Temperature of suspension (T) [˚C]	25.1
Time under vacuum [min]	Overnight
Mass of Tare + Dry Ash [g]	18.90
Specific Gravity of water at 20 ˚C	1.00
Mass of Ash [g]	0.12
Mass of Flask + Water at T [g]	72.08
Specific Gravity of Water at T	1.00
Specific Gravity of Soil	**2.71**
Dry Ash Density [kg/m^3]	2708.70

Pipe Series 3a	
Mass Tare [g]	18.658
Mass of Flask + Water + Ash [g]	72.246
Temperature of suspension (T) [˚C]	24.9
Time under vacuum [min]	Overnight
Mass of Tare + Dry Ash [g]	19.02
Specific Gravity of water at 20 ˚C	1.00
Mass of Ash [g]	0.37
Mass of Flask + Water at T [g]	72.08
Specific Gravity of Water at T	1.00
Specific Gravity of Soil	**1.84**
Dry Ash Density [kg/m^3]	1838.72

Pipe Series 3b	
Mass Tare [g]	18.69
Mass of Flask + Water + Ash [g]	72.263
Temperature of suspension (T) [˚C]	25.7
Time under vacuum [min]	Overnight
Mass of Tare + Dry Ash [g]	19.08
Specific Gravity of water at 20 ˚C	1.00
Mass of Ash [g]	0.39
Mass of Flask + Water at T [g]	72.08
Specific Gravity of Water at T	1.00
Specific Gravity of Soil	**1.92**
Dry Ash Density [kg/m^3]	1918.28

Pipe Series 4a	
Mass Tare [g]	18.624
Mass of Flask + Water + Ash [g]	72.264
Temperature of suspension (T) [˚C]	24.4
Time under vacuum [min]	Overnight
Mass of Tare + Dry Ash [g]	18.98
Specific Gravity of water at 20 ˚C	1.00
Mass of Ash [g]	0.36
Mass of Flask + Water at T [g]	72.08
Specific Gravity of Water at T	1.00
Specific Gravity of Soil	**2.07**
Dry Ash Density [kg/m^3]	2070.52

Pipe Series 4b	
Mass Tare [g]	18.623
Mass of Flask + Water + Ash [g]	72.441
Temperature of suspension (T) [˚C]	24
Time under vacuum [min]	Overnight
Mass of Tare + Dry Ash [g]	19.22
Specific Gravity of water at 20 ˚C	1.00
Mass of Ash [g]	0.60
Mass of Flask + Water at T [g]	72.08
Specific Gravity of Water at T	1.00
Specific Gravity of Soil	**2.51**
Dry Ash Density [kg/m^3]	2511.91

Pipe Series 5a	
Mass Tare [g]	18.274
Mass of Flask + Water + Ash [g]	72.672
Temperature of suspension (T) [˚C]	25.3
Time under vacuum [min]	Overnight
Mass of Tare + Dry Ash [g]	19.34
Specific Gravity of water at 20 ˚C	1.00
Mass of Ash [g]	1.07
Mass of Flask + Water at T [g]	72.08
Specific Gravity of Water at T	1.00
Specific Gravity of Soil	**2.25**
Dry Ash Density [kg/m^3]	2254.64

Pipe Series 5b	
Mass Tare [g]	18.661
Mass of Flask + Water + Ash [g]	72.41
Temperature of suspension (T) [˚C]	25.8
Time under vacuum [min]	Overnight
Mass of Tare + Dry Ash [g]	19.27
Specific Gravity of water at 20 ˚C	1.00
Mass of Ash [g]	0.61
Mass of Flask + Water at T [g]	72.08
Specific Gravity of Water at T	1.00
Specific Gravity of Soil	**2.22**
Dry Ash Density [kg/m^3]	2218.58

Pipe Series 6a	
Mass Tare [g]	18.679
Mass of Flask + Water + Ash [g]	72.489
Temperature of suspension (T) [˚C]	24.2
Time under vacuum [min]	Overnight
Mass of Tare + Dry Ash [g]	19.37
Specific Gravity of water at 20 ˚C	1.00
Mass of Ash [g]	0.69
Mass of Flask + Water at T [g]	72.08
Specific Gravity of Water at T	1.00
Specific Gravity of Soil	**2.47**
Dry Ash Density [kg/m^3]	2466.46

Pipe Series 6b	
Mass Tare [g]	18.195
Mass of Flask + Water + Ash [g]	72.269
Temperature of suspension (T) [˚C]	26.5
Time under vacuum [min]	Overnight
Mass of Tare + Dry Ash [g]	18.52
Specific Gravity of water at 20 ˚C	1.00
Mass of Ash [g]	0.33
Mass of Flask + Water at T [g]	72.07
Specific Gravity of Water at T	1.00
Specific Gravity of Soil	**2.47**
Dry Ash Density [kg/m^3]	2469.18

Pipe Series 7a	
Mass Tare [g]	18.754
Mass of Flask + Water + Ash [g]	72.601
Temperature of suspension (T) [˚C]	25.3
Time under vacuum [min]	Overnight
Mass of Tare + Dry Ash [g]	19.63
Specific Gravity of water at 20 ˚C	1.00
Mass of Ash [g]	0.88
Mass of Flask + Water at T [g]	72.08
Specific Gravity of Water at T	1.00
Specific Gravity of Soil	**2.47**
Dry Ash Density [kg/m^3]	2468.38

Pipe Series 7b	
Mass Tare [g]	18.711
Mass of Flask + Water + Ash [g]	72.651
Temperature of suspension (T) [˚C]	25.8
Time under vacuum [min]	Overnight
Mass of Tare + Dry Ash [g]	19.77
Specific Gravity of water at 20 ˚C	1.00
Mass of Ash [g]	1.06
Mass of Flask + Water at T [g]	72.08
Specific Gravity of Water at T	1.00
Specific Gravity of Soil	**2.18**
Dry Ash Density [kg/m^3]	2184.04

Pipe Series 8a	
Mass Tare [g]	18.569
Mass of Flask + Water + Ash [g]	72.53
Temperature of suspension (T) [˚C]	25
Time under vacuum [min]	Overnight
Mass of Tare + Dry Ash [g]	19.37
Specific Gravity of water at 20 ˚C	1.00
Mass of Ash [g]	0.80
Mass of Flask + Water at T [g]	72.08
Specific Gravity of Water at T	1.00
Specific Gravity of Soil	**2.30**
Dry Ash Density [kg/m^3]	2303.91

Pipe Series 8b	
Mass Tare [g]	18.694
Mass of Flask + Water + Ash [g]	72.577
Temperature of suspension (T) [˚C]	25.2
Time under vacuum [min]	Overnight
Mass of Tare + Dry Ash [g]	19.53
Specific Gravity of water at 20 ˚C	1.00
Mass of Ash [g]	0.83
Mass of Flask + Water at T [g]	72.08
Specific Gravity of Water at T	1.00
Specific Gravity of Soil	**2.49**
Dry Ash Density [kg/m^3]	2491.34

ii. Pipe Ring 3

Pipe Series 1a	
Mass Tare [g]	18.622
Mass of Flask + Water + Ash [g]	48.754
Temperature of suspension (T) [˚C]	23.3
Time under vacuum [min]	Overnight
Mass of Tare + Dry Ash [g]	18.775
Specific Gravity of water at 20 ˚C	0.9982
Mass of Ash [g]	0.153
Mass of Flask + Water at T [g]	48.66
Specific Gravity of Water at T	1.00
Specific Gravity of Soil	**2.68**
Dry Ash Density [kg/m^3]	2678.94

Pipe Series 1b	
Mass Tare [g]	18.705
Mass of Flask + Water + Ash [g]	48.844
Temperature of suspension (T) [˚C]	23.2
Time under vacuum [min]	Overnight
Mass of Tare + Dry Ash [g]	18.98
Specific Gravity of water at 20 ˚C	0.9982
Mass of Ash [g]	0.275
Mass of Flask + Water at T [g]	48.66
Specific Gravity of Water at T	1.00
Specific Gravity of Soil	**3.08**
Dry Ash Density [kg/m^3]	3080.72

Pipe Series 2a	
Mass Tare [g]	18.769
Mass of Flask + Water + Ash [g]	48.694
Temperature of suspension (T) [˚C]	25.2
Time under vacuum [min]	Overnight
Mass of Tare + Dry Ash [g]	18.84
Specific Gravity of water at 20 ˚C	1.00
Mass of Ash [g]	0.07
Mass of Flask + Water at T [g]	48.65
Specific Gravity of Water at T	1.00
Specific Gravity of Soil	**2.19**
Dry Ash Density [kg/m^3]	2185.45

Pipe Series 2b	
Mass Tare [g]	18.619
Mass of Flask + Water + Ash [g]	48.741
Temperature of suspension (T) [˚C]	25.2
Time under vacuum [min]	Overnight
Mass of Tare + Dry Ash [g]	18.75
Specific Gravity of water at 20 ˚C	1.00
Mass of Ash [g]	0.14
Mass of Flask + Water at T [g]	48.65
Specific Gravity of Water at T	1.00
Specific Gravity of Soil	**2.79**
Dry Ash Density [kg/m^3]	2788.07

Pipe Series 3a	
Mass Tare [g]	18.748
Mass of Flask + Water + Ash [g]	48.761
Temperature of suspension (T) [˚C]	25.2
Time under vacuum [min]	Overnight
Mass of Tare + Dry Ash [g]	19.00
Specific Gravity of water at 20 ˚C	1.00
Mass of Ash [g]	0.25
Mass of Flask + Water at T [g]	48.65
Specific Gravity of Water at T	1.00
Specific Gravity of Soil	**1.76**
Dry Ash Density [kg/m^3]	1757.63

Pipe Series 3b	
Mass Tare [g]	18.566
Mass of Flask + Water + Ash [g]	48.776
Temperature of suspension (T) [˚C]	24.4
Time under vacuum [min]	Overnight
Mass of Tare + Dry Ash [g]	18.82
Specific Gravity of water at 20 ˚C	1.00
Mass of Ash [g]	0.26
Mass of Flask + Water at T [g]	48.66
Specific Gravity of Water at T	1.00
Specific Gravity of Soil	**1.88**
Dry Ash Density [kg/m^3]	1884.14

Pipe Series 4a	
Mass Tare [g]	18.651
Mass of Flask + Water + Ash [g]	49.004
Temperature of suspension (T) [˚C]	25
Time under vacuum [min]	Overnight
Mass of Tare + Dry Ash [g]	19.26
Specific Gravity of water at 20 ˚C	1.00
Mass of Ash [g]	0.61
Mass of Flask + Water at T [g]	48.65
Specific Gravity of Water at T	1.00
Specific Gravity of Soil	**2.34**
Dry Ash Density [kg/m^3]	2335.73

Pipe Series 4b	
Mass Tare [g]	18.61
Mass of Flask + Water + Ash [g]	49.002
Temperature of suspension (T) [˚C]	24.8
Time under vacuum [min]	Overnight
Mass of Tare + Dry Ash [g]	19.21
Specific Gravity of water at 20 ˚C	1.00
Mass of Ash [g]	0.59
Mass of Flask + Water at T [g]	48.66
Specific Gravity of Water at T	1.00
Specific Gravity of Soil	**2.39**
Dry Ash Density [kg/m^3]	2393.34

Pipe Series 5a	
Mass Tare [g]	18.644
Mass of Flask + Water + Ash [g]	48.889
Temperature of suspension (T) [˚C]	23.5
Time under vacuum [min]	Overnight
Mass of Tare + Dry Ash [g]	19.07
Specific Gravity of water at 20 ˚C	1.00
Mass of Ash [g]	0.42
Mass of Flask + Water at T [g]	48.66
Specific Gravity of Water at T	1.00
Specific Gravity of Soil	**2.22**
Dry Ash Density [kg/m^3]	2216.52

Pipe Series 5b	
Mass Tare [g]	18.687
Mass of Flask + Water + Ash [g]	48.844
Temperature of suspension (T) [˚C]	25
Time under vacuum [min]	Overnight
Mass of Tare + Dry Ash [g]	19.05
Specific Gravity of water at 20 ˚C	1.00
Mass of Ash [g]	0.36
Mass of Flask + Water at T [g]	48.65
Specific Gravity of Water at T	1.00
Specific Gravity of Soil	**2.10**
Dry Ash Density [kg/m^3]	2098.13

Pipe Series 6a	
Mass Tare [g]	18.188
Mass of Flask + Water + Ash [g]	49.221
Temperature of suspension (T) [˚C]	26
Time under vacuum [min]	Overnight
Mass of Tare + Dry Ash [g]	19.22
Specific Gravity of water at 20 ˚C	1.00
Mass of Ash [g]	1.03
Mass of Flask + Water at T [g]	48.65
Specific Gravity of Water at T	1.00
Specific Gravity of Soil	**2.24**
Dry Ash Density [kg/m^3]	2236.01

Pipe Series 6b	
Mass Tare [g]	18.671
Mass of Flask + Water + Ash [g]	48.956
Temperature of suspension (T) [˚C]	26.2
Time under vacuum [min]	Overnight
Mass of Tare + Dry Ash [g]	19.22
Specific Gravity of water at 20 ˚C	1.00
Mass of Ash [g]	0.55
Mass of Flask + Water at T [g]	48.65
Specific Gravity of Water at T	1.00
Specific Gravity of Soil	**2.23**
Dry Ash Density [kg/m^3]	2232.24

Pipe Series 7a	
Mass Tare [g]	18.655
Mass of Flask + Water + Ash [g]	48.777
Temperature of suspension (T) [˚C]	24.7
Time under vacuum [min]	Overnight
Mass of Tare + Dry Ash [g]	18.89
Specific Gravity of water at 20 ˚C	1.00
Mass of Ash [g]	0.23
Mass of Flask + Water at T [g]	48.66
Specific Gravity of Water at T	1.00
Specific Gravity of Soil	**2.08**
Dry Ash Density [kg/m^3]	2076.62

Pipe Series 7b	
Mass Tare [g]	18.764
Mass of Flask + Water + Ash [g]	48.85
Temperature of suspension (T) [˚C]	24
Time under vacuum [min]	Overnight
Mass of Tare + Dry Ash [g]	19.07
Specific Gravity of water at 20 ˚C	1.00
Mass of Ash [g]	0.31
Mass of Flask + Water at T [g]	48.66
Specific Gravity of Water at T	1.00
Specific Gravity of Soil	**2.68**
Dry Ash Density [kg/m^3]	2676.47

Pipe Series 8a	
Mass Tare [g]	18.678
Mass of Flask + Water + Ash [g]	48.823
Temperature of suspension (T) [˚C]	24.2
Time under vacuum [min]	Overnight
Mass of Tare + Dry Ash [g]	19.01
Specific Gravity of water at 20 ˚C	1.00
Mass of Ash [g]	0.33
Mass of Flask + Water at T [g]	48.66
Specific Gravity of Water at T	1.00
Specific Gravity of Soil	**2.03**
Dry Ash Density [kg/m^3]	2027.75

Pipe Series 8b	
Mass Tare [g]	18.266
Mass of Flask + Water + Ash [g]	48.869
Temperature of suspension (T) [˚C]	24.7
Time under vacuum [min]	Overnight
Mass of Tare + Dry Ash [g]	18.63
Specific Gravity of water at 20 ˚C	1.00
Mass of Ash [g]	0.37
Mass of Flask + Water at T [g]	48.66
Specific Gravity of Water at T	1.00
Specific Gravity of Soil	**2.41**
Dry Ash Density [kg/m^3]	2405.67

iii. Pipe Ring 4

Pipe Series 1a	
Mass Tare [g]	18.187
Mass of Flask + Water + Ash [g]	48.707
Temperature of suspension (T) [˚C]	25.1
Time under vacuum [min]	1 Hour
Mass of Tare + Dry Ash [g]	18.262
Specific Gravity of water at 20 ˚C	0.9982
Mass of Ash [g]	0.075
Mass of Flask + Water at T [g]	48.65
Specific Gravity of Water at T	1.00
Specific Gravity of Soil	**3.31**
Dry Ash Density [kg/m^3]	3312.40

Pipe Series 1b	
Mass Tare [g]	18.684
Mass of Flask + Water + Ash [g]	48.731
Temperature of suspension (T) [˚C]	25.1
Time under vacuum [min]	1 Hour
Mass of Tare + Dry Ash [g]	18.808
Specific Gravity of water at 20 ˚C	0.9982
Mass of Ash [g]	0.124
Mass of Flask + Water at T [g]	48.65
Specific Gravity of Water at T	1.00
Specific Gravity of Soil	**2.60**
Dry Ash Density [kg/m^3]	2601.14

Pipe Series 2a	
Mass Tare [g]	18.747
Mass of Flask + Water + Ash [g]	48.699
Temperature of suspension (T) [˚C]	26.2
Time under vacuum [min]	3 Hours
Mass of Tare + Dry Ash [g]	18.82
Specific Gravity of water at 20 ˚C	1.00
Mass of Ash [g]	0.07
Mass of Flask + Water at T [g]	48.65
Specific Gravity of Water at T	1.00
Specific Gravity of Soil	**2.73**
Dry Ash Density [kg/m^3]	2725.04

Pipe Series 2b	
Mass Tare [g]	18.63
Mass of Flask + Water + Ash [g]	48.704
Temperature of suspension (T) [˚C]	25.2
Time under vacuum [min]	4 Hours
Mass of Tare + Dry Ash [g]	18.69
Specific Gravity of water at 20 ˚C	1.00
Mass of Ash [g]	0.06
Mass of Flask + Water at T [g]	48.65
Specific Gravity of Water at T	1.00
Specific Gravity of Soil	**4.45**
Dry Ash Density [kg/m^3]	4450.58

Pipe Series 3a	
Mass Tare [g]	18.62
Mass of Flask + Water + Ash [g]	48.701
Temperature of suspension (T) [˚C]	24.5
Time under vacuum [min]	3 Hours
Mass of Tare + Dry Ash [g]	18.71
Specific Gravity of water at 20 ˚C	1.00
Mass of Ash [g]	0.09
Mass of Flask + Water at T [g]	48.66
Specific Gravity of Water at T	1.00
Specific Gravity of Soil	**1.96**
Dry Ash Density [kg/m^3]	1955.54

Pipe Series 3b	
Mass Tare [g]	18.647
Mass of Flask + Water + Ash [g]	48.719
Temperature of suspension (T) [˚C]	24.3
Time under vacuum [min]	3 Hours
Mass of Tare + Dry Ash [g]	18.73
Specific Gravity of water at 20 ˚C	1.00
Mass of Ash [g]	0.09
Mass of Flask + Water at T [g]	48.66
Specific Gravity of Water at T	1.00
Specific Gravity of Soil	**3.67**
Dry Ash Density [kg/m^3]	3670.50

Pipe Series 4a	
Mass Tare [g]	18.706
Mass of Flask + Water + Ash [g]	48.804
Temperature of suspension (T) [˚C]	25.8
Time under vacuum [min]	1 Hour
Mass of Tare + Dry Ash [g]	18.98
Specific Gravity of water at 20 ˚C	1.00
Mass of Ash [g]	0.27
Mass of Flask + Water at T [g]	48.65
Specific Gravity of Water at T	1.00
Specific Gravity of Soil	**2.26**
Dry Ash Density [kg/m^3]	2260.74

Pipe Series 4b	
Mass Tare [g]	18.613
Mass of Flask + Water + Ash [g]	48.775
Temperature of suspension (T) [˚C]	25.9
Time under vacuum [min]	1 Hour
Mass of Tare + Dry Ash [g]	18.79
Specific Gravity of water at 20 ˚C	1.00
Mass of Ash [g]	0.18
Mass of Flask + Water at T [g]	48.65
Specific Gravity of Water at T	1.00
Specific Gravity of Soil	**3.17**
Dry Ash Density [kg/m^3]	3168.64

Pipe Series 5a	
Mass Tare [g]	18.665
Mass of Flask + Water + Ash [g]	48.779
Temperature of suspension (T) [˚C]	24.6
Time under vacuum [min]	3 Hours
Mass of Tare + Dry Ash [g]	18.85
Specific Gravity of water at 20 ˚C	1.00
Mass of Ash [g]	0.18
Mass of Flask + Water at T [g]	48.66
Specific Gravity of Water at T	1.00
Specific Gravity of Soil	**3.09**
Dry Ash Density [kg/m^3]	3092.87

Pipe Series 5b	
Mass Tare [g]	23.928
Mass of Flask + Water + Ash [g]	48.734
Temperature of suspension (T) [˚C]	24.5
Time under vacuum [min]	4 Hours
Mass of Tare + Dry Ash [g]	24.05
Specific Gravity of water at 20 ˚C	1.00
Mass of Ash [g]	0.12
Mass of Flask + Water at T [g]	48.66
Specific Gravity of Water at T	1.00
Specific Gravity of Soil	**2.90**
Dry Ash Density [kg/m^3]	2899.63

Pipe Series 6a	
Mass Tare [g]	18.557
Mass of Flask + Water + Ash [g]	48.721
Temperature of suspension (T) [˚C]	25.4
Time under vacuum [min]	4 Hours
Mass of Tare + Dry Ash [g]	18.66
Specific Gravity of water at 20 ˚C	1.00
Mass of Ash [g]	0.10
Mass of Flask + Water at T [g]	48.65
Specific Gravity of Water at T	1.00
Specific Gravity of Soil	**3.04**
Dry Ash Density [kg/m^3]	3041.46

Pipe Series 6b	
Mass Tare [g]	24.78
Mass of Flask + Water + Ash [g]	48.755
Temperature of suspension (T) [˚C]	25
Time under vacuum [min]	4 Hours
Mass of Tare + Dry Ash [g]	24.93
Specific Gravity of water at 20 ˚C	1.00
Mass of Ash [g]	0.15
Mass of Flask + Water at T [g]	48.65
Specific Gravity of Water at T	1.00
Specific Gravity of Soil	**3.05**
Dry Ash Density [kg/m^3]	3045.92

Pipe Series 7a	
Mass Tare [g]	18.654
Mass of Flask + Water + Ash [g]	48.792
Temperature of suspension (T) [˚C]	24.8
Time under vacuum [min]	3 Hours
Mass of Tare + Dry Ash [g]	18.91
Specific Gravity of water at 20 ˚C	1.00
Mass of Ash [g]	0.25
Mass of Flask + Water at T [g]	48.66
Specific Gravity of Water at T	1.00
Specific Gravity of Soil	**2.17**
Dry Ash Density [kg/m^3]	2172.37

Pipe Series 7b	
Mass Tare [g]	18.7
Mass of Flask + Water + Ash [g]	48.762
Temperature of suspension (T) [˚C]	24.7
Time under vacuum [min]	3 Hours
Mass of Tare + Dry Ash [g]	18.90
Specific Gravity of water at 20 ˚C	1.00
Mass of Ash [g]	0.20
Mass of Flask + Water at T [g]	48.66
Specific Gravity of Water at T	1.00
Specific Gravity of Soil	**2.11**
Dry Ash Density [kg/m^3]	2111.54

Pipe Series 8a	
Mass Tare [g]	18.263
Mass of Flask + Water + Ash [g]	48.711
Temperature of suspension (T) [˚C]	24.3
Time under vacuum [min]	3 Hours
Mass of Tare + Dry Ash [g]	18.44
Specific Gravity of water at 20 ˚C	1.00
Mass of Ash [g]	0.17
Mass of Flask + Water at T [g]	48.66
Specific Gravity of Water at T	1.00
Specific Gravity of Soil	**1.46**
Dry Ash Density [kg/m^3]	1455.78

Pipe Series 8b	
Mass Tare [g]	18.614
Mass of Flask + Water + Ash [g]	48.779
Temperature of suspension (T) [˚C]	24.2
Time under vacuum [min]	3 Hours
Mass of Tare + Dry Ash [g]	18.81
Specific Gravity of water at 20 ˚C	1.00
Mass of Ash [g]	0.19
Mass of Flask + Water at T [g]	48.66
Specific Gravity of Water at T	1.00
Specific Gravity of Soil	**2.76**
Dry Ash Density [kg/m^3]	2755.91

iv. Pipe Ring 5

Pipe Series 1a	
Mass Tare [g]	18.557
Mass of Flask + Water + Ash [g]	48.722
Temperature of suspension (T) [˚C]	25.3
Time under vacuum [min]	2 Hours
Mass of Tare + Dry Ash [g]	18.67
Specific Gravity of water at 20 ˚C	0.9982
Mass of Ash [g]	0.113
Mass of Flask + Water at T [g]	48.65
Specific Gravity of Water at T	1.00
Specific Gravity of Soil	**2.50**
Dry Ash Density [kg/m^3]	2502.29

Pipe Series 1b	
Mass Tare [g]	18.756
Mass of Flask + Water + Ash [g]	48.736
Temperature of suspension (T) [˚C]	26.3
Time under vacuum [min]	2 Hours
Mass of Tare + Dry Ash [g]	18.871
Specific Gravity of water at 20 ˚C	0.9982
Mass of Ash [g]	0.115
Mass of Flask + Water at T [g]	48.65
Specific Gravity of Water at T	1.00
Specific Gravity of Soil	**3.81**
Dry Ash Density [kg/m^3]	3807.46

Pipe Series 2a	
Mass Tare [g]	18.612
Mass of Flask + Water + Ash [g]	48.808
Temperature of suspension (T) [˚C]	25.1
Time under vacuum [min]	2 Hours
Mass of Tare + Dry Ash [g]	18.84
Specific Gravity of water at 20 ˚C	1.00
Mass of Ash [g]	0.22
Mass of Flask + Water at T [g]	48.65
Specific Gravity of Water at T	1.00
Specific Gravity of Soil	**3.17**
Dry Ash Density [kg/m^3]	3168.40

Pipe Series 2b	
Mass Tare [g]	18.661
Mass of Flask + Water + Ash [g]	48.789
Temperature of suspension (T) [˚C]	25.7
Time under vacuum [min]	2 Hours
Mass of Tare + Dry Ash [g]	18.86
Specific Gravity of water at 20 ˚C	1.00
Mass of Ash [g]	0.20
Mass of Flask + Water at T [g]	48.65
Specific Gravity of Water at T	1.00
Specific Gravity of Soil	**3.15**
Dry Ash Density [kg/m^3]	3154.43

Pipe Series 3a	
Mass Tare [g]	18.18
Mass of Flask + Water + Ash [g]	48.795
Temperature of suspension (T) [˚C]	25
Time under vacuum [min]	2 Hours
Mass of Tare + Dry Ash [g]	18.39
Specific Gravity of water at 20 ˚C	1.00
Mass of Ash [g]	0.21
Mass of Flask + Water at T [g]	48.65
Specific Gravity of Water at T	1.00
Specific Gravity of Soil	**3.09**
Dry Ash Density [kg/m^3]	3092.39

Pipe Series 3b	
Mass Tare [g]	18.65
Mass of Flask + Water + Ash [g]	48.779
Temperature of suspension (T) [˚C]	23.8
Time under vacuum [min]	2 Hours
Mass of Tare + Dry Ash [g]	18.85
Specific Gravity of water at 20 ˚C	1.00
Mass of Ash [g]	0.20
Mass of Flask + Water at T [g]	48.66
Specific Gravity of Water at T	1.00
Specific Gravity of Soil	**2.57**
Dry Ash Density [kg/m^3]	2571.57

Pipe Series 4a	
Mass Tare [g]	18.616
Mass of Flask + Water + Ash [g]	48.706
Temperature of suspension (T) [˚C]	25.6
Time under vacuum [min]	2 Hours
Mass of Tare + Dry Ash [g]	18.71
Specific Gravity of water at 20 ˚C	1.00
Mass of Ash [g]	0.09
Mass of Flask + Water at T [g]	48.65
Specific Gravity of Water at T	1.00
Specific Gravity of Soil	**2.45**
Dry Ash Density [kg/m^3]	2449.45

Pipe Series 4b	
Mass Tare [g]	18.632
Mass of Flask + Water + Ash [g]	48.703
Temperature of suspension (T) [˚C]	24.9
Time under vacuum [min]	2 Hours
Mass of Tare + Dry Ash [g]	18.72
Specific Gravity of water at 20 ˚C	1.00
Mass of Ash [g]	0.09
Mass of Flask + Water at T [g]	48.66
Specific Gravity of Water at T	1.00
Specific Gravity of Soil	**2.25**
Dry Ash Density [kg/m^3]	2254.57

Pipe Series 5a	
Mass Tare [g]	18.681
Mass of Flask + Water + Ash [g]	48.791
Temperature of suspension (T) [˚C]	25.3
Time under vacuum [min]	2 Hours
Mass of Tare + Dry Ash [g]	18.88
Specific Gravity of water at 20 ˚C	1.00
Mass of Ash [g]	0.20
Mass of Flask + Water at T [g]	48.65
Specific Gravity of Water at T	1.00
Specific Gravity of Soil	**3.35**
Dry Ash Density [kg/m^3]	3351.99

Pipe Series 5b	
Mass Tare [g]	18.606
Mass of Flask + Water + Ash [g]	48.761
Temperature of suspension (T) [˚C]	25.1
Time under vacuum [min]	2 Hours
Mass of Tare + Dry Ash [g]	18.80
Specific Gravity of water at 20 ˚C	1.00
Mass of Ash [g]	0.19
Mass of Flask + Water at T [g]	48.65
Specific Gravity of Water at T	1.00
Specific Gravity of Soil	**2.23**
Dry Ash Density [kg/m^3]	2225.64

Pipe Series 6a	
Mass Tare [g]	18.261
Mass of Flask + Water + Ash [g]	48.742
Temperature of suspension (T) [˚C]	24.5
Time under vacuum [min]	2 Hours
Mass of Tare + Dry Ash [g]	18.41
Specific Gravity of water at 20 ˚C	1.00
Mass of Ash [g]	0.15
Mass of Flask + Water at T [g]	48.66
Specific Gravity of Water at T	1.00
Specific Gravity of Soil	**2.28**
Dry Ash Density [kg/m^3]	2281.33

Pipe Series 6b	
Mass Tare [g]	18.567
Mass of Flask + Water + Ash [g]	48.75
Temperature of suspension (T) [˚C]	25.5
Time under vacuum [min]	2 Hours
Mass of Tare + Dry Ash [g]	18.72
Specific Gravity of water at 20 ˚C	1.00
Mass of Ash [g]	0.15
Mass of Flask + Water at T [g]	48.65
Specific Gravity of Water at T	1.00
Specific Gravity of Soil	**2.76**
Dry Ash Density [kg/m^3]	2763.78

Pipe Series 7a	
Mass Tare [g]	24.778
Mass of Flask + Water + Ash [g]	48.754
Temperature of suspension (T) [˚C]	25
Time under vacuum [min]	2 Hours
Mass of Tare + Dry Ash [g]	24.92
Specific Gravity of water at 20 ˚C	1.00
Mass of Ash [g]	0.14
Mass of Flask + Water at T [g]	48.65
Specific Gravity of Water at T	1.00
Specific Gravity of Soil	**3.55**
Dry Ash Density [kg/m^3]	3546.96

Pipe Series 7b	
Mass Tare [g]	18.636
Mass of Flask + Water + Ash [g]	48.744
Temperature of suspension (T) [˚C]	25.8
Time under vacuum [min]	2 Hours
Mass of Tare + Dry Ash [g]	18.78
Specific Gravity of water at 20 ˚C	1.00
Mass of Ash [g]	0.15
Mass of Flask + Water at T [g]	48.65
Specific Gravity of Water at T	1.00
Specific Gravity of Soil	**2.61**
Dry Ash Density [kg/m^3]	2606.19

Pipe Series 8a	
Mass Tare [g]	18.623
Mass of Flask + Water + Ash [g]	48.746
Temperature of suspension (T) [˚C]	24.8
Time under vacuum [min]	2 Hours
Mass of Tare + Dry Ash [g]	18.76
Specific Gravity of water at 20 ˚C	1.00
Mass of Ash [g]	0.14
Mass of Flask + Water at T [g]	48.66
Specific Gravity of Water at T	1.00
Specific Gravity of Soil	**2.80**
Dry Ash Density [kg/m^3]	2798.14

Pipe Series 8b	
Mass Tare [g]	23.926
Mass of Flask + Water + Ash [g]	48.761
Temperature of suspension (T) [˚C]	24.6
Time under vacuum [min]	2 Hours
Mass of Tare + Dry Ash [g]	24.10
Specific Gravity of water at 20 ˚C	1.00
Mass of Ash [g]	0.18
Mass of Flask + Water at T [g]	48.66
Specific Gravity of Water at T	1.00
Specific Gravity of Soil	**2.51**
Dry Ash Density [kg/m^3]	2505.14

APPENDIX H : CLOGGING Na^+ COMPOSITION DATA FROM THE PIPE RINGS (FROM RING# 2) AT DIFFERENT ELAPSED TIMES.

a. Summary of average (μ) and standard deviation (σ) values of Na^+ ($mg \cdot kg^{-1}$) sampled from clogging collected form the pipes rings of the pipe series at different elapsed times

Pipe Series #	Na^+ concentration [mg/L] Pipe Ring #							
	2		3		4		5	
	μ	σ	μ	σ	μ	σ	μ	σ
1	3671	86.27	2041	375.78	3850	139.30	3814	250.37
2	1933	1166.13	13658	7219.56	4306	25.46	5827	1936.32
3	6778	86.83	1475	225.16	3164	118.09	3575	565.85
4	5223	1223.36	1822	111.58	1944	208.60	2702	1120.19
5	6927	297.30	1319	85.93	4885	3897.57	3580	2708.54
6	5188	19.50	1407	48.34	1040	41.72	1303	322.09
7	2641	795.30	1119	27.98	3853	70.00	3853	69.60
8	2977	1477.70	1662	681.67	2629	1161.07	2629	1160.43

APPENDIX I : XRD ANALYSES OF CLOGGING ACCUMULATED WITHIN THE PIPE RINGS (FROM RING #2) COLLECTED FROM THE PIPE SERIES AT DIFFERENT ELAPSED TIMES.

a. XRD results

i. 2nd ring

Pipe Series 1a

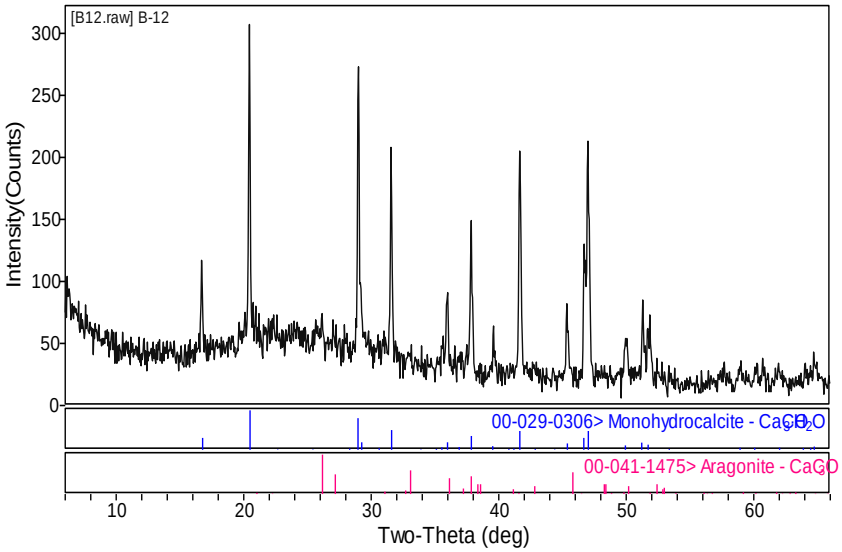

Pipe Series 1b

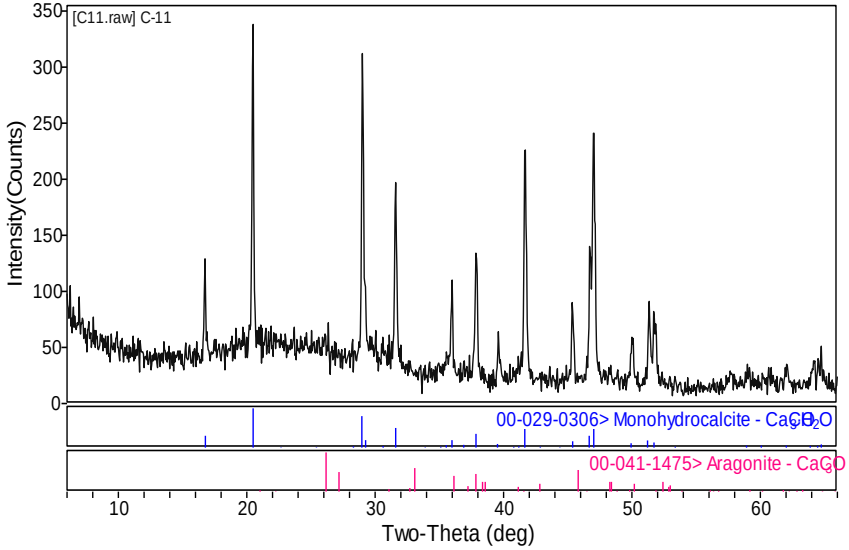

Pipe Series 2a

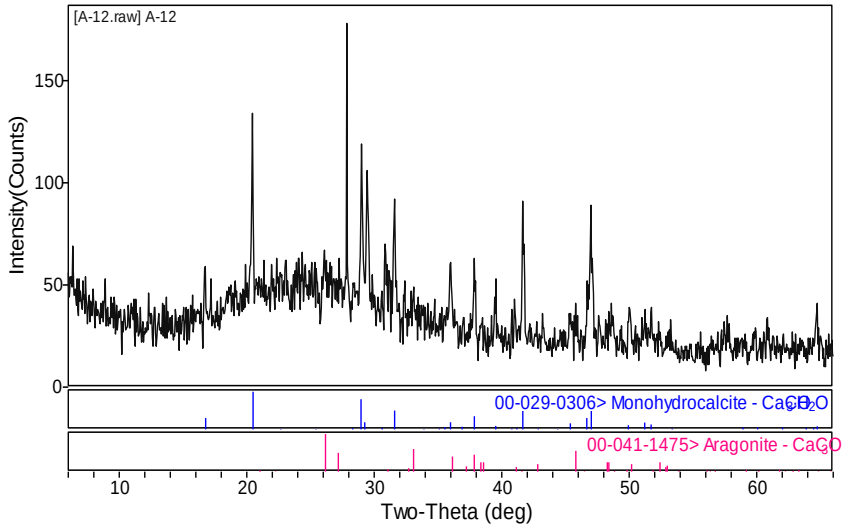

Pipe Series 2b

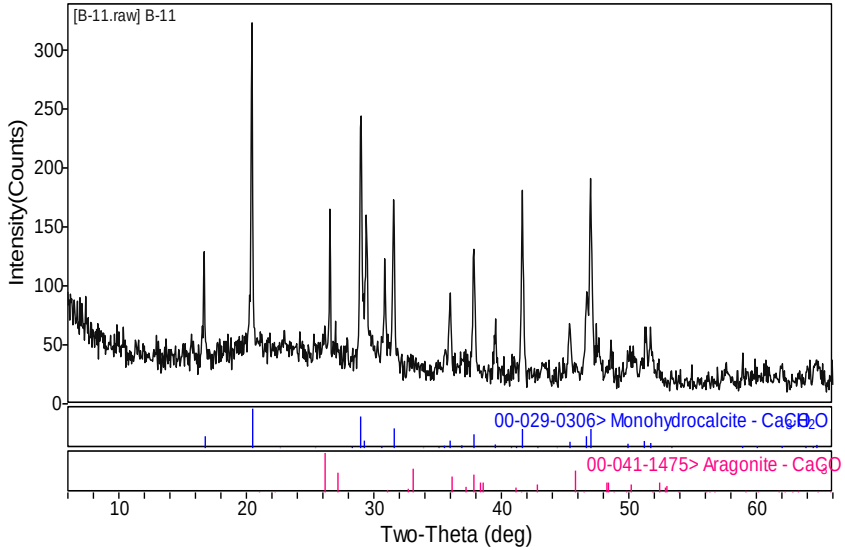

Pipe Series 3a

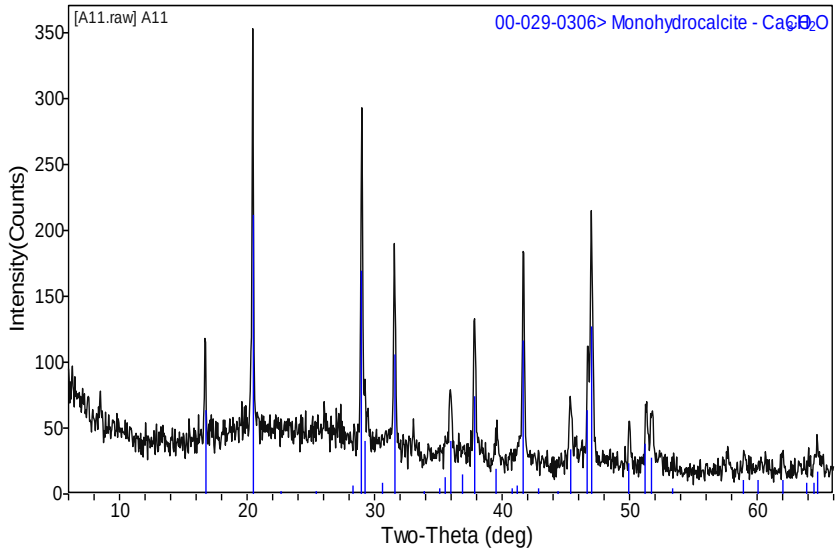

Pipe Series 3b

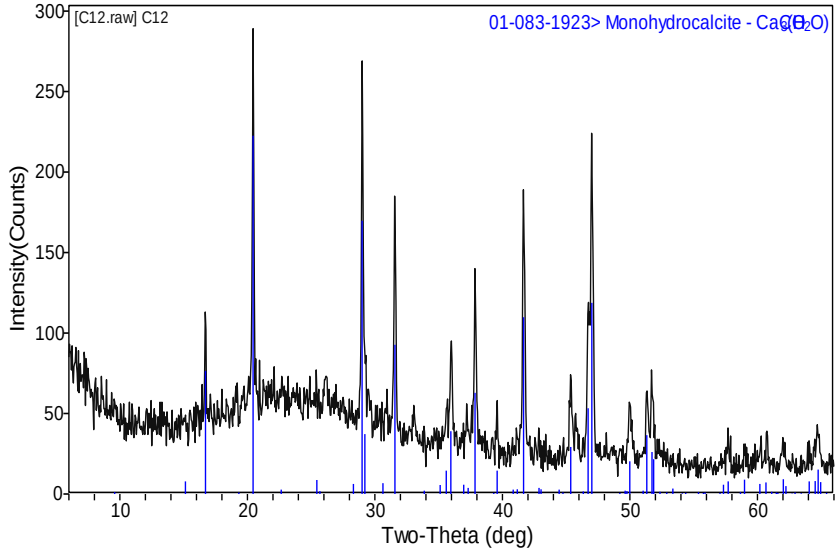

Pipe Series 4a

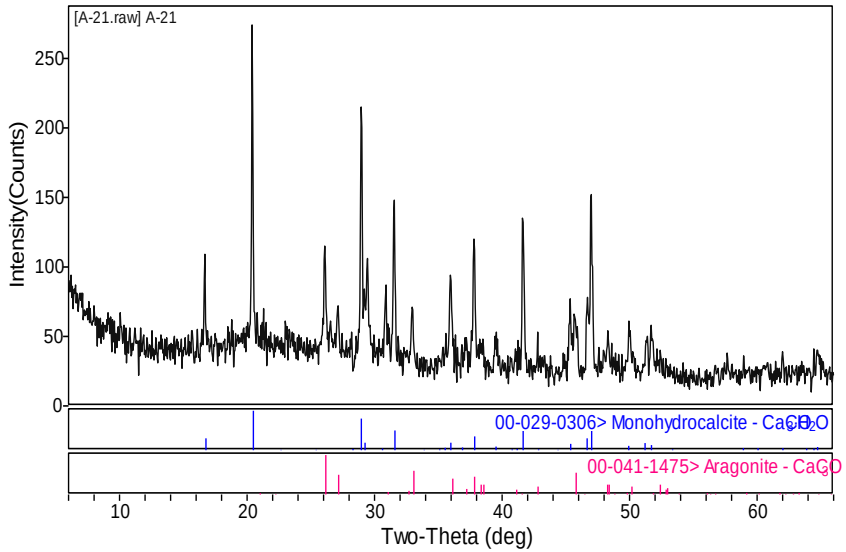

Pipe Series 4b

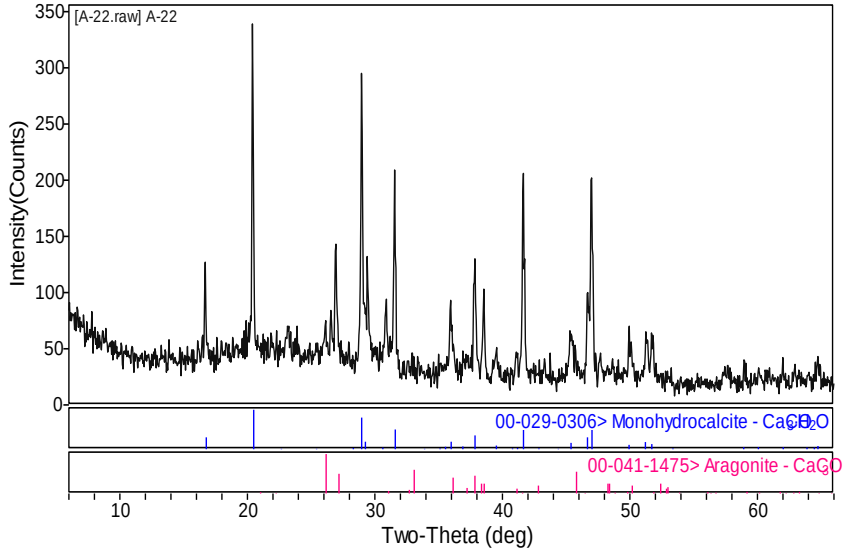

Pipe Series 5a

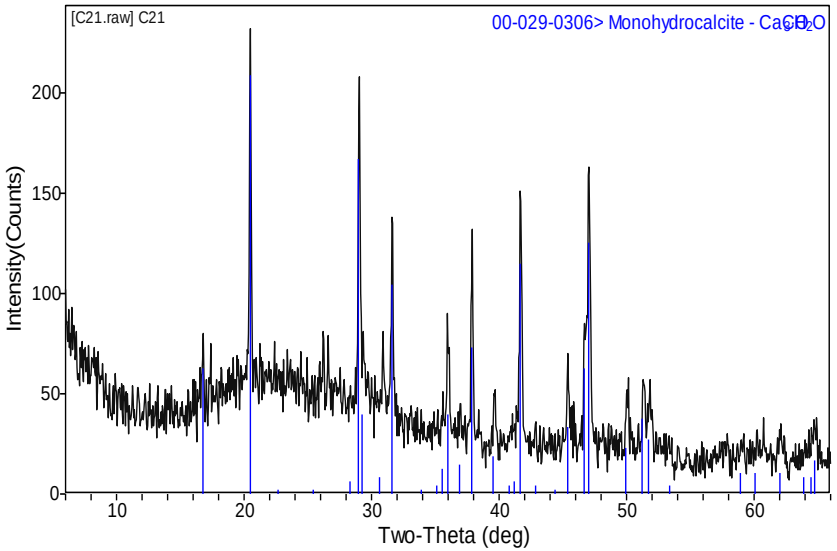

Pipe Series 5b

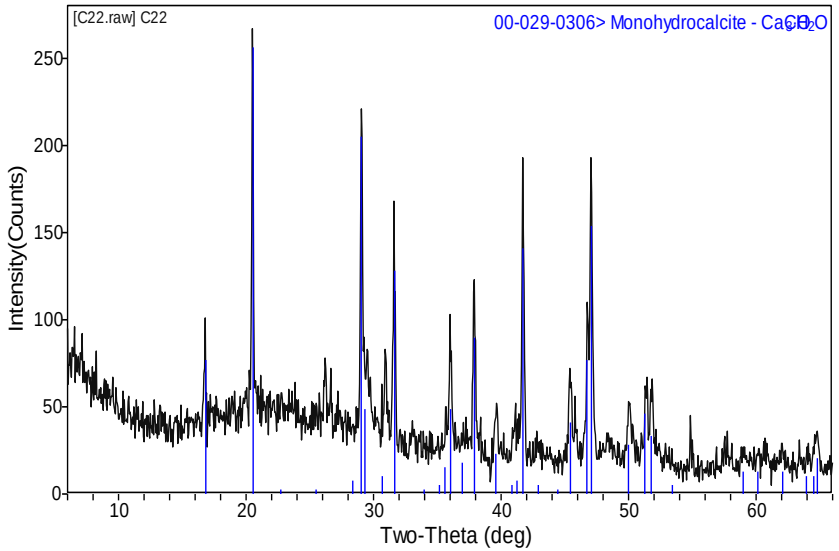

Pipe Series 6a

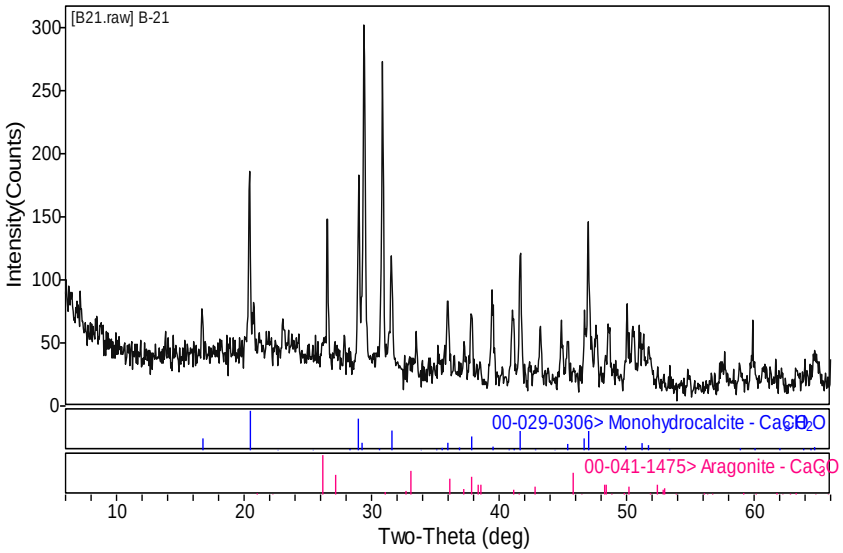

Pipe Series 6b

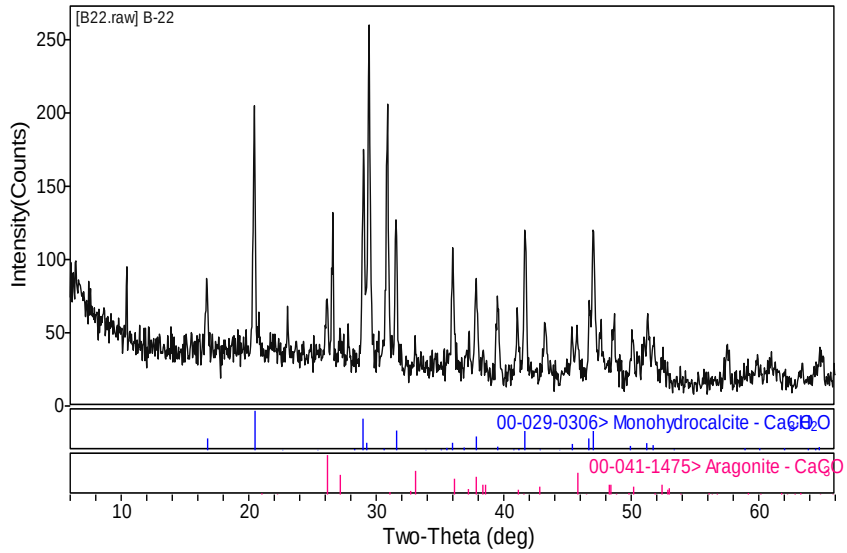

Pipe Series 7a

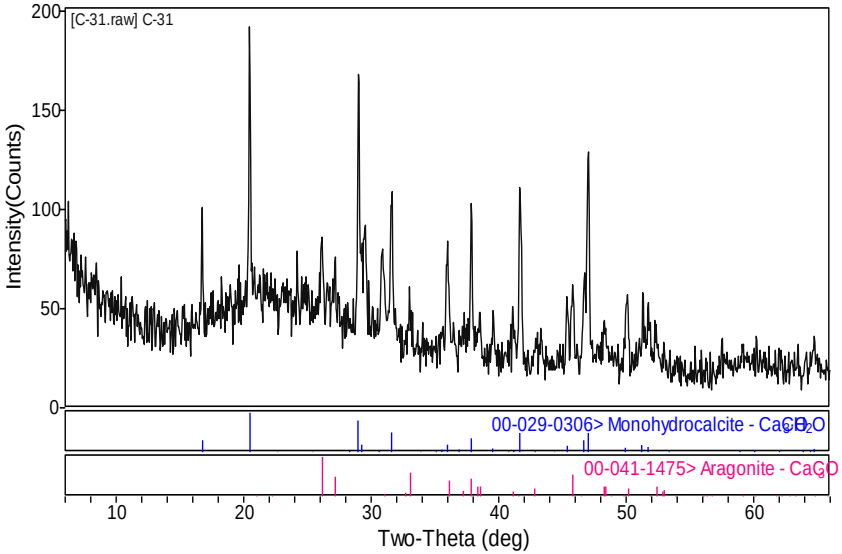

Pipe Series 7b

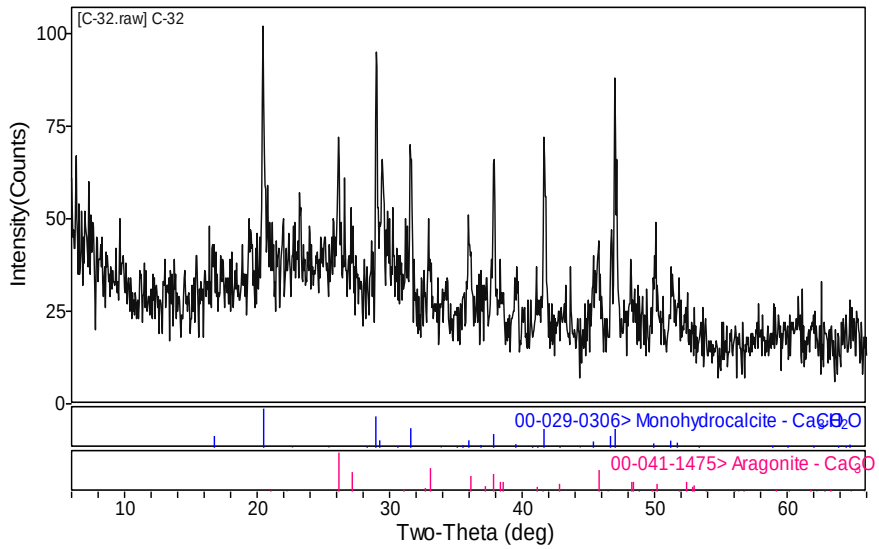

Pipe Series 8a

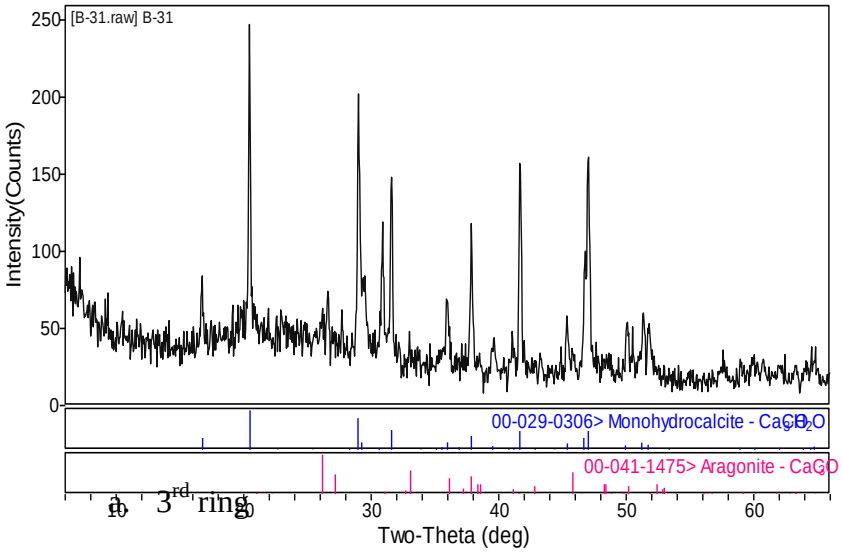

a 3rd ring

Pipe Series 8b

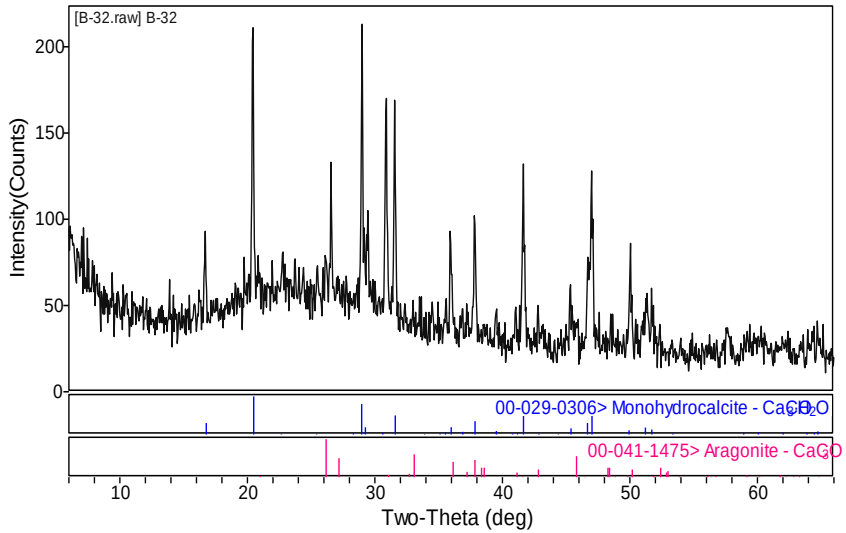

ii. 3rd ring

Pipe Series 1a

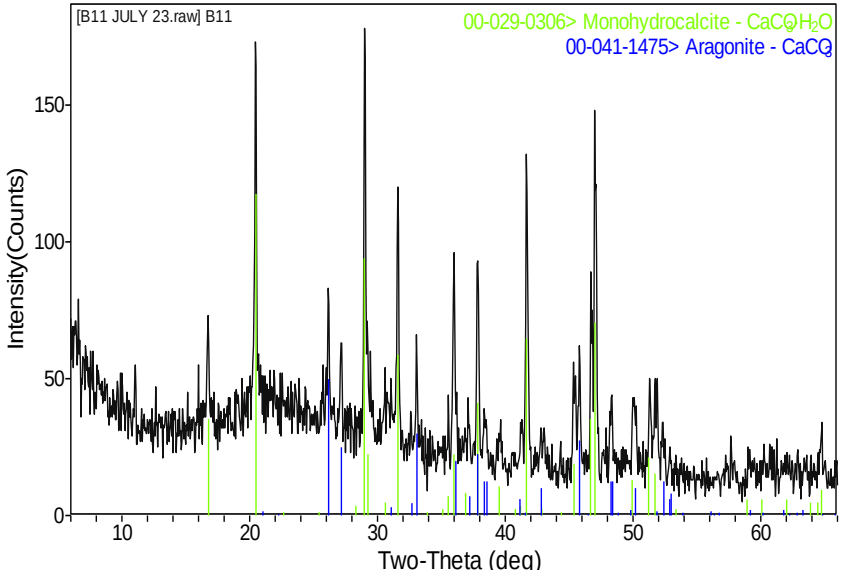

Pipe Series 1b

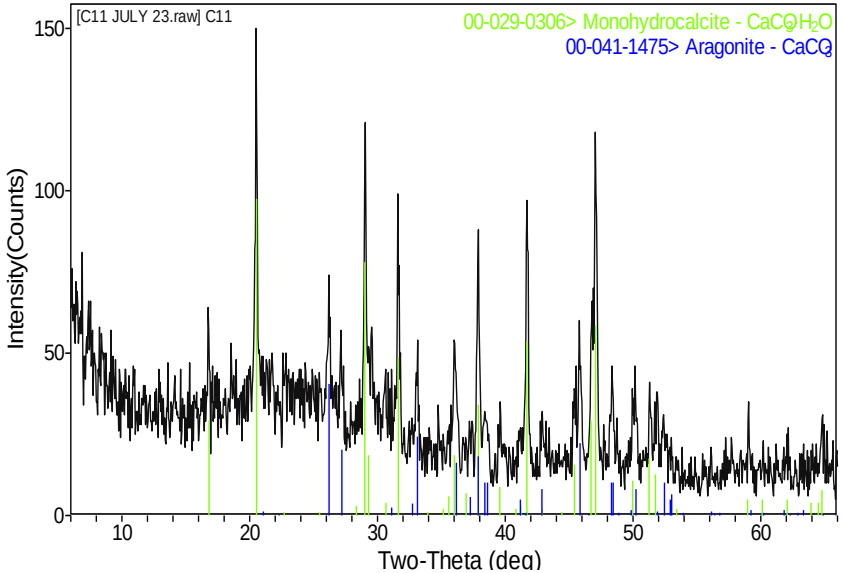

Pipe Series 2a

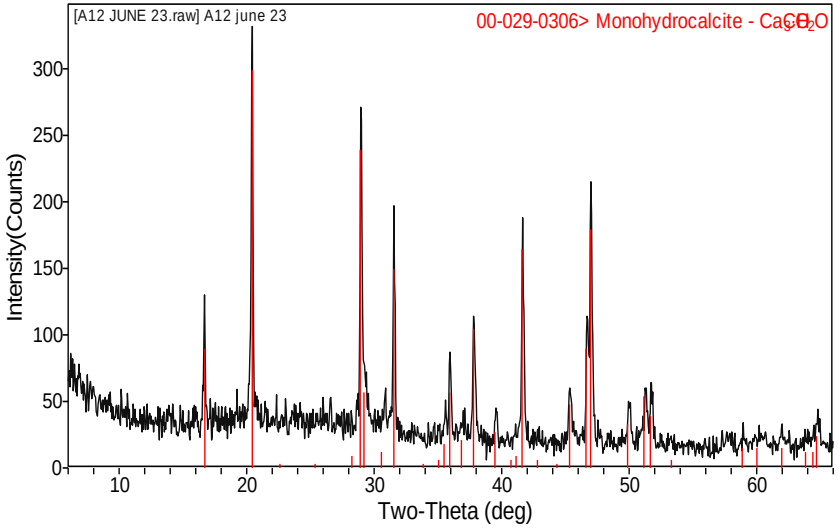

Pipe Series 2b

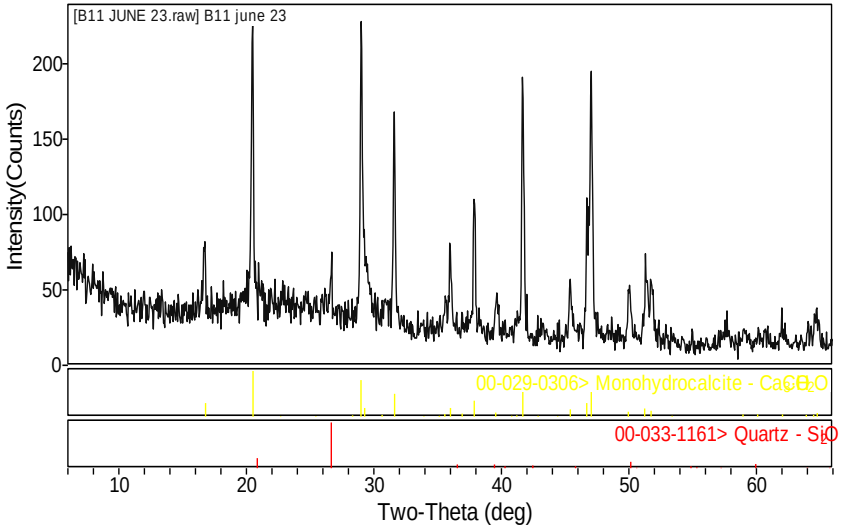

Pipe Series 3a

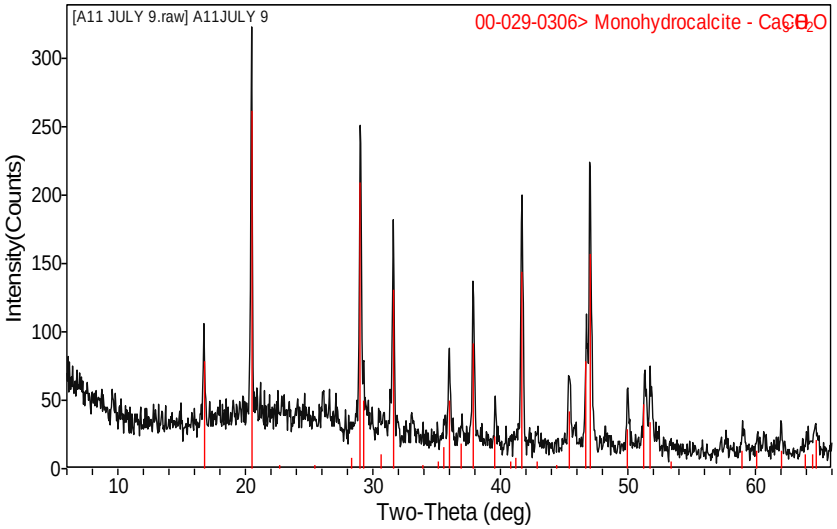

Pipe Series 3b

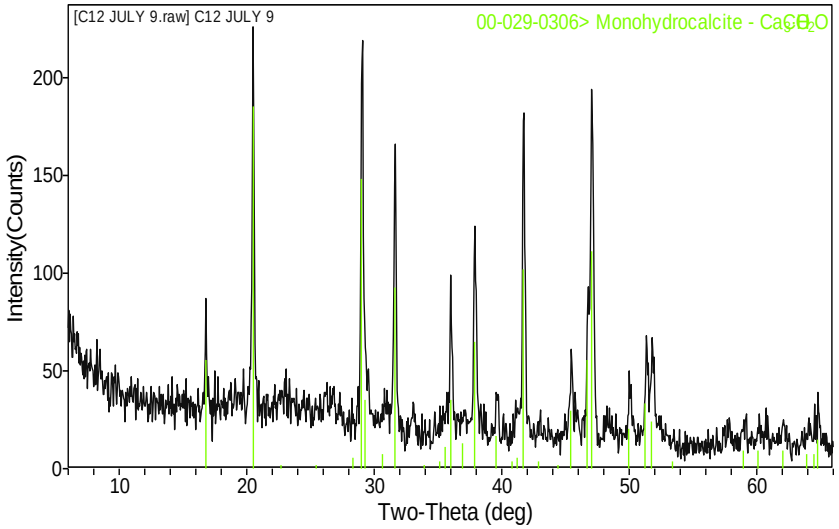

Pipe Series 4a

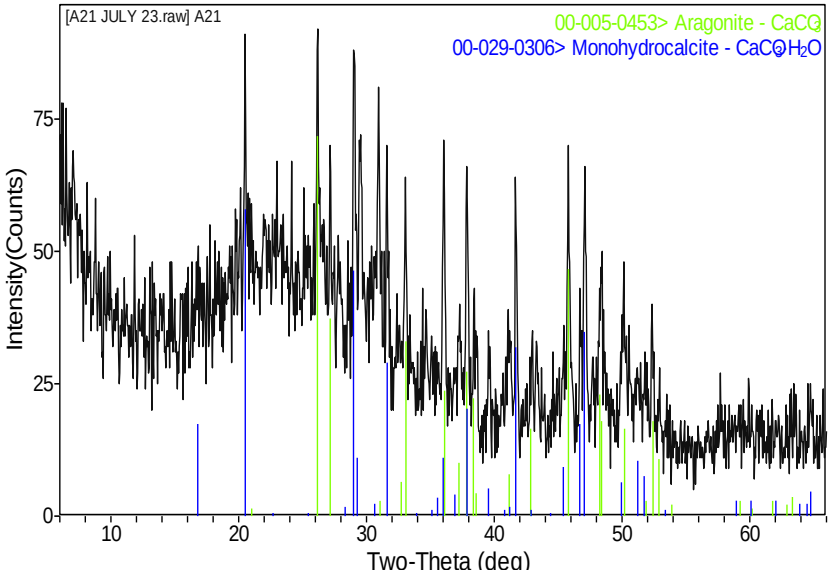

Pipe Series 4b

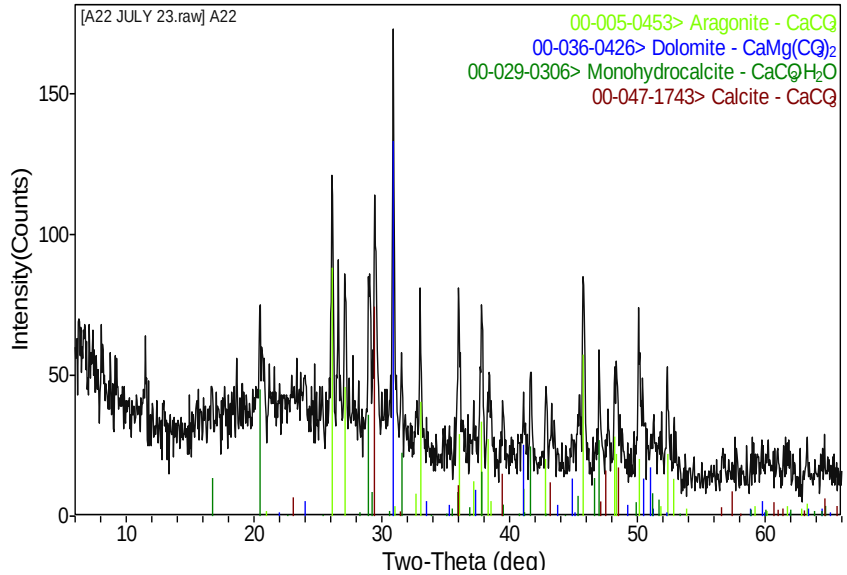

Pipe Series 5a

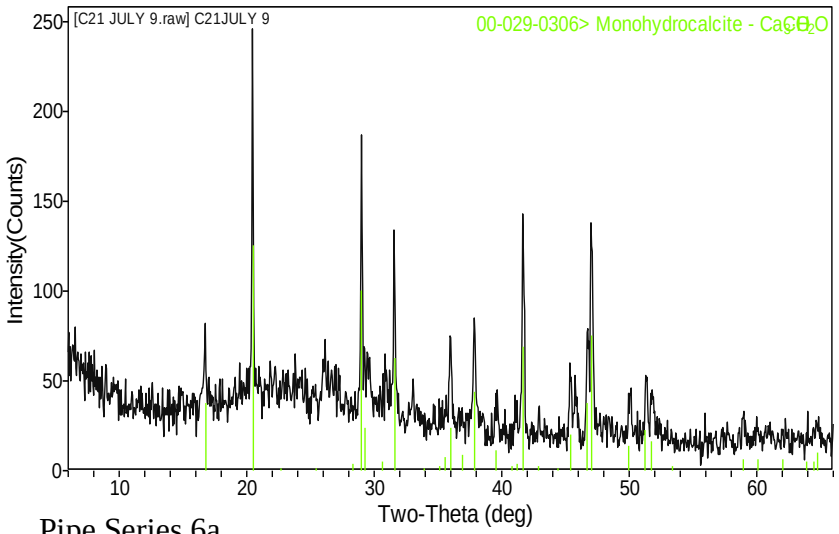

Pipe Series 5b

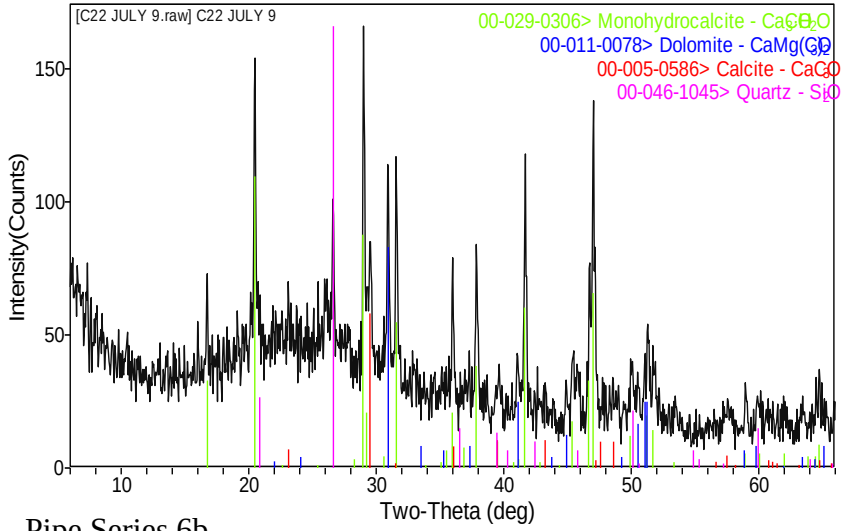

Pipe Series 6a

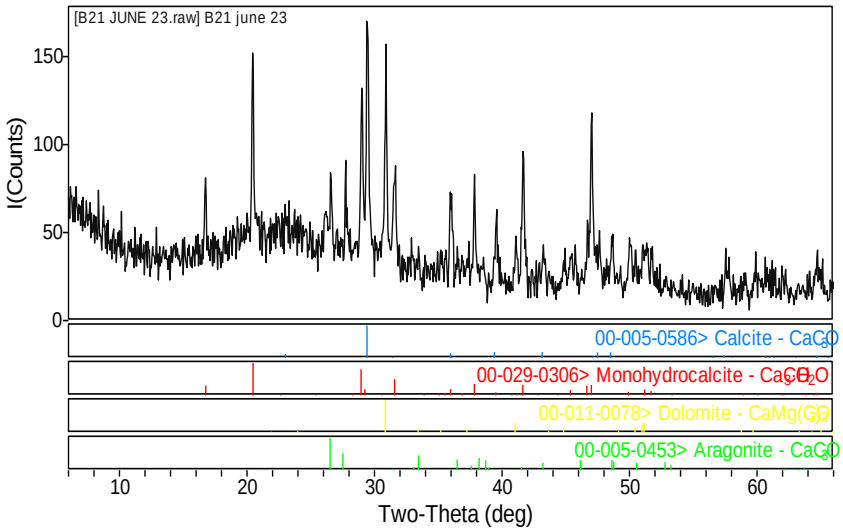

Pipe Series 6b

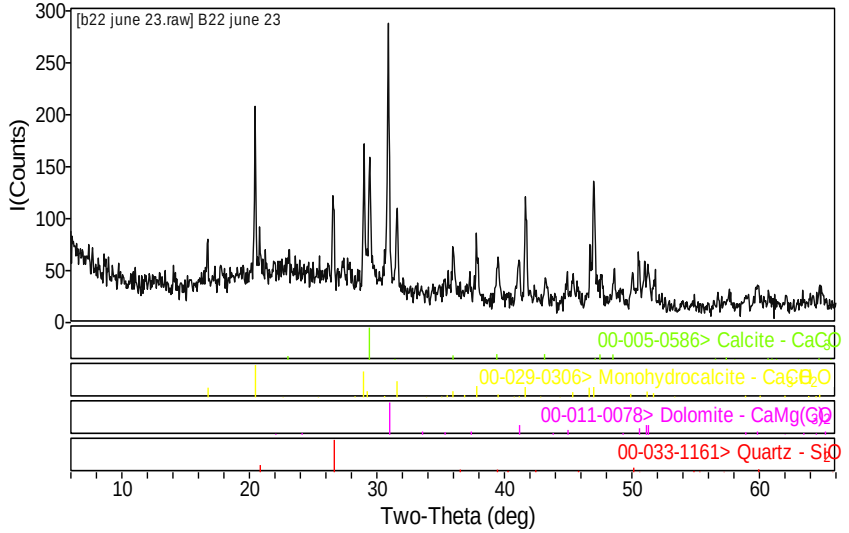

Pipe Series 7a

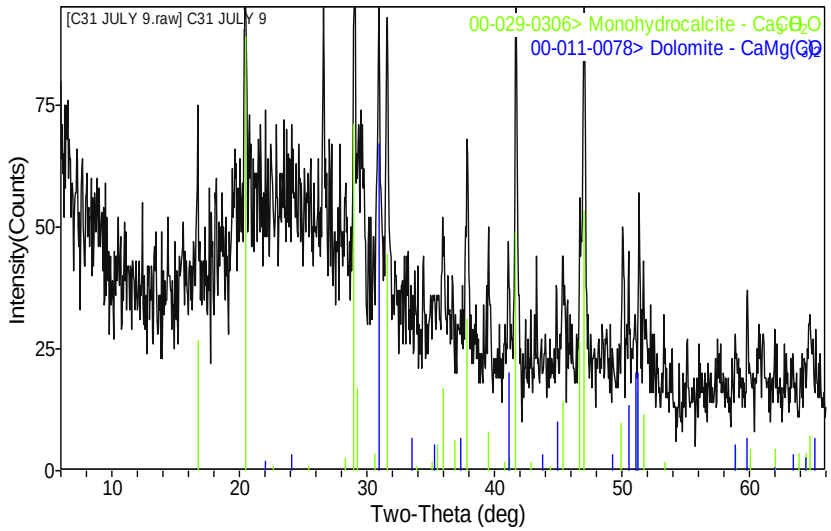

Pipe Series 7b

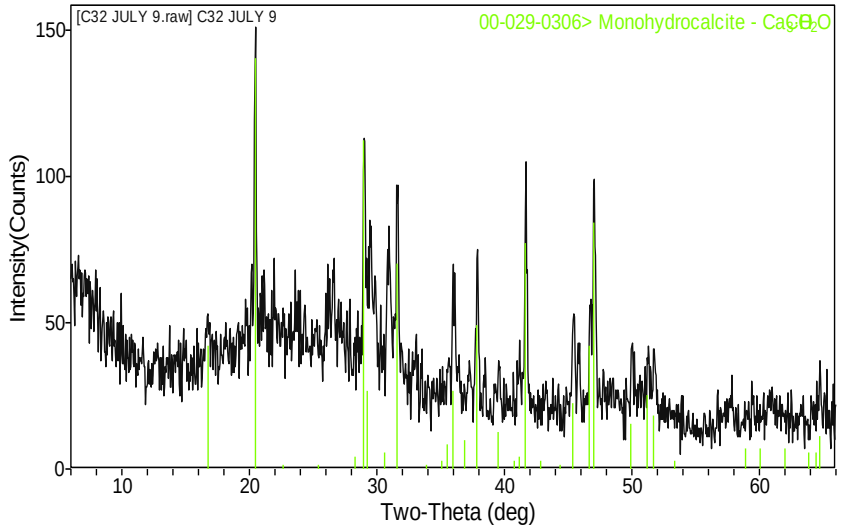

Pipe Series 8a

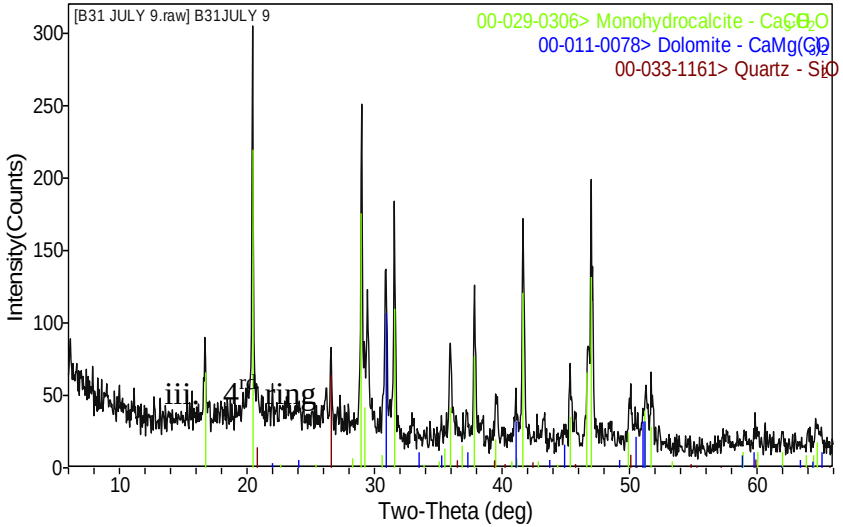

iii. 4th ring

Pipe Series 8b

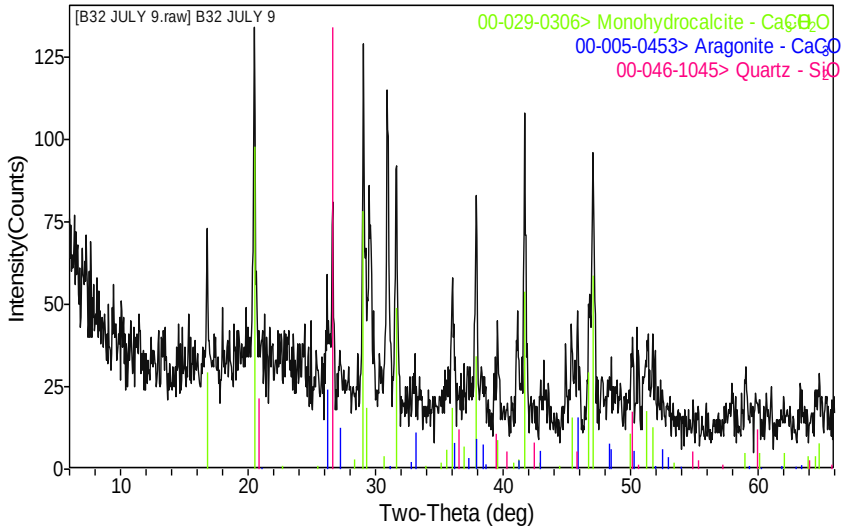

Pipe Series 1a

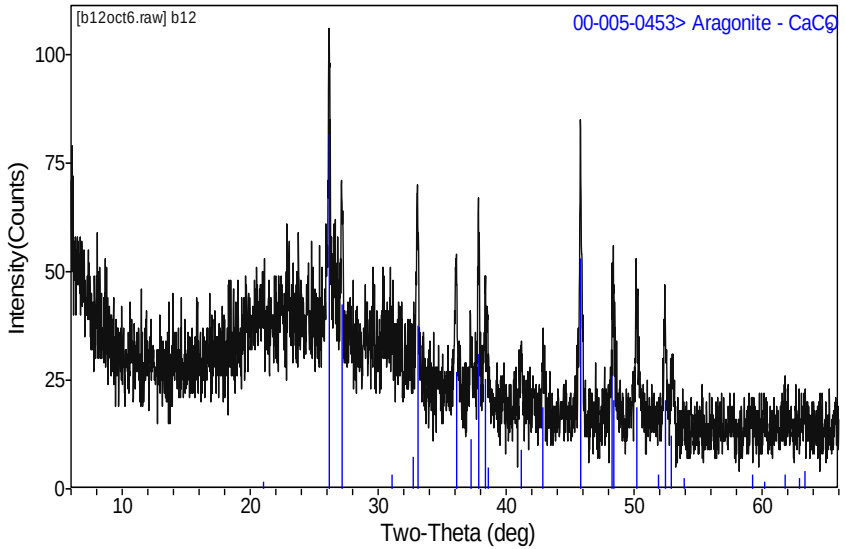

Pipe Series 1b

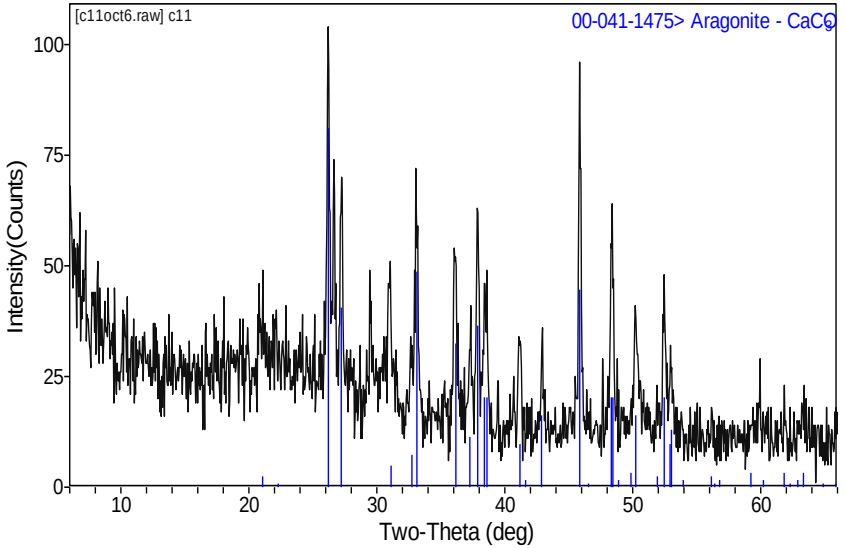

Pipe Series 2a

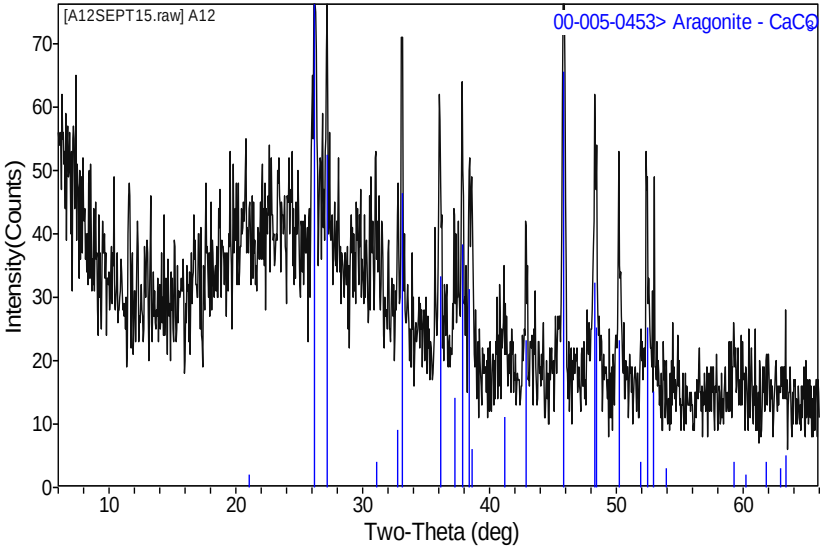

Pipe Series 2b

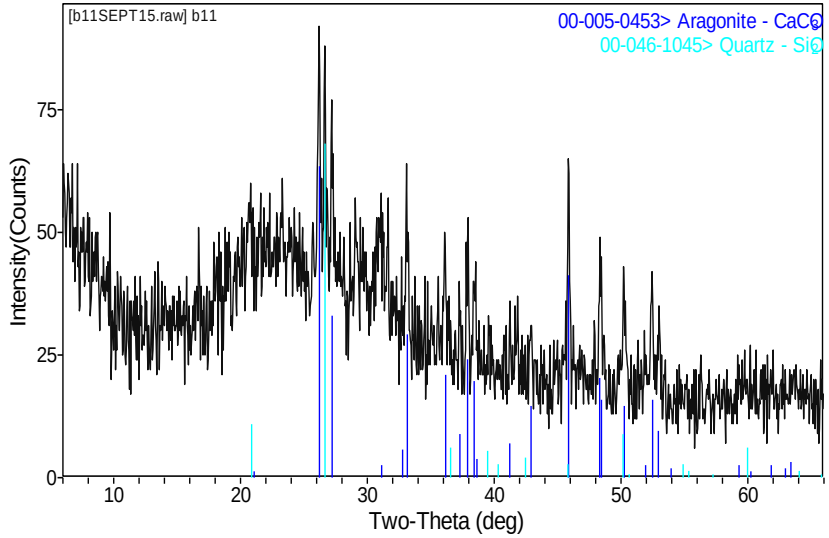

Pipe Series 3a

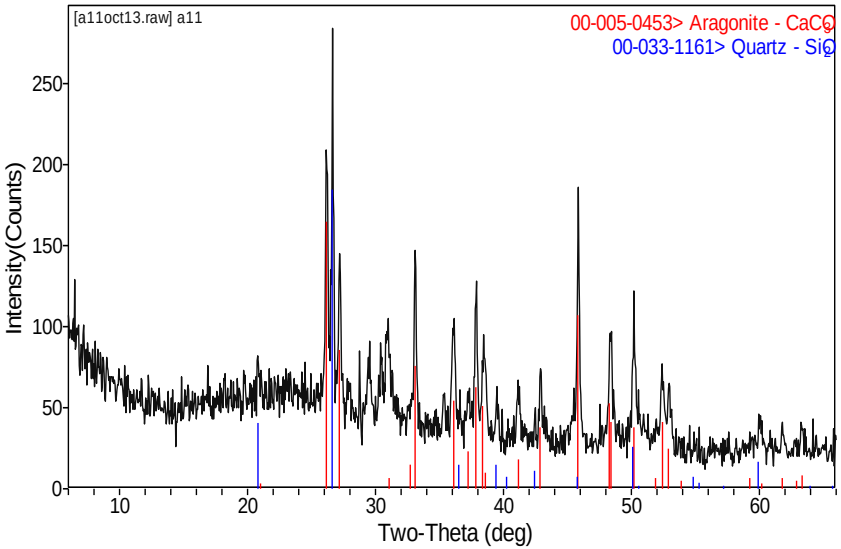

Pipe Series 3b

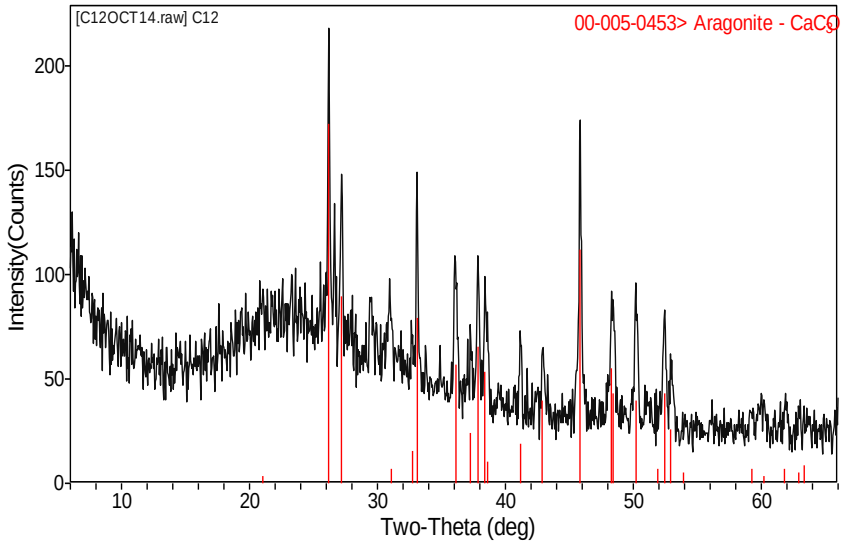

Pipe Series 4a

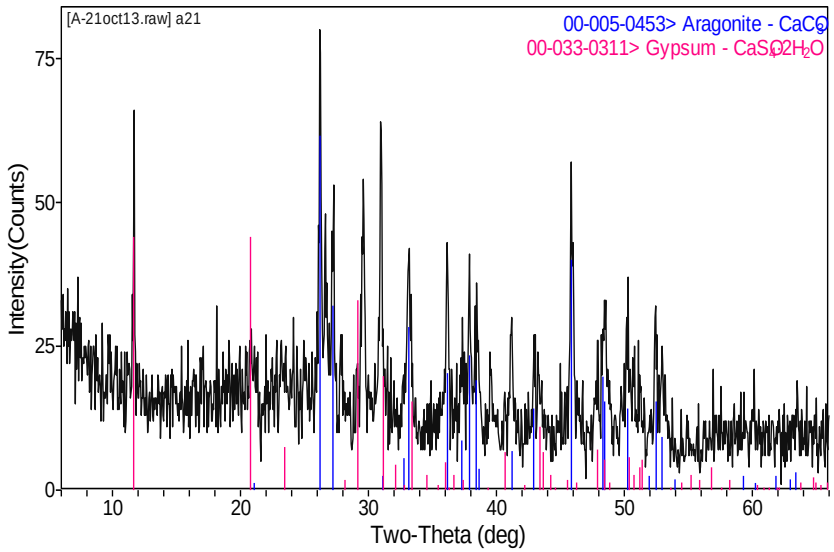

Pipe Series 4b

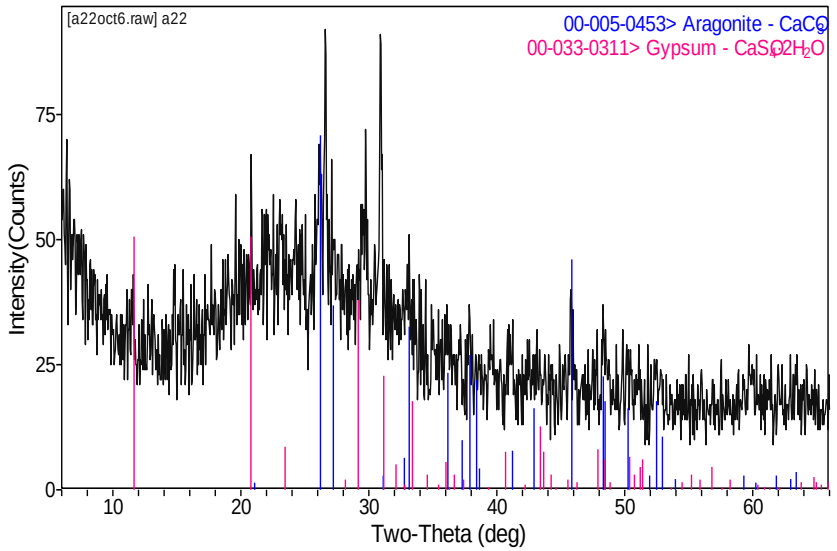

Pipe Series 5a

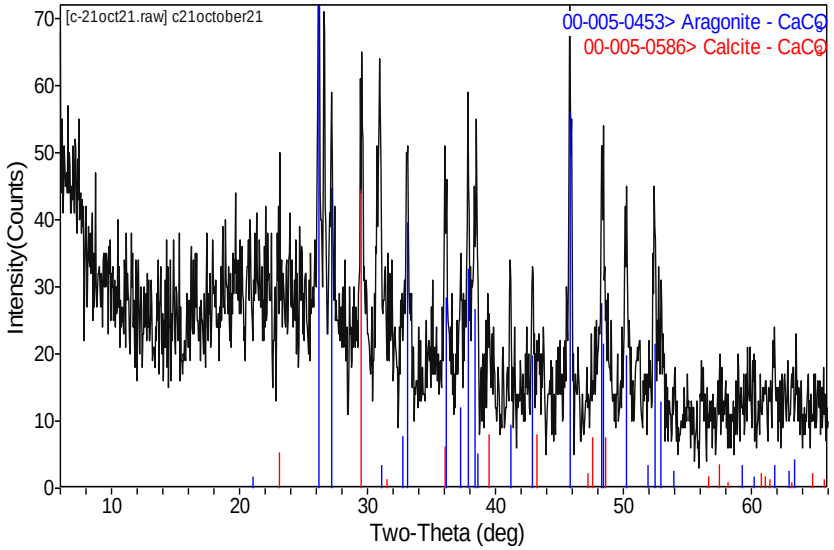

Pipe Series 5b

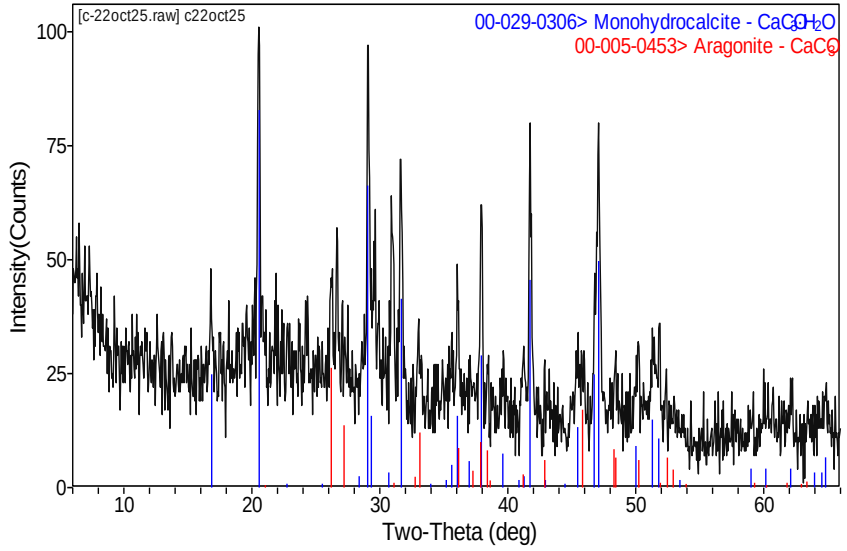

Pipe Series 6a

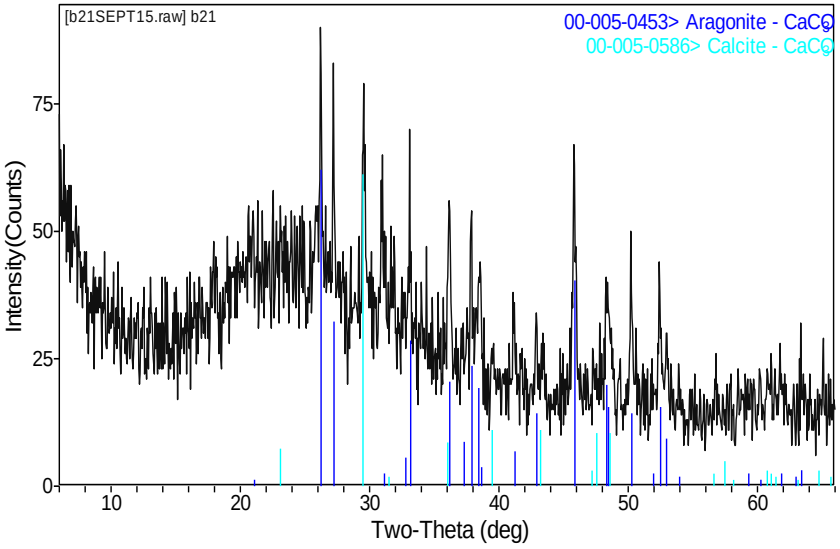

Pipe Series 6b

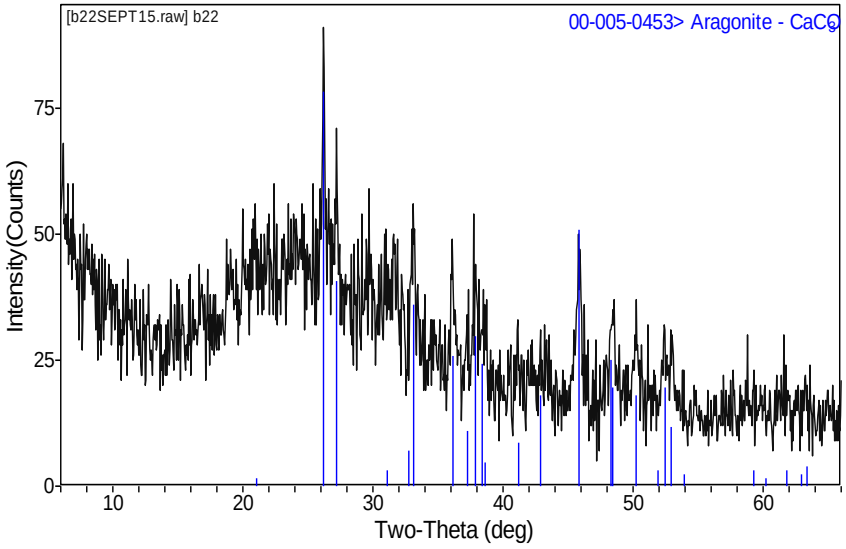

Pipe Series 7a

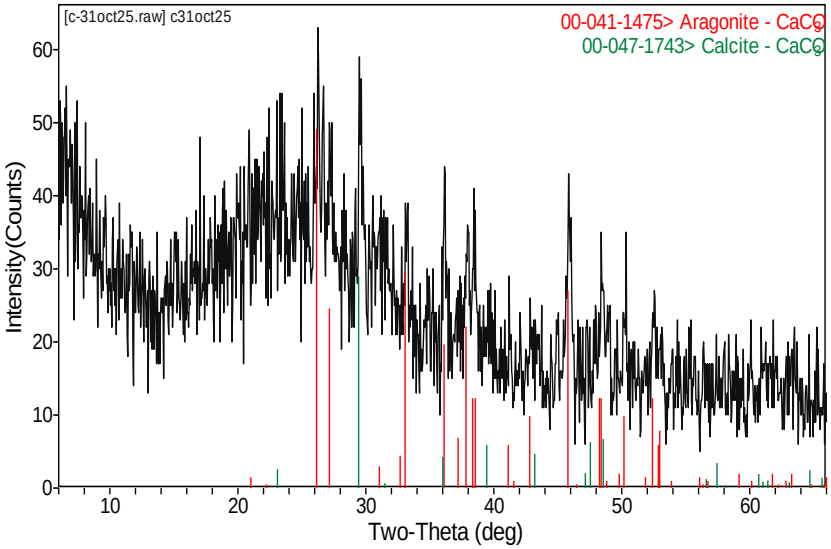

Pipe Series 7b

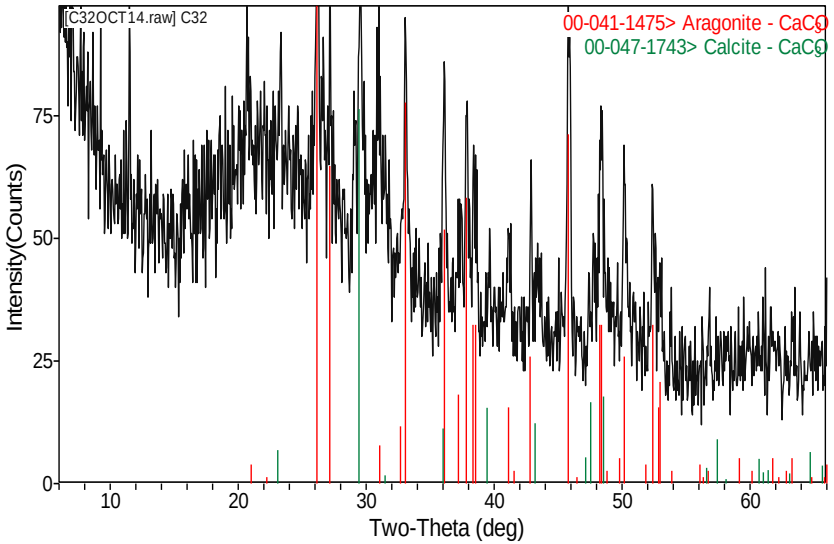

Pipe Series 8a

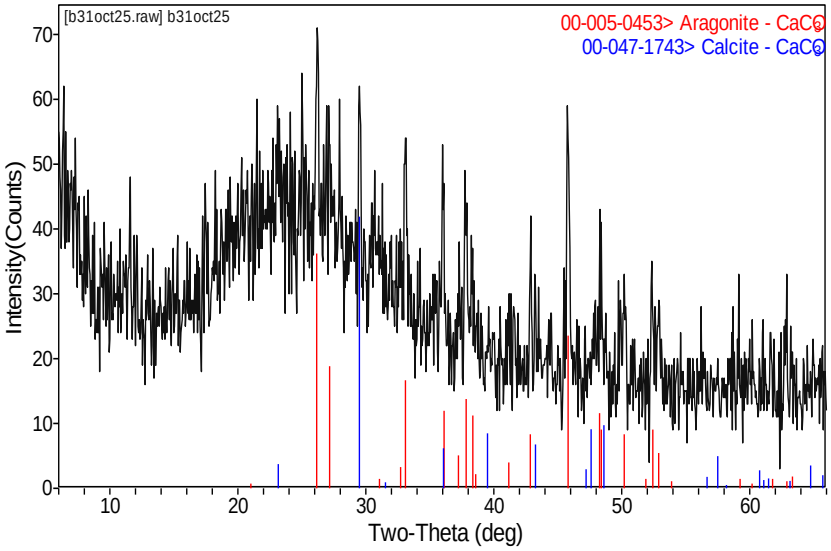

Pipe Series 8b

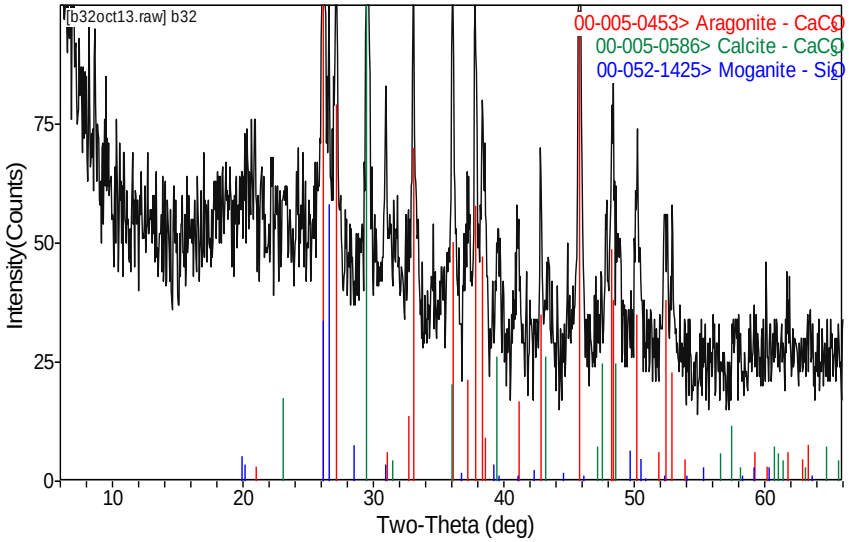

iv. 5th ring

Pipe Series 1a

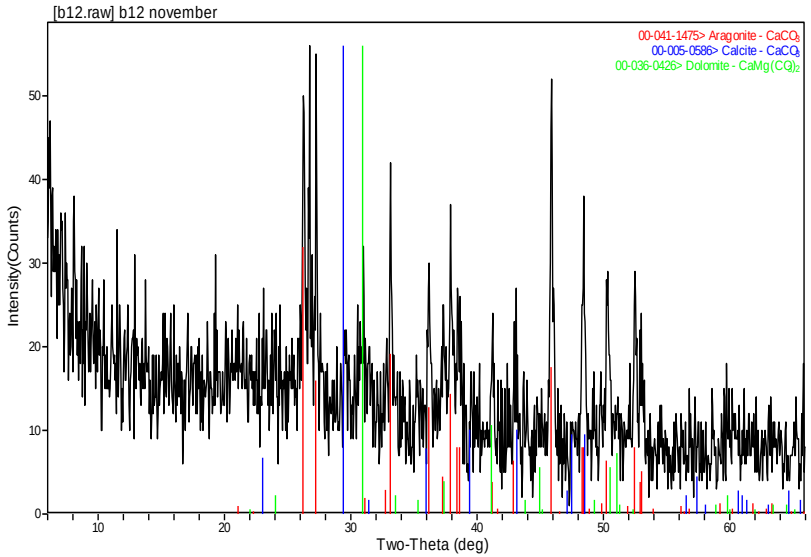

Pipe Series 1b

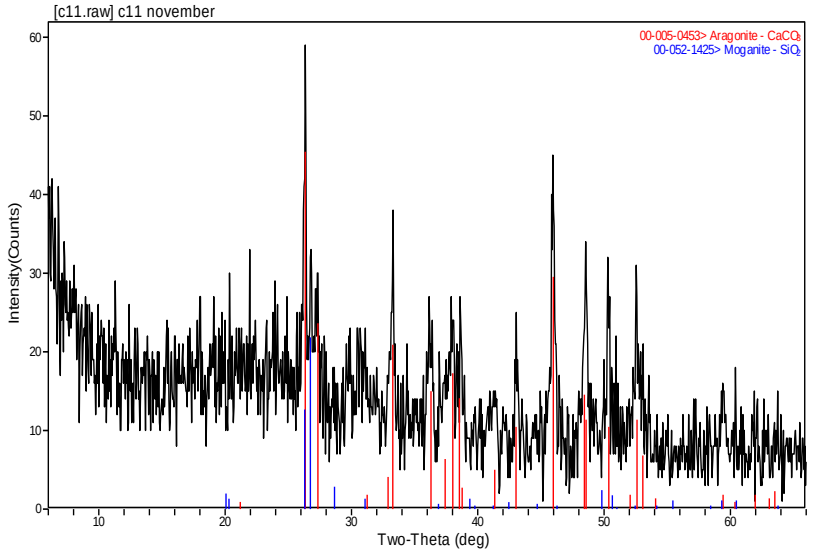

Pipe Series 2a

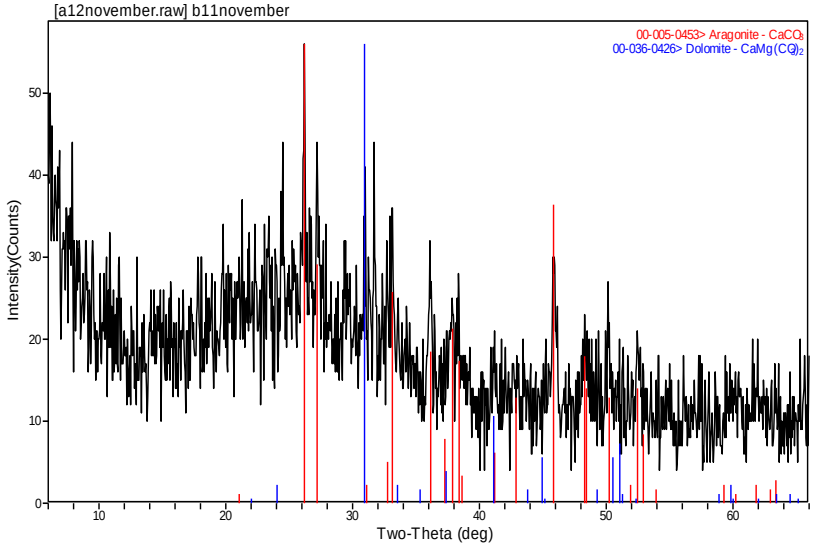

Pipe Series 2b

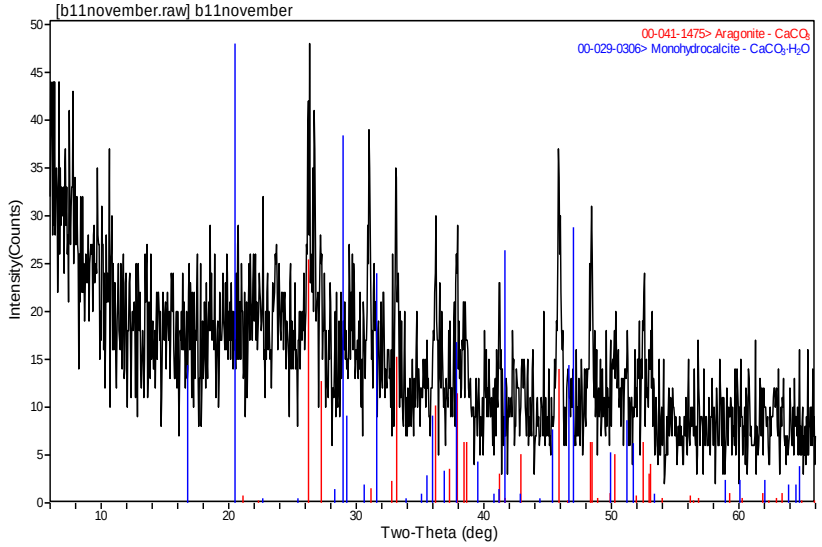

Pipe Series 3a

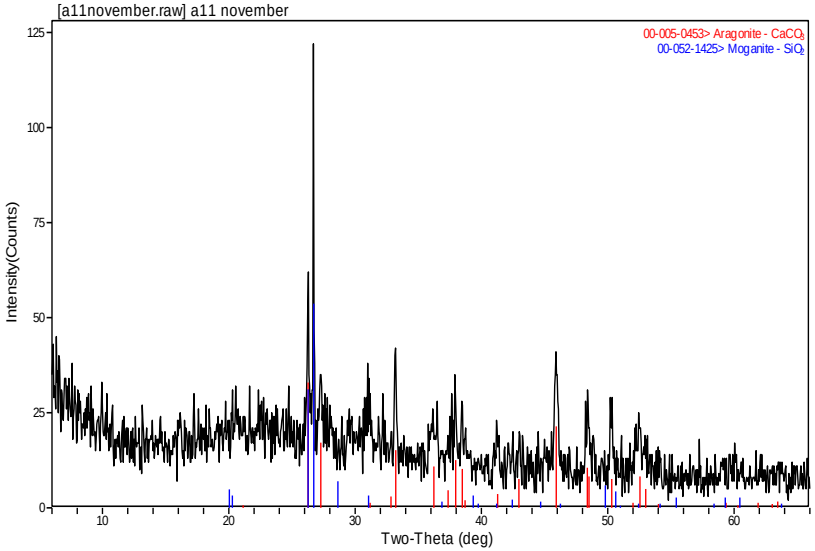

Pipe Series 3b

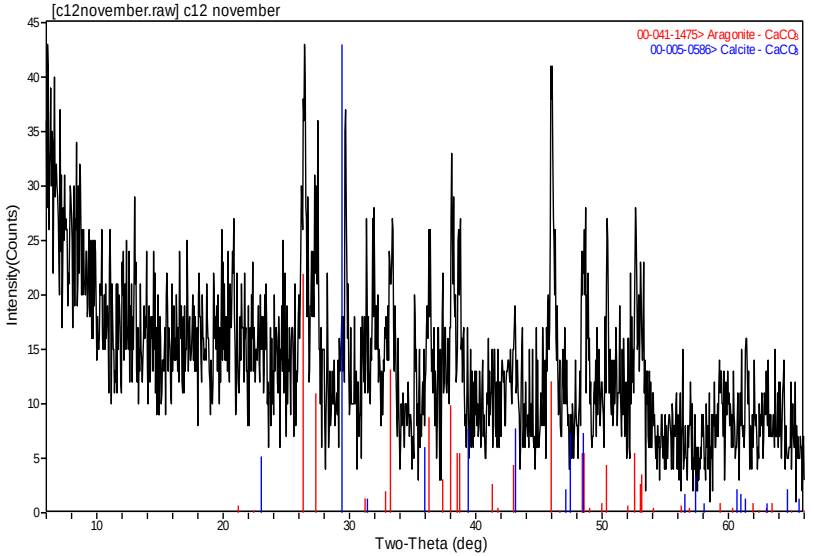

Pipe Series 4a

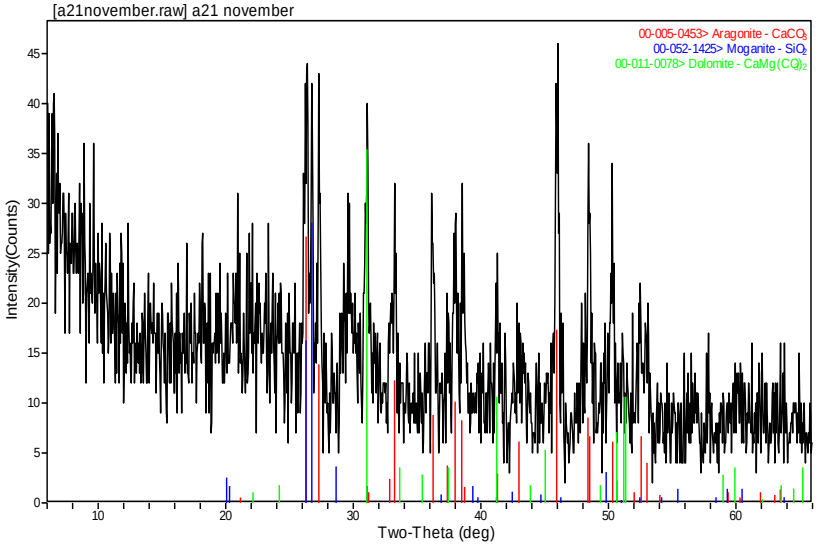

Pipe Series 4b

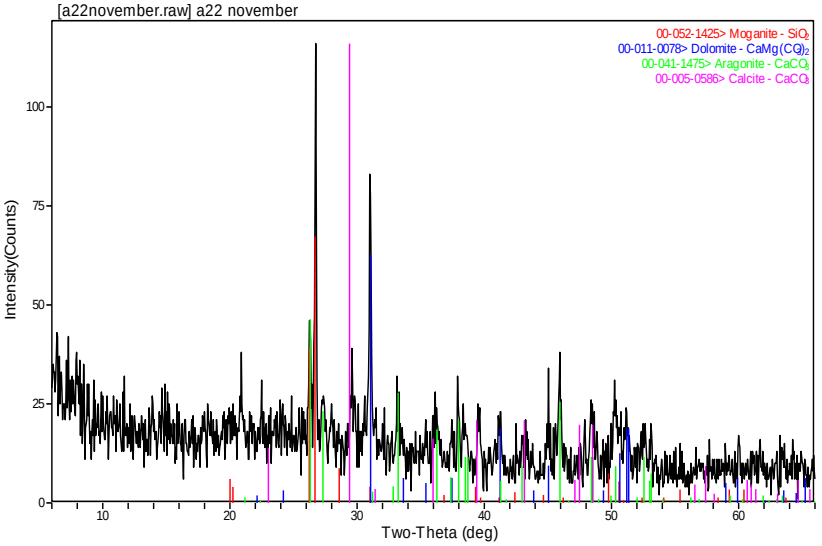

Pipe Series 5a

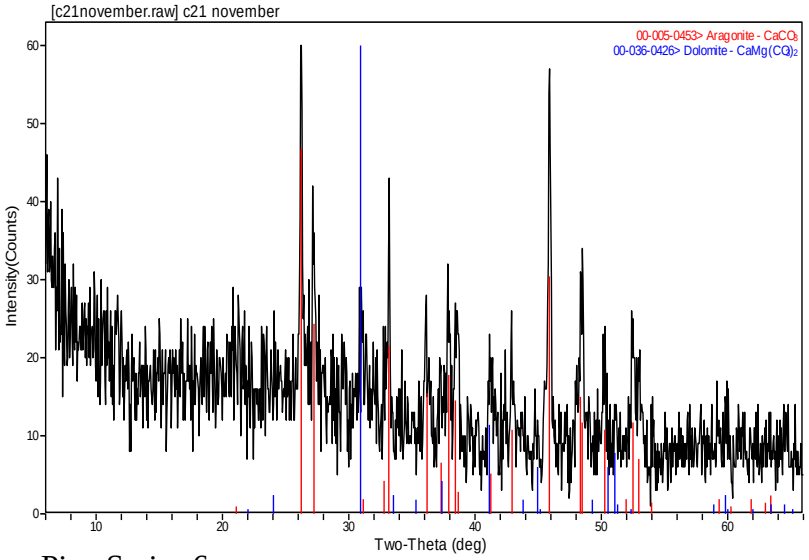

Pipe Series 5b

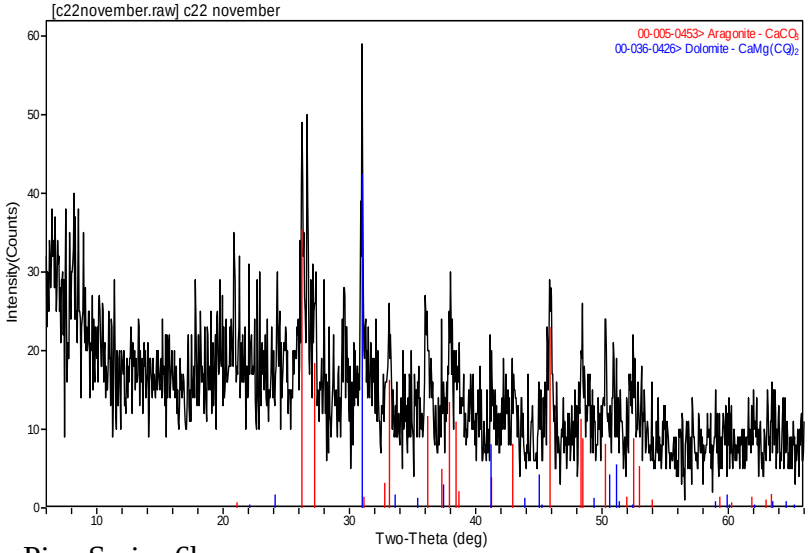

Pipe Series 6a

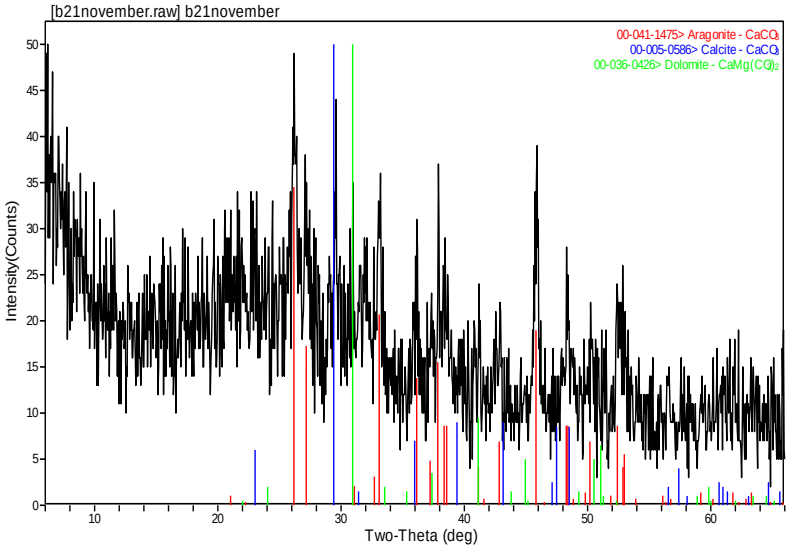

Pipe Series 6b

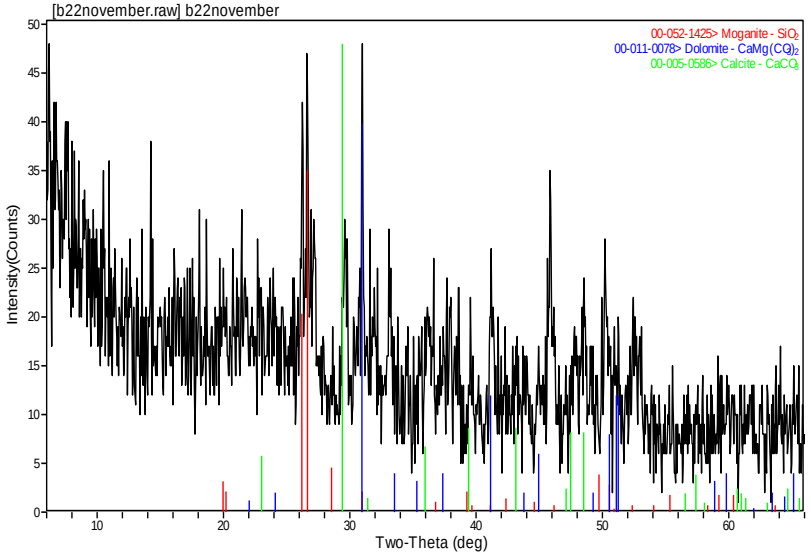

Pipe Series 7a

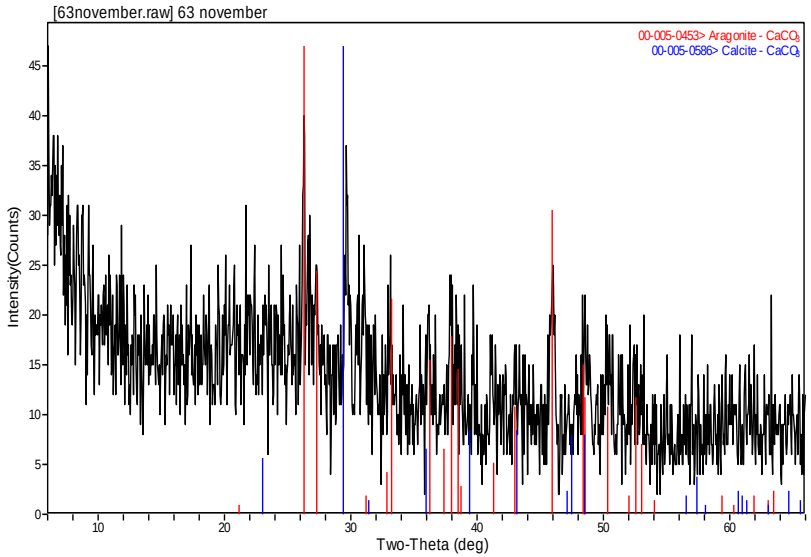

Pipe Series 7b

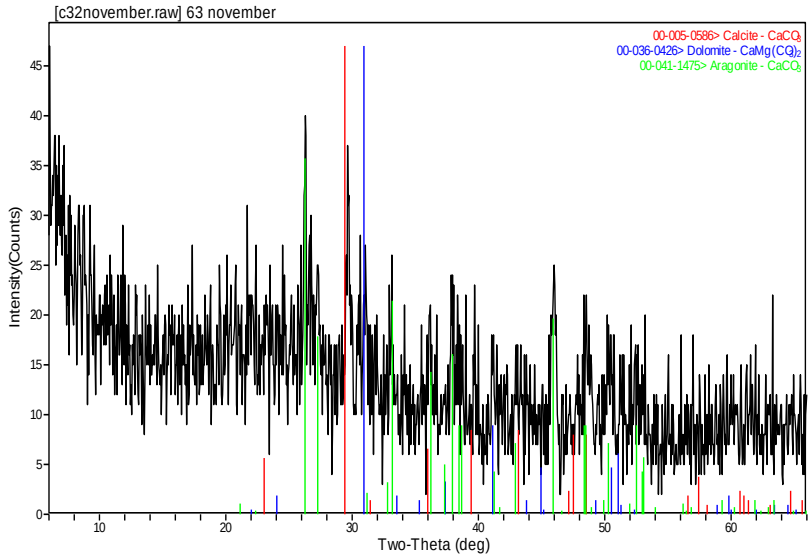

Pipe Series 8a

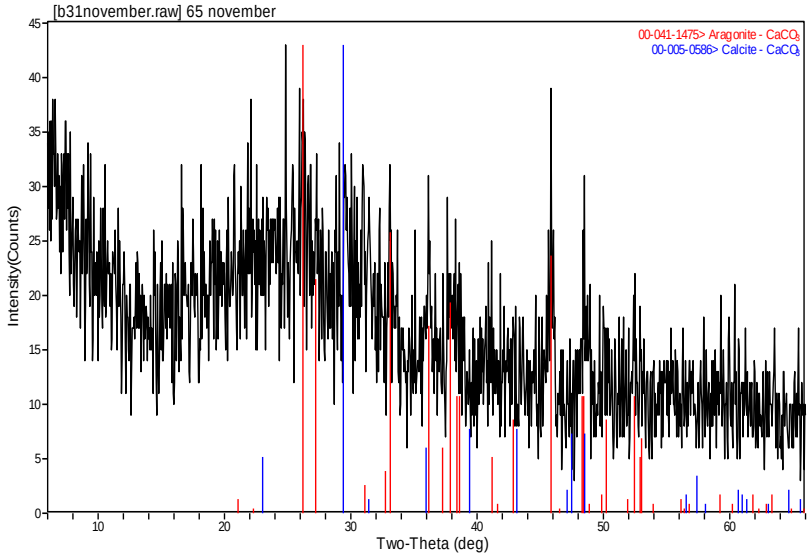

Pipe Series 8b

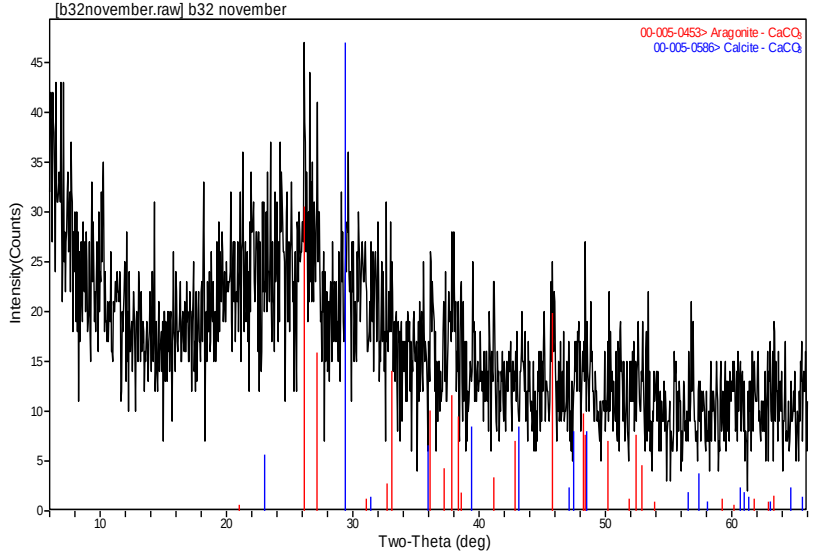

APPENDIX J : INLET HEAD AND HEAD LOSSES DATA FROM THE PIPE SERIES AT DIFFERENT ELAPSED TIMES

Pipe Series 1a

Date	Flow	Initial Head	Head Loss		Friction Factor
			PT1	PT2	Measured
	L/sec	m	mm	mm	[-]
2009-09-14	0.76	0.82		20.28	0.040
2009-09-14	1.39	1.65		33.93	0.020
2009-09-30	0.8	1.16		25.5	0.045
2009-10-14	0.8	1.21		26.97	0.048
2009-11-01	0.8	1.30		27.18	0.048
2009-11-15	1.52	1.34		22.03	0.011
2010-02-23	1.34	1.13		20.71	0.013
2010-03-02	1.39	1.06		19.57	0.012
2010-03-10	1.42	1.06		27.67	0.016
2010-05-08	1.72	1.26		36.39	0.014
2010-06-01	1.59	1.24		36.55	0.016
2010-06-15	1.72	1.87		45.81	0.018
2010-10-27	1.87	1.89		40.71	0.013
2010-11-12	1.87	1.98		44.50	0.015

Pipe Series 1b

Date	Flow	Initial Head	Head Loss		Friction Factor
			PT1	PT2	Measured
	L/sec	m	mm	mm	[-]
2009-09-14	1.17	1.80		45.07	0.035
2009-09-14	1.8	3.06		74.03	0.024
2009-09-30	0.82	1.23		35.74	0.057
2009-10-14	0.8	1.21		34.66	0.058
2009-11-01	0.81	1.26		33.93	0.055
2009-11-15	1.7	1.34		32.34	0.012
2010-02-23	1.71	2.08		44.77	0.016
2010-03-02	1.71	2.17		48.91	0.018
2010-03-10	1.73	1.62		46.42	0.017
2010-05-08	1.73	1.24		39.46	0.014
2010-06-01	1.73	1.66		55.84	0.020
2010-06-15	1.73	1.92		62.42	0.022
2010-10-27	1.84	2.10		56.28	0.018
2010-11-12	1.83	2.31		61.95	0.020

Pipe Series 2a

Date	Flow	Initial Head	Head Loss		Friction Factor
			PT1	PT2	Measured
	L/sec	m	mm	mm	[-]
2009-09-13	2.3			77.43	0.016
2009-09-16	2.28			80.15	0.017
2009-09-16	2.3			79.21	0.017
2009-09-30	1.53	1.24		40.95	0.020
2009-10-12	1.53	1.21		40.63	0.020
2009-11-01	1.53	1.25		40.91	0.020
2009-11-15	1.53	1.31		39.7	0.019
2010-01-14	1.53	1.25		35.11	0.017
2010-02-24	1.53	1.01		31.28	0.015
2010-03-08	1.53	1.16		35.3	0.017
2010-03-17	1.53	1.56		52.32	0.025
2010-05-08	1.53	1.11		48.65	0.023
2010-06-01	1.53	1.16		46.59	0.022
2010-06-15	1.53	1.50		59.58	0.029
2010-10-23	1.9594	2.41		80.22	0.024
2010-11-08	1.9723	2.46		83.67	0.024

Pipe Series 2b

Date	Flow	Initial Head	Head Loss		Friction Factor
			PT1	PT2	Measured
	L/sec	m	mm	mm	[-]
2009-09-13	2.28			70.19	0.015
2009-09-16	2.1			73.23	0.018
2009-09-16	2.26			72.32	0.015
2009-09-30	1.53	1.33		40.07	0.018
2009-10-12	1.55	1.35		41.15	0.018
2009-11-01	1.53	1.07		34.1	0.016
2009-11-15	1.53	1.10		33.63	0.015
2010-01-14	1.53	1.25		59.15	0.027
2010-02-24	1.52	1.40		35.68	0.017
2010-03-08	1.53	1.44		47.19	0.022
2010-03-17	1.53	1.61		47.76	0.022
2010-05-08	1.53	1.13		43.94	0.020
2010-06-01	1.53	1.19		44.55	0.020
2010-06-15	1.53	1.18		47.94	0.022
2010-10-23	1.53	1.46		45.99	0.021
2010-11-08	1.53	1.64		51.88	0.024

Pipe Series 3a						Pipe Series 3b					
			Head Loss		Friction Factor				Head Loss		Friction Factor
Date	Flow	Initial Head	PT1	PT2	Measured	Date	Flow	Initial Head	PT1	PT2	Measured
	L/sec	m	mm	mm	[-]		L/sec	m	mm	mm	[-]
2009-09-16	0.97	0.65		14.23	0.017	2009-09-16	1.03	0.55		12.27	0.014
2009-09-16	1.03	0.77		15.98	0.017	2009-09-16	1.1	0.64		13.96	0.014
2009-09-30	0.95	0.50		13.04	0.016	2009-09-30	0.96	0.31		9.91	0.013
2009-10-12	0.84	0.32		7.24	0.011	2009-10-12	0.96	0.51		7.28	0.010
2009-10-21	0.8	0.25	11.08		0.019	2009-10-21	0.96	0.66	12.93		0.017
2009-10-30	0.77	0.23	9.96		0.019	2009-10-30	0.97	0.53	10.87		0.014
2009-11-18	0.77	0.25	8.41		0.016	2009-11-18	0.98	0.55	10.03		0.013
2010-03-03	0.97	0.53	19.23		0.023	2010-03-03	0.57	0.10	11.05		0.041
2010-03-15	0.95	0.47	17.85		0.022	2010-03-15	0.65	0.15	5.55		0.016
2010-05-15	0.95	0.50	22.87		0.028	2010-05-15	0.81	0.39	15.45		0.028
2010-06-01	0.95	0.61	19.02		0.023	2010-06-01	0.76	0.34	12.73		0.027
2010-06-16	0.95	0.61	18.44		0.023	2010-06-16	0.96	0.72		32.40	0.042
2010-10-29	0.98	0.72		21.52	0.025	2010-10-29	0.93	0.55		17.42	0.024
2010-11-13	0.98	0.66		17.40	0.020	2010-11-13	0.96	0.63		16.82	0.022

Pipe Series 4a

Date	Flow	Initial Head	Head Loss		Friction Factor
			PT1	PT2	Measured
	L/sec	m	mm	mm	[-]
2009-09-14	0.85	0.71		1.38	0.004
2009-09-14	1.6	1.24		1.71	0.001
2009-09-30	1.08	0.36		-2.32	-0.004
2009-10-14	0.98	-			
2009-10-18	1.01	0.67		-2.98	-0.007
2009-11-01	1.18	0.47	-0.49		-0.001
2009-11-15	1.16	0.45	-0.91		-0.002
2010-02-23	1.61	0.98	-0.06		0.000
2010-03-02	1.63	1.13	-6.76		-0.006
2010-03-10	1.61	1.06	6.66		0.006
2010-03-10	1.61	1.06	-1.20		-0.001
2010-05-08	1.61	1.13	4.28		0.004
2010-06-01	1.61	1.12	1.94		0.002
2010-06-15	1.61	1.25	0.86		0.001
2010-10-27	1.61	0.99		-1.12	-0.001
2010-11-16	1.61	0.96		-3.39	-0.003

Pipe Series 4b

Date	Flow	Initial Head	Head Loss		Friction Factor
			PT1	PT2	Measured
	L/sec	m	mm	mm	[-]
2009-09-14	1.42	0.92		2.29	0.003
2009-09-14	1.6	1.05		3.93	0.003
2009-09-30	0.65	0.62		-1.81	-0.010
2009-10-14	0.98	0.70		-0.62	-0.001
2009-11-01	0.91	1.39	6.26		0.017
2009-11-15	1.29	0.31	-0.98		-0.001
2010-02-23	1.63	1.20	-0.3		0.000
2010-03-02	1.63	1.08	-2.89		-0.002
2010-03-10	1.61	1.01	6.46		0.006
2010-03-10	1.61	1.01	-0.46		0.000
2010-05-08	1.64	0.84	4.51		0.004
2010-06-01	1.63	1.16	1.734		0.001
2010-06-15	1.61	1.06	1.551		0.001
2010-10-27	1.63	1.36		-0.98	-0.001
2010-11-16	1.63	0.83		-2.43	-0.002

Pipe Series 5a						Pipe Series 5b					
			Head Loss		Friction Factor				Head Loss		Friction Factor
Date	Flow	Initial Head	PT1	PT2	Measured	Date	Flow	Initial Head	PT1	PT2	Measured
	L/sec		mm	mm	[-]		L/sec	m	mm	mm	[-]
2009-09-16	1.69	1.32		0.84	0.001	2009-09-16	1.73	1.45		1.22	0.001
2009-09-16	1.82	1.64		0.93	0.001	2009-09-16	1.77	1.50		1.11	0.001
2009-09-30	1.4	0.59		0.61	0.001	2009-09-30	1.4	0.61		0.53	0.001
2009-10-12	1.44	0.55		-2.13	-0.002	2009-10-12	1.44	0.70		-2.2	-0.002
2009-10-21	1.42	0.55	1.06		0.001	2009-10-21	1.42	0.70	0.98		0.001
2009-10-30	1.41	0.53	-0.02		0.000	2009-10-30	1.4	0.54	-0.01		0.000
2009-11-18	1.41	0.55	-1.96		-0.002	2009-11-18	1.4	0.63	-1.61		-0.002
2010-02-24	1.47	0.55	2.28		0.002	2010-02-24	1.4	0.59	2.28		0.003
2010-03-06	1.41	0.54	6.29		0.007	2010-03-06	1.4	0.58	6.37		0.007
2010-03-14	1.41	0.63	2.24		0.003	2010-03-14	1.4	0.59	2.09		0.002
2010-05-15	1.41	0.66	2.98		0.003	2010-05-15	1.4	0.64	2.75		0.003
2010-06-01	1.41	0.67	2.10		0.002	2010-06-01	1.41	0.58	1.82		0.002
2010-06-16	1.41	0.60	2.015		0.002	2010-06-16	1.4	0.67	2.75		0.003
2010-10-29	0.72	0.02		-2.67	-0.011	2010-10-29	0.95	0.18		0.53	0.001
2010-11-13	1.406	0.57		-2.42	-0.003	2010-11-13	1.40	0.52		-1.52	-0.002

Pipe Series 6a

Date	Flow	Initial Head	Head Loss PT1	Head Loss PT2	Friction Factor Measured
	L/sec	m	mm	mm	[-]
2009-09-13	0.89			1.02	0.003
2009-09-16	0.87			3.48	0.010
2009-09-16	0.94	0.37		-0.14	0.000
2009-09-30	0.84	0.17		-1.57	-0.005
2009-10-12	0.86	0.16		-2.74	-0.008
2009-11-01	0.85	0.19	-0.14		0.000
2009-11-15	0.84	0.18	0.86		0.003
2010-01-14	0.85	0.18		-9.41	-0.029
2010-02-24	0.84	0.12	0.02		0.000
2010-03-08	0.84	0.15	6.77		0.021
2010-03-12	0.84	0.15	0.08		0.000
2010-03-17	0.84	0.06	-0.31		-0.001
2010-05-08	0.84	0.08	4.589		0.014
2010-06-01	0.84	0.13	1.491		0.005
2010-06-15	0.84	0.09	-0.19		-0.001
2010-10-27	0.82	0.30		-2.47	-0.008
2010-11-12	0.85	0.22		-2.71	-0.008

Pipe Series 6b

Date	Flow	Initial Head	Head Loss PT1	Head Loss PT2	Friction Factor Measured
	L/sec	m	mm	mm	[-]
2009-09-13	0.95			1.46	0.003
2009-09-16	0.89			3.23	0.009
2009-09-16	0.95			2.93	0.007
2009-09-16	0.98	0.38		0.33	0.001
2009-09-30	0.84	0.16		-1.52	-0.005
2009-10-12	0.84	0.11		-1.73	-0.005
2009-11-01	0.84	0.14	-0.14		0.000
2009-11-15	0.84	0.08	-1.62		-0.005
2010-01-14	0.85	0.09		-8.55	-0.025
2010-02-24	0.84	0.11	0.36		0.001
2010-03-08	0.84	0.13	6.32		0.019
2010-03-12	0.84	0.13	0.46		0.001
2010-03-17	0.84	0.10	1.501		0.005
2010-03-17	-	0.00	1.472		0.004
2010-05-08	0.84	0.09	4.55		0.014
2010-06-01	0.84	0.11	1.009		0.003
2010-06-15	0.84	0.19	1.052		0.003
2010-10-27	0.84	0.15		-0.43	-0.001
2010-11-12	0.84	0.17		-0.21	-0.001

Pipe Series 7a

Date	Flow	Initial Head	Head Loss PT1	Head Loss PT2	Friction Factor Measured
	L/sec	m	mm	mm	[-]
2009-09-16	0.26	0.08		0.73	0.037
2009-09-16	0.33	0.07		0.56	0.018
2009-09-30	0.38	0.04		0.11	0.003
2009-10-14	0.32	0.05		-2.67	-0.090
2009-10-21	0.32	0.06	-0.25		-0.008
2009-10-30	0.33	0.06	-0.97		-0.031
2009-11-18	0.34	0.06	-2.22		-0.066
2010-02-24	0.32	0.08	1.38		0.046
2010-03-15	0.32	0.08	-1.40		-0.047
2010-06-01	0.32	0.07	0.92		0.031
2010-06-16	0.32	0.08	1.15		0.039
2010-10-29	0.32	0.03		0.025	0.001
2010-11-13	0.17	-0.01		-2.67	-0.315

Pipe Series 7b

Date	Flow	Initial Head	Head Loss PT1	Head Loss PT2	Friction Factor Measured
	L/sec	m	mm	mm	[-]
2009-09-16	0.22	0.09		0.49	0.033
2009-09-16	0.32	0.09		0.93	0.030
2009-09-30	0.37	0.06		0.28	0.007
2009-10-14	0.23	0.01		-2.89	-0.180
2009-10-18	0.22	0.02		-3.21	-0.219
2009-10-19	0.22	0.11		-3.45	-0.235
2009-10-21	0.19	0.11	-0.35		-0.032
2009-10-30	0.2	0.11	0.06		0.005
2009-11-18	0.2	0.12	-2.31		-0.190
2010-02-24	0.18	0.13	1.14		0.116
2010-03-15	0.26	0.13	-1.58		-0.077
2010-06-01	0.19	0.12	0.7		0.064
2010-06-16	0.31	0.09	1.193		0.041
2010-10-29	0.31	0.00		0.08	0.003
2010-11-13	0.31	0.01		-2.04	-0.072

Pipe Series 8a

Date	Flow	Initial Head	Head Loss		Friction Factor
			PT1	PT2	Measured
	L/sec	m	mm	mm	[-]
2009-09-16	0.14	0.13		1.17	0.191
2009-09-16	0.18	0.13		0.86	0.085
2009-09-30	0.18	0.10		-0.3	-0.030
2009-10-14	0.16	0.00		-3.05	-0.381
2009-10-18	0.16	0.00		-3.17	-0.396
2009-10-19	0.16	0.14		-0.63	-0.079
2009-10-21	0.16	0.13	0.1		0.012
2009-10-30	0.16	0.14	0.51		0.064
2009-11-18	0.18	0.13	-2.49		-0.246
2010-03-03	0.16	0.13	4.99		0.624
2010-03-14	0.16	0.13	-0.09		-0.011
2010-06-01	0.16	-0.01	1.44		0.179
2010-06-16	0.16	0.01	1.421		0.177
2010-10-29	0.16	0.00		-0.34	-0.042
2010-11-13	0.1644	0.04		-2.55	-0.302

Pipe Series 8b

Date	Flow	Initial Head	Head Loss		Friction Factor
			PT1	PT2	Measured
	L/sec	m	mm	mm	[-]
2009-09-16	0.15	0.14		-1	-0.142
2009-09-16	0.17	0.14		0.63	0.070
2009-09-30	0.18	0.10		-0.04	-0.004
2009-10-14	0.16	0.10		-2.75	-0.343
2009-10-21	0.16	0.06	0.82		0.102
2009-10-30	0.15	0.11	-0.49		-0.070
2009-11-18	0.14	0.09	-1.75		-0.285
2010-03-03	0.16	0.07	4.93		0.615
2010-03-14	0.16	0.08	-0.39		-0.049
2010-06-01	0.16	0.09	1.01		0.126
2010-06-16	0.16	0.10	1.77		0.221
2010-10-29	0.16	0.10		-0.42	-0.053
2010-11-13	0.16	0.13		-2.06	-0.245

APPENDIX K : PHOTOGRAPHS OF PUMP CLOGGED AFTER 9 MONTHS OF OPERATION AND CHEMICAL CLEANING ATTEMPT.

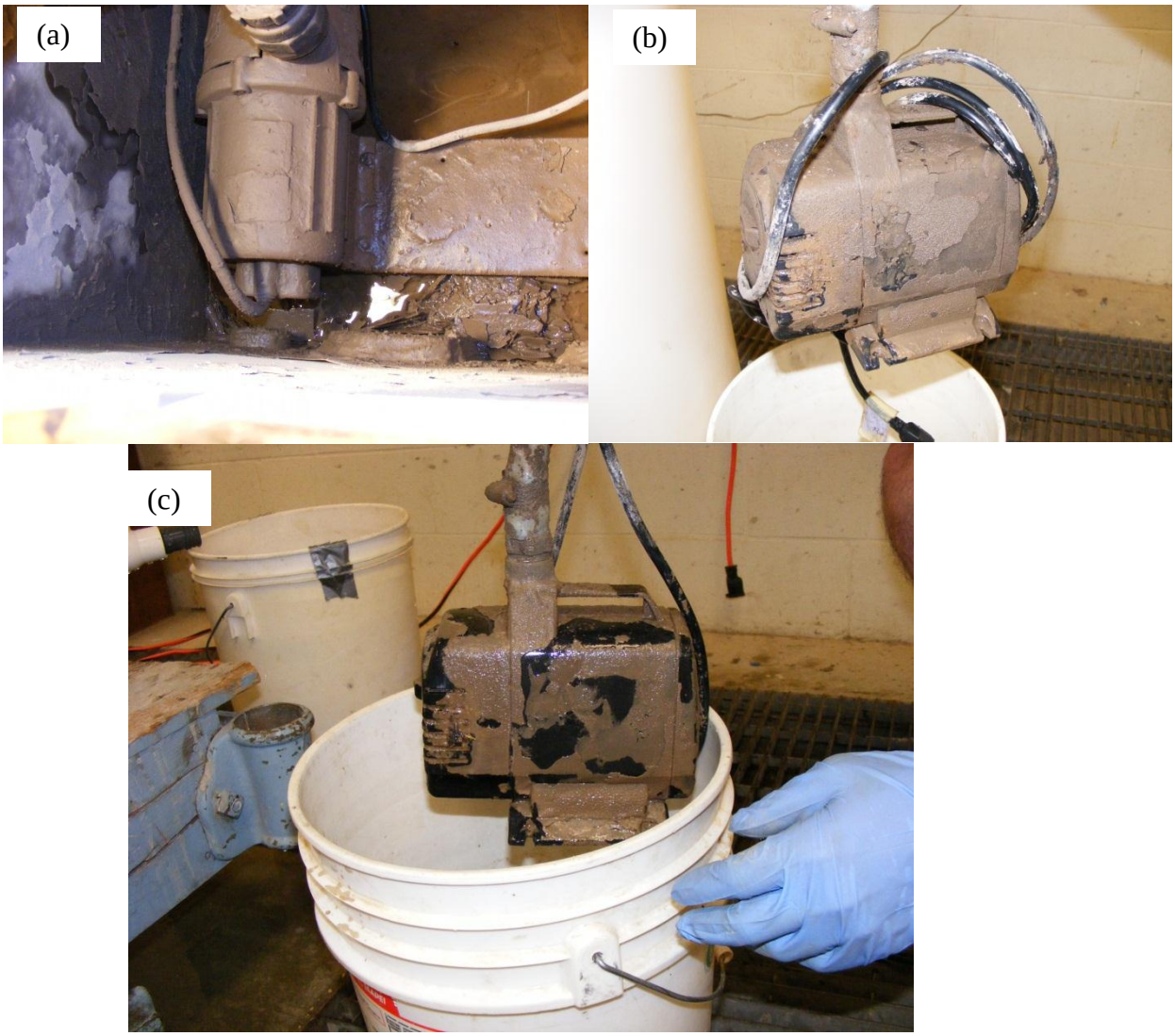

Figure (a) shows the pump totally coated on clogging inside of the feeding tank at the field study after 9 months of operation. Figure (b) shows the pump prior chemical cleaning at environmental engineering laboratory at the University of Manitoba and (c) shows the pump after 15 min of chemical cleaning.

APPENDIX L : PHOTOGRAPHS OF CLOG ACCUMULATED AND COLLECTED FROM PIPE INLET AND OUTLET AFTER PUMPS WERE TURNED OFF

Figure (d) shows the tool built at the mechanical engineering laboratory to collect clogging from the inlet and outlet of the pipe series at 13 cm of distance inside of the pipes. Figure (e) shows how important was the difference of clogging accumulated between inlet versus outlet for the pipe series 8.

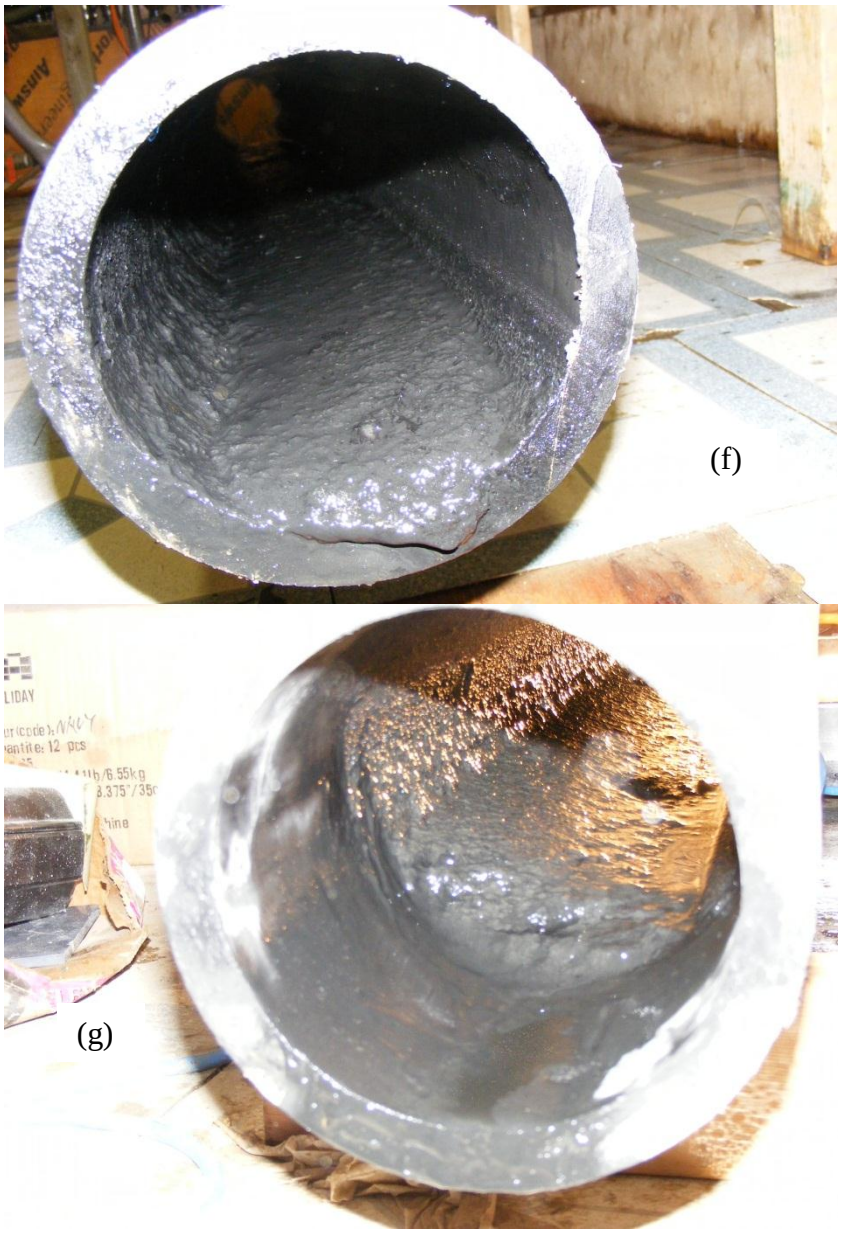

Figure (f) shows the clog accumulated within the pipe 7a after the pumps were turned off. Figure (g) shows the performance of the tool shown in (d) after clog was removed from the pipe outlet.

APPENDIX M : MIXER'S PHOTOGRAPHS

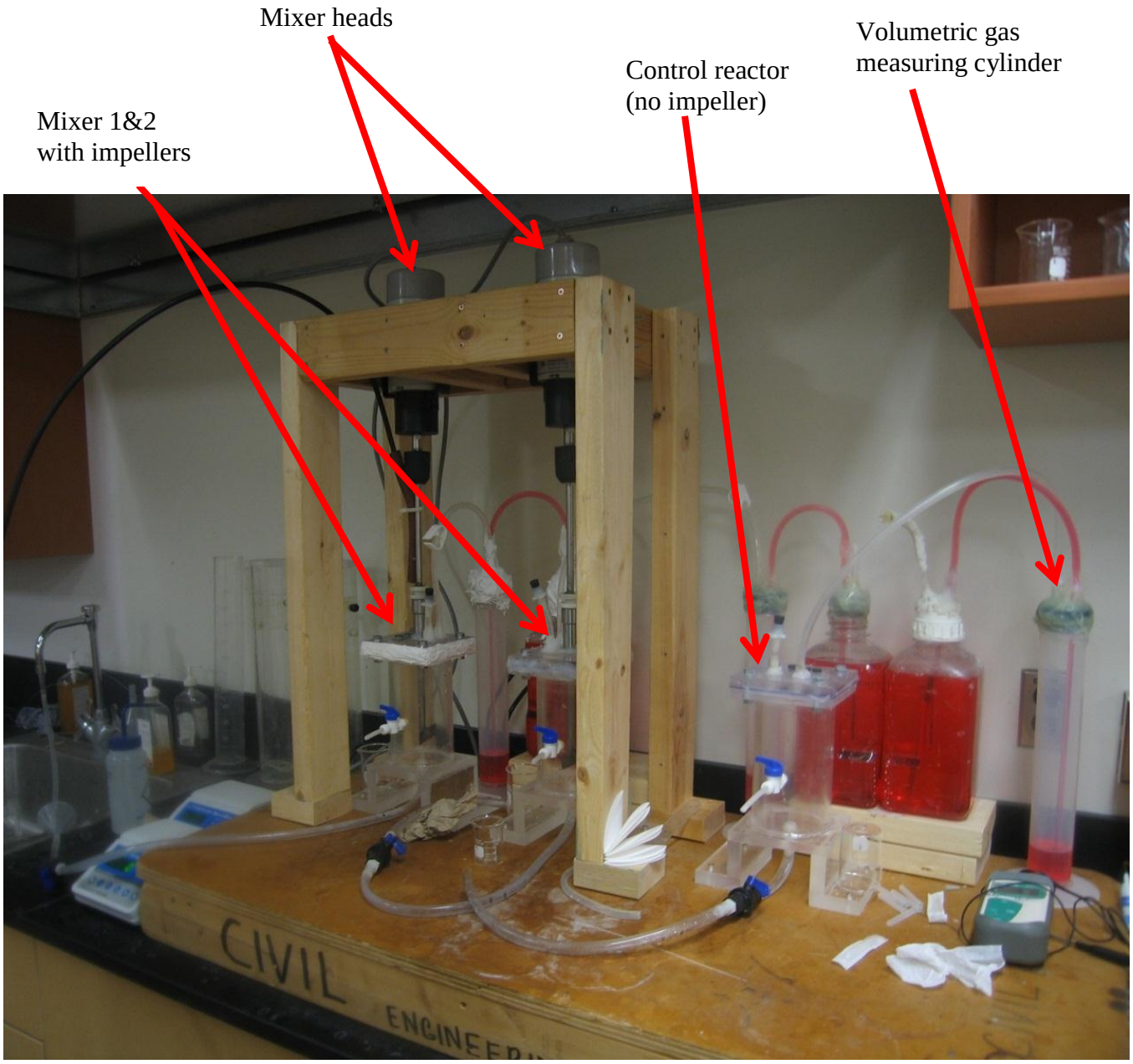

Figure a: Mixers set-up at the Environmental Engineering laboratory

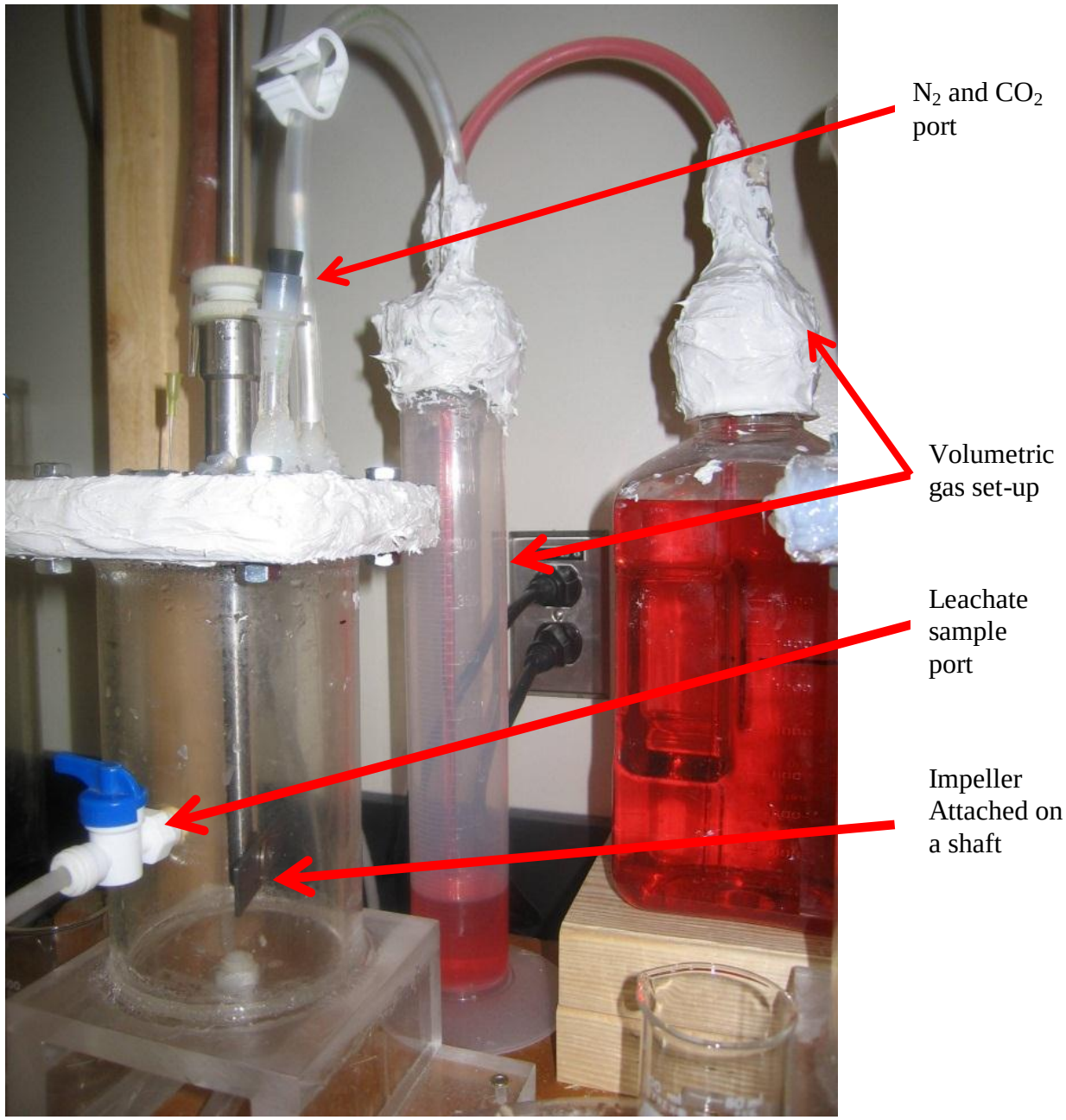

Figure b: Reactor configuration

APPENDIX N : REACTORS DATA

a. Evolved CO_2 (mL), pH and Ca^{2+} [mg/L] from the mixers after 6 hrs of operation at different mixing conditions (rpm's).

Parameter	Unit	0 rpm			32 rpm		83 rpm		180 rpm	
$CO_{2\ (gas)}$	mL	2.74	1.7	2.86	8.81	8.09	8.83	8.46	11.26	10.21
pH	-	7.06	7.02	7	7.06	7.08	7.01	7.03	7.01	7.03
Temperature	(˚C)	21.7	22	21.6	21.6	21.8	22	21.9	22.3	22.4
Ca^{2+}	[mg/L]	1072	1040	1064	1064	1056	1032	1048	1055	1048

b. pH, temperature (˚C) and Ca^{2+} [mg/L] values from the mixers after 18 hrs of atmospheric exposure after different mixing conditions (rpm's) were performed.

Parameter	Unit	0 rpm			32 rpm		83 rpm		180 rpm	
pH	-	8.14	8.06	7.89	8.12	8.14	8.12	8.18	8.1	8.23
Temperature	(˚C)	21.8	20.9	21	21.1	21.3	20.7	20.9	21.6	21.3
Ca^{2+}	[mg/L]	160	164	180	180	186	140	146	136	150.4
		168	204	196	174	166	166	168	128	122

c. pH, dissolved Ca^{2+} (mg/L), CO_2 evolved and temperature values of real leachate from the mixers and control reactor under sealed conditions

	T = 0 hrs			T = 6 hrs				T = 24 hrs		
	pH	T	Ca^{2+}	pH	T	Ca^{2+}	CO_2 [mL]	pH	T	Ca^{2+}
Mixer 1	7.47	13	390	7.4	23	390	8.20	7.04	22.9	280
Mixer 2	7.48	15	380	7.39	23	380	8.17	7.11	22.8	280
Control	7.48	15	380	7.33	23	360	0.87	7.17	23	340

	T = 0 hrs			T = 6 hrs				T = 24 hrs		
	pH	T	Ca^{2+}	pH	T	Ca^{2+}	CO_2 [mL]	pH	T	Ca^{2+}
Mixer 1	7.56	15	380	7.6	23	360	4.96	7.25	22	224
Mixer 2	7.57	16	360	7.57	23	350	3.61	7.26	21.9	224
Control	7.57	18	370	7.55	22	320	0.42	7.26	21.8	224

d. pH, dissolved Ca^{2+} (mg/L) and temperature (˚C) values of real leachate from the mixers and control reactor after being exposed to atmospheric conditions for 18 hrs after being mixed for 6 hrs at 180 rpm.

		Study a			Study b		
Time	Reactor	pH	T	Ca^{2+}	pH	T	Ca^{2+}
T = 24 hrs	Mixer 1	7.8	22.3	132	7.8	21.5	192
	Mixer 2	7.86	22.2	144	7.86	21.3	200
	Control	7.78	22.2	152	7.78	21.4	200

APPENDIX O : REAL LEACHATE TREATMENT USING METHANOGENESIS: SET-UP AND DATA

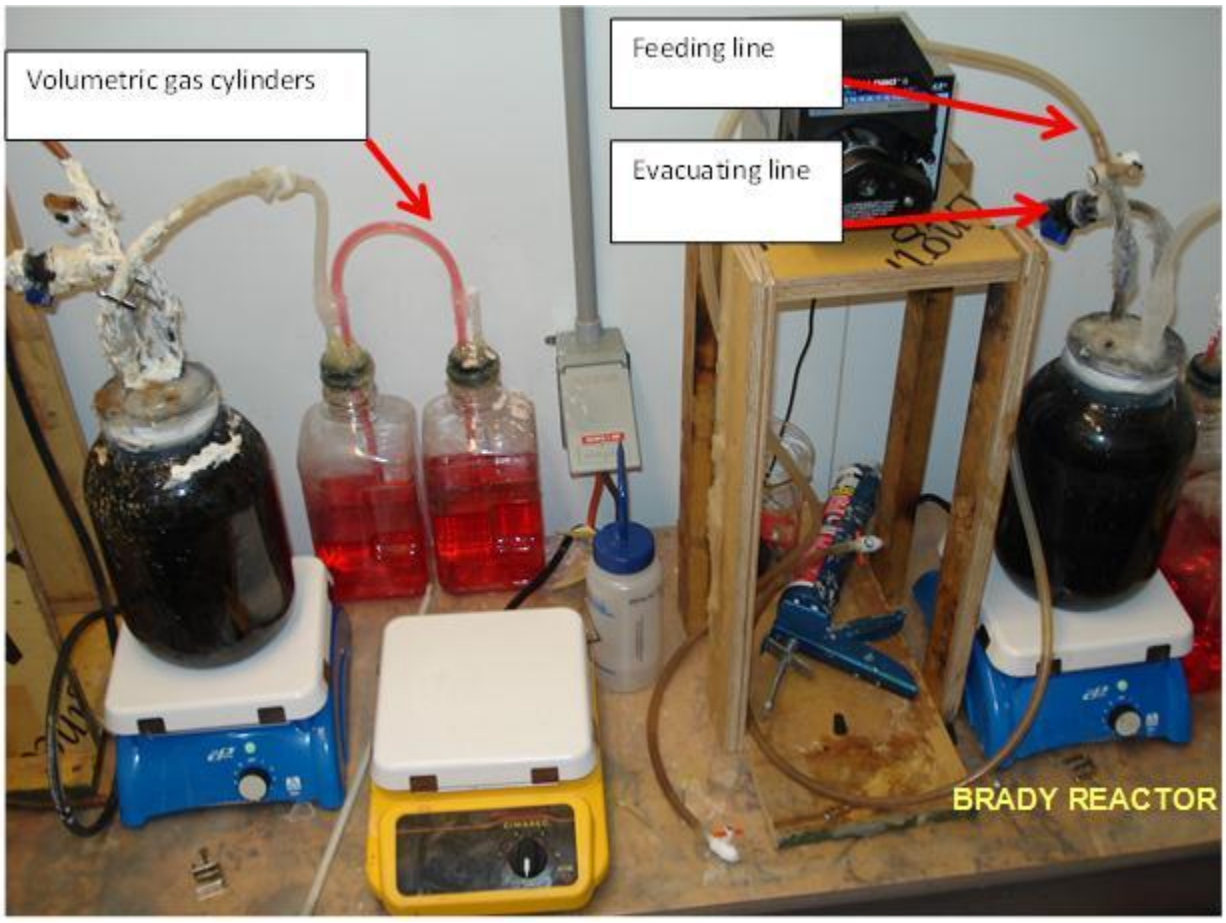

Figure. Set up of SBR and liquid displacement jars

APPENDIX P : REAL LEACHATE TREATMENT USING METHANOGENESIS - DATA

a. Total COD and soluble COD removed sampled from the digester between cycles over time

Date	TCOD [mg/L]		sCOD [mg/L]		Date	TCOD [mg/L]		sCOD [mg/L]	
	Influent	Effluent	Influent	Effluent		Influent	Effluent	Influent	Effluent
10-Jul-08	6720	3690	1710	1950	5-Aug-08	3120	2160	2610	1117.5
11-Jul-08	7237.5	8377.5	3022.5	2377.5	7-Aug-08	2812.5	2070	2152.5	1252.5
12-Jul-08	6780	6412.5	2655	2602.5	9-Aug-08	2902.5	2587.5	1995	1417.5
13-Jul-08	6345	6705	2452.5	3540	11-Aug-08	3457.5	1770	2602.5	1117.5
14-Jul-08	6210	6180	3082.5	2917.5	13-Aug-08	2977.5	1912.5	1957.5	1207.5
15-Jul-08	5865	6465	3300	3052.5	15-Aug-08	2782.5	1747.5	2107.5	1027.5
16-Jul-08	5332.5	5272.5	3315	2692.5	17-Aug-08	2842.5	2160	2235	1657.5
17-Jul-08	4882.5	4725	2895	2670	23-Aug-08	3547.5	2085	2460	1297.5
18-Jul-08	4192.5	4905	3150	2955	29-Aug-08	3705	2640	3480	1590
19-Jul-08	4350	-	3090	-	31-Aug-08	2797.5	1972.5	1462.5	1222.5
20-Jul-08	-	-	-	-	2-Sep-08	2437.5	2572.5	2287.5	1245
21-Jul-08	-	3862.5	-	3652.5	4-Sep-08	3195	2715	1875	1222.5
22-Jul-08	4282.5	3525	2977.5	2707.5	6-Sep-08	3015	1282.5	2437.5	630
23-Jul-08	3472.5	3157.5	2430	2197.5	8-Sep-08	2940	1432.5	2565	1380
24-Jul-08	3187.5	2767.5	2535	2235	10-Sep-08	2625	2100	2107.5	1372.5
25-Jul-08	3277.5	3345	2452.5	2197.5	12-Sep-08	3727.5	2677.5	2655	1770
26-Jul-08	3067.5	-	2902.5	-	14-Sep-08	3555	1725	3067.5	1380
27-Jul-08	-	-	-	-	16-Sep-08	2700	1837.5	2047.5	1305
28-Jul-08	3660	3060	2940	2355	18-Sep-08	2707.5	1762.5	1837.5	1200
29-Jul-08	3300	2872.5	2805	2775	22-Sep-08	2220	1710	1012.5	472.5
30-Jul-08	3345	3397.5	2662.5	2062.5	26-Sep-08	4762.5	3307.5	4762.5	3307.5
31-Jul-08	3555	3135	3105	2835	28-Sep-08	4762.5	3225	4762.5	3225
2-Aug-08	3060	3180	2205	1890	30-Sep-08	5422.5	2842.5	5422.5	2842.5

Date	TCOD [mg/L]		sCOD [mg/L]		Date	TCOD [mg/L]		sCOD [mg/L]	
	Influent	Effluent	Influent	Effluent		Influent	Effluent	Influent	Effluent
2-Oct-08	6315	2910	6315	2910	27-Nov-08	9495	0	4800	0
4-Oct-08	5745	3705	5745	3705	29-Nov-08	7222.5	4882.5	4327.5	2370
6-Oct-08	5872.5	2325	5872.5	2325	1-Dec-08	6937.5	5070	3960	2092.5
8-Oct-08	4920	2655	4920	2655	3-Dec-08	7740	4980	4500	2137.5
10-Oct-08	8077.5	4785	8077.5	4785	5-Dec-08	6645	4935	4215	1927.5
12-Oct-08	9645	5295	9645	5295	7-Dec-08	6870	5437.5	3907.5	2085
14-Oct-08	9510	4965	9510	4087.5	9-Dec-08	7080	5085	4125	2182.5
16-Oct-08	8932.5	5505	8932.5	5505	24-Dec-08	6322.5	4237.5	3007.5	1245
18-Oct-08	9915	5047.5	9915	3337.5	2-Jan-09	6720	4687.5	3360	1147.5
28-Oct-08	9592.5	6217.5	7522.5	3855	12-Jan-09	6810	4500	3810	1035
30-Oct-08	8205	5730	8205	2970	18-Jan-09	6772.5	4410	3285	885
1-Nov-08	10680	5490	8010	3135					
3-Nov-08	10440	5745	7740	3742.5					
5-Nov-08	10710	5422.5	8430	3682.5					
9-Nov-08	6060	6517.5	3382.5	3247.5					
11-Nov-08	9885	6225	7365	3285					
13-Nov-08	10042.5	6637.5	7672.5	5325					
15-Nov-08	10222.5	7050	7837.5	5910					
17-Nov-08	9592.5	6165	6975	3195					
19-Nov-08	7777.5	5880	5272.5	3105					
21-Nov-08	7605	6787.5	4830	2820					
23-Nov-08	7777.5	6555	4800	3600					
25-Nov-08	7905	6622.5	4440	2895					

b. Variation in pH within the digester versus time

Date	pH		Date	pH		Date	pH		Date	pH	
	Influent	Effluent		Influent	Effluent		Influent	Effluent		Influent	Effluent
10-Jul-08	7.39	7.53	5-Aug-08	7.41	7.45	2-Oct-08	7.19	7.47	27-Nov-08	7.16	7.42
11-Jul-08	7.43	7.3	7-Aug-08	7.43	7.57	4-Oct-08	7.28	7.53	29-Nov-08	7.22	7.44
12-Jul-08	7.24	7.51	9-Aug-08	7.46	7.42	6-Oct-08	7.31	7.59	1-Dec-08	7.2	7.54
13-Jul-08	7.43	7.54	11-Aug-08	7.41	7.75	8-Oct-08	7.46	7.55	3-Dec-08	7.27	7.39
14-Jul-08	7.56	7.55	13-Aug-08	7.28	7.65	10-Oct-08	7.1	7.56	5-Dec-08	7.19	7.52
15-Jul-08	7.55	7.57	15-Aug-08	7.41	7.62	12-Oct-08	7.05	7.53	7-Dec-08	7.27	7.36
16-Jul-08	7.54	7.24	17-Aug-08	7.39	7.42	14-Oct-08	7.09	7.51	9-Dec-08	7.23	7.42
17-Jul-08	7.16	7.37	23-Aug-08	7.25	7.39	16-Oct-08	7.08	7.54	24-Dec-08	7.23	7.47
18-Jul-08	7.17	7.3	29-Aug-08	7.37	7.36	18-Oct-08	7.21	7.57	2-Jan-09	7.24	7.37
19-Jul-08	7.21	-	31-Aug-08	7.38	7.39	28-Oct-08	7.19	7.62	12-Jan-09	7.2	7.56
20-Jul-08	-	-	2-Sep-08	7.28	7.31	30-Oct-08	6.99	7.4	18-Jan-09	7.34	7.55
21-Jul-08	-	7.14	4-Sep-08	7.31	7.28	1-Nov-08	7.05	7.5			
22-Jul-08	7.25	7.19	6-Sep-08	7.3	7.31	3-Nov-08	7.11	7.48			
23-Jul-08	7.3	7.22	8-Sep-08	7.26	7.25	5-Nov-08	7.01	7.56			
24-Jul-08	7.38	7.26	10-Sep-08	7.25	7.3	9-Nov-08	7.23	7.29			
25-Jul-08	7.43	7.29	12-Sep-08	7.31	7.29	11-Nov-08	6.97	7.42			
26-Jul-08	7.37	-	14-Sep-08	7.27	7.24	13-Nov-08	7.2	7.36			
27-Jul-08	-	-	16-Sep-08	7.23	7.29	15-Nov-08	7.19	7.27			
28-Jul-08	7.32	7.29	18-Sep-08	7.28	7.26	17-Nov-08	7.23	7.41			
29-Jul-08	7.37	7.41	22-Sep-08	7.28	7.29	19-Nov-08	7.2	7.43			
30-Jul-08	7.38	7.28	26-Sep-08	7.1	7.46	21-Nov-08	7.21	7.37			
31-Jul-08	7.34	7.49	28-Sep-08	7.1	7.45	23-Nov-08	7.23	7.3			
2-Aug-08	7.47	7.35	30-Sep-08	7.26	7.45	25-Nov-08	7.18	7.41			

c. Variation in (i) acetate, (ii) propionate and (iii) butyrate concentrations within the digester versus time

i. Variation in Acetate within the digester over time (mg/L)

Date	Acetate [mg/L]		Date	Acetate [mg/L]		Date	Acetate [mg/L]	
	Influent	Effluent		Influent	Effluent		Influent	Effluent
13-Jul-08	602	619.5	2-Sep-08	326	34	30-Oct-08	1074.9	43.5
14-Jul-08	592.5	653	4-Sep-08	156.5	27	1-Nov-08	1190.1	0
15-Jul-08	622	663.5	6-Sep-08	319.5	75	3-Nov-08	1064.1	38.1
16-Jul-08	608	684	8-Sep-08	370	24.5	5-Nov-08	1111.2	24.3
17-Jul-08	605	1863	10-Sep-08	284.5	0	9-Nov-08	891.9	23
18-Jul-08	1626	1492	12-Sep-08	288.5	0	11-Nov-08	931.5	21.7
22-Jul-08	747	709	14-Sep-08	294.5	0	13-Nov-08	906.1	1002.9
23-Jul-08	608.5	703	16-Sep-08	226	334.5	15-Nov-08	1525.2	856.9
25-Jul-08	646.5	731.5	18-Sep-08	546	24.1	17-Nov-08	1052	0
29-Jul-08	498.5	656	22-Sep-08	425	33.7	19-Nov-08	697.4	72.9
30-Jul-08	524.5	603	26-Sep-08	622.3	70.9	21-Nov-08	577	52.5
31-Jul-08	516	622.5	28-Sep-08	634	205.9	23-Nov-08	708.2	38
2-Aug-08	505	419	30-Sep-08	664.9	0	25-Nov-08	555.1	36.6
5-Aug-08	393.5	298	2-Oct-08	596.4	0	27-Nov-08	668.3	34.6
7-Aug-08	348	222.5	4-Oct-08	608.8	16.1	29-Nov-08	767	121
9-Aug-08	320.5	312.5	6-Oct-08	631	0	1-Dec-08	639.8	37.8
11-Aug-08	283	540.5	8-Oct-08	1025.7	0	3-Dec-08	630.3	41
13-Aug-08	366.5	500	10-Oct-08	1087.1	390.5	5-Dec-08	623.9	43.2
15-Aug-08	2299.5	4710	12-Oct-08	1275.4	381.9	7-Dec-08	615	0
17-Aug-08	4749.5	317.5	14-Oct-08	1195.4	378.7	9-Dec-08	627.6	22.7
23-Aug-08	360	39	16-Oct-08	1160.7	1110.5	24-Dec-08	661.6	98.2
29-Aug-08	298.5	73.5	18-Oct-08	952.7	1110.5	2-Jan-09	786.8	40.6
31-Aug-08	316.5	132.5	28-Oct-08	1137.5	0	12-Jan-09	782.8	60.3

ii. Variation in Butyrate within the digester over time (mg/L)

Date	Butyrate [mg/L]		Date	Butyrate [mg/L]		Date	Butyrate [mg/L]	
	Influent	Effluent		Influent	Effluent		Influent	Effluent
13-Jul-08	136	91.50	2-Sep-08	136.5	44	30-Oct-08	1085.1	51.5
14-Jul-08	137	92.00	4-Sep-08	59	22	1-Nov-08	1043.8	0
15-Jul-08	137	71.00	6-Sep-08	43	2141	3-Nov-08	1113.1	0
16-Jul-08	120	62.00	8-Sep-08	96	0	5-Nov-08	721.5	0
17-Jul-08	101	748.50	10-Sep-08	43.5	0	9-Nov-08	928	0
18-Jul-08	660	548.00	12-Sep-08	46.5	0	11-Nov-08	924.1	0
22-Jul-08	315.5	218.5	14-Sep-08	46	0	13-Nov-08	897.7	37.5
23-Jul-08	215.5	194.5	16-Sep-08	42	24	15-Nov-08	744.7	152.7
25-Jul-08	44	49	18-Sep-08	100	5.4	17-Nov-08	587	0
29-Jul-08	129	147.5	22-Sep-08	18.5	6.6	19-Nov-08	547.4	0
30-Jul-08	140	142.5	26-Sep-08	350.3	0	21-Nov-08	314.1	0
31-Jul-08	132.5	139	28-Sep-08	298.5	0	23-Nov-08	362	0
2-Aug-08	118.5	120	30-Sep-08	282.8	0	25-Nov-08	283.9	0
5-Aug-08	119	127	2-Oct-08	274.2	0	27-Nov-08	346.3	0
7-Aug-08	86.5	52.5	4-Oct-08	320.4	0	29-Nov-08	388.7	0
9-Aug-08	102.5	113.5	6-Oct-08	334.7	0	1-Dec-08	347.9	0
11-Aug-08	115	90.5	8-Oct-08	757.6	0	3-Dec-08	255.9	0
13-Aug-08	101	507.5	10-Oct-08	756.9	0	5-Dec-08	303.2	0
15-Aug-08	1151	5306	12-Oct-08	705.6	13.2	7-Dec-08	234.1	0
17-Aug-08	3741.5	41.5	14-Oct-08	674.4	14.6	9-Dec-08	301.9	0
23-Aug-08	26.5	0	16-Oct-08	720.4	38.7	24-Dec-08	268.2	43.9
29-Aug-08	52	32.5	18-Oct-08	715.4	38.7	2-Jan-09	204.7	24.7
31-Aug-08	81	61	28-Oct-08	1210.5	0	12-Jan-09	180.3	38.2

iii. Variation in Propionate within the digester over time (mg/L)

Date	Propionate [mg/L]		Date	Propionate [mg/L]		Date	Propionate [mg/L]	
	Influent	Effluent		Influent	Effluent		Influent	Effluent
13-Jul-08	208	167.50	2-Sep-08	185.5	114.5	30-Oct-08	1064.7	984.9
14-Jul-08	220	172.50	4-Sep-08	100.5	105.5	1-Nov-08	1092.6	989.2
15-Jul-08	197	178.50	6-Sep-08	112.5	3041	3-Nov-08	1100.3	816.6
16-Jul-08	188	158.00	8-Sep-08	149	65	5-Nov-08	788	883.4
17-Jul-08	166	276.00	10-Sep-08	78.5	66.5	9-Nov-08	919.8	962.2
18-Jul-08	374	330.00	12-Sep-08	88.5	65.5	11-Nov-08	929.8	893.4
22-Jul-08	259	261	14-Sep-08	98.5	58	13-Nov-08	871.9	714.8
23-Jul-08	207	215	16-Sep-08	86.5	255.5	15-Nov-08	816.1	834.2
25-Jul-08	162	177	18-Sep-08	241	34.3	17-Nov-08	915.5	0
29-Jul-08	165.5	210.5	22-Sep-08	93.6	46.3	19-Nov-08	1006	966
30-Jul-08	172.5	201	26-Sep-08	296.9	0	21-Nov-08	917.1	806.7
31-Jul-08	170.5	204	28-Sep-08	345.8	280.5	23-Nov-08	759.5	811.1
2-Aug-08	168.5	201	30-Sep-08	382.6	292.6	25-Nov-08	698.1	616.8
5-Aug-08	158.5	206.5	2-Oct-08	365	223.5	27-Nov-08	626.4	640.3
7-Aug-08	148	176	4-Oct-08	370.6	258.3	29-Nov-08	706	0
9-Aug-08	162	203	6-Oct-08	383.7	192.1	1-Dec-08	653.3	478.8
11-Aug-08	172	190	8-Oct-08	1265.6	194.9	3-Dec-08	515.6	367.1
13-Aug-08	153	536	10-Oct-08	643.5	455.7	5-Dec-08	517.7	448.7
15-Aug-08	1541	3155	12-Oct-08	735.1	593.4	7-Dec-08	523.2	418.6
17-Aug-08	3142	67.5	14-Oct-08	769.9	631.6	9-Dec-08	514	372
23-Aug-08	122	84.5	16-Oct-08	860.6	975.4	24-Dec-08	232.7	152.5
29-Aug-08	85	160.5	18-Oct-08	888.9	975.4	2-Jan-09	273.4	113.2
31-Aug-08	116	104	28-Oct-08	1090.9	989.8	12-Jan-09	233.9	147.6

d. Variation in total suspend solids (TSS) and volatile suspend solids (VSS) within the digester versus time

Date	TSS [mg/L]		VSS [mg/L]		Date	TSS [mg/L]		VSS [mg/L]	
	Influent	Effluent	Influent	Effluent		Influent	Effluent	Influent	Effluent
10-Jul-08	9590	11200		6300	5-Aug-08	3490	4810	710	870
11-Jul-08	7840	12770	4210	6660	7-Aug-08	4320	4080	890	850
12-Jul-08	7850	12670	3960	5850	9-Aug-08	4480	4980	1700	840
13-Jul-08	5590	5060	2840	2560	11-Aug-08	7210	4370	2550	760
14-Jul-08	4270	4570	2140	2340	13-Aug-08	4570	4250	800	750
15-Jul-08	3780	4060	1890	2070	15-Aug-08	5420	4280	1960	1210
16-Jul-08	9940	3880	4240	1790	17-Aug-08	4120	5460	1050	1310
17-Jul-08	4790	26900	2200	13320	23-Aug-08	5960	-	910	-
18-Jul-08	2540	26570	1220	13090	29-Aug-08	6090	6050	1750	1060
19-Jul-08	2430	-	1090	-	31-Aug-08	6140	5390	1220	980
20-Jul-08	-	-	-	-	2-Sep-08	4360	5470	1470	930
21-Jul-08	-	2630	-	1050	4-Sep-08	5050	6230	980	1230
22-Jul-08	2160	4050	850	1740	6-Sep-08	4930	22060	1380	8190
23-Jul-08	2420	2690	910	1060	8-Sep-08	4730	4860	900	730
24-Jul-08	9530	2560	4230	790	10-Sep-08	4750	4910	790	810
25-Jul-08	3700	2510	1470	730	12-Sep-08	4560	4830	770	630
26-Jul-08	2430	-	730	-	14-Sep-08	4410	4780	650	1410
27-Jul-08	-	-	-	-	16-Sep-08	4400	4880	1310	910
28-Jul-08	3250	10180	1280	4450	18-Sep-08	4440	4520	940	930
29-Jul-08	4400	3280	1730	930	22-Sep-08	5020	5130	1400	950
30-Jul-08	4040	3980	1650	800	26-Sep-08	5350	5900	-	-
31-Jul-08	3120	3540	700	940	28-Sep-08	5710	6300	2480	1800
2-Aug-08	3300	4240	900	720	30-Sep-08	5980	6510	1430	2400

Date	TSS [mg/L]		VSS [mg/L]		Date	TSS [mg/L]		VSS [mg/L]	
	Influent	Effluent	Influent	Effluent		Influent	Effluent	Influent	Effluent
2-Oct-08	6340	6800	1420	1410	27-Nov-08	15800	16500	3460	3260
4-Oct-08	6320	6830	1390	1480	29-Nov-08	15620	16660	3110	3240
6-Oct-08	6640	7150	1560	1500	1-Dec-08	16320	17810	3320	7710
8-Oct-08	6910	7430	1660	1490	3-Dec-08	17750	17280	5380	3990
10-Oct-08	7020	7900	1600	2410	5-Dec-08	17180	17140	4070	3590
12-Oct-08	15580	9030	5070	1950	7-Dec-08	16780	16860	3660	3110
14-Oct-08	8500	9410	1970	2720	9-Dec-08	16270	16320	3130	2860
16-Oct-08	8450	9980	2800	2340	24-Dec-08	16980	16970	3700	3540
18-Oct-08	9660	10410	2340	2280	2-Jan-09	19690	19180	3740	4690
28-Oct-08	12820	14000	3040	3450	12-Jan-09	19350	20260	3320	3890
30-Oct-08	13810	14660	3500	3140	18-Jan-09	20300	19790	3370	3300
1-Nov-08	13770	14770	3130	3210					
3-Nov-08	14470	15260	3360	5790					
5-Nov-08	14180	15100	5270	5310					
9-Nov-08	16600	16080	5060	3660					
11-Nov-08	15270	16070	3600	4550					
13-Nov-08	14770	11700	4250	3640					
15-Nov-08	15360	9010	4630	3530					
17-Nov-08	15610	15940	4260	3630					
19-Nov-08	15790	16640	3710	3660					
21-Nov-08	17410	16790	3870	4740					
23-Nov-08	16650	16210	4340	4310					
25-Nov-08	14870	16600	4400	4520					

e. Variation of (a) percentage of CH_4 and CO_2 within the biogas produced and (b) CH_4 produced per gram of COD removed within the digester versus time

Table (a)

Date	CH_4 [%]	CO_2 [%]
26-Jul-08	32.39	41.96
30-Jul-08	38.17	40.6
13-Aug-08	60.72	28
15-Aug-08	54.71	37.14
23-Aug-08	56.89	29.37
29-Aug-08	62.41	33.52
31-Aug-08	59.4	29.43
6-Sep-08	58.77	35.41
10-Sep-08	54.44	33.43
16-Sep-08	60.67	32.62
28-Sep-08	61.53	36.29
4-Oct-08	69.72	25.25
10-Oct-08	71.18	25.14
14-Oct-08	74.77	24.55
30-Oct-08	75.44	24.1
3-Nov-08	78.23	24.51
17-Nov-08	74.96	25.01
23-Nov-08	71.72	28.22
24-Dec-08	72.17	25.21

Table (b)

Date	L Ch_4/g COD removed [L/g]
13-Aug-08	0.44
15-Aug-08	0.43
23-Aug-08	0.33
31-Aug-08	0.58
28-Sep-08	0.35
4-Oct-08	0.43
14-Oct-08	0.26
30-Oct-08	0.61
3-Nov-08	0.24
5-Nov-08	0.29
11-Nov-08	0.33
17-Nov-08	0.23
19-Nov-08	0.36
21-Nov-08	0.84
23-Nov-08	0.64
25-Nov-08	0.49
27-Nov-08	0.06
29-Nov-08	0.30
1-Dec-08	0.15
3-Dec-08	0.24
5-Dec-08	0.45
7-Dec-08	0.41
9-Dec-08	0.32
24-Dec-08	0.35
2-Jan-09	0.40
12-Jan-09	0.35

f. Variation of pH and total soluble calcium within the reactor (separated study using synthetic leachate at open atmospheric conditions)

pH [-]	Dissolved Ca2+ mg/L
6.5	894
7	830
7.21	810
7.35	784
7.4	292
7.46	182
8.04	96

APPENDIX Q : SYNTHETIC LEACHATE TREATMENT - DATA

a. Acetate, butyrate, propionate, pH values and dissolved Ca^{2+} of synthetic leachate at 0, 24 and 48 h from tests 1, 2, 3, 4, 5 and 6 performed during week 1 and 2.

Acetate [mg/L]

Test 1				Test 2				Test 3			
t=0	t=24	t=48	t=72	t=0	t=24	t=48	t=72	t=0	t=24	t=48	t=72
2220	2700	2100	876	1800	1920	1020	0	1560	1560	1320	270
2460	3060	2160	848	1800	1920	960	0	1500	1620	1380	0
2400	2820	1800	1026	1860	1920	540	1114	1500	1500	840	0
2460	4260	1860	1040	1920	2040	540	1080	1560	1680	840	0
2400	2640	1860	1694	1800	1920	1320	0	1500	1740	0	0
2460	2640	1920	1707	1860	1980	1320	0	1560	1860	240	0

Acetate [mg/L]

Test 4				Test 5				Test 6			
t=0	t=24	t=48	t=72	t=0	t=24	t=48	t=72				
1796	1500	540	0	1085	1200	420	0	547	540	600	0
1932	1560	480	0	1144	1200	420	0	546	540	600	0
1513	1560	1380	0	1127	1080	1080	0	454	540	0	51.56
1572	1560	1260	0	1173	1140	1020	0	461	540	0	51.56
1653	1560	1560	0	1121	1200	1080	43.6	506	540	540	51.56
1718	1620	1500	0	1096	1140	1080	41.56	516	540	480	51.56

Propionate [mg/L]

Test 1				Test 2				Test 3			
t=0	t=24	t=48	t=72	t=0	t=24	t=48	t=72	t=0	t=24	t=48	t=72
592	592	518	587	1036	962	888	785	1776	1628	1628	1279
592	666	518	601	1036	888	888	796	1776	1628	1702	1312
592	740	444	671	1036	1036	814	831	1776	1554	1406	1323
592	888	444	623	1036	962	814	776	1776	1776	1480	1356
592	592	518	691	1036	962	962	902	1776	1850	1332	1445
592	518	444	699	962	962	962	919	1776	2072	1406	1448

Propionate [mg/L]											
Test 4				Test 5				Test 6			
t=0	t=24	t=48	t=72	t=0	t=24	t=48	t=72	t=0	t=24	t=48	t=72
1900	1628	1850	1332	2229	2072	1998	1406	3554	3626	2960	3256
1846	1702	1702	1480	2116	2220	1702	1332	3639	3700	3182	3626
1674	1628	1924	1258	2236	2294	1628	1480	2882	3700	3552	3256
1592	1554	1554	1480	2197	2294	1850	1480	2960	3626	3552	3478
1751	1702	1850	1554	2122	2220	1776	1998	3482	3552	3108	3108
1645	1702	1702	1554	2105	2146	1702	1924	3361	3478	3108	3256

Butyrate [mg/L]											
Test 1				Test 2				Test 3			
t=0	t=24	t=48	t=72	t=0	t=24	t=48	t=72	t=0	t=24	t=48	t=72
880	880	792	616	1056	880	616	486	1056	968	880	546
968	968	792	578	968	880	704	442	1144	880	968	580
968	1144	704	772	1056	968	616	644	1056	880	704	499
880	1408	704	696	968	880	528	781	1056	1056	704	514
880	880	704	862	968	968	792	196	1056	1056	528	701
968	792	704	864	968	880	792	195	1056	1144	616	426

Butyrate [mg/L]											
Test 4				Test 5				Test 6			
t=0	t=24	t=48	t=72	t=0	t=24	t=48	t=72	t=0	t=24	t=48	t=72
1192	880	968	528	1173	1056	968	616	786	792	616	616
1130	968	1056	528	1069	1144	880	704	795	792	704	704
1037	968	1056	528	1156	1144	1056	704	673	792	616	704
930	880	880	616	1108	1144	1056	704	686	792	616	704
1030	1056	1144	616	1061	1144	1056	704	760	792	616	704
923	1056	1056	616	1079	1056	1144	704	730	792	704	704

pH

Test 1				Test 2				Test 3			
t=0	t=24	t=48	t=72	t=0	t=24	t=48	t=72	t=0	t=24	t=48	t=72
6.98	7.07	7.13	7.24	7.01	7.06	7.17	7.42	6.96	7.06	7.16	7.39
6.96	7.08	7.1	7.16	6.99	7.11	7.27	7.25	6.98	7.07	7.12	7.34
6.97	7.03	7.1	7.2	6.99	7.04	7.29	7.45	6.97	7.06	7.28	7.39

pH

Test 4				Test 5				Test 6			
t=0	t=24	t=48	t=72	t=0	t=24	t=48	t=72	t=0	t=24	t=48	t=72
6.99	7.08	7.38	7.46	6.99	7.13	7.32	7.34	6.97	7.05	7.27	7.29
6.99	7.09	7.35	7.43	7	7.11	7.29	7.35	6.98	7.07	7.28	7.3
7	7.1	7.35	7.43	6.98	7.09	7.27	7.33	6.96	7.06	7.25	7.29

Ca^{2+}

Test 1				Test 2				Test 3			
t=0	t=24	t=48	t=72	t=0	t=24	t=48	t=72	t=0	t=24	t=48	t=72
260	272	208	172	176	240	144	72	200	256	176	80
280	288	224	180	192	256	160	76	180	224	192	88

Ca^{2+}

Test 4				Test 5				Test 6			
t=0	t=24	t=48	t=72	t=0	t=24	t=48	t=72	t=0	t=24	t=48	t=72
180	128	100	76	240	160	160	128	280	256	220	188
140	112	108	84	220	176	164	132	260	272	200	172

b. CO_2 and CH_4 values (mg/L) measured in the headspace of the Balch tubes after 24, 48 and 72 h of digestion for tests 1 to 6.

Test	CO_2 [mg/L]			CH4 [mg/L]		
#	t=24	t=48	t=72	t=24	t=48	t=72
	31.54	31.40	37.47	1.00	1.18	20.01
1	36.25	32.15	52.89	0.90	2.11	33.08
	32.77	74.31	66.33	1.77	4.79	25.07
	27.51	56.72	33.68	1.32	20.31	27.05
2	38.81	58.62	43.18	0.92	37.07	6.42
	29.15	30.15	64.24	0.95	7.10	68.56
	44.40	59.45	29.78	0.90	7.48	19.90
3	27.64	70.82	34.17	0.93	16.43	23.09
	36.00	77.51	32.44	0.92	37.63	22.21
	52.53	52.53	31.54	1.80	20.42	25.32
4	44.46	47.63	27.51	1.28	5.27	23.92
	39.64	41.99	47.68	1.00	1.61	31.93
	41.23	49.84	51.26	0.93	11.08	23.24
5	31.63	28.48	36.96	0.89	1.29	15.05
	25.49	30.20	32.10	0.89	1.06	8.03
	28.88	26.68	31.21	0.90	0.94	4.80
6	31.26	56.22	46.08	0.89	6.10	1.23
	25.15	58.24	35.30	0.97	1.63	1.08